

Cover Page



Universiteit Leiden



The handle <http://hdl.handle.net/1887/73850> holds various files of this Leiden University dissertation.

**Author:** Keijzer, J. de

**Title:** A proteomic portrait of Mycobacterium tuberculosis

**Issue Date:** 2019-06-06

**A Proteomic Portrait of**  
***Mycobacterium tuberculosis***

Jeroen de Keijzer

The research described in this thesis was funded by strategic research fund (SOR) of the National Institute for Public Health and the Environment (RIVM). (SOR Project S/000134)

**ISBN:** 978-94-6323-651-5  
**Cover:** Scientist generating a proteomic portrait of *Mycobacterium tuberculosis*.  
**Cover concept:** Jeroen de Keijzer  
**Cover design:** Ilse Modder, [www.ilsemodder.nl](http://www.ilsemodder.nl)  
**Lay-out:** Ilse Modder, [www.ilsemodder.nl](http://www.ilsemodder.nl)  
**Printing:** Gildeprint, Enschede, The Netherlands



© 2019 Jeroen de Keijzer

All rights reserved. No part of this publication may be reproduced or transmitted in any form by any means without permission of the author.

# **A Proteomic Portrait of *Mycobacterium tuberculosis***

Proefschrift

ter verkrijging van  
de graad van Doctor aan de Universiteit Leiden,  
op gezag van Rector Magnificus prof.mr. C.J.J.M. Stolker,  
volgens besluit van het College voor Promoties  
te verdedigen op donderdag 6 juni 2019  
klokke 16.15 uur

door

**Jeroen de Keijzer**

geboren te Rotterdam  
in 1988

## **Promotiecommissie**

### **Promotores:**

Prof. dr. F. Koning

Prof. dr. D. van Soolingen (Radboud University, University Medical Center, Nijmegen)

### **Co-promotor:**

Dr. P.A. van Veelen

### **Leden promotiecommissie:**

Prof. dr. M. Wuhler

Prof. dr. M.W. Borgdorff (University of Amsterdam, Academic Medical Center, Amsterdam)

Prof. dr. C.R. Jimenez (Vrije University Amsterdam, University Medical Center, Amsterdam)

## Table of contents

Chapter 1:	Introduction	09
Chapter 2:	Disclosure of selective advantages in the “modern” sublineage of the <i>Mycobacterium tuberculosis</i> Beijing genotype family by quantitative proteomics	33
Chapter 3:	Mechanisms of phenotypic rifampicin tolerance in <i>Mycobacterium tuberculosis</i> Beijing genotype strain B0/W148 revealed by proteomics	71
Chapter 4:	Parallel reaction monitoring of clinical <i>Mycobacterium tuberculosis</i> lineages reveals pre-existent markers of rifampicin tolerance in the emerging Beijing lineage	107
Chapter 5:	Thioridazine alters the cell envelope permeability of <i>Mycobacterium tuberculosis</i>	139
Chapter 6:	Identification of phylogenetic relationships in the <i>Mycobacterium</i> genus by direct comparison of shared spectral content	169
Chapter 7:	General discussion	189
Addendum:	Nederlandstalige samenvatting	213
	List of publications	221
	Curriculum Vitae	222
	Dankwoord	223



# 1

## Introduction



# Proteomic analysis of *Mycobacterium tuberculosis*: towards the etiology of drug resistance

## BACKGROUND

*Mycobacterium tuberculosis*, the causative agent of tuberculosis (TB), is an airborne and highly contagious bacterium. *M. tuberculosis* generally causes a pulmonary disease, but can also manifest itself in other parts of the body. Approximately 90% of the individuals infected by *M. tuberculosis* carry an inactive, asymptomatic, non-contagious, latent form of TB that could eventually progress to an active form of TB.<sup>(1)</sup> Currently, an estimated 2 billion individuals worldwide have a latent form of TB, while >10 million cases of active TB are registered each year.<sup>(2)</sup> With a total of 1.4 million individuals that die annually due to this pathogen, TB is the global leading cause of death by a single bacterial infection.<sup>(2)</sup>

To answer the question how *M. tuberculosis* has developed into the notorious pathogen we experience today, one should go back to the time of early humans, roughly 70,000 years ago. One theory suggests that the early modern humans in Africa were already infected by *M. tuberculosis*.<sup>(3)</sup> Since in this theory humans encountered *M. tuberculosis* at the start of existence, it is believed that man and pathogen followed parallel paths during the course of evolution. When early humans, accompanied by *M. tuberculosis*, migrated from Africa into Europe and Asia, isolated human populations were formed, leading to separate paths of evolution. Over time, both man and pathogen co-evolved in geographically separated populations. This 'isolated evolution' ultimately resulted in the seven *M. tuberculosis* lineages that are known today; see Box 1. Each of these seven *M. tuberculosis* lineages adapted to the human population it co-evolved with.<sup>(4)</sup> For example, the *M. tuberculosis* lineages that evolved in high density human populations became more infectious and easy to transmit, since large human populations prevent extinction of the bacterium once the hosts pass away. In contrast, *M. tuberculosis* lineages that infected low density populations evolved by becoming less aggressive, and included periods of latency followed by reactivation to prevent their extinction. Due to this specialized refinement, the pathogen was able to manifest itself as one of the greatest killers in history, killing one in five European adults between the 17<sup>th</sup> and 19<sup>th</sup> century.<sup>(5)</sup>

Until the 19<sup>th</sup> century, the cause of TB was unknown. To describe the pathology, the term 'consumption' was used, referring to the dramatic weight loss that occurs in TB patients, i.e. the patients were 'consumed' by the disease. In 1882 Robert Koch identified *M. tuberculosis* as the pathogen responsible for the spread of TB, and from that time on mankind knew what caused the disease they were fighting.<sup>(6)</sup> With the introduction of the antibiotic streptomycin some 65 years later, humans gained the upper hand and TB could be efficiently treated.<sup>(7, 8)</sup> In the following years, several anti-TB drugs became available, leading to the standard multidrug

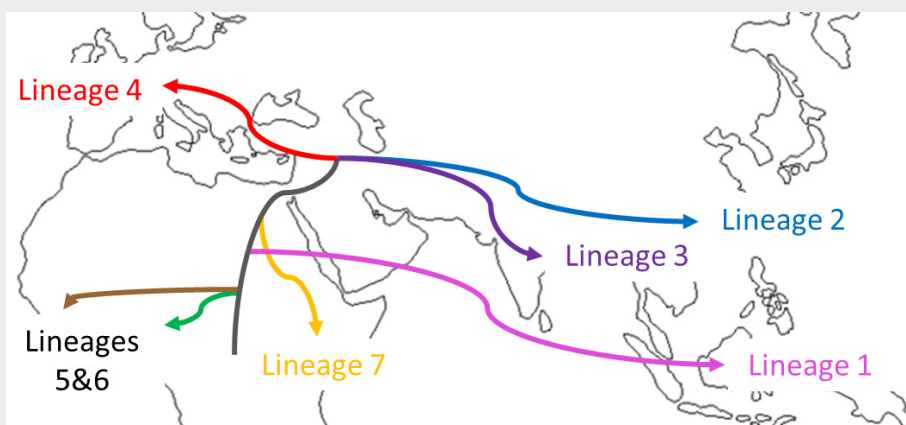
treatment regimens that are currently being used over the last 50 years.

With the means available to cure TB, the American Medical Association's Advisory Council for the Elimination of TB predicted in 1987 that by 2010 TB would be extinct worldwide.<sup>(9)</sup> While given the unique opportunity to eliminate this deadly disease, limited access to resources, poverty, non-adherence to therapy, neglect, and the HIV epidemic prevented eradication of the disease and ultimately resulted into the emergence of a new threat; drug-resistant *M. tuberculosis*.<sup>(10)</sup>

#### BOX 1: Out-of-Africa migration of *Mycobacterium tuberculosis*

Genetic evidence suggests that the long, 70,000 years of shared history between *M. tuberculosis* and humans led to isolated evolution of seven *M. tuberculosis* lineages as humans migrated out of Africa; see Figure adapted from Hershberg *et al.*, 2008<sup>(4)</sup> During this time, each of the *M. tuberculosis* lineages have been able to adapt to the various human population structures.

To date, knowledge about lineage specific diversity within *M. tuberculosis* is becoming increasingly important to understand the observed inter-lineage variation in virulence, transmission and emergence of drug resistance.<sup>(11)</sup> Regarding drug resistance, Lineage 2, largely consisting of the Beijing genotype family, is largely responsible for the dissemination of drug resistant TB in Eurasia.<sup>(12, 13)</sup> Compared to the other *M. tuberculosis* lineages, Beijing strains have been shown to possess, yet to be identified, selective advantages to develop antibiotic resistance.<sup>(14-17)</sup>



## Drug resistance in *Mycobacterium tuberculosis*

Antibiotics are essential to treat TB patients and prevent further transmission and dissemination of the disease. Despite the presence of multiple effective antibiotics, *M. tuberculosis* is increasingly found to be resistant to one or several antibiotics.<sup>(18)</sup>

The development of antibiotic resistance in *M. tuberculosis* is a typical example of Darwin's evolution theory. The selective pressure provided by the usage of antibiotics in the 20<sup>th</sup> and 21<sup>st</sup> century made antibiotic tolerance a favorable trait for *M. tuberculosis*. The positive selection for more antibiotic tolerant bacteria, combined with non-curative treatment, pushed evolution to select for drug resistant strains.<sup>(19)</sup> This positive selection for drug resistant strains led to the global occurrence of multidrug resistant strains that are currently isolated from TB patients.

Multidrug resistant TB, also referred to as MDR-TB, is resistant to at least rifampicin and isoniazid, two of the most potent drugs in anti-TB therapy. Globally, at least 3.5% of all new TB cases are caused by MDR-TB, whereas the reported levels of MDR-TB are around 20% for patients previously treated for TB.<sup>(18)</sup> Despite being resistant to the first-line antibiotics rifampicin and isoniazid, MDR-TB can in principle be treated successfully using second-line antibiotics such as fluoroquinolone and aminoglycoside. However, there is a progression of MDR-TB to extensively drug resistant TB (XDR-TB), which, in addition to resistance for isoniazid and rifampicin, also involves resistance to any of the fluoroquinolones and at least one aminoglycoside.<sup>(20)</sup> Finally, the term totally drug resistant TB (TDR-TB) has been introduced in 2009 to describe *M. tuberculosis* that acquired resistance against all known TB drugs available in a particular setting.<sup>(21-23)</sup> Due to the absence of novel anti-TB drugs that can be used to treat drug resistant TB, there is a growing concern that the emergence of MDR-TB, XDR-TB and TDR-TB will reverse the gains obtained in the last century that aided humans in the enduring fight against *M. tuberculosis*.<sup>(24)</sup>

Massive rates of drug resistant TB have been reported from several central Asian and Eastern European countries like for instance Belarus, where MDR-TB was found in 35% of newly infected patients and more than 75% in patients previously treated for TB.<sup>(25)</sup> One explanation for the drug resistant TB burden in Belarus and other former Soviet Union states is the collapse of healthcare systems following the fall of the Soviet Union.<sup>(26)</sup> Similarly, the relatively fragile healthcare system in India is thought to accelerate the evolution of *M. tuberculosis* towards drug resistance.<sup>(27)</sup> Due to the absence of sufficient medical knowledge and appropriate means to treat TB in multiple high burden countries, it is evident that there is a human factor contributing to the development and spread of antibiotic resistance.<sup>(28)</sup>

Next to human factors, bacterial factors can also contribute to the emergence of drug resistance. In Eurasia, the dissemination of MDR-TB is largely attributable to the *M. tuberculosis* lineage 2,

that largely consist out of the Beijing genotype.<sup>(12, 13)</sup> Members of the *M. tuberculosis* the Beijing genotype have been reported to be more transmissible than other *M. tuberculosis* lineages and seem to possess selective advantages to development resistance against the first line antibiotic rifampicin.<sup>(14-17, 29-32)</sup> Despite the current knowledge of *M. tuberculosis*, it remains difficult to pinpoint the exact mechanism employed by the pathogen to develop antibiotic resistance. All *M. tuberculosis* lineages have a shared, broad variety of known, and possibly unknown, molecular mechanisms that can be utilized to by-pass and ultimately survive antibiotic treatment. These mechanisms can express themselves in either the genotype or the phenotype of the pathogen. Genotypic resistance, or inheritable resistance, in bacteria can occur either due to chromosomal changes of drug target genes or by horizontal transfer of resistance conferring genes between bacteria. In *M. tuberculosis*, genotypic resistance is exclusively caused by chromosomal changes, after which drug resistant mutants can outgrow susceptible bacteria under the selective pressure of antibiotics.<sup>(33)</sup> The vast majority of antibiotic resistance in *M. tuberculosis* is caused by a genetic modification of the drug target gene, followed by selection of these mutants in the patient. In new patients, MDR-TB can be contracted by an infection of an MDR-TB strain (primary resistance) and by a bad quality treatment (acquired resistance). In case of the first-line antibiotic rifampicin, the drug target *rpoB* is genetically altered in approximately 95% of all the rifampicin resistant cases.<sup>(34)</sup>

Next to modifications of the genotype, *M. tuberculosis* has several intrinsic and phenotypic traits that can contribute to antibiotic tolerance already prior exposure to drugs; see Box 2. Phenotypic drug resistance mechanisms do usually not provide the level of resistance that is conferred by genotypic resistance, hence it is also referred to as phenotypic drug tolerance. One major obstacle in the design of antibiotics is to get clinically relevant concentrations of drugs inside the pathogen. The first hurdle for antibiotics is the remarkable hydrophobic cell wall of *M. tuberculosis*, that consists of unusual long-chain fatty acids, named mycolic acids. These fatty acids surround the pathogen and form an impermeable shell that provides resistance to a broad variety of antibiotics.<sup>(35)</sup> The cell wall acts together with specific proteins, referred to as porins, that can form channel-like structures in the mycobacterial cell wall. By regulating the abundance of porins, mycobacteria can adjust the permeability of their cell wall.<sup>(36)</sup> The presence of porins allows the pathogen to more easily take up hydrophilic nutrients such as glucose.<sup>(37)</sup> In contrast, the absence of porins makes it more difficult for hydrophilic antibiotics to cross the cell wall and accumulate inside the pathogen.<sup>(36, 38)</sup>

Antibiotics that do manage to cross the hydrophobic cell wall of *M. tuberculosis* can be secreted by a specific class of proteins, known as efflux pumps. These proteins actively decrease the intracellular drug concentration by exporting antibiotics from the intracellular to the extracellular environment.<sup>(39-41)</sup> To date, more than 30 putative efflux pump genes have been

described in *M. tuberculosis*.<sup>(40)</sup> With this large collection of efflux pumps, *M. tuberculosis* is capable of reducing the intracellular concentration of a variety of antibiotics including, but not limited to, tetracycline, fluoroquinolones and aminoglycosides.<sup>(42)</sup>

The hydrophobic cell wall, in combination with porins and efflux pumps, brings the intracellular concentration of antibiotics to a minimum for specific molecules. Other molecules, such as beta-lactams, can be accumulated in the pathogen. However, mycobacteria possess at least four enzymes that provide beta-lactamase activity to degrade beta-lactam containing drugs.

<sup>(43-45)</sup>

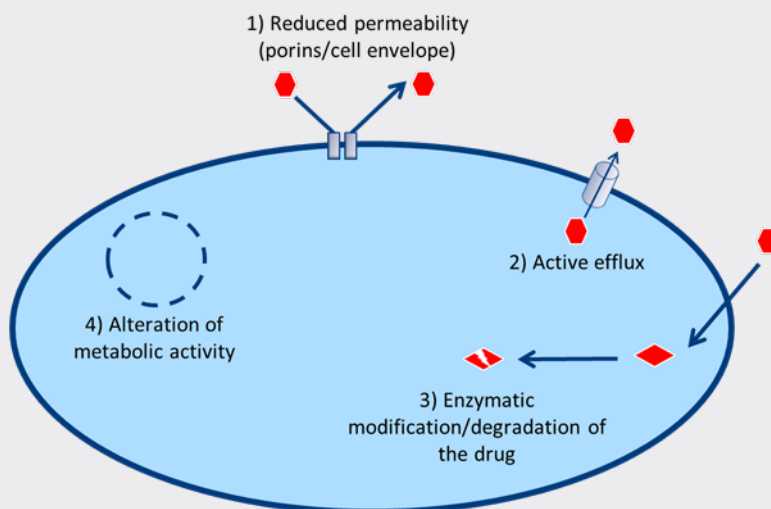
Finally, drug tolerance in *M. tuberculosis* can also be conferred by the slow growth rate of the pathogen, since the majority of antibiotics target mechanisms involved in active cell growth and division.<sup>(46, 47)</sup> Compared to the well-studied bacterium *Escherichia coli*, the doubling time of *M. tuberculosis* in nutrient rich media is approximately 40 times longer than that of *E. coli*.<sup>(48)</sup> Consequently, it takes approximately 40 times longer to kill 99% of *M. tuberculosis* in culture using antibiotics than it would to kill *E. coli*.<sup>(49)</sup> Next to its slow growth rate, *M. tuberculosis* can regulate its metabolic activity. When the pathogen becomes metabolically hypoactive, the potency of various antibiotics is lowered.<sup>(50)</sup>

*In vivo*, the intrinsic, genotypic and phenotypic drug resistance mechanisms are related. During the initial exposure to antibiotics, *M. tuberculosis* can persist in its host due to intrinsic and phenotypic drug resistance mechanisms. As a consequence, the pathogen gains time to develop a more durable drug resistant genotype.<sup>(51, 52)</sup>

Although intrinsic, genotypic and phenotypic mechanisms are known to exist in *M. tuberculosis*, it is unclear whether these mechanisms are actively induced simultaneously by the pathogen when challenged by antibiotics. Since both intrinsic and phenotypic drug resistance mechanisms facilitate the development of genotypic resistance, it is of increasing interest to pinpoint which biological processes drive the development of drug resistance within the various *M. tuberculosis* lineages. This is not only important to increase our understanding of the 'traditional' first line antibiotics, but also to prevent the occurrence of resistance for the novel second-line antibiotics bedaquiline and delamanid that have proven efficacy for treatment of drug resistant TB.<sup>(53, 54)</sup>

### BOX 2: The molecular toolbox of *Mycobacterium tuberculosis*

*M. tuberculosis* strains possess a variety of tools that allow the pathogen to protect itself against antibiotics. Depicted are the four most general phenotypic mechanisms used by *M. tuberculosis* to increase its tolerance towards antibiotics; see Figure adapted from Vranakis *et al.*, 2014 (55). The first barrier, which is conserved throughout the *Mycobacterium* genus, is the highly hydrophobic cell wall. This barrier, in combination with the regulation of porins, increases antibiotic resistance by reducing the cells permeability to antibiotics, which makes it difficult to intracellularly accumulate antibiotics to a clinically relevant concentration.(35, 36, 38) Antibiotics that manage to cross the cell envelope face a second hurdle: efflux pumps that can export a variety of intracellular compounds, such as antibiotics. By working together with the cell wall and porins, efflux pumps can keep the intracellular concentration of drugs to a minimum.(40) Third, some antibiotics that manage to accumulate inside the pathogen, can be degraded by intracellular enzymes. For example, beta-lactam based antibiotics can be actively degraded by cytoplasmic enzymes known as beta-lactamases.(43-45) Finally, *M. tuberculosis* can alter its metabolic activity. When the pathogen makes the transition to a metabolically hypoactive state, it becomes far less susceptible to a variety of antibiotics.(46, 50)



## Quantitative Proteomics to study *Mycobacterium tuberculosis*

Current curative anti-TB drug treatment regimens require 6-9 months with multiple antibiotics, to avoid re-emergence of the disease.<sup>(56)</sup> The length of the treatment often leads to adverse drug reactions and poor compliance to therapy, which contributes to the occurrence of drug resistance.<sup>(57)</sup> In the case of MDR-TB and XDR-TB, curative treatment requires the use of second-line antibiotics that are often associated with even more severe adverse events, that could ultimately result in discontinuation of treatment and more resistant bacteria.<sup>(58)</sup>

Treatment regimens for both drug susceptible and drug resistant TB are based on the assumption that the microbial physiology of drug-susceptible *M. tuberculosis* is similar to that of drug-resistant variants and strains that are more prone to develop drug resistance, i.e. our understanding of drug resistance is limited to the established relationship between specific mutations and resistance to specific anti-TB drugs.<sup>(59)</sup> However, considering the phenotypic drug tolerance mechanisms available to *M. tuberculosis*, it is to be expected that drug resistant strains, and variants that are more likely to develop resistance, differ physiologically from drug susceptible strains.

A better knowledge of the mechanisms of action of anti-TB drugs, the evolution of drug resistance and the biology of drug resistance development will allow for the identification of new drug targets, more strategic use of available antibiotics and improved diagnostic assays to detect drug resistance. To fully understand the development of antibiotic resistance, one needs tools to monitor and examine the various known and unknown mechanisms that contribute to the formation of drug resistance.

Modern 'omic' approaches can provide an unbiased, quantitative and holistic view to study specific classes of biomolecules. The DNA, which may contain drug resistance conferring mutations present in the genome of *M. tuberculosis*, is studied within the field of genomics. The genome itself is generally considered a blueprint for proteins that can be synthesized by an organism. The proteins, synthesized as dictated by the genome, that are present at a given time point within the cell, are referred to as the proteome. In contrast to the genome, the proteome is highly dynamic: the abundance of proteins can vary under different environmental conditions; proteins can be modified post- and co-translational; proteins can be secreted or only be present within a specific compartment of the cell. The field of proteomics aims to identify and quantify the proteome of organisms under various environmental conditions.

The mass spectrometer, or mass analyzer, is a central piece of equipment in mass spectrometric based proteomic workflows. Essentially, mass spectrometers determine the mass-to-charge

( $m/z$ ) ratio of charged peptides and proteins in the gas-phase. Based on the observed mass-to-charge ratio, the mass of intact proteins and peptides can be determined. This process is referred to as peptide mass fingerprinting.<sup>(60)</sup> Tandem mass spectrometry, also known as MS/MS or MS<sup>2</sup>, is used to determine the amino acid sequence of proteins and peptides.<sup>(61)</sup> First, the intact mass of a molecule is determined using a process similar to that of peptide mass fingerprinting. Subsequently, using a single or a combination of fragmentation techniques, the peptide backbone of the molecule can be broken. By determining the masses of these fragments, one can identify the sequence of building blocks, or amino acids, of which the protein or peptide is composed.

The first mycobacterial proteomic studies focused on enriched cellular fractions, including the culture supernatant, cell envelope or cytoplasm, using two-dimensional gel electrophoresis after which selected “spots” were analyzed using tandem mass spectrometry.<sup>(62-71)</sup> Using this approach, a cumulative number of approximately 300 *M. tuberculosis* proteins were identified. In 1998, the entire *M. tuberculosis* genome was mapped.<sup>(33)</sup> In the case of *M. tuberculosis*, the genome contained blueprints for roughly 4,000 proteins. Based on homology studies, nearly 3,500 proteins could, often weakly, be associated to a function.<sup>(72)</sup> Equipped with the knowledge that less than 10% of the *M. tuberculosis* proteome was yet observed, it was evident that in order to analyze the entire mycobacterial proteome in a single experiment, significant changes in workflow and equipment were necessary.

One major step forward was around the turn of the century, with the introduction of novel proteomic workflows in which multidimensional liquid chromatography (LC) was hyphenated to tandem mass spectrometry, of which the spectra could be automatically matched to a genome using proteomic search engines.<sup>(73)</sup> Currently, proteomic workflows are still based on the same principles, albeit with more advanced instrumentation and bioinformatics.

A schematic, modern proteomics approach for *M. tuberculosis* is outlined in Box 3. The described approach, applied with minor modifications, has resulted in the identification of >3000 mycobacterial proteins, which corresponds to 95% of the observable proteome during logarithmic growth of *M. tuberculosis*.<sup>(74)</sup> The identification of a proteins N-terminal and C-terminal sequence can be used to verify and improve genome annotations. This specific field is referred to as proteogenomics. Mass spectrometry based proteogenomic analysis of *M. tuberculosis* led to translational start site correction for >30 genes, and identification >40 novel protein coding genes.<sup>(74-76)</sup> However, to study the dynamics of the proteome, and its relation to drug resistance, quantification of proteins is often a necessity.<sup>(55)</sup> This is especially relevant when researchers want to compare the proteome composition of a drug-resistant strain with that of a drug susceptible strain or monitor the proteomic response of a strain exposed to sub-lethal concentrations of antibiotics.



Using mass spectrometry, also quantitative information of the proteome can be obtained.<sup>(77)</sup> Although there are multiple quantitative proteomic methods, one can separate label-free strategies from isotopically labelled methods.<sup>(78)</sup> With a label-free proteomic approach, data is acquired as presented in Box 3. Subsequently, the abundance of peptides is compared between two or multiple runs. The main advantages of label-free proteomic approaches is that they are cost-efficient, relatively straight forward and have a high dynamic range.<sup>(77, 79)</sup> For *M. tuberculosis*, label-free proteomic analyses have been used to compare drug susceptible with drug resistant strains, and avirulent to virulent *M. tuberculosis* strains.<sup>(80-83)</sup> Although powerful, label-free approaches have the disadvantage that they are relatively prone to experimental and technical variation.

In order to achieve a more robust proteomic quantification method with more throughput, a variety of mass labels, or mass tags, have been introduced.<sup>(77, 78)</sup> Since mass spectrometers are able to determine masses, one can discriminate peptides with a “heavy” or “light” mass label in a single analysis. By comparing the intensities of mass labelled peptides, one can determine their relative abundance. One elegant technique to label, or tag proteins is to culture cells in the presence of stable isotopically labelled amino acids (SILAC).<sup>(84)</sup> Unfortunately, this type of metabolic labeling for *M. tuberculosis* is challenging because amino acids are used as carbon and nitrogen source for the synthesis of new amino acids, causing the isotopic label to end in a variety of amino acids.<sup>(83, 85)</sup>

To overcome these limitations, post-metabolic labeling strategies can be used. Post-metabolic labeling strategies have the advantage that they do not rely on specific culture media and virtually every sample can be labelled, including clinically derived material. Most post-metabolic labels are incorporated at the peptide level. Depending on the number of the samples and capabilities of the equipment available, one can decide to use isobaric tags or isotope-coded tags. Isobaric tags such as tandem mass tags (TMT) or isobaric tags for relative and absolute quantitation (iTRAQ) can be used to analyze 2-10 samples in a single analysis. Quantitative data is obtained after fragmentation of the peptide and its isobaric label.<sup>(86, 87)</sup> A major drawback of isobaric mass tags is that they are not compatible with all types of mass spectrometers due to the low mass of the reporter ion. Furthermore, the occurrence of precursor ions with similar masses leads to co-isolation of peptides with inaccurate quantification as a result.<sup>(88, 89)</sup>

Finally, quantification can also be performed by dimethylation, also known as reductive amination, which uses isotope coded tags.<sup>(90)</sup> The dimethyl label is incorporated after protein digestion, providing the peptides with a “light” (+28 Da), “medium” (+32 Da) or “heavy” (+36 Da) methyl tag. Subsequently, the samples are mixed and co-analyzed using LC-MS/MS. Since there is no chemical difference between the three dimethyl labels, the labelled peptides will co-elute

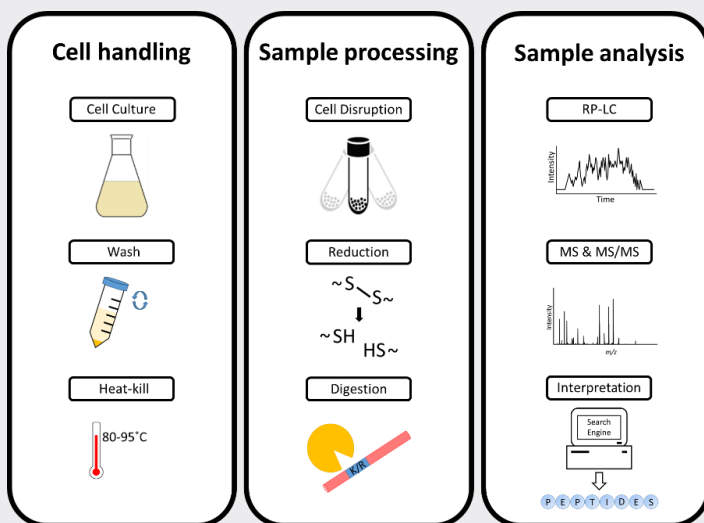
from the LC system, after which they are analyzed by the mass spectrometer, where the relative abundance is calculated based on the precursors ion chromatogram peak area. Compared to isobaric mass tags, dimethylation has a lower throughput due to limited multiplexing, and more complex mass spectra, which could lead to less peptide identifications. However, isobaric mass tags have several advantages compared to dimethylation mass tags including: compatibility with all tandem mass spectrometers; more accurate quantification; and more affordable reagents.<sup>(91)</sup> In this thesis, we decided to use dimethylation as the method of choice to quantitatively assess the proteome of *M. tuberculosis* in a robust manner.

Quantitative mass spectrometry can be used to study the abundance of proteins. However, more layers of information are present within the proteome. Post-translational modifications of proteins can impact the functionality of proteins, their compartmentalization, but also how they are organized in complexes and interact with other proteins.<sup>(92)</sup> Several post-translational modifications have been reported within the proteome of *M. tuberculosis*, including phosphorylation, glycosylation, acetylation, lipidation and pupylation.<sup>(93-97)</sup> Despite their presence, there is only a single quantitative phosphoproteomic study that demonstrated the potential impact of post-translational modifications on bacterial virulence.<sup>(98)</sup>

Despite being in its infancy, modern day proteomic approaches are powerful enough to study, without bias, phenotypic changes in the *M. tuberculosis* proteome, which could contribute to the development of antibiotic tolerance.

### BOX 3: Interpreting the mycobacterial proteome using mass spectrometry

A typical, schematic, *M. tuberculosis* proteomic workflow can roughly be divided into three steps: 1. Cell culture in a biosafety level 3 laboratory, 2. Sample processing, generally outside of the biosafety level 3 laboratory, 3. Analysis of the processed sample. 1) Cell culture is the starting point for a majority of bacterial proteomic studies. Since the proteome is highly dynamic, one needs to select culture conditions that allow for reproducible culture of the pathogen. Following cell culture, media components, including proteins, that can interfere with the downstream processing and analysis of the samples need to be removed. Subsequently, the cells need to be killed before they can be moved safely from the biosafety level 3 laboratory. 2) For the processing of the samples, the proteins are extracted from the cell with a combination of lysis buffer, heat and mechanical disruption to obtain an unbiased protein extract of the mycobacterial proteome.(99) The extracted proteins are denatured, reduced and alkylated after which they are proteolytically digested: trypsin is the common choice since it often yields peptides of favorable length and charge state for analysis by mass spectrometry. At this stage, the peptides can be dimethylated for quantitative purposes, or fractionated to reduce the complexity of the digest and increase proteomic coverage. 3) The analysis of the protein digest encompasses a reverse phase based separation of peptides, followed by analysis using tandem mass spectrometry. The recorded fragment spectra are matched against theoretical spectra, generated on the basis of the available genomic information by a proteomic search engine.



## Outline of this thesis

Over the last decade, it became apparent that global efforts, which make use of the currently available antibiotics, vaccines and diagnostic assays, fall short to reverse the global TB epidemic and spread of MDR-TB. In this thesis, we used mass spectrometry based proteomics as a tool to study the interplay between the proteome of *M. tuberculosis* and antibiotic resistance.

**Chapter 1** provides an overview of *M. tuberculosis*, its family structure, its mechanisms to cope with antibiotics and the potential of proteomics to pinpoint which proteins contribute to the transition of *M. tuberculosis* to its multidrug resistant form.

**In chapter 2**, we investigate which bacterial factor present in *M. tuberculosis* Beijing, provides a selective evolutionary advantage. The *M. tuberculosis* Beijing family is often associated with drug resistance. Compared to other *M. tuberculosis* lineages, the Beijing genotype is considered to be one of the most prevalent and genetically conserved *M. tuberculosis* families. Despite being genetically conserved, the Beijing family can be divided into the more ancient (atypical) and more modern (typical) Beijing strains. Even though the ancient and modern Beijing strains are closely related on the genetic level, it is the modern Beijing strain that is responsible for the dissemination of drug resistance in Eurasia. Using a pooled proteomics approach, alongside traditional individual duplex analyses, we search for proteins that contribute to the successful phenotype of modern Beijing strains. Using enzymatic and quantitative polymerase chain reaction analysis of selected genes in a large cohort of Beijing strains, we establish a relation between the genotype and phenotype of modern Beijing strains that could ultimately provide the pathogen with an inheritable selective advantage over other *M. tuberculosis* strains.

**In chapter 3**, we determine which phenotypic mechanisms contribute to drug tolerance during the initial 24 hrs after antibiotic treatment. Since there is a strong correlation between modern Beijing strains and drug resistance, we follow the (phospho)proteome of a clinically relevant *M. tuberculosis* modern Beijing strain during the first 24 hrs of rifampicin exposure. Based on the findings generated by the (phosphor)proteomic analysis, we make use of cellular assays to confirm the physiological adaptations made by *M. tuberculosis* Beijing to cope with rifampicin.

**In chapter 4**, we examine whether other *M. tuberculosis* strains respond to rifampicin in the same manner as *M. tuberculosis* Beijing strains. We start by comparing the proteome of *M. tuberculosis* Beijing with the proteome of *M. tuberculosis* H37Rv. Based on the outcomes of this study we select differentially regulated proteins that can contribute to antibiotic tolerance in *M. tuberculosis* and quantify these proteins in a large cohort of clinically relevant strains using parallel reaction monitoring.

**In chapter 5**, the mechanism of action of thioridazine is investigated. Thioridazine is a neuroleptic that might be used off-label to treat *M. tuberculosis*. The anti-mycobacterial potency of thioridazine has been reported not to be affected by the selective advantages present in *M. tuberculosis* Beijing. However, the mechanism through which thioridazine is capable of killing mycobacteria is yet unknown. By comparing the proteome of *M. tuberculosis* in the presence and absence of thioridazine, we want to generate a first hypothesis of thioridazines mechanism of action. Subsequently, this hypothesis is tested using cellular assays, so we can establish a model of thioridazines mechanism of action.

**In chapter 6**, the potential of tandem mass spectrometry as a highly discriminatory phenotypic tool to identify mycobacteria is explored. Using a proteomic workflow in combination with a 10 minute LC-MS/MS gradient, we examine phylogenetic relationships between various well conserved mycobacteria. The outcomes and feasibility of the method is compared with the methods that are routinely used in a clinical setting.

**In chapter 7**, we summarize the outcomes of this thesis. Furthermore, we discuss the relevance of our findings, how they should be seen into context with our current knowledge of TB and suggest directions for future studies.

## References

1. Lee, S. H., Tuberculosis Infection and Latent Tuberculosis. *Tuberc Respir Dis (Seoul)* **2016**, 79, (4), 201-206.
2. WHO, Global tuberculosis report 2016. **2016**.
3. Comas, I.; Coscolla, M.; Luo, T.; Borrell, S.; Holt, K. E.; Kato-Maeda, M.; Parkhill, J.; Malla, B.; Berg, S.; Thwaites, G.; Yeboah-Manu, D.; Bothamley, G.; Mei, J.; Wei, L.; Bentley, S.; Harris, S. R.; Niemann, S.; Diel, R.; Aseffa, A.; Gao, Q.; Young, D.; Gagneux, S., Out-of-Africa migration and Neolithic coexpansion of *Mycobacterium tuberculosis* with modern humans. *Nat Genet* **2013**, 45, (10), 1176-82.
4. Hershberg, R.; Lipatov, M.; Small, P. M.; Sheffer, H.; Niemann, S.; Homolka, S.; Roach, J. C.; Kremer, K.; Petrov, D. A.; Feldman, M. W.; Gagneux, S., High functional diversity in *Mycobacterium tuberculosis* driven by genetic drift and human demography. *PLoS Biol* **2008**, 6, (12), e311.
5. Wilson, L. G., Commentary: Medicine, population, and tuberculosis. *Int J Epidemiol* **2005**, 34, (3), 521-4.
6. Koch, R., Die Aetiologie der Tuberkulose. *Berliner Klinische Wochenschrift* **1882**, 15, (April 10), 221-230.
7. Investigation, A. M. R. C., STREPTOMYCIN treatment of pulmonary tuberculosis. *Br Med J* **1948**, 2, (4582), 769-82.
8. Schatz, A.; Bugie, E.; Waksman, S. A., Streptomycin, a substance exhibiting antibiotic activity against gram-positive and gram-negative bacteria. 1944. *Clin Orthop Relat Res* **2005**, (437), 3-6.
9. Koehler, C. W., Consumption, the great killer. *Modern Drug Discovery* **2002**, 5, (2), 47-49.
10. Kurz, S. G.; Furin, J. J.; Bark, C. M., Drug-Resistant Tuberculosis: Challenges and Progress. *Infect Dis Clin North Am* **2016**, 30, (2), 509-22.
11. Reiling, N.; Homolka, S.; Walter, K.; Brandenburg, J.; Niwinski, L.; Ernst, M.; Herzmann, C.; Lange, C.; Diel, R.; Ehlers, S.; Niemann, S., Clade-specific virulence patterns of *Mycobacterium tuberculosis* complex strains in human primary macrophages and aerogenically infected mice. *MBio* **2013**, 4, (4).
12. Casali, N.; Nikolayevskyy, V.; Balabanova, Y.; Harris, S. R.; Ignatyeva, O.; Kontsevaya, I.; Corander, J.; Bryant, J.; Parkhill, J.; Nejentsev, S.; Horstmann, R. D.; Brown, T.; Drobniowski, F., Evolution and transmission of drug-resistant tuberculosis in a Russian population. *Nat Genet* **2014**, 46, (3), 279-86.
13. Mokrousov, I., Insights into the origin, emergence, and current spread of a successful Russian clone of *Mycobacterium tuberculosis*. *Clin Microbiol Rev* **2013**, 26, (2), 342-60.
14. Ford, C. B.; Shah, R. R.; Maeda, M. K.; Gagneux, S.; Murray, M. B.; Cohen, T.; Johnston, J. C.; Gardy, J.; Lipsitch, M.; Fortune, S. M., *Mycobacterium tuberculosis* mutation rate estimates from different lineages predict substantial differences in the emergence of drug-resistant tuberculosis. *Nat Genet* **2013**, 45, (7), 784-90.
15. Ebrahimi-Rad, M.; Bifani, P.; Martin, C.; Kremer, K.; Samper, S.; Rauzier, J.; Kreiswirth, B.; Blazquez, J.; Jouan, M.; van Soolingen, D.; Gicquel, B., Mutations in putative mutator genes of *Mycobacterium tuberculosis* strains of the W-Beijing family. *Emerg Infect Dis* **2003**, 9, (7), 838-45.
16. de Steenwinkel, J. E.; ten Kate, M. T.; de Knecht, G. J.; Kremer, K.; Aarnoutse, R. E.; Boeree, M. J.; Verbrugh, H. A.; van Soolingen, D.; Bakker-Woudenberg, I. A., Drug susceptibility of *Mycobacterium tuberculosis*

- Beijing genotype and association with MDR TB. *Emerg Infect Dis* **2012**, 18, (4), 660-3.
17. den Hertog, A. L.; Menting, S.; van Soolingen, D.; Anthony, R. M., Mycobacterium tuberculosis Beijing genotype resistance to transient rifampin exposure. *Emerg Infect Dis* **2014**, 20, (11), 1932-3.
  18. WHO, Multidrug-resistant tuberculosis (MDR-TB) 2013 Update. Factsheet. Available at: [http://www.who.int/tb/challenges/mdr/MDR\\_TB\\_FactSheet.pdf](http://www.who.int/tb/challenges/mdr/MDR_TB_FactSheet.pdf) **2013**, (Accessed: 16 January 2015).
  19. Nguyen, L., Antibiotic resistance mechanisms in M. tuberculosis: an update. *Arch Toxicol* **2016**, 90, (7), 1585-604.
  20. Centers for Disease, C.; Prevention, Plan to combat extensively drug-resistant tuberculosis: recommendations of the Federal Tuberculosis Task Force. *MMWR Recomm Rep* **2009**, 58, (RR-3), 1-43.
  21. Udwadia, Z. F.; Amale, R. A.; Ajbani, K. K.; Rodrigues, C., Totally drug-resistant tuberculosis in India. *Clin Infect Dis* **2012**, 54, (4), 579-81.
  22. Velayati, A. A.; Masjedi, M. R.; Farnia, P.; Tabarsi, P.; Ghanavi, J.; Ziazarifi, A. H.; Hoffner, S. E., Emergence of new forms of totally drug-resistant tuberculosis bacilli: super extensively drug-resistant tuberculosis or totally drug-resistant strains in iran. *Chest* **2009**, 136, (2), 420-5.
  23. Migliori, G. B.; De Iaco, G.; Besozzi, G.; Centis, R.; Cirillo, D. M., First tuberculosis cases in Italy resistant to all tested drugs. *Euro Surveill* **2007**, 12, (5), E070517 1.
  24. Garfein, R. S.; Catanzaro, D. G.; Rodwell, T. C.; Avalos, E.; Jackson, R. L.; Kaping, J.; Evasco, H.; Rodrigues, C.; Crudu, V.; Lin, S. Y.; Groessl, E.; Hillery, N.; Trollip, A.; Ganiats, T.; Victor, T. C.; Eisenach, K.; Valafar, F.; Channick, J.; Qian, L.; Catanzaro, A., Phenotypic and genotypic diversity in a multinational sample of drug-resistant Mycobacterium tuberculosis isolates. *Int J Tuberc Lung Dis* **2015**, 19, (4), 420-7.
  25. Skrahina, A.; Hurevich, H.; Zalutskaya, A.; Sahalchyk, E.; Astrauko, A.; van Gemert, W.; Hoffner, S.; Rusovich, V.; Zignol, M., Alarming levels of drug-resistant tuberculosis in Belarus: results of a survey in Minsk. *Eur Respir J* **2012**, 39, (6), 1425-31.
  26. Merker, M.; Blin, C.; Mona, S.; Duforet-Frebourg, N.; Lecher, S.; Willery, E.; Blum, M. G.; Rusch-Gerdes, S.; Mokrousov, I.; Aleksic, E.; Allix-Beguec, C.; Antierens, A.; Augustynowicz-Kopec, E.; Ballif, M.; Barletta, F.; Beck, H. P.; Barry, C. E., 3rd; Bonnet, M.; Borroni, E.; Campos-Herrero, I.; Cirillo, D.; Cox, H.; Crowe, S.; Crudu, V.; Diel, R.; Drobniewski, F.; Fauville-Dufaux, M.; Gagneux, S.; Ghebremichael, S.; Hanekom, M.; Hoffner, S.; Jiao, W. W.; Kalon, S.; Kohl, T. A.; Kontsevaya, I.; Lillebaek, T.; Maeda, S.; Nikolayevskyy, V.; Rasmussen, M.; Rastogi, N.; Samper, S.; Sanchez-Padilla, E.; Savic, B.; Shamputa, I. C.; Shen, A.; Sng, L. H.; Stakenas, P.; Toit, K.; Varaine, F.; Vukovic, D.; Wahl, C.; Warren, R.; Supply, P.; Niemann, S.; Wirth, T., Evolutionary history and global spread of the Mycobacterium tuberculosis Beijing lineage. *Nat Genet* **2015**, 47, (3), 242-9.
  27. Udwadia, Z. F.; Pinto, L. M.; Uplekar, M. W., Tuberculosis management by private practitioners in Mumbai, India: has anything changed in two decades? *PLoS One* **2010**, 5, (8), e12023.
  28. Eldholm, V.; Balloux, F., Antimicrobial Resistance in Mycobacterium tuberculosis: The Odd One Out. *Trends Microbiol* **2016**, 24, (8), 637-48.
  29. Tounghoussova, O. S.; Mariandyshev, A.; Bjune, G.; Sandven, P.; Caugant, D. A., Molecular epidemiology and drug resistance of Mycobacterium tuberculosis isolates in the Archangel prison in Russia:

- predominance of the W-Beijing clone family. *Clin Infect Dis* **2003**, 37, (5), 665-72.
30. Wada, T.; Fujihara, S.; Shimouchi, A.; Harada, M.; Ogura, H.; Matsumoto, S.; Hase, A., High transmissibility of the modern Beijing *Mycobacterium tuberculosis* in homeless patients of Japan. *Tuberculosis (Edinb)* **2009**, 89, (4), 252-5.
  31. Buu, T. N.; van Soolingen, D.; Huyen, M. N.; Lan, N. T.; Quy, H. T.; Tiemersma, E. W.; Kremer, K.; Borgdorff, M. W.; Cobelens, F. G., Increased transmission of *Mycobacterium tuberculosis* Beijing genotype strains associated with resistance to streptomycin: a population-based study. *PLoS One* **2012**, 7, (8), e42323.
  32. Yang, C.; Luo, T.; Sun, G.; Qiao, K.; Sun, G.; DeRiemer, K.; Mei, J.; Gao, Q., *Mycobacterium tuberculosis* Beijing strains favor transmission but not drug resistance in China. *Clin Infect Dis* **2012**, 55, (9), 1179-87.
  33. Cole, S. T.; Brosch, R.; Parkhill, J.; Garnier, T.; Churcher, C.; Harris, D.; Gordon, S. V.; Eiglmeier, K.; Gas, S.; Barry, C. E., 3rd; Tekaia, F.; Badcock, K.; Basham, D.; Brown, D.; Chillingworth, T.; Connor, R.; Davies, R.; Devlin, K.; Feltwell, T.; Gentles, S.; Hamlin, N.; Holroyd, S.; Hornsby, T.; Jagels, K.; Krogh, A.; McLean, J.; Moule, S.; Murphy, L.; Oliver, K.; Osborne, J.; Quail, M. A.; Rajandream, M. A.; Rogers, J.; Rutter, S.; Seeger, K.; Skelton, J.; Squares, R.; Squares, S.; Sulston, J. E.; Taylor, K.; Whitehead, S.; Barrell, B. G., Deciphering the biology of *Mycobacterium tuberculosis* from the complete genome sequence. *Nature* **1998**, 393, (6685), 537-44.
  34. Somoskovi, A.; Parsons, L. M.; Salfinger, M., The molecular basis of resistance to isoniazid, rifampin, and pyrazinamide in *Mycobacterium tuberculosis*. *Respir Res* **2001**, 2, (3), 164-8.
  35. Daffe, M.; Draper, P., The envelope layers of mycobacteria with reference to their pathogenicity. *Adv Microb Physiol* **1998**, 39, 131-203.
  36. Danilchanka, O.; Pavlenok, M.; Niederweis, M., Role of porins for uptake of antibiotics by *Mycobacterium smegmatis*. *Antimicrob Agents Chemother* **2008**, 52, (9), 3127-34.
  37. Stahl, C.; Kubetzko, S.; Kaps, I.; Seeber, S.; Engelhardt, H.; Niederweis, M., MspA provides the main hydrophilic pathway through the cell wall of *Mycobacterium smegmatis*. *Mol Microbiol* **2001**, 40, (2), 451-64.
  38. Stephan, J.; Mailaender, C.; Etienne, G.; Daffe, M.; Niederweis, M., Multidrug resistance of a porin deletion mutant of *Mycobacterium smegmatis*. *Antimicrob Agents Chemother* **2004**, 48, (11), 4163-70.
  39. Nikaido, H., Preventing drug access to targets: cell surface permeability barriers and active efflux in bacteria. *Semin Cell Dev Biol* **2001**, 12, (3), 215-23.
  40. Louw, G. E.; Warren, R. M.; Gey van Pittius, N. C.; McEvoy, C. R.; Van Helden, P. D.; Victor, T. C., A balancing act: efflux/influx in mycobacterial drug resistance. *Antimicrob Agents Chemother* **2009**, 53, (8), 3181-9.
  41. Louw, G. E.; Warren, R. M.; Gey van Pittius, N. C.; Leon, R.; Jimenez, A.; Hernandez-Pando, R.; McEvoy, C. R.; Grobbelaar, M.; Murray, M.; van Helden, P. D.; Victor, T. C., Rifampicin reduces susceptibility to ofloxacin in rifampicin-resistant *Mycobacterium tuberculosis* through efflux. *Am J Respir Crit Care Med* **2011**, 184, (2), 269-76.
  42. De Rossi, E.; Ainsa, J. A.; Riccardi, G., Role of mycobacterial efflux transporters in drug resistance: an unresolved question. *FEMS Microbiol Rev* **2006**, 30, (1), 36-52.



43. Flores, A. R.; Parsons, L. M.; Pavelka, M. S., Jr., Genetic analysis of the beta-lactamases of *Mycobacterium tuberculosis* and *Mycobacterium smegmatis* and susceptibility to beta-lactam antibiotics. *Microbiology* **2005**, 151, (Pt 2), 521-32.
44. Nampoothiri, K. M.; Rubex, R.; Patel, A. K.; Narayanan, S. S.; Krishna, S.; Das, S. M.; Pandey, A., Molecular cloning, overexpression and biochemical characterization of hypothetical beta-lactamases of *Mycobacterium tuberculosis* H37Rv. *J Appl Microbiol* **2008**, 105, (1), 59-67.
45. Sala, C.; Haouz, A.; Saul, F. A.; Miras, I.; Rosenkrands, I.; Alzari, P. M.; Cole, S. T., Genome-wide regulon and crystal structure of Blal (Rv1846c) from *Mycobacterium tuberculosis*. *Mol Microbiol* **2009**, 71, (5), 1102-16.
46. Gomez, J. E.; McKinney, J. D., *M. tuberculosis* persistence, latency, and drug tolerance. *Tuberculosis (Edinb)* **2004**, 84, (1-2), 29-44.
47. Barry, C. E., 3rd; Boshoff, H. I.; Dartois, V.; Dick, T.; Ehrt, S.; Flynn, J.; Schnappinger, D.; Wilkinson, R. J.; Young, D., The spectrum of latent tuberculosis: rethinking the biology and intervention strategies. *Nat Rev Microbiol* **2009**, 7, (12), 845-55.
48. Manina, G.; Dhar, N.; McKinney, J. D., Stress and host immunity amplify *Mycobacterium tuberculosis* phenotypic heterogeneity and induce nongrowing metabolically active forms. *Cell Host Microbe* **2015**, 17, (1), 32-46.
49. Brauner, A.; Fridman, O.; Gefen, O.; Balaban, N. Q., Distinguishing between resistance, tolerance and persistence to antibiotic treatment. *Nat Rev Microbiol* **2016**, 14, (5), 320-30.
50. de Steenwinkel, J. E.; de Knecht, G. J.; ten Kate, M. T.; van Belkum, A.; Verbrugh, H. A.; Kremer, K.; van Soolingen, D.; Bakker-Woudenberg, I. A., Time-kill kinetics of anti-tuberculosis drugs, and emergence of resistance, in relation to metabolic activity of *Mycobacterium tuberculosis*. *J Antimicrob Chemother* **2010**, 65, (12), 2582-9.
51. Jiang, X.; Zhang, W.; Zhang, Y.; Gao, F.; Lu, C.; Zhang, X.; Wang, H., Assessment of efflux pump gene expression in a clinical isolate *Mycobacterium tuberculosis* by real-time reverse transcription PCR. *Microb Drug Resist* **2008**, 14, (1), 7-11.
52. Rodrigues, L.; Machado, D.; Couto, I.; Amaral, L.; Viveiros, M., Contribution of efflux activity to isoniazid resistance in the *Mycobacterium tuberculosis* complex. *Infect Genet Evol* **2012**, 12, (4), 695-700.
53. Esposito, S.; Bianchini, S.; Blasi, F., Bedaquiline and delamanid in tuberculosis. *Expert Opin Pharmacother* **2015**, 16, (15), 2319-30.
54. Migliori, G. B.; Pontali, E.; Sotgiu, G.; Centis, R.; D'Ambrosio, L.; Tiberi, S.; Tadolini, M.; Esposito, S., Combined Use of Delamanid and Bedaquiline to Treat Multidrug-Resistant and Extensively Drug-Resistant Tuberculosis: A Systematic Review. *Int J Mol Sci* **2017**, 18, (2).
55. Vranakis, I.; Goniatis, I.; Psaroulaki, A.; Sandalakis, V.; Tselentis, Y.; Gevaert, K.; Tsiotis, G., Proteome studies of bacterial antibiotic resistance mechanisms. *J Proteomics* **2014**, 97, 88-99.
56. Hopewell, P. C., Updating the international standards for tuberculosis care. *Int J Tuberc Lung Dis* **2014**, 18, (3), 253.
57. Castelnuovo, B., A review of compliance to anti tuberculosis treatment and risk factors for defaulting

- treatment in Sub Saharan Africa. *Afr Health Sci* **2010**, 10, (4), 320-4.
58. Isaakidis, P.; Varghese, B.; Mansoor, H.; Cox, H. S.; Ladamiriska, J.; Saranchuk, P.; Da Silva, E.; Khan, S.; Paryani, R.; Udawadia, Z.; Migliori, G. B.; Sotgiu, G.; Reid, T., Adverse events among HIV/MDR-TB co-infected patients receiving antiretroviral and second line anti-TB treatment in Mumbai, India. *PLoS One* **2012**, 7, (7), e40781.
  59. de Souza, G. A.; Wiker, H. G., A proteomic view of mycobacteria. *Proteomics* **2011**, 11, (15), 3118-27.
  60. Henzel, W. J.; Billeci, T. M.; Stults, J. T.; Wong, S. C.; Grimley, C.; Watanabe, C., Identifying proteins from two-dimensional gels by molecular mass searching of peptide fragments in protein sequence databases. *Proc Natl Acad Sci U S A* **1993**, 90, (11), 5011-5.
  61. Yates, J. R., 3rd, Mass spectrometry and the age of the proteome. *J Mass Spectrom* **1998**, 33, (1), 1-19.
  62. Wallis, R. S.; Paranjape, R.; Phillips, M., Identification by two-dimensional gel electrophoresis of a 58-kilodalton tumor necrosis factor-inducing protein of *Mycobacterium tuberculosis*. *Infect Immun* **1993**, 61, (2), 627-32.
  63. Lee, B. Y.; Horwitz, M. A., Identification of macrophage and stress-induced proteins of *Mycobacterium tuberculosis*. *J Clin Invest* **1995**, 96, (1), 245-9.
  64. Sonnenberg, M. G.; Belisle, J. T., Definition of *Mycobacterium tuberculosis* culture filtrate proteins by two-dimensional polyacrylamide gel electrophoresis, N-terminal amino acid sequencing, and electrospray mass spectrometry. *Infect Immun* **1997**, 65, (11), 4515-24.
  65. Urquhart, B. L.; Cordwell, S. J.; Humphery-Smith, I., Comparison of predicted and observed properties of proteins encoded in the genome of *Mycobacterium tuberculosis* H37Rv. *Biochem Biophys Res Commun* **1998**, 253, (1), 70-9.
  66. Wong, D. K.; Lee, B. Y.; Horwitz, M. A.; Gibson, B. W., Identification of fur, aconitase, and other proteins expressed by *Mycobacterium tuberculosis* under conditions of low and high concentrations of iron by combined two-dimensional gel electrophoresis and mass spectrometry. *Infect Immun* **1999**, 67, (1), 327-36.
  67. Jungblut, P. R.; Schaible, U. E.; Mollenkopf, H. J.; Zimny-Arndt, U.; Raupach, B.; Mattow, J.; Halada, P.; Lamer, S.; Hagens, K.; Kaufmann, S. H., Comparative proteome analysis of *Mycobacterium tuberculosis* and *Mycobacterium bovis* BCG strains: towards functional genomics of microbial pathogens. *Mol Microbiol* **1999**, 33, (6), 1103-17.
  68. Betts, J. C.; Dodson, P.; Quan, S.; Lewis, A. P.; Thomas, P. J.; Duncan, K.; McAdam, R. A., Comparison of the proteome of *Mycobacterium tuberculosis* strain H37Rv with clinical isolate CDC 1551. *Microbiology* **2000**, 146 Pt 12, 3205-16.
  69. Rosenkrands, I.; King, A.; Weldingh, K.; Moniatte, M.; Moertz, E.; Andersen, P., Towards the proteome of *Mycobacterium tuberculosis*. *Electrophoresis* **2000**, 21, (17), 3740-56.
  70. Rosenkrands, I.; Weldingh, K.; Jacobsen, S.; Hansen, C. V.; Florio, W.; Gianetri, I.; Andersen, P., Mapping and identification of *Mycobacterium tuberculosis* proteins by two-dimensional gel electrophoresis, microsequencing and immunodetection. *Electrophoresis* **2000**, 21, (5), 935-48.
  71. Mattow, J.; Schaible, U. E.; Schmidt, F.; Hagens, K.; Siejak, F.; Brestrich, G.; Haeselbarth, G.; Muller, E. C.;

- Jungblut, P. R.; Kaufmann, S. H., Comparative proteome analysis of culture supernatant proteins from virulent *Mycobacterium tuberculosis* H37Rv and attenuated *M. bovis* BCG Copenhagen. *Electrophoresis* **2003**, 24, (19-20), 3405-20.
72. Doerks, T.; van Noort, V.; Minguéz, P.; Bork, P., Annotation of the *M. tuberculosis* hypothetical orfeome: adding functional information to more than half of the uncharacterized proteins. *PLoS One* **2012**, 7, (4), e34302.
  73. Washburn, M. P.; Wolters, D.; Yates, J. R., 3rd, Large-scale analysis of the yeast proteome by multidimensional protein identification technology. *Nat Biotechnol* **2001**, 19, (3), 242-7.
  74. Schubert, O. T.; Mouritsen, J.; Ludwig, C.; Rost, H. L.; Rosenberger, G.; Arthur, P. K.; Claassen, M.; Campbell, D. S.; Sun, Z.; Farrah, T.; Gengenbacher, M.; Maiolica, A.; Kaufmann, S. H.; Moritz, R. L.; Aebersold, R., The *Mtb* proteome library: a resource of assays to quantify the complete proteome of *Mycobacterium tuberculosis*. *Cell Host Microbe* **2013**, 13, (5), 602-12.
  75. de Souza, G. A.; Malen, H.; Softeland, T.; Saelensminde, G.; Prasad, S.; Jonassen, I.; Wiker, H. G., High accuracy mass spectrometry analysis as a tool to verify and improve gene annotation using *Mycobacterium tuberculosis* as an example. *BMC Genomics* **2008**, 9, 316.
  76. Kelkar, D. S.; Kumar, D.; Kumar, P.; Balakrishnan, L.; Muthusamy, B.; Yadav, A. K.; Shrivastava, P.; Marimuthu, A.; Anand, S.; Sundaram, H.; Kingsbury, R.; Harsha, H. C.; Nair, B.; Prasad, T. S.; Chauhan, D. S.; Katoch, K.; Katoch, V. M.; Kumar, P.; Chaerkady, R.; Ramachandran, S.; Dash, D.; Pandey, A., Proteogenomic analysis of *Mycobacterium tuberculosis* by high resolution mass spectrometry. *Mol Cell Proteomics* **2011**, 10, (12), M111 011627.
  77. Bantscheff, M.; Lemeer, S.; Savitski, M. M.; Kuster, B., Quantitative mass spectrometry in proteomics: critical review update from 2007 to the present. *Anal Bioanal Chem* **2012**, 404, (4), 939-65.
  78. Ong, S. E.; Mann, M., Mass spectrometry-based proteomics turns quantitative. *Nat Chem Biol* **2005**, 1, (5), 252-62.
  79. Patel, V. J.; Thalassinou, K.; Slade, S. E.; Connolly, J. B.; Crombie, A.; Murrell, J. C.; Scrivens, J. H., A comparison of labeling and label-free mass spectrometry-based proteomics approaches. *J Proteome Res* **2009**, 8, (7), 3752-9.
  80. Phong, T. Q.; Ha do, T. T.; Volker, U.; Hammer, E., Using a Label Free Quantitative Proteomics Approach to Identify Changes in Protein Abundance in Multidrug-Resistant *Mycobacterium tuberculosis*. *Indian J Microbiol* **2015**, 55, (2), 219-30.
  81. Jhingan, G. D.; Kumari, S.; Jamwal, S. V.; Kalam, H.; Arora, D.; Jain, N.; Kumaar, L. K.; Samal, A.; Rao, K. V.; Kumar, D.; Nandicoori, V. K., Comparative Proteomic Analyses of Avirulent, Virulent, and Clinical Strains of *Mycobacterium tuberculosis* Identify Strain-specific Patterns. *J Biol Chem* **2016**, 291, (27), 14257-73.
  82. Bespyatykh, J.; Shitikov, E.; Butenko, I.; Altukhov, I.; Alexeev, D.; Mokrousov, I.; Dogonadze, M.; Zhuravlev, V.; Yablonsky, P.; Ilina, E.; Govorun, V., Proteome analysis of the *Mycobacterium tuberculosis* Beijing B0/W148 cluster. *Sci Rep* **2016**, 6, 28985.
  83. de Souza, G. A.; Fortuin, S.; Aguilar, D.; Pando, R. H.; McEvoy, C. R.; van Helden, P. D.; Koehler, C. J.; Thiede, B.; Warren, R. M.; Wiker, H. G., Using a label-free proteomics method to identify differentially

- abundant proteins in closely related hypo- and hypervirulent clinical *Mycobacterium tuberculosis* Beijing isolates. *Mol Cell Proteomics* **2010**, 9, (11), 2414-23.
84. Ong, S. E.; Blagoev, B.; Kratchmarova, I.; Kristensen, D. B.; Steen, H.; Pandey, A.; Mann, M., Stable isotope labeling by amino acids in cell culture, SILAC, as a simple and accurate approach to expression proteomics. *Mol Cell Proteomics* **2002**, 1, (5), 376-86.
  85. Hampel, A.; Huber, C.; Geffers, R.; Spona-Friedl, M.; Eisenreich, W.; Bange, F. C., *Mycobacterium tuberculosis* Is a Natural Ornithine Aminotransferase (rocD) Mutant and Depends on Rv2323c for Growth on Arginine. *PLoS One* **2015**, 10, (9), e0136914.
  86. Thompson, A.; Schafer, J.; Kuhn, K.; Kienle, S.; Schwarz, J.; Schmidt, G.; Neumann, T.; Johnstone, R.; Mohammed, A. K.; Hamon, C., Tandem mass tags: a novel quantification strategy for comparative analysis of complex protein mixtures by MS/MS. *Anal Chem* **2003**, 75, (8), 1895-904.
  87. Ross, P. L.; Huang, Y. N.; Marchese, J. N.; Williamson, B.; Parker, K.; Hattan, S.; Khainovski, N.; Pillai, S.; Dey, S.; Daniels, S.; Purkayastha, S.; Juhasz, P.; Martin, S.; Bartlett-Jones, M.; He, F.; Jacobson, A.; Pappin, D. J., Multiplexed protein quantitation in *Saccharomyces cerevisiae* using amine-reactive isobaric tagging reagents. *Mol Cell Proteomics* **2004**, 3, (12), 1154-69.
  88. Trinh, H. V.; Grossmann, J.; Gehrig, P.; Roschitzki, B.; Schlapbach, R.; Greber, U. F.; Hemmi, S., iTRAQ-Based and Label-Free Proteomics Approaches for Studies of Human Adenovirus Infections. *Int J Proteomics* **2013**, 2013, 581862.
  89. Rauniyar, N.; Yates, J. R., 3rd, Isobaric labeling-based relative quantification in shotgun proteomics. *J Proteome Res* **2014**, 13, (12), 5293-309.
  90. Boersema, P. J.; Raijmakers, R.; Lemeer, S.; Mohammed, S.; Heck, A. J., Multiplex peptide stable isotope dimethyl labeling for quantitative proteomics. *Nat Protoc* **2009**, 4, (4), 484-94.
  91. Ji, C.; Guo, N.; Li, L., Differential dimethyl labeling of N-termini of peptides after guanidination for proteome analysis. *J Proteome Res* **2005**, 4, (6), 2099-108.
  92. van Els, C. A.; Corbiere, V.; Smits, K.; van Gaans-van den Brink, J. A.; Poelen, M. C.; Mascart, F.; Meiring, H. D.; Locht, C., Toward Understanding the Essence of Post-Translational Modifications for the *Mycobacterium tuberculosis* Immunoproteome. *Front Immunol* **2014**, 5, 361.
  93. Prisic, S.; Dankwa, S.; Schwartz, D.; Chou, M. F.; Locasale, J. W.; Kang, C. M.; Bemis, G.; Church, G. M.; Steen, H.; Husson, R. N., Extensive phosphorylation with overlapping specificity by *Mycobacterium tuberculosis* serine/threonine protein kinases. *Proc Natl Acad Sci U S A* **2010**, 107, (16), 7521-6.
  94. Smith, G. T.; Sweredoski, M. J.; Hess, S., O-linked glycosylation sites profiling in *Mycobacterium tuberculosis* culture filtrate proteins. *J Proteomics* **2014**, 97, 296-306.
  95. Okkels, L. M.; Muller, E. C.; Schmid, M.; Rosenkrands, I.; Kaufmann, S. H.; Andersen, P.; Jungblut, P. R., CFP10 discriminates between nonacetylated and acetylated ESAT-6 of *Mycobacterium tuberculosis* by differential interaction. *Proteomics* **2004**, 4, (10), 2954-60.
  96. Sutcliffe, I. C.; Harrington, D. J., Lipoproteins of *Mycobacterium tuberculosis*: an abundant and functionally diverse class of cell envelope components. *FEMS Microbiol Rev* **2004**, 28, (5), 645-59.
  97. Pearce, M. J.; Mintseris, J.; Ferreyra, J.; Gygi, S. P.; Darwin, K. H., Ubiquitin-like protein involved in the

proteasome pathway of *Mycobacterium tuberculosis*. *Science* **2008**, 322, (5904), 1104-7.

98. Fortuin, S.; Tomazella, G. G.; Nagaraj, N.; Sampson, S. L.; Gey van Pittius, N. C.; Soares, N. C.; Wiker, H. G.; de Souza, G. A.; Warren, R. M., Phosphoproteomics analysis of a clinical *Mycobacterium tuberculosis* Beijing isolate: expanding the mycobacterial phosphoproteome catalog. *Front Microbiol* **2015**, 6, 6.
99. Rabodoarivelo, M. S.; Aerts, M.; Vandamme, P.; Palomino, J. C.; Rasolofo, V.; Martin, A., Optimizing of a protein extraction method for *Mycobacterium tuberculosis* proteome analysis using mass spectrometry. *J Microbiol Methods* **2016**, 131, 144-147.





Disclosure of selective advantages in the “modern”  
sublineage of the *Mycobacterium tuberculosis* Beijing  
genotype family by quantitative proteomics

Jeroen de Keijzer<sup>1</sup>, Petra E. de Haas<sup>2</sup>, Arnoud H. de Ru<sup>1</sup>,  
Peter A. van Veelen<sup>1#</sup>, Dick van Soolingen<sup>2,3#</sup>

<sup>1</sup> Department of Immunohematology and Blood Transfusion, Leiden University Medical Centre (LUMC), Leiden,  
2300 RC, The Netherlands

<sup>2</sup> Tuberculosis Reference Laboratory, National Institute for Public Health and the Environment (RIVM),  
Bilthoven, 3720 BA, The Netherlands

<sup>3</sup> Departments of Pulmonary Diseases and Medical Microbiology, Radboud University Medical Centre,  
Nijmegen, 6500 HB, The Netherlands

#PAvV and DvS share senior authorship



## Abstract

The *Mycobacterium tuberculosis* Beijing genotype, consisting of the more ancient (atypical) and modern (typical) emerging sublineage, is one of the most prevalent and genetically conserved genotype families and has often been associated with multidrug resistance. In this study, we employed a 2D-LC-FTICR MS approach, combined with dimethylation of tryptic peptides, to systematically compare protein abundance levels of ancient- and modern Beijing strains and identify differences that could be associated with successful spread of the modern sublineage. The data is available via ProteomeXchange using the identifier PXD000931. Despite the highly uniform protein abundance ratios in both sublineages, we identified four proteins as differentially regulated between both sublineages, which could explain the apparent increased adaptation of the modern Beijing strains. These proteins are; Rv0450c/MmpL4, Rv1269c, Rv3137 and Rv3283/sseA. Transcriptional and functional analysis of these proteins in a large cohort of 29 Beijing strains showed that the mRNA levels of Rv0450c/MmpL4 are significantly higher in modern Beijing strains, whereas we also provide evidence that Rv3283/sseA is less abundant in the modern Beijing sublineage. Our findings provide a possible explanation for the increased virulence and success of the modern Beijing sublineage. In addition, in the established dataset of 1817 proteins, we demonstrate the pre-existence of several, possibly unique, antibiotic efflux pumps in the proteome of the Beijing strains. This may reflect an increased ability of Beijing strains to escape exposure to anti-tuberculosis drugs.

## Introduction

*Mycobacterium tuberculosis*, the causative agent of tuberculosis (TB), is one of the most successful pathogens worldwide. Nowadays, still about 8-9 million new cases and 1.5 million deaths are recorded annually.<sup>(1)</sup>

DNA fingerprinting of the *Mycobacterium tuberculosis* complex has revolutionized studies on transmission of TB in the last two decades<sup>(2)</sup>, but also disclosed the phylogeny of this important grouping of bacteria.<sup>(3, 4)</sup> In essence there are six major *M. tuberculosis* lineages. The first one was described in 1995 and designated the 'Beijing' genotype family, which is highly prevalent in Asia, the Former Soviet Union states, and South Africa.<sup>(5-8)</sup> Recently, the Beijing genotype family was identified as the major genotype family in the 'East Asia clade' defined on single nucleotide polymorphism (SNP) typing.<sup>(4)</sup> In the years after its disclosure, the Beijing genotype family drew attention because it seemed genetically highly conserved on basis of the available genetic markers, which could be related to active and recent spread, presumably due to selective advantages over other *M. tuberculosis* genotypes.<sup>(5-8)</sup> Selective pressure on this group of bacteria could be induced by the introduction of mass BCG vaccination and treatment by anti-TB drugs.<sup>(9)</sup> Consequently, in many geographic areas, Beijing strains were found significantly correlated with (multi)drug resistance, treatment failure, relapses after curative treatment, and transmission of resistant TB.<sup>(6, 7, 10-12)</sup> In TB mouse models, Beijing strains revealed an upregulated virulence and a higher ability to escape BCG vaccination.<sup>(13-15)</sup> This is particularly alarming since there are indications that the Beijing genotype strains are emerging in multiple geographic areas, as they are associated with lower ages of patients and, hence, active transmission.<sup>(6, 16, 17)</sup> Increased odds of *M. tuberculosis* Beijing are also observed for patients with a polymorphism in their natural resistance associated macrophage protein 1 (*NRAMP1*), encoded by the *SLC11A1* gene.<sup>(18)</sup> This supports the theory of a co-evolution of *M. tuberculosis* Beijing with their human host.

Initially, mechanisms underlying a higher adaptability were assumed to be related to alterations in DNA repair, but polymorphisms in related genes were also observed in strains of other genotype families.<sup>(19)</sup> Although not yet explained in detail, a study published in 2012 revealed that a part of the Beijing strains revealed a much higher frequency of naturally occurring rifampicin resistant mutants than the traditionally measured 1 in 10<sup>8</sup>.<sup>(20)</sup> This important observation was recently confirmed by Ford *et al*, who pointed out that the correlation between the Beijing genotype and resistance could indeed be explained by a higher mutation frequency.<sup>(21)</sup> Not surprisingly, resistance against anti-TB drugs is especially a major problem in former Soviet Union States, China, and South Africa, where the Beijing genotype strains are highly prevalent.<sup>(22-26)</sup>

In 2002, the Beijing genotype family was divided into the modern (typical) and ancient (atypical) lineage.<sup>(27)</sup> Beijing strains without insertion of IS6110 in the NTF region were referred to as ancient Beijing strains and seem to resemble the ancestors of the Beijing family.<sup>(27)</sup> In most countries, modern Beijing strains are much more prevalent than ancient ones, suggesting an active spread, except for Japan, where the ancient type of Beijing strains is more wide spread.<sup>(28)</sup> The two Beijing lineages were also divided on basis of large genomic deletions, also referred to as Regions of Difference (RDs). RD105 is thought to be characteristic of all Beijing strains, whereas deletion of RD181 was found associated with modern Beijing strains.<sup>(29)</sup> Although the modern and ancient Beijing strains seem to be closely related on the genetic level<sup>(30)</sup>, differences in association with (multi) drug resistance and in the ability to cause and spread disease<sup>(31)</sup> have been described between both sublineages. Moreover, after several studies suggested enhanced ability of Beijing strains in general to circumvent BCG-vaccine induced immunity<sup>(13, 14)</sup>, one study reported that modern Beijing strains were isolated more frequently from BCG-vaccinated patients than non-vaccinated individuals.<sup>(9)</sup> The observation that the interaction of modern Beijing strains with the immune system is different than that of ancient strains was further confirmed by a recent study that described differences in pro-inflammatory cytokine induction for both strains.<sup>(32)</sup> If modern Beijing strains indeed have selective advantages over other *M. tuberculosis* strains and spread more prosperously, this should be reflected in the degree of genetic conservation. This assumption was confirmed by whole genome sequencing (WGS) of Beijing strains from a wide spread geographic area. Three modern Beijing strains from China, Vietnam, and South Africa were found genetically highly conserved in comparison to three ancient strains from the same regions.<sup>(30)</sup> This confirms the evolutionary advantage of the modern Beijing genotype over the closely related ancient Beijing and other *M. tuberculosis* strains. In fact, Schürch *et al.* traced only 31 non synonymous single nucleotide polymorphisms (nsSNPs) mutations characteristic of modern Beijing strains.<sup>(30)</sup> However, the presence of these 31 nsSNPs is not sufficient to explain the consequences in terms of evolutionary development and adaptation. Therefore, we performed an in-depth comparison of the protein abundances of both sublineages. Comparative proteomic analysis of different *M. tuberculosis* strains has been reported before.<sup>(33)</sup> So far, one study examined the proteomes of a single hyper- and hypo virulent *M. tuberculosis* Beijing strain by a label-free quantitative technique, and reported the differential regulation of virulence factors, such as Rv3875/ESAT-6 and other Esx-like proteins.<sup>(34)</sup> However, biological variation limits the value of a traditional individual duplex (one-versus-one) experimental approach. In addition, individual characteristics that are not always representative of the entire grouping cannot be distinguished from structural differences between the two genotypes. To obtain a more reliable insight, multiple measurements of individual samples of each grouping are required. Furthermore, to limit the influence of biological and inter-strain variation, we generated a sample pool comprising five modern and five ancient Beijing strains, which were selected to optimally represent the full spectrum of both *M. tuberculosis* Beijing

sublineages.

Sample pooling was previously successfully applied in proteomic experiments, and used in case there was insufficient individual sample material available.<sup>(35, 36)</sup> Sample pooling has also been applied to create an internal reference sample in a so called 'super-SILAC mix'<sup>(37, 38)</sup>, that can be combined with clinical samples. Use of the super-SILAC approach resulted in a narrower distribution of protein abundance ratios. The narrower protein ratio distribution increased the significance of the altered protein ratios.<sup>(35)</sup> Next to the pooled sample approach, we compared three ancient Beijing strains with three modern Beijing strains using traditional individual duplexes. We identified and quantified a cumulative number of 2392 proteins ( $\pm 60\%$  of the *M. tuberculosis* protein coding genome), of which 1817 were present in all of the analyses performed. We demonstrate the presence of multiple antibiotic extruding efflux pumps in the proteome of *M. tuberculosis* Beijing, notably without exposure of the pathogen to a drug. Three of these efflux pumps were previously not quantified in the proteome of *M. tuberculosis* H37Rv by a proteome-wide selected reaction monitoring approach.<sup>(39)</sup>

Despite the highly uniform protein ratio distribution in both strains, we identified four proteins to be more abundant in the modern Beijing strains that can explain their emergence and perhaps higher virulence. We complemented our proteomic data with transcriptional analysis of selected genes in a larger cohort of 14 ancient Beijing and 15 modern Beijing strains. To verify the differential regulation of a particular virulence factor the experiments were supplemented with functional analysis.

## Materials and methods

### Molecular typing methods

*M. tuberculosis* Beijing strains were selected from a previously published selection of 259 Beijing strains.<sup>(40)</sup> Fourteen ancient- and 14 modern Beijing strains were included in the study to optimally represent the *M. tuberculosis* family. In addition, the successful modern Beijing strain B0/W148 was added to the selection.<sup>(41-43)</sup> Using the *M. tuberculosis* Beijing characteristic marker RD105, we ensured that all the strains investigated indeed belong to the *M. tuberculosis* Beijing family. Additionally, mutT2/ogt were used to differentiate ancient from modern Beijing strains.<sup>(29, 31)</sup> To exclude the possibility of contamination, or the selection of clonal isolates for proteomic analysis, we performed standard MIRU (mycobacterial interspersed repeat units) 24-loci VNTR (variable number of tandem repeats) with a few minor modifications.<sup>(44)</sup> The in-house VNTR method based on the protocol of the MIRU-VNTR typing manual was used with minor modifications: the amount of DNA polymerase used was 0.75 units per multiplex PCR, and the initial concentration of labeled primers was increased to 8  $\mu$ M for locus 2165 and locus 2163b. The amplicon sizes were determined by using the automated ABI 3730 DNA analyzer (Applied Biosystems, CA).

### Mycobacterial culture conditions

All *M. tuberculosis* isolates were derived from the reference database of clinical isolates at the National Institute for Public Health and the Environment (RIVM) in Bilthoven, the Netherlands. Strains were re-cultured from frozen stocks in 5 ml Tween-Albumin liquid culture broth (Tritium Microbiologie, the Netherlands) at 36°C without shaking until an O.D. at 600 nm of 0.4 AU was reached. Of the mycobacterial pre-culture, 1 ml was transferred to a 250 ml Erlenmeyer flask containing 100 ml Tween-Albumin broth and incubated under shaking conditions at 36°C with constant aeration. Once the cultures reached an O.D. at 600 nm of 0.6 AU, representing the mid-log phase, the cells for proteome analysis were washed three times with ice cold PBS, dissolved in 5 ml Lysis-buffer (4% SDS, 100 mM Tris-HCl, pH 7.6) and heat-killed at 95°C for 10 min. Lysates were stored at -20°C until further usage. *M. tuberculosis* Beijing strains used for qPCR analysis were harvested at early log phase and stored in L6-buffer at -20°C until use.<sup>(45)</sup>

### Minimal inhibitory concentration determination

Susceptibility to the first line anti-mycobacterial drugs; rifampicin, isoniazid, ethambutol and pyrazinamid, was determined according to Clinical and Laboratory Standards Institute guidelines<sup>(46)</sup>, using the BACTEC MGIT-960 system (Becton, Dickinson and Co., Franklin Lakes, NJ).

### Protein sample preparation and dimethylation isotope labeling

Heat inactivated cells for proteomic experiments were mechanically lysed by bead-beating in a mini bead-beater 16 (BioSpec) for 5 min using glass beads. Thereafter, the cells were cooled down on ice for 5 min and the procedure was repeated twice. The cell lysates were cleaned from cell debris by centrifugation for 1 min at 14,000g and the supernatant was transferred to another tube. Proteins were digested using the filter aided sample preparation (FASP) method.<sup>(47)</sup> In brief, 100 µg of DTT reduced proteins was loaded on a 30kDa filter. SDS was removed in three washes with 8M urea. The proteins were reduced and carbamidomethylated, and the excess reagent was removed by three additional washes with 8M urea. Proteins were then overnight digested using endoproteinase Lys-C (endoLysC) followed by a four hrs digestion using trypsin at RT. Tryptic peptides were desalted on C18 SepPak columns and derivatized on column by dimethyl labeling.<sup>(48)</sup> Peptides derived from ancient Beijing strains were labeled with a light label (+28Da), whereas modern Beijing strains were labeled with heavy labels (+36Da). In addition, two sample pools consisting of five light labeled ancient Beijing strains and five heavy labeled modern Beijing strains were prepared by mixing the respective tryptic digests in a 1:1:1:1:1 manner before fractionation.

### Strong Cation Exchange Chromatography

In total 100 µg of labeled peptides were fractionated by strong cation exchange (SCX) on a Agilent 1100 system equipped with an in-house packed SCX-column (320 µm ID, 15 cm, polysulfoethyl A 3 µm, Poly LC), run at 4 µl/min. The gradient started with a 10 min run at 100% solvent A (70/30/0.1 (water/acetonitrile/formic acid)), after which a linear gradient reached 100% solvent B (250 mM KCl, 35% acetonitrile, 0.1% formic acid) in 15 min, followed by 100 % solvent C (500 mM KCl, 35% acetonitrile 0.1% formic acid) in the following 15 min. The gradient was held at 100 % solvent C for 5 min to clean the column, then switched back to 100 % solvent A. Thereafter, 15 fractions were collected in 1 min intervals, lyophilized and reconstituted in 30 µl 95/3/0.1 (water/acetonitrile/formic acid).

### NanoLC-MS/MS

Dissolved fractions were analyzed by on-line nano-HPLC MS with a system consisting of a Agilent 1100 gradient HPLC system (Agilent, Waldbronn, Germany) as described previously<sup>(49)</sup>, and a LTQ-FT Ultra mass spectrometer (Thermo, Bremen, Germany). Of each fraction 5 µl was injected onto a home-made pre-column (100 µm×15 mm; Reprosil-Pur C18-AQ 3 µm, Dr Maisch, Ammerbuch, Germany) and eluted via a home-made analytical nano-HPLC column (15 cm×50 µm; Reprosil-Pur C18-AQ 3 µm). The gradient was run from 0% to 30% solvent B (10/90/0.1 water/acetonitrile/formic acid) in 10-155 min. A tip of approximately 5 µm was drawn at the tip of the nano-HPLC column to act as electrospray needle. Full scan mass spectra were acquired in the FT-ICR with a resolution of 25,000 at a target value of  $5 \times 10^6$ . The five most intense ions

were selected and fragmented in the linear ion trap using collision-induced dissociation at a target value of 10,000.

### Search Databases

MSMSpddb was used to generate concatenated protein databases in FASTA format.<sup>(50)</sup> Genomic sequences and annotational information of *M. tuberculosis* H37Rv (3996 entries)<sup>(51)</sup> were used, together with the genetic information of *M. tuberculosis* Beijing strain NITR203 (4071 entries).<sup>(52)</sup> This concatenated database contains all previously described mutations that are specific for modern Beijing strains, as well as the ancient Beijing “wild-type” sequence (4327 entries).<sup>(30)</sup> Protein products larger than 50 amino acids were considered for stop-to-stop translation. Peptides describing varying sequences or different translational start sites between both strains were only used when the sequence was longer than seven- and shorter than 35 amino acids. Proteins that were clustered received the accession number and description of control strain *M. tuberculosis* H37Rv. Translated entries, which did not cluster with any of the annotated genes, were discarded. To use the database with MaxQuant software, the artificial J and O amino acid residues were replaced by a lysine residue. Alongside the concatenated data base we searched FASTA databases based on *M. tuberculosis* H37Rv<sup>(51)</sup> and *M. tuberculosis* Beijing NITR203.<sup>(52)</sup>

### Data Interpretation

Peptide and protein identification and quantitation was accomplished using MaxQuant 1.4.0.3.<sup>(53)</sup> The false discovery rate (FDR) was set to 0.01 for both proteins and peptides. Minimal peptide length was set to 6 amino acids. The first search was performed using 20 ppm, while the main search was conducted with 10 ppm. Search of MS/MS spectra was performed with 20 ppm using the Andromeda search engine.<sup>(54)</sup> In total 262 common contaminants were included in the searches by Andromeda. Enzyme specificity was set as C-terminal to arginine and lysine without proline restriction. A maximum of two missed cleavages was allowed. Variable modifications included N-terminal protein acetylation, methionine oxidation and corresponding dimethyl labels.

Carbamidomethylation of cysteine was selected as a fixed modification. Proteins considered for quantification required a minimal peptide count of two, including unique and razor peptides. Proteins identified by site, matched against the reverse database or identified as a contamination, were excluded for further analysis. Statistical analysis of the outcomes was performed by Perseus using the significance B test with a Benjamini-Hochberg FDR <5%. Data files have been deposited in the publicly available ProteomeXchange Consortium (proteomecentral.proteomexchange.org) and can be accessed through the code: PXD000931. General properties of the proteome were examined using “Batch MW and pI Finder” tool and the gravity index was calculated using the “gravity-calculator.de” web tool, whereas PSORTb v3.0<sup>(55)</sup> was used to determine protein

localization and the TMHMM Server V.2.0<sup>(56)</sup> for the determination of transmembrane helices.

### Transcriptional analysis of selected genes by quantitative Real Time PCR

RNA was isolated and purified from bacteria using the PureLink RNA Mini Kit (life technologies) according to the manufacturer's instructions. In addition, on column digestion was performed with RNase free DNase (Qiagen). The quality and quantity of RNA was examined by spectrophotometric measurements (260/280 nm). Thereafter, 0.5 µg of purified RNA was reverse transcribed using the High Capacity cDNA Reverse Transcription Kit (life technologies). Genomic DNA control samples were incubated without reverse transcriptase. Primers were designed using Primer3Plus<sup>(57)</sup> or derived from previous studies.<sup>(34)</sup> The following forward and reverse primer sequences were used: 16s forward 5'-TCCGGGCCTTGACACA-3'; reverse 5'-CCACTGGCTTCGGGTGTTA-3', Rv0450c/MmpL4 forward 5'-GTGTTCAAGGAAGGCGATTC-3'; reverse 5'-CAAGGGGTGGTTACCCTCT-3', Rv1269c forward 5'-CAAGGTGCTCACCAGTTTCA-3'; reverse 5'-CTGGTATGCCCTATCGTTGG-3', Rv3137 forward 5'-GGTTGACCGATACCGTGTG-3', reverse 5'-GCCACCAGGCAGTAAGACAG-3', Rv3283/sseA forward 5'-ATACCTGGTTCGTGCTCACA-3'; reverse 5'-AGCCGTCGTAGTTCGTACA-3'. LightCycler 480 SYBR Green I Master (Roche Applied Science) was used as qPCR master mix. Samples were analyzed in a LightCycler 480 (Roche Applied Science). The following cycling conditions were used: The thermal cycler program was initiated by 10 min at 95°C followed 35-40 cycles for 10 s at 95°C, 10 s at 60°C and 10 s at 72°C. High Resolution Melt analysis was performed after each program. mRNA quantities were determined in triplicate and normalized on 16s rRNA levels using the  $2^{-\Delta Ct}$  method. Mann-Whitney U-test was used to determine p-values.

### Prediction of protein stability upon mutation

Three independent algorithms were used to predict the effect of a previously described mutation<sup>(30)</sup> on the stability of Rv3283/sseA: PolyPhen-2<sup>(58)</sup>, I-Mutant3.0 (sequence mode)<sup>(59)</sup> and (Protein ANALysis THrough Evolutionary Relationships) PANTHER.<sup>(60)</sup> The respective protein sequence was derived from tdbb.org<sup>(61)</sup>, using the conversion of a glutamic acid residue to a lysine residue in position 276.

### Quantitative rhodanese activity assay

To perform quantitative rhodanese activity analysis, all chemicals were derived from Sigma-Aldrich Chemie B.V. (Zwijndrecht, Netherlands). Rhodanese activity was examined as described previously with minor modifications.<sup>(62)</sup> In brief, cells were cultured to early-log phase and disrupted by bead-beating. Unbroken cells and cell debris was separated by centrifugation and discarded. The collected supernatant was filtered twice through a 0.2 µm filter and stored until use at -70°C in PBS-containing 20% glycerol. The reaction mixture contained 50 µl of 125 mM sodium thiosulfate, 25 µl of 250 mM potassium cyanide, and 30 µl of 200 mM potassium



phosphate buffer, pH 8.6. 20  $\mu$ l of cell lysate was added to this reaction mixture. The reaction was carried out for 15 min at room temperature and was stopped by the addition of 25  $\mu$ l of 38% formaldehyde. In the control set, formaldehyde was added prior to the addition of the cell lysate. The concentration of thiocyanate was determined by the addition of 125  $\mu$ l 410 mM ferric nitrate in 14% (w/v) nitric acid. Rhodanese activity is reported as specific activity (unit/mg protein) of which the biological replicates were averaged for each of the isolates examined. One unit of enzyme activity was defined as micromoles of thiocyanate formed per min at pH 8.6.

## Results

### Selection of *M. tuberculosis* Beijing genotype isolates

To quantify differences in the proteomes of modern and ancient *M. tuberculosis* Beijing sublineages we set out to generate two sample pools containing five strains of each genotype. Therefore, 14 ancient Beijing and 15 modern Beijing strains were selected from a published collection of 259 Beijing strains.<sup>(40)</sup> The selected strains were representative of 13 countries on four continents i.e. the strains were isolated in that country or isolated from a patient born in the respective country. RD105 was determined to ensure all strains represent the *M. tuberculosis* Beijing genotype. *MutT2/ogt* were determined to differentiate between modern and ancient *M. tuberculosis* Beijing strains.<sup>(31)</sup> MIRU-24 VNTR was determined to ensure a heterogeneous selection *M. tuberculosis* Beijing isolates; Figure S1.

### Qualitative proteome analysis of *M. tuberculosis* Beijing strains

We set out to identify proteins that are differentially regulated in either modern Beijing or ancient Beijing strains. To this end, we utilized a pooled approach, in which we mixed the digests of five ancient Beijing strains and five modern Beijing strains. We also analyzed three individual duplexes, in which single ancient Beijing strains were compared to single modern Beijing strains. In each individual duplex, different strains were selected at random from our set of Beijing strains described above.

Three different search databases were used to analyze the peptides yielded; 1. a FASTA database based on the genome of *M. tuberculosis* H37Rv<sup>(51)</sup>, a well annotated *M. tuberculosis* laboratory strain. 2. a database based on the genome of *M. tuberculosis* Beijing strain NITR203<sup>(52)</sup>, which contains all modern Beijing specific nsSNPs, and 3. a concatenated database comprising both H37Rv and NITR203; Figure S2B. The combined analyses yielded a total of 30,748 unique peptides with a FDR <1% for all samples measured; see Table S1. None of the searched databases clearly outperformed the others in terms of peptide identifications. Therefore, we continued with the concatenated database, as it contains all major sequence variation caused by SNPs.

The cumulative number of unique protein identifications and quantifications was 2392; of which 1817 proteins were identified and quantified in all proteome experiments, constituting >75% of all the quantified proteins; see Figure S2A and Table S2. These results represent the most comprehensive proteome description of a clinical *M. tuberculosis* genotype to date. When we compared the identified proteins of the individual duplexes with the pooled duplex, an overlap of >80% was achieved using our shotgun proteomics approach.

To confirm the quality of our proteomic dataset, we investigated if specific proteins were

underrepresented on the basis of several physicochemical properties; see Figure S3A-C. As can be concluded from the distribution of proteins based on mass, pI, or hydrophobicity (i.e., gravy index) which follows the theoretical database distribution. All categories are represented to the same extent. In addition, there is no bias on the basis of protein localization<sup>(55)</sup> and transmembrane proteins<sup>(56)</sup>, even for proteins predicted to contain 13 predicted transmembrane helices; see Figure S3D-E. In summary, from the above we conclude there is no skewing of the proteome we obtained.

### Functional classification of proteins and efflux pumps

We categorized the proteins that were quantified in all four analyses, according to their functionality as given by Tuberculist.<sup>(63)</sup> Proteins that were considered to be specific for *M. tuberculosis* Beijing NITR203<sup>(52)</sup> by MSMSpddb<sup>(50)</sup> were categorized as “other”; see Figure 1A. The proteins of different functional categories are represented to the same extent, except for the PE/PPE family, the insertion sequences and phages and the proteins that we categorized as “other”.<sup>(63)</sup>

Beijing strains are linked to (multi)drug resistance in many geographical areas.<sup>(16, 22-26)</sup> Initially, the DNA repair mechanism was thought to be involved in the development of antibiotic resistance.<sup>(19)</sup> Although not based on studying the DNA repair in detail, two recent studies confirmed this hypothesis by showing that several Beijing strains have a much higher frequency of rifampicin resistant mutants.<sup>(20, 21)</sup> However, proteins such as efflux pumps can also play a crucial part in reduced susceptibility to antibiotics by lowering the intra bacterial concentration of drugs and hence creating a higher tolerance to particular compounds. To determine whether such pre-existing factors are present in the proteome of *M. tuberculosis* Beijing, we categorized putative efflux pump genes and transporters that play a role in drug resistance in *M. tuberculosis*, as previously listed.<sup>(64)</sup> As presented in Figure 1B, indeed several antibiotic transporting efflux pumps were disclosed in the proteome of *in vitro* cultured *M. tuberculosis* Beijing strains.

The pre-existence of these efflux pumps can potentially be caused by the analysis of multidrug resistant strains. We therefore determined the MICs for the first line antibiotics (rifampicin, isoniazid, ethambutol and pyrazinamide) of the analyzed strains. Both the modern and ancient Beijing strains used in this study were susceptible to all first line drugs (data not shown).

The pre-existing presence of efflux pumps is not a unique characteristic of *M. tuberculosis* Beijing strains. Efflux pumps were also identified in the proteome of *M. tuberculosis* H37Rv by a proteome-wide selected reaction monitoring approach.<sup>(39)</sup> We compared this comprehensive dataset of 2195 *M. tuberculosis* H37Rv proteins with the proteins we identified. Three of these proteins (Rv0341/iniB, Rv2688c&Rv3728) were exclusively identified by our proteomic analysis of *M. tuberculosis* Beijing.

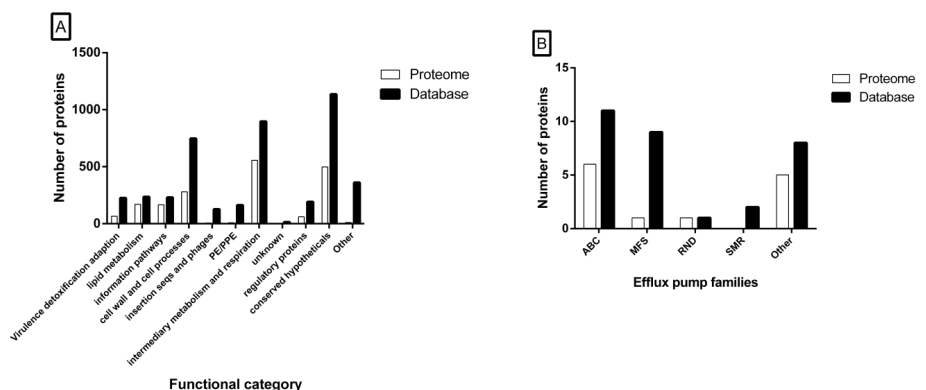


**FIGURE 1:** Functional distribution of the proteome of *M. tuberculosis* Beijing

Proteins present in our MS-database (filled black bars) and our dataset (white bars) were categorized by:

- A) Functional class categories as given by Tuberculist
- B) Bacterial efflux transporter families

ABC: ATP Binding Cassette, MFS: Major Facilitator Superfamily, RND: Resistance Nodulation cell Division, SMR: Small Multidrug Resistance

### Quantitative proteomic profiling of modern and ancient *M. tuberculosis* Beijing strains

WGS revealed that the modern- and ancient Beijing strains are highly conserved on the genetic level.<sup>(30)</sup> However, multiple studies have shown that modern Beijing strains are more “successful” in terms of transmission and development of antibiotic resistance.<sup>(13, 14, 31, 65, 66)</sup> Moreover, in most geographic areas with a higher density of Beijing strains the modern Beijing strain are predominant, except for Japan.<sup>(28)</sup> To determine whether bacterial factors on the protein level may be associated with the emergence of modern Beijing strains, we quantitatively compared the proteomes of five modern Beijing and five ancient Beijing strains. Therefore, we performed a pooled approach and three individual duplex analyses. The protein ratio distribution was only slightly narrower when the samples were pooled; see Figure S4.

Forty-seven proteins were identified as differentially abundant using our pooled approach. The three individual duplex experiments identified respectively 74, 111 and 55 proteins of which the abundance was significantly different; see Table S3. We categorized all differentially abundant proteins according to their functionality, as given by Tuberculist.<sup>(63)</sup> To identify proteins that are specifically more abundant in either the modern, or the ancient Beijing strains, we selected proteins that were over represented in the three individual approaches and the pooled approach; see Table 1. Rv0450c/MmpL4 and Rv3137 were significantly more abundant in the modern Beijing strains, whereas Rv1269c, and Rv3283/sseA were identified to be more

abundant in the ancient Beijing strains examined.

**TABLE 1:** Differentially abundant proteins between modern Beijing and ancient Beijing strains

Rv identifier	Gene name	Description	PEP	Fold	Unique peptides
Rv0450c	MmpL4	Transmembrane transport protein	0	3,3-3,8	34
Rv1269c	-	Conserved probable secreted protein	3.96E-34	<0,1-0,3	5
Rv3137	-	Probable monophosphatase	8.69E-143	3,1-4,3	12
Rv3283	sseA	Probable thiosulfate sulfurtransferase	0	<0,1-0,2	22

### Transcriptional analysis of selected genes in a large cohort of *M. tuberculosis* Beijing strains

To evaluate whether the mRNA levels of Rv0450c/MmpL4, Rv1269c, Rv3137 and Rv3283/sseA are differentially regulated throughout the entire modern Beijing or ancient Beijing genotypes, we complemented our MS-based proteomic observations with qPCR analysis in a larger cohort of *M. tuberculosis* Beijing strains by qPCR. Therefore, 14 ancient Beijing strains and 15 modern Beijing strains, including the strains used for the proteome analyses, as presented in Figure S1, were analyzed.

For Rv0450c/MmpL4 both the mRNA and the protein product were more abundant in the modern Beijing strains examined; see Figure 2. In contrast, Rv1269c and Rv3137 did not show significant differences in the larger cohort of *M. tuberculosis* Beijing strains examined. Nevertheless, Rv3137 showed a trend in line with the obtained protein ratios, but the effect observed on the protein level was larger than the fold change observed on the mRNA level. An opposite trend between mRNA levels and protein levels was observed for Rv3283/sseA. Our proteome analysis showed a 5-10 fold higher abundance of Rv3283/sseA in ancient Beijing strains. Contrary to these observations, higher transcriptional levels were observed for Rv3283/sseA in modern Beijing strains compared to ancient Beijing strains.

### Functional prediction of amino-acid residue substitution in Rv3283/sseA

To investigate if the observed lower protein abundance of the protein Rv3283/sseA in modern Beijing strains could be caused by destabilization of the protein structure by the altered amino acid at position 276, due to the nsSNP, reported to be specific for modern Beijing lineage strains<sup>(30)</sup>, we applied the protein stability prediction programs, PolyPhen-2<sup>(58)</sup> and I-Mutant3.0<sup>(59)</sup> and the protein functionality prediction program PANTHER.<sup>(60)</sup>

The 3D structure of 3HZU, a homologue of Rv3283/sseA was used by PolyPhen-2 among other information. Based on the calculation, PolyPhen-2 designates the mutation as being “benign”, “possibly damaging”, and “probably damaging”. The conversion of the glutamic acid residue towards a lysine residue in position 276 of Rv3283/sseA is considered to be “probably

damaging” by PolyPhen-2.

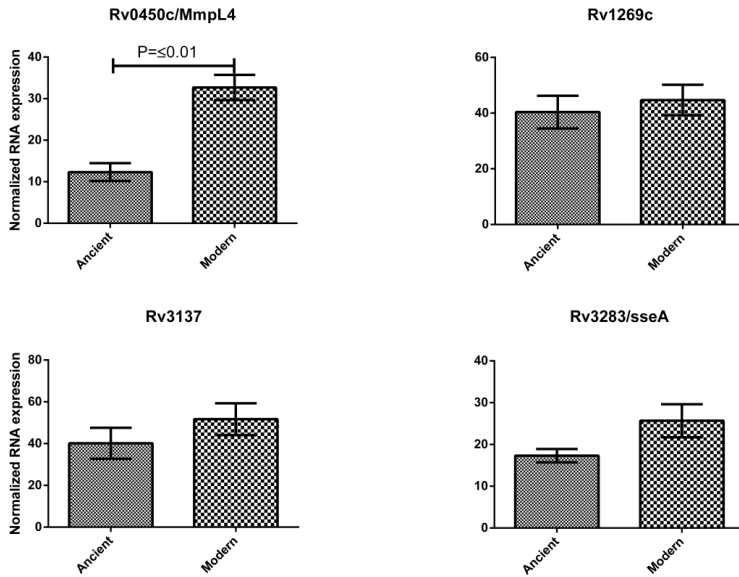


**FIGURE 2:** Observed mRNA levels for selected genes

mRNA levels of the selected protein candidates were analyzed in 14 ancient Beijing strains and 15 modern Beijing strains using qPCR. Each sample was analyzed in triplicate. Data are expressed as mean  $\pm$  standard error of the mean.

As a second independent control, we also determined the impact of the mutation using the sequence option of I-Mutant3.0<sup>(59)</sup>, which evaluates changes in stability of proteins based upon a single site mutation. The amino acid substitution in the active domain of Rv3283/sseA was predicted to result in a free energy change of 1.02 Kcal/mol. This is calculated from the unfolding Gibbs free energy change of the mutated protein minus the unfolding free energy value of the native protein (Kcal/mol). A change of 1.02 Kcal/mol in predicted free energy is considerable, and therefore expected to largely decrease the stability of Rv3283/sseA.

Finally, we predicted the functionality of the mutant and wild-type version of Rv3283/sseA using PANTHER.<sup>(60)</sup> This software considers site-specific variation between evolutionary related proteins to calculate substitution position-specific evolutionary conservation(subPSEC) score. When we calculated the functional consequence of a mutation in Rv3283/sseA the subPSEC score was -4.74 and the corresponding Pdeleterious (probability of functional impairment) was 0.85. All together, three independent prediction algorithms predict that the mutation in

Rv3283/sseA will have a large impact on the proteins' function and stability.

To support the observation that Rv3283/sseA is less abundant in modern Beijing strains than in ancient Beijing strains, we determined its activity. Rv3283/sseA is one of the at least four rhodanese domain containing proteins in our proteomic dataset of *M. tuberculosis* Beijing. Two of the proteins with potential rhodanese activity, Rv0815c/cysA2 & Rv3117/cysA3, could not be distinguished from one another, due to their high sequence similarity, but could be distinguished from Rv3283/sseA in the proteome analysis. Rv0815c/cysA2, Rv3117/cysA3 and Rv2291/sseB were not identified to be differentially abundant in all of the ancient or modern Beijing strains examined. Rhodanese proteins can detoxify cyanide by converting thiosulfate to thiocyanate and sulfite (EC 2.8.1.1). This reaction can be monitored in a quantitative manner by the formation of a blood red iron(III) thiocyanate complex.<sup>(62)</sup>

Rhodanese activity of cell lysates, containing all proteins with potential rhodanese activity, was determined in triplicate of the strains used for the proteomic analysis; see Figure 3. The average rhodanese activity observed in the cell lysate of ancient Beijing strains was approximately 23% higher than the rhodanese activity observed in the modern Beijing strains.

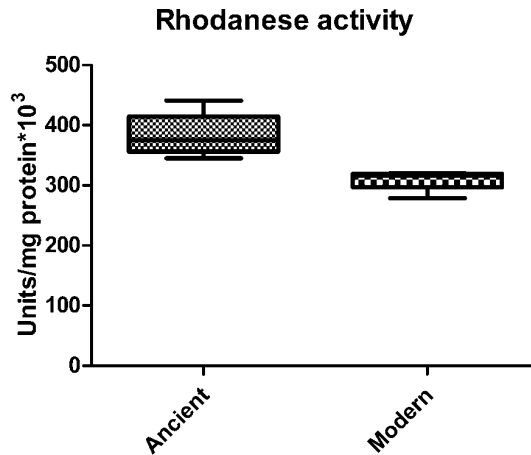


**FIGURE 3:** Rhodanese activity in *M. tuberculosis* Beijing sublineages

Rhodanese activity was determined in whole cell lysates of five ancient Beijing and five modern Beijing strains. Biological triplicates were taken and samples were analyzed in triplicate. The median is shown by the horizontal black line, with vertical whiskers representing the range.

## Discussion

The Beijing lineage of *M. tuberculosis* is one of the most successful *M. tuberculosis* genotypes worldwide, as indicated by its degree of genetic conservation and emergence.<sup>(67, 68)</sup> Previous studies showed an increase of TB incidence caused by *M. tuberculosis* Beijing, combined with higher odds on drug resistance for these strains.<sup>(6)</sup> Characterization of the Beijing strains revealed the presence of two sublineages, the modern and ancient Beijing strains.<sup>(27)</sup> Although the two sublineages are highly conserved on the genetic level, epidemiological studies suggested a possible evolutionary advantage of the modern Beijing strains, as this lineage is most prevalent in many geographic areas, except for Japan. In addition, whole genome analysis demonstrated the presence of only 31 nsSNPs that are characteristic of modern Beijing lineage strains from China, Japan and South Africa and this suggests a relative short time of divergence and successful spread.<sup>(30)</sup> To understand the evolutionary success of these pathogens, it is essential to identify factors that contribute to their high transmissibility and propagation in the human population, possibly associated with enhanced antibiotic resistance and ability to circumvent BCG induced immunity.<sup>(10, 13, 14, 31, 65, 66)</sup> We employed a pooled proteomics approach alongside three traditional individual duplex analyses to identify proteins that contribute to the successful phenotype of modern Beijing strains.

### Selection of a heterogeneous set of *M. tuberculosis* Beijing genotype strains

To cover the full spectrum of the genotype family, we selected 14 ancient and 14 modern Beijing strains from a previous selection of 259 *M. tuberculosis* strains.<sup>(40)</sup> Furthermore, we included the successful modern Beijing strain B0/W148, that comprises one-fourth of the *M. tuberculosis* Beijing isolates in different parts of Russia.<sup>(41-43)</sup> The Beijing strains in our selection originated from 13 countries distributed over four continents. We determined RD105 to assure that all strains in our selection truly belonged to the *M. tuberculosis* Beijing genotype.<sup>(29)</sup> A deletion of RD181 is considered to be characteristic of the modern sublineage.<sup>(29)</sup> However, deletions of RD181 were also identified in “late” ancient Beijing strains.<sup>(69, 70)</sup> Therefore, stringent differentiation between modern and ancient Beijing strains was accomplished using the *M. tuberculosis* modern Beijing genetic markers of putative DNA repair genes *mutT2* and *ogt*.<sup>(31)</sup> To exclude the possibility of mixed strains, contamination or the selection of clonal isolates we performed MIRU-24 VNTR-typing; see Figure S1. Five modern and five ancient Beijing strains were randomly selected from this heterogeneous set of *M. tuberculosis* Beijing strains.

### Description of the *M. tuberculosis* proteome

The combined analysis of pooled and individual duplex approaches yielded a total of 2392 unique proteins, the highest reported number of quantified proteins in any clinical strain of *M. tuberculosis* to date. Comparison of the individual duplexes with the pooled duplex approach



showed an overlap of 80-95% in identified proteins; see Figure S2A. In total 1817 proteins were quantified in all four analyses using a concatenated database. A high overlap, achieved by a shotgun proteomics approach is typically achieved when one reaches high proteome coverage. Furthermore, this high overlap of protein identifications and quantifications in all four analyses suggests a low inter-strain and low biological variation in the strains examined.

In mycobacterial proteomics, the solid, thick cell wall of mycobacteria presents a major obstacle to full proteome recovery. In particular reproducible extraction of cell wall and membrane bound proteins can be difficult. Therefore, we examined the general physicochemical properties of the obtained proteome to assure a representative coverage of the proteome, and to prevent a bias towards easy-to-extract proteins. The concatenated search database was utilized to represent the theoretically maximal observable proteome; see Figure S3. In the general properties that we assessed (Protein MW/pI/hydrophobicity), the observed proteome followed a distribution highly similar to that of the theoretically observable proteome, from which we conclude that our workflow is not biased regarding proteins with certain physicochemical properties. This was further confirmed by TMHMM<sup>(56)</sup> and protein localization analysis; see Figure S3 D-E.<sup>(55)</sup>

Approximately 42% of the proteins present in our database were reproducibly quantified in the four analyses. Two third of the proteins that were predicted to be localized in the thick cell wall were included in this dataset. In addition, we were able to reproducibly quantify proteins with  $\geq 13$  transmembrane helices. The high coverage of even the highly hydrophobic cell wall bound proteins suggests that our dataset provides a reliable representation of the *M. tuberculosis* Beijing proteome without discrimination of the more hydrophobic proteins.

### Categorization of the identified proteins

Functional categorization, as given by Tuberculist(63), showed a homogeneous distribution of the 1817 proteins present in our dataset for most of the listed categories, except for the PE/PPE family and the insertion sequences and phages; see Figure 1A. The categories containing the PE/PPE-family and insertion sequences and phages are notoriously difficult to identify. A recent study using ‘proteome-wide selected reaction monitoring’ also suffered from an under representation of the PE/PPE-family.<sup>(39)</sup> The PE/PPE family is named after their PE proline-glutamic acid and PPE proline-proline-glutamic acid N-terminal motif. Members of this family are characterized by a high number of glycine and alanine residues in combination with repetitive sequences. As a result, there are relatively few tryptic cleavage sites.<sup>(39)</sup> This lack of tryptic digestion sites makes our workflow with endoLys-c and trypsin digestion less suitable for the detection of members from this protein family. A reported method for the optimal identification of PE/PPE proteins includes the extraction of proteins from the mycobacterial cell wall followed by a double tryptic digestion and a triple chymotrypsin digestion.<sup>(71)</sup>

### Identification of pre-existing efflux pumps in the Beijing genotype

Throughout many geographic areas, Beijing strains were reported to significantly correlate with (multi) drug resistance, treatment, relapses after curative treatment and transmission of resistant TB.<sup>(6, 7, 10-12)</sup> Initially, altered DNA repair mechanisms in the *M. tuberculosis* Beijing genotype family were assumed to be responsible for the strong correlation with antibiotic resistance, due to mutations in three putative mutator genes in modern Beijing strains.<sup>(19)</sup> More support for this hypothesis was gained after a recent study showed that Beijing strains in Vietnam have an increased frequency of rifampicin resistant mutants compared to strains of the East African Asian (EAI) genotype family.<sup>(20)</sup> Unfortunately, the effects of variations in the DNA repair mechanism of *M. tuberculosis* Beijing has not been studied in full detail. Our systematic study did not reveal any quantitative difference for the genes involved in DNA repair, i.e. *mutT2*, *mutT4* and *ogt*. This suggests that mutations or post-translational mutations, but not protein abundance, are important for the aberrant DNA repair mechanism in *M. tuberculosis* Beijing.

The role of efflux pumps, which are able to transport antibiotics over the cell wall, has only been slightly touched upon in *M. tuberculosis* Beijing strains.<sup>(72, 73)</sup> We examined whether efflux pumps are present in the proteome of *M. tuberculosis* Beijing strains in the absence of selective pressure of antibiotics. We therefore used a previously listed selection of *M. tuberculosis* efflux pumps to categorize the proteins included in our dataset.<sup>(64)</sup> As presented in Figure 1B, several types of efflux pumps are present in the proteome of *in vitro* cultured *M. tuberculosis* Beijing. To ensure that this observation is not caused by the presence of (multi)drug resistant strains potentially present in our selection, we determined the MICs of first line antibiotics for the strains analyzed. None of the *M. tuberculosis* strains examined were identified to be resistant for any of the tested drugs. This observation shows that the presence of the efflux pumps alone, present in the proteome of *M. tuberculosis* Beijing, is not sufficient to cause antibiotic resistance. However, expression of these antibiotic extruding proteins can potentially cause a higher tolerance to drugs or makes it more difficult to eliminate all pathogens by antibiotic therapy. Moreover, a reduced susceptibility to drugs such as rifampicin, as observed previously, may be responsible for more durable persistence and hence the selection of drug resistant bacteria.<sup>(20)</sup> As recently reported, a much higher dosage of rifampicin was required to achieve a 100% killing of *M. tuberculosis* Beijing strains.<sup>(20)</sup> Taken together, this suggests a potential role for efflux pumps in the development of (multi)drug resistance in *M. tuberculosis* Beijing strains. The pre-existing presence of efflux pumps is, however, not necessarily a unique characteristic for *M. tuberculosis* Beijing. Therefore, we compared the presence of efflux pumps in our dataset with those that were recently identified and quantified in the proteome of *M. tuberculosis* H37Rv.<sup>(39)</sup> The used comprehensive *M. tuberculosis* H37Rv dataset was generated using proteome-wide selected reaction monitoring and contains 2195 proteins. Three efflux pumps, Rv0341/iniB, Rv2688c and Rv3728, were exclusively identified in our dataset on Beijing strains. However,

a proteogenomic approach that studied the proteome of *M. tuberculosis* H37Rv identified the respective proteins, Rv0341/iniB, Rv2688c and Rv3728.<sup>(74)</sup> It should be noted that 123 LC-MS/MS analyses were performed, which resulted in the identification of Rv2688c by a single peptide. In contrast, we identified  $\geq 4$  unique peptides in each of the duplex analyses performed. This combined information is a strong indication that Rv2688c is more abundant in *M. tuberculosis* Beijing strains than in the proteome of *M. tuberculosis* H37Rv. Rv3728 was reported to be present in the proteome of *M. tuberculosis* H37Rv as well.<sup>(74)</sup> However, peptides corresponding to Rv3728 were only identified by the Sequest algorithm, whereas Mascot and MassWiz failed to identify any peptide belonging to Rv3728. Therefore, as these proteins may preexist exclusively in the *M. tuberculosis* Beijing proteome, or be more abundant in the proteome of *M. tuberculosis* Beijing, they might contribute to the success of the Beijing family as a whole in the development of antibiotic resistance.

### Identification of differentially abundant proteins within the Beijing genotype

With the pooled sample approach alongside three individual duplex approaches, we achieved reproducible high proteome coverage using shotgun proteomics. Furthermore, we demonstrated a highly uniform ratio distribution for a majority of the proteins in the *M. tuberculosis* Beijing strains analyzed. On average, the pooled approach and the individual comparisons yielded approximately the same number of differentially abundant proteins (pooled duplex 47, individual duplexes 74, 111 and 55, Table S3). Therefore, it is conceivable that not only the modern and ancient Beijing strains are highly similar on the genetic level<sup>(30)</sup>, but that also protein regulation is conserved throughout the *M. tuberculosis* Beijing family as a whole; Figure S4.

As expected, not all proteins identified as differentially abundant in the pooled approach were also identified as differentially abundant in the individual duplexes. A logical explanation is that very abundant proteins in single isolates cannot be averaged out. Furthermore, individual duplex approaches are prone to false positives due to inter-strain and biological variation. It is important to keep in mind that both the pooled approach and the individual approaches can still yield false positives and are best used in parallel to identify sublineage specific differences. From our dataset of 1817 proteins that were reproducibly quantified in each analysis, only four proteins showed to be differentially regulated in all strains examined; see Table 1. This further confirms that most traits are highly conserved in the *M. tuberculosis* Beijing family. Therefore, our data suggests that the success of the modern Beijing strains compared to the ancient Beijing strains is caused by only a limited number of virulence factors.

### Transcriptional analysis of differentially abundant proteins in a large cohort of *M. tuberculosis* Beijing strains

Of the 1817 proteins present in our dataset only four proteins were differentially abundant in

all four proteomic analyses (Rv0450c/MmpL4, Rv1269c, Rv3137, Rv3283/sseA). To determine whether the mRNA levels of the corresponding proteins are differentially regulated throughout the entire modern Beijing or ancient Beijing genotypes, we complemented our MS-based proteomic observations with quantitative mRNA analysis in a larger cohort of *M. tuberculosis* Beijing strains by qPCR. Although mRNA does not always correlate with protein abundance levels present within the cell, it provides insight into the regulation of these specific genes.<sup>(75-77)</sup> The strains listed in Figure S1 were selected to represent the full repertoire of *M. tuberculosis* Beijing strains. This selection consisted out of 14 ancient Beijing and 15 modern Beijing strains and included the strains used for proteomic analysis.

The probable secreted protein Rv1269c was identified by MS to be >3 fold more abundant in ancient Beijing strains. However, we analyzed the cell lysate of *M. tuberculosis* Beijing, not the secretome. Quantitative mRNA analysis revealed that Rv1269c is equally transcribed by both modern and ancient Beijing strains; see Figure 2. Therefore, we cannot rule out the possibility that Rv1269c is more efficiently secreted by modern Beijing strains as the proteomic data clearly pointed out that Rv1269c is less abundant in modern Beijing strains.

Subsequently, we analyzed the mRNA levels for Rv3137, a probable monophosphatase that is essential for the *in vitro* growth of *M. tuberculosis* H37Rv.<sup>(78, 79)</sup> A trend similar to the ratios obtained by our proteomic experiments was detected. However, the average difference was much smaller on the mRNA level than observed on the protein level. Further separation of the modern Beijing strains from our selection with several genetic markers<sup>(31)</sup> will potentially allow us to identify a sub species of modern Beijing strains that contains high levels of Rv3137. However, this indicates that Rv3137 is not a virulence factor that is upregulated throughout the modern Beijing genotype as a whole.

The relative mRNA quantities of Rv0450c/MmpL4 were in agreement with the results obtained by our proteomic experiments. Previous studies identified Rv0450c/MmpL4 as a potential virulence factor of *M. tuberculosis* by signature-tagged transposon mutagenesis.<sup>(80)</sup> In addition, this protein has been reported to be essential for growth in mouse models of TB.<sup>(81)</sup> A recent study reported Rv0450c/MmpL4, together with Rv0451c/MmpS4 or Rv0677c/MmpS5 and Rv0676c/MmpL5, are needed for the secretion of iron-scavenging siderophores in *M. tuberculosis*.<sup>(82)</sup> Our results demonstrate a clear upregulation of both protein and mRNA throughout the modern Beijing genotype. Taken together with the previously reported modern Beijing specific mutation in Rv0676c/MmpL5<sup>(30)</sup>, this suggests that siderophores could be differentially expressed in the two Beijing sublineages. If the increased levels of Rv0450c/MmpL4 work as a compensating mechanism for the mutated Rv0676c/MmpL5 gene in modern Beijing strains remains to be determined. Nevertheless, the results point to differences in iron metabolism between both

*M. tuberculosis* Beijing genotypes. This hypothesis is reinforced by a study which revealed that patients with a mutation in *SLC11A1/NRAMP1*, a divalent transition metal transporter involved in iron metabolism, have been associated with higher odds of TB caused by *M. tuberculosis* Beijing.<sup>(18)</sup> The altered quantities of Rv0450c/MmpL4 in association with the modern Beijing specific mutation in Rv0676c/MmpL5 is possibly the missing link that explains the success of *M. tuberculosis* Beijing strains within individuals that possess a mutation in *SLC11A1/NRAMP1*. Therefore, our findings support the idea of *M. tuberculosis* coevolution with their human host. Next to the secretion of siderophores, Rv0450c/MmpL4 & Rv0676c/MmpL5 has been identified as differentially regulated in rifampicin-resistant *M. tuberculosis* strains upon rifampicin exposure.<sup>(83)</sup> Build around the already known function of these MmpL genes and the upregulation of MmpL mRNA in a *M. tuberculosis*-rifampicin microarray model the authors suggested an involvement of Rv0450c/MmpL4 & Rv0676c/MmpL5 in the rifampicin efflux out of the cell.<sup>(83)</sup>

For Rv3283/sseA, the mRNA levels showed a trend opposite to the results we obtained by proteomics. Where the protein appeared to be strongly upregulated, and was quantitated by as much as 22 unique peptides on the protein level of ancient Beijing strains, we observed a slightly, but not significant, increase in the mRNA levels of modern Beijing strains. The discrepancy between the results obtained by proteomics and qPCR might be explained by the presence of a nsSNP in the genome of modern *M. tuberculosis* Beijing strains.<sup>(30)</sup>

### Enzymatic activity of Rv3283/sseA

Several studies have linked the expression of Rv3283/sseA to a virulent *M. tuberculosis* phenotype. One study demonstrated the differential regulation of Rv3283/sseA by *M. tuberculosis* within the host cell.<sup>(84)</sup> The association between the protein and an increase in virulence was further supported by a study that showed how a mutation in Rv3283/sseA leads to enhanced growth of *M. tuberculosis* in macrophages relative to *in vitro* growth of *M. tuberculosis*.<sup>(85)</sup> Finally, the predicted rhodanese activity of Rv3283/sseA potentially helps to cope with oxidative stress, as the knock-out of a rhodanese domain containing protein in *Azotobacter vinelandii* altered their sensitivity towards oxidative damages.<sup>(86)</sup>

In contrast to our proteomic data, the transcription levels of the Rv3283/sseA were higher, on average, in modern Beijing strains compared to ancient Beijing strains. We set out to determine whether a previously reported modern Beijing specific mutation could contribute to this discrepancy. This nsSNP confers a glutamic acid residue to a lysine residue which has been shown to be specific for modern Beijing strains.<sup>(30)</sup> Three independent bioinformatic algorithms were used to determine the effect of the mutation on the stability and function of the respective protein. PolyPhen-2, which uses the 3D crystal structure of Rv3283/sseA homologue 3HZU among other information, predicted that the mutation is “probably damaging” for the protein.

<sup>(58)</sup> Next to PolyPhen-2, we also used I-Mutant 3.0 in sequence mode.<sup>(59)</sup> The calculated free energy change upon substitution of glutamic acid by a lysine residue was -1.02 kcal/mol, which indicates a significant loss of stability of Rv3283/sseA in modern Beijing strains. Analysis of the protein and the corresponding mutation by PANTHER pointed towards a functional impairment of the mutated protein (subPSEC=-4.74& Pdeleterious=0.85).<sup>(60)</sup> The predicted instability, and thereby a potential short half-life time of Rv3283/sseA in modern Beijing strains can explain the lower level of Rv3283/sseA observed in modern Beijing strains compared to ancient Beijing strains.

To further confirm our results we measured the rhodanese activity in whole cell lysates of the ten *M. tuberculosis* Beijing strains used for the comparative proteomic analysis. Besides Rv3283/sseA there are at least three additional proteins (Rv0815c/cysA2, Rv2291/sseB & Rv3117/cysA3) that contain a rhodanese domain. The presence of these proteins makes our rhodanese activity assay on whole cell lysate level not rhodanese enzyme specific. However, as the additional rhodanese domain containing proteins appeared to occur in equal quantities in most modern and ancient Beijing strains, this is not expected to yield any difference in the total rhodanese activity. We observed approximately 23% more rhodanese activity in the ancient Beijing strains examined compared to modern Beijing strains. The relative predicted instability of the mutated Rv3283/sseA, together with the observed rhodanese activity, supports the results obtained by proteomics. In summary; our data suggests that modern Beijing strains possess, on average, less Rv3283/sseA than ancient Beijing strains.

### Comparative study

We compared the results of our systematic approach with a previous comparative proteomic study that described the differences between a hyper- and a hypovirulent Beijing strain.<sup>(34)</sup> In that study 23 proteins were reported to be more abundant in the hypo virulent strain. Of these 23 proteins, 17 were quantified in all four of our analyses, but none showed to be specifically more abundant in either the modern or the ancient Beijing strains; see Table S4. When we compared the 54 proteins that were reported to be more abundant in the previously reported hypervirulent strain, we identified 39 of those 54 proteins in all four of our analyses. Only one protein, Rv2680, showed to be more abundant in several modern Beijing strains. Two out of our three individual duplex approaches and the pooled approach demonstrated the upregulation of Rv2680 in modern Beijing strains. Together these observations show that comparison of two individual isolates can be useful to identify virulence factors, but not to describe specific differences between the two Beijing sublineages. The proteins Rv0450c/MmpL4, Rv1269c, Rv3137 and Rv3283/sseA were identified as differentially abundant in both our pooled approach and our three individual duplex analyses. Of these proteins, Rv3137 was solely identified in the previously reported *M. tuberculosis* Beijing proteome dataset.<sup>(34)</sup> However, Rv3137 was not

reported to be upregulated in the hypervirulent strain. This observation supports our hypothesis that Rv3137 is upregulated in several, but not all modern Beijing strains.

### Other differentially regulated proteins

The W-Beijing strain, a distinct phylogenetic branch within the modern Beijing genotype mainly observed in the early 1990s in the USA<sup>(87)</sup>, is known for the expression of a glycosylated variant of phthiocerol dimycocerosate (PDIM), the phenolic glycolipid (PGL-tb). W-Beijing strains are capable of synthesizing PGL-tb due to a mutation in their *pks15/1* gene.<sup>(88)</sup> Production of PGL-tb is thought to be one of the success factors of the W-Beijing strains.<sup>(89)</sup> However, not all *M. tuberculosis* Beijing strains produce PGL-tb, even when they possess a functional *pks15/1* gene.<sup>(90)</sup> In our dataset, Rv2946c/pks1 is significantly less abundant in both the pooled approach and two out of three separate duplexes. This observation suggests that *M. tuberculosis* Beijing strains do not necessarily express equal amounts of PDIM and PGL-tb.

In this study we identified Rv2688c in the proteome of *M. tuberculosis* Beijing, whereas this protein was not observed in the extensively studied proteome of *M. tuberculosis* H37Rv.<sup>(39)</sup> Rv2688c is often described as a fluoroquinolones (FQ) export ATP-binding protein.<sup>(91)</sup> The presence of Rv2688c was not only observed in the proteome of *M. tuberculosis* Beijing strains, but was also relatively high abundant in several of the modern Beijing strains studied. Interestingly, Beijing genotype isolates that are resistant to FQs occur significantly more than FQ-resistant isolates of other genotypes in Vietnam.<sup>(92)</sup> A mutation in the *gyrA* gene was associated with this high-level FQ-resistance. However, an increased abundance of the FQ efflux pump, Rv2688c, possibly leads to a better tolerance of modern *M. tuberculosis* Beijing strains against FQs, which can eventually result in mutations that cause resistance.

Our study showed that Rv2946c/PKS1 and Rv2688c are not upregulated in all modern Beijing strains. However, further characterization of the modern Beijing family might yield subfamilies in which this trait is conserved.

The DosR regulon, which is transcribed during the latent stage of infection, is reported to be constitutively upregulated in W-Beijing strains.<sup>(90)</sup> Our combined pooled and individual approach did not reveal differential abundance of proteins from the DosR regulon between modern and ancient Beijing strains. This suggests that upregulation of DosR might be conserved throughout all *M. tuberculosis* Beijing strains in general compared to other *M. tuberculosis* lineages.

## Conclusions

We identified an important virulence factor for modern Beijing strains in the form of Rv0450c/MmpL4. This observation is the first link between the proteome of modern *M. tuberculosis* Beijing strains and the higher odds of *M. tuberculosis* Beijing in individuals with a mutation in their *SLC11A1/NRAMP1* gene. We further provide evidence for the lower abundance of Rv3283/sseA in modern Beijing strains, which seems to be a direct consequence of a previously described nsSNP. In addition, we listed several proteins previously reported as potential virulence factors, such as Rv2946c/PKS1 and FQ efflux pump Rv2688c, which could contribute to the success of modern Beijing strains. Taken together our observations contribute to a better understanding of the successful spread of modern Beijing strains, and may assist in combatting this serious threat in TB control. If the spread of Beijing strains is not controlled the current epidemic of TB may transform into an epidemic of resistant TB.



## References

1. Organisation, W. H., Global Tuberculosis Report 2013. **2013**, 306.
2. Schurch, A. C.; van Soolingen, D., DNA fingerprinting of *Mycobacterium tuberculosis*: from phage typing to whole-genome sequencing. *Infect Genet Evol* **2012**, 12, (4), 602-9.
3. Brosch, R.; Gordon, S. V.; Marmiesse, M.; Brodin, P.; Buchrieser, C.; Eiglmeier, K.; Garnier, T.; Gutierrez, C.; Hewinson, G.; Kremer, K.; Parsons, L. M.; Pym, A. S.; Samper, S.; van Soolingen, D.; Cole, S. T., A new evolutionary scenario for the *Mycobacterium tuberculosis* complex. *Proc Natl Acad Sci U S A* **2002**, 99, (6), 3684-9.
4. Hershberg, R.; Lipatov, M.; Small, P. M.; Sheffer, H.; Niemann, S.; Homolka, S.; Roach, J. C.; Kremer, K.; Petrov, D. A.; Feldman, M. W.; Gagneux, S., High functional diversity in *Mycobacterium tuberculosis* driven by genetic drift and human demography. *PLoS Biol* **2008**, 6, (12), e311.
5. van Soolingen, D.; Qian, L.; de Haas, P. E.; Douglas, J. T.; Traore, H.; Portaels, F.; Qing, H. Z.; Enkhsaikan, D.; Nymadawa, P.; van Embden, J. D., Predominance of a single genotype of *Mycobacterium tuberculosis* in countries of east Asia. *J Clin Microbiol* **1995**, 33, (12), 3234-8.
6. Glynn, J. R.; Whiteley, J.; Bifani, P. J.; Kremer, K.; van Soolingen, D., Worldwide occurrence of Beijing/W strains of *Mycobacterium tuberculosis*: a systematic review. *Emerg Infect Dis* **2002**, 8, (8), 843-9.
7. Parwati, I.; Alisjahbana, B.; Apriani, L.; Soetikno, R. D.; Ottenhoff, T. H.; van der Zanden, A. G.; van der Meer, J.; van Soolingen, D.; van Crevel, R., *Mycobacterium tuberculosis* Beijing genotype is an independent risk factor for tuberculosis treatment failure in Indonesia. *J Infect Dis* **2010**, 201, (4), 553-7.
8. Kremer, K.; Glynn, J. R.; Lillebaek, T.; Niemann, S.; Kurepina, N. E.; Kreiswirth, B. N.; Bifani, P. J.; van Soolingen, D., Definition of the Beijing/W lineage of *Mycobacterium tuberculosis* on the basis of genetic markers. *J Clin Microbiol* **2004**, 42, (9), 4040-9.
9. Kremer, K.; van-der-Werf, M. J.; Au, B. K.; Anh, D. D.; Kam, K. M.; van-Doorn, H. R.; Borgdorff, M. W.; van-Soolingen, D., Vaccine-induced immunity circumvented by typical *Mycobacterium tuberculosis* Beijing strains. *Emerg Infect Dis* **2009**, 15, (2), 335-9.
10. Devaux, I.; Kremer, K.; Heersma, H.; Van Soolingen, D., Clusters of multidrug-resistant *Mycobacterium tuberculosis* cases, Europe. *Emerg Infect Dis* **2009**, 15, (7), 1052-60.
11. Buu, T. N.; van Soolingen, D.; Huyen, M. N.; Lan, N. T.; Quy, H. T.; Tiemersma, E. W.; Kremer, K.; Borgdorff, M. W.; Cobelens, F. G., Increased transmission of *Mycobacterium tuberculosis* Beijing genotype strains associated with resistance to streptomycin: a population-based study. *PLoS One* **2012**, 7, (8), e42323.
12. Buu, T. N.; Huyen, M. N.; Lan, N. T.; Quy, H. T.; Hen, N. V.; Zignol, M.; Borgdorff, M. W.; Cobelens, F. G.; van Soolingen, D., The Beijing genotype is associated with young age and multidrug-resistant tuberculosis in rural Vietnam. *Int J Tuberc Lung Dis* **2009**, 13, (7), 900-6.
13. Lopez, B.; Aguilar, D.; Orozco, H.; Burger, M.; Espitia, C.; Ritacco, V.; Barrera, L.; Kremer, K.; Hernandez-Pando, R.; Huygen, K.; van Soolingen, D., A marked difference in pathogenesis and immune response induced by different *Mycobacterium tuberculosis* genotypes. *Clin Exp Immunol* **2003**, 133, (1), 30-7.

14. Abebe, F.; Bjune, G., The emergence of Beijing family genotypes of *Mycobacterium tuberculosis* and low-level protection by bacille Calmette-Guerin (BCG) vaccines: is there a link? *Clin Exp Immunol* **2006**, *145*, (3), 389-97.
15. Grode, L.; Seiler, P.; Baumann, S.; Hess, J.; Brinkmann, V.; Nasser Eddine, A.; Mann, P.; Goosmann, C.; Bander mann, S.; Smith, D.; Bancroft, G. J.; Rey rat, J. M.; van Soolingen, D.; Raupach, B.; Kaufmann, S. H., Increased vaccine efficacy against tuberculosis of recombinant *Mycobacterium bovis* bacille Calmette-Guerin mutants that secrete listeriolysin. *J Clin Invest* **2005**, *115*, (9), 2472-9.
16. Anh, D. D.; Borgdorff, M. W.; Van, L. N.; Lan, N. T.; van Gorkom, T.; Kremer, K.; van Soolingen, D., *Mycobacterium tuberculosis* Beijing genotype emerging in Vietnam. *Emerg Infect Dis* **2000**, *6*, (3), 302-5.
17. van der Spuy, G. D.; Kremer, K.; Ndabambi, S. L.; Beyers, N.; Dunbar, R.; Marais, B. J.; van Helden, P. D.; Warren, R. M., Changing *Mycobacterium tuberculosis* population highlights clade-specific pathogenic characteristics. *Tuberculosis (Edinb)* **2009**, *89*, (2), 120-5.
18. van Crevel, R.; Parwati, I.; Sahiratmadja, E.; Marzuki, S.; Ottenhoff, T. H.; Netea, M. G.; van der Ven, A.; Nelwan, R. H.; van der Meer, J. W.; Alisjahbana, B.; van de Vosse, E., Infection with *Mycobacterium tuberculosis* Beijing genotype strains is associated with polymorphisms in SLC11A1/NRAMP1 in Indonesian patients with tuberculosis. *J Infect Dis* **2009**, *200*, (11), 1671-4.
19. Ebrahimi-Rad, M.; Bifani, P.; Martin, C.; Kremer, K.; Samper, S.; Rauzier, J.; Kreiswirth, B.; Blazquez, J.; Jouan, M.; van Soolingen, D.; Gicquel, B., Mutations in putative mutator genes of *Mycobacterium tuberculosis* strains of the W-Beijing family. *Emerg Infect Dis* **2003**, *9*, (7), 838-45.
20. de Steenwinkel, J. E.; ten Kate, M. T.; de Knecht, G. J.; Kremer, K.; Aarnoutse, R. E.; Boeree, M. J.; Verbrugh, H. A.; van Soolingen, D.; Bakker-Woudenberg, I. A., Drug susceptibility of *Mycobacterium tuberculosis* Beijing genotype and association with MDR TB. *Emerg Infect Dis* **2012**, *18*, (4), 660-3.
21. Ford, C. B.; Shah, R. R.; Maeda, M. K.; Gagneux, S.; Murray, M. B.; Cohen, T.; Johnston, J. C.; Gardy, J.; Lipsitch, M.; Fortune, S. M., *Mycobacterium tuberculosis* mutation rate estimates from different lineages predict substantial differences in the emergence of drug-resistant tuberculosis. *Nat Genet* **2013**, *45*, (7), 784-90.
22. Dong, H.; Shi, L.; Zhao, X.; Sang, B.; Lv, B.; Liu, Z.; Wan, K., Genetic diversity of *Mycobacterium tuberculosis* isolates from Tibetans in Tibet, China. *PLoS One* **2012**, *7*, (3), e33904.
23. Yu, Q.; Su, Y.; Lu, B.; Ma, Y.; Zhao, X.; Yang, X.; Dong, H.; Liu, Y.; Lian, L.; Wan, L.; Wu, Y.; Wan, K., Genetic diversity of *Mycobacterium tuberculosis* isolates from Inner Mongolia, China. *PLoS One* **2013**, *8*, (5), e57660.
24. Casali, N.; Nikolayevskyy, V.; Balabanova, Y.; Ignatyeva, O.; Kontsevaya, I.; Harris, S. R.; Bentley, S. D.; Parkhill, J.; Nejentsev, S.; Hoffner, S. E.; Horstmann, R. D.; Brown, T.; Drobniewski, F., Microevolution of extensively drug-resistant tuberculosis in Russia. *Genome Res* **2012**, *22*, (4), 735-45.
25. Johnson, R.; Warren, R. M.; van der Spuy, G. D.; Gey van Pittius, N. C.; Theron, D.; Streicher, E. M.; Bosman, M.; Coetzee, G. J.; van Helden, P. D.; Victor, T. C., Drug-resistant tuberculosis epidemic in the Western Cape driven by a virulent Beijing genotype strain. *Int J Tuberc Lung Dis* **2010**, *14*, (1), 119-21.

26. European Concerted Action on New Generation Genetic, M.; Techniques for the, E.; Control of, T., Beijing/W genotype Mycobacterium tuberculosis and drug resistance. *Emerg Infect Dis* **2006**, *12*, (5), 736-43.
27. Mokrousov, I.; Narvskaya, O.; Otten, T.; Vyazovaya, A.; Limeschenko, E.; Steklova, L.; Vyshnevskiy, B., Phylogenetic reconstruction within Mycobacterium tuberculosis Beijing genotype in northwestern Russia. *Res Microbiol* **2002**, *153*, (10), 629-37.
28. Iwamoto, T., [Population structure analysis of Mycobacterium tuberculosis Beijing family in Japan]. *Kekkaku* **2009**, *84*, (12), 755-9.
29. Tsolaki, A. G.; Gagneux, S.; Pym, A. S.; Goguet de la Salmoniere, Y. O.; Kreiswirth, B. N.; Van Soolingen, D.; Small, P. M., Genomic deletions classify the Beijing/W strains as a distinct genetic lineage of Mycobacterium tuberculosis. *J Clin Microbiol* **2005**, *43*, (7), 3185-91.
30. Schurch, A. C.; Kremer, K.; Warren, R. M.; Hung, N. V.; Zhao, Y.; Wan, K.; Boeree, M. J.; Siezen, R. J.; Smith, N. H.; van Soolingen, D., Mutations in the regulatory network underlie the recent clonal expansion of a dominant subclone of the Mycobacterium tuberculosis Beijing genotype. *Infect Genet Evol* **2011**, *11*, (3), 587-97.
31. Hanekom, M.; van der Spuy, G. D.; Streicher, E.; Ndabambi, S. L.; McEvoy, C. R.; Kidd, M.; Beyers, N.; Victor, T. C.; van Helden, P. D.; Warren, R. M., A recently evolved sublineage of the Mycobacterium tuberculosis Beijing strain family is associated with an increased ability to spread and cause disease. *J Clin Microbiol* **2007**, *45*, (5), 1483-90.
32. van Laarhoven, A.; Mandemakers, J. J.; Kleinnijenhuis, J.; Enaimi, M.; Lachmandas, E.; Joosten, L. A.; Ottenhoff, T. H.; Netea, M. G.; van Soolingen, D.; van Crevel, R., Low induction of proinflammatory cytokines parallels evolutionary success of modern strains within the Mycobacterium tuberculosis Beijing genotype. *Infect Immun* **2013**, *81*, (10), 3750-6.
33. Jungblut, P. R.; Schaible, U. E.; Mollenkopf, H. J.; Zimny-Arndt, U.; Raupach, B.; Mattow, J.; Halada, P.; Lamer, S.; Hagens, K.; Kaufmann, S. H., Comparative proteome analysis of Mycobacterium tuberculosis and Mycobacterium bovis BCG strains: towards functional genomics of microbial pathogens. *Mol Microbiol* **1999**, *33*, (6), 1103-17.
34. de Souza, G. A.; Fortuin, S.; Aguilar, D.; Pando, R. H.; McEvoy, C. R.; van Helden, P. D.; Koehler, C. J.; Thiede, B.; Warren, R. M.; Wiker, H. G., Using a label-free proteomics method to identify differentially abundant proteins in closely related hypo- and hypervirulent clinical Mycobacterium tuberculosis Beijing isolates. *Mol Cell Proteomics* **2010**, *9*, (11), 2414-23.
35. Neubauer, H.; Clare, S. E.; Kurek, R.; Fehm, T.; Wallwiener, D.; Sotlar, K.; Nordheim, A.; Wozny, W.; Schwall, G. P.; Poznanovic, S.; Sastri, C.; Hunzinger, C.; Stegmann, W.; Schrattenholz, A.; Cahill, M. A., Breast cancer proteomics by laser capture microdissection, sample pooling, 54-cm IPG IEF, and differential iodine radioisotope detection. *Electrophoresis* **2006**, *27*, (9), 1840-52.
36. Diz, A. P.; Truebano, M.; Skibinski, D. O., The consequences of sample pooling in proteomics: an empirical study. *Electrophoresis* **2009**, *30*, (17), 2967-75.
37. Geiger, T.; Cox, J.; Ostasiewicz, P.; Wisniewski, J. R.; Mann, M., Super-SILAC mix for quantitative

- proteomics of human tumor tissue. *Nat Methods* **2010**, 7, (5), 383-5.
38. Deeb, S. J.; D'Souza, R. C.; Cox, J.; Schmidt-Supprian, M.; Mann, M., Super-SILAC allows classification of diffuse large B-cell lymphoma subtypes by their protein expression profiles. *Mol Cell Proteomics* **2012**, 11, (5), 77-89.
  39. Schubert, O. T.; Mouritsen, J.; Ludwig, C.; Rost, H. L.; Rosenberger, G.; Arthur, P. K.; Claassen, M.; Campbell, D. S.; Sun, Z.; Farrah, T.; Gengenbacher, M.; Maiolica, A.; Kaufmann, S. H.; Moritz, R. L.; Aebersold, R., The Mtb proteome library: a resource of assays to quantify the complete proteome of *Mycobacterium tuberculosis*. *Cell Host Microbe* **2013**, 13, (5), 602-12.
  40. Schurch, A. C.; Kremer, K.; Hendriks, A. C.; Freyee, B.; McEvoy, C. R.; van Crevel, R.; Boeree, M. J.; van Helden, P.; Warren, R. M.; Siezen, R. J.; van Soolingen, D., SNP/RD typing of *Mycobacterium tuberculosis* Beijing strains reveals local and worldwide disseminated clonal complexes. *PLoS One* **2011**, 6, (12), e28365.
  41. Bifani, P. J.; Mathema, B.; Kurepina, N. E.; Kreiswirth, B. N., Global dissemination of the *Mycobacterium tuberculosis* W-Beijing family strains. *Trends Microbiol* **2002**, 10, (1), 45-52.
  42. Narvskaya, O. V.; Mokrousov, I. V.; Otten, T. F.; Vishnevskii, B. I., [Genetic marking of polyresistant mycobacterium tuberculosis strains isolated in the north-west of Russia]. *Probl Tuberk* **1999**, (3), 39-41.
  43. Narvskaya, O. M. I. O., T; Vishnevsky, B, Molecular markers: application for studies of *Mycobacterium tuberculosis* population in Russia. *Trends in DNA fingerprinting research* **2005**, 15.
  44. Supply, P.; Allix, C.; Lesjean, S.; Cardoso-Oelemann, M.; Rusch-Gerdes, S.; Willery, E.; Savine, E.; de Haas, P.; van Deutekom, H.; Roring, S.; Bifani, P.; Kurepina, N.; Kreiswirth, B.; Sola, C.; Rastogi, N.; Vatin, V.; Gutierrez, M. C.; Fauville, M.; Niemann, S.; Skuce, R.; Kremer, K.; Locht, C.; van Soolingen, D., Proposal for standardization of optimized mycobacterial interspersed repetitive unit-variable-number tandem repeat typing of *Mycobacterium tuberculosis*. *J Clin Microbiol* **2006**, 44, (12), 4498-510.
  45. Boom, R.; Sol, C. J.; Salimans, M. M.; Jansen, C. L.; Wertheim-van Dillen, P. M.; van der Noordaa, J., Rapid and simple method for purification of nucleic acids. *J Clin Microbiol* **1990**, 28, (3), 495-503.
  46. Woods, G. L.; Brown-Elliott, B. A.; Desmond, E. P.; Hall, G. S.; Heifets, L.; Pfyffer, G. E.; Ridderhof, J. C.; Wallace, R. J.; Warren, N. G.; Witebsky, F. G., Susceptibility Testing of Mycobacteria, Nocardiae, and Other Aerobic Actinomycetes; Approved Standard, second edition. *Clinical and Laboratory Standards Institute* **2011**.
  47. Wisniewski, J. R.; Zougman, A.; Nagaraj, N.; Mann, M., Universal sample preparation method for proteome analysis. *Nat Methods* **2009**, 6, (5), 359-62.
  48. Boersema, P. J.; Raijmakers, R.; Lemeer, S.; Mohammed, S.; Heck, A. J., Multiplex peptide stable isotope dimethyl labeling for quantitative proteomics. *Nat Protoc* **2009**, 4, (4), 484-94.
  49. Meiring, H. D.; van der Heeft, E.; ten Hove, G. J.; de Jong, A. P. J. M., Nanoscale LC-MS(n): technical design and applications to peptide and protein analysis. *Journal of Separation Science* **2002**, 25, (9), 12.
  50. de Souza, G. A.; Arntzen, M. O.; Wiker, H. G., MSMSpddb: providing protein databases of closely

related organisms to improve proteomic characterization of prokaryotic microbes. *Bioinformatics* **2010**, 26, (5), 698-9.

51. Cole, S. T.; Brosch, R.; Parkhill, J.; Garnier, T.; Churcher, C.; Harris, D.; Gordon, S. V.; Eiglmeier, K.; Gas, S.; Barry, C. E., 3rd; Tekaia, F.; Badcock, K.; Basham, D.; Brown, D.; Chillingworth, T.; Connor, R.; Davies, R.; Devlin, K.; Feltwell, T.; Gentles, S.; Hamlin, N.; Holroyd, S.; Hornsby, T.; Jagels, K.; Krogh, A.; McLean, J.; Moule, S.; Murphy, L.; Oliver, K.; Osborne, J.; Quail, M. A.; Rajandream, M. A.; Rogers, J.; Rutter, S.; Seeger, K.; Skelton, J.; Squares, R.; Squares, S.; Sulston, J. E.; Taylor, K.; Whitehead, S.; Barrell, B. G., Deciphering the biology of *Mycobacterium tuberculosis* from the complete genome sequence. *Nature* **1998**, 393, (6685), 537-44.
52. Narayanan, S.; Deshpande, U., Whole-Genome Sequences of Four Clinical Isolates of *Mycobacterium tuberculosis* from Tamil Nadu, South India. *Genome Announc* **2013**, 1, (3).
53. Cox, J.; Mann, M., MaxQuant enables high peptide identification rates, individualized p.p.b.-range mass accuracies and proteome-wide protein quantification. *Nat Biotechnol* **2008**, 26, (12), 1367-72.
54. Cox, J.; Neuhauser, N.; Michalski, A.; Scheltema, R. A.; Olsen, J. V.; Mann, M., Andromeda: a peptide search engine integrated into the MaxQuant environment. *J Proteome Res* **2011**, 10, (4), 1794-805.
55. Yu, N. Y.; Wagner, J. R.; Laird, M. R.; Melli, G.; Rey, S.; Lo, R.; Dao, P.; Sahinalp, S. C.; Ester, M.; Foster, L. J.; Brinkman, F. S., PSORTb 3.0: improved protein subcellular localization prediction with refined localization subcategories and predictive capabilities for all prokaryotes. *Bioinformatics* **2010**, 26, (13), 1608-15.
56. Krogh, A.; Larsson, B.; von Heijne, G.; Sonnhammer, E. L., Predicting transmembrane protein topology with a hidden Markov model: application to complete genomes. *J Mol Biol* **2001**, 305, (3), 567-80.
57. Untergasser, A.; Nijveen, H.; Rao, X.; Bisseling, T.; Geurts, R.; Leunissen, J. A., Primer3Plus, an enhanced web interface to Primer3. *Nucleic Acids Res* **2007**, 35, (Web Server issue), W71-4.
58. Adzhubei, I. A.; Schmidt, S.; Peshkin, L.; Ramensky, V. E.; Gerasimova, A.; Bork, P.; Kondrashov, A. S.; Sunyaev, S. R., A method and server for predicting damaging missense mutations. *Nat Methods* **2010**, 7, (4), 248-9.
59. Capriotti, E.; Fariselli, P.; Rossi, I.; Casadio, R., A three-state prediction of single point mutations on protein stability changes. *BMC Bioinformatics* **2008**, 9 Suppl 2, S6.
60. Brunham, L. R.; Singaraja, R. R.; Pape, T. D.; Kejariwal, A.; Thomas, P. D.; Hayden, M. R., Accurate prediction of the functional significance of single nucleotide polymorphisms and mutations in the ABCA1 gene. *PLoS Genet* **2005**, 1, (6), e83.
61. Reddy, T. B.; Riley, R.; Wymore, F.; Montgomery, P.; DeCaprio, D.; Engels, R.; Gellesch, M.; Hubble, J.; Jen, D.; Jin, H.; Koehrsen, M.; Larson, L.; Mao, M.; Nitzberg, M.; Sisk, P.; Stolte, C.; Weiner, B.; White, J.; Zachariah, Z. K.; Sherlock, G.; Galagan, J. E.; Ball, C. A.; Schoolnik, G. K., TB database: an integrated platform for tuberculosis research. *Nucleic Acids Res* **2009**, 37, (Database issue), D499-508.
62. Vandenberg, P. A. B., R.E.; Berk, R.S., Rapid Test for Determining the Intracellular Rhodanese Activity of Various Bacteria *International Journal of Systematic Bacteriology* **1979**, 29, (4), 6.
63. Lew, J. M.; Kapopoulou, A.; Jones, L. M.; Cole, S. T., TubercuList--10 years after. *Tuberculosis (Edinb)*

- 2011, 91, (1), 1-7.
64. Louw, G. E.; Warren, R. M.; Gey van Pittius, N. C.; McEvoy, C. R.; Van Helden, P. D.; Victor, T. C., A balancing act: efflux/influx in mycobacterial drug resistance. *Antimicrob Agents Chemother* **2009**, 53, (8), 3181-9.
  65. Mokrousov, I.; Jiao, W. W.; Sun, G. Z.; Liu, J. W.; Valcheva, V.; Li, M.; Narvskaya, O.; Shen, A. D., Evolution of drug resistance in different sublineages of Mycobacterium tuberculosis Beijing genotype. *Antimicrob Agents Chemother* **2006**, 50, (8), 2820-3.
  66. Iwamoto, T.; Yoshida, S.; Suzuki, K.; Wada, T., Population structure analysis of the Mycobacterium tuberculosis Beijing family indicates an association between certain sublineages and multidrug resistance. *Antimicrob Agents Chemother* **2008**, 52, (10), 3805-9.
  67. Parwati, I.; van Crevel, R.; van Soolingen, D., Possible underlying mechanisms for successful emergence of the Mycobacterium tuberculosis Beijing genotype strains. *Lancet Infect Dis* **2010**, 10, (2), 103-11.
  68. Borgdorff, M. W.; van Soolingen, D., The re-emergence of tuberculosis: what have we learnt from molecular epidemiology? *Clin Microbiol Infect* **2013**, 19, (10), 889-901.
  69. Faksri, K.; Drobniowski, F.; Nikolayevskyy, V.; Brown, T.; Prammananan, T.; Palittapongarnpim, P.; Prayoonwiwat, N.; Chaiprasert, A., Genetic diversity of the Mycobacterium tuberculosis Beijing family based on IS6110, SNP, LSP and VNTR profiles from Thailand. *Infect Genet Evol* **2011**, 11, (5), 1142-9.
  70. Lu, B.; Zhao, P.; Liu, B.; Dong, H.; Yu, Q.; Zhao, X.; Wan, K., Genetic diversity of Mycobacterium tuberculosis isolates from Beijing, China assessed by Spoligotyping, LSPs and VNTR profiles. *BMC Infect Dis* **2012**, 12, 372.
  71. Bell, C.; Smith, G. T.; Sweredoski, M. J.; Hess, S., Characterization of the Mycobacterium tuberculosis proteome by liquid chromatography mass spectrometry-based proteomics techniques: a comprehensive resource for tuberculosis research. *J Proteome Res* **2012**, 11, (1), 119-30.
  72. Louw, G. E.; Warren, R. M.; Gey van Pittius, N. C.; Leon, R.; Jimenez, A.; Hernandez-Pando, R.; McEvoy, C. R.; Grobbelaar, M.; Murray, M.; van Helden, P. D.; Victor, T. C., Rifampicin reduces susceptibility to ofloxacin in rifampicin-resistant Mycobacterium tuberculosis through efflux. *Am J Respir Crit Care Med* **2011**, 184, (2), 269-76.
  73. Villellas, C.; Aristimuno, L.; Vitoria, M. A.; Prat, C.; Blanco, S.; Garcia de Viedma, D.; Dominguez, J.; Samper, S.; Ainsa, J. A., Analysis of mutations in streptomycin-resistant strains reveals a simple and reliable genetic marker for identification of the Mycobacterium tuberculosis Beijing genotype. *J Clin Microbiol* **2013**, 51, (7), 2124-30.
  74. Kelkar, D. S.; Kumar, D.; Kumar, P.; Balakrishnan, L.; Muthusamy, B.; Yadav, A. K.; Shrivastava, P.; Marimuthu, A.; Anand, S.; Sundaram, H.; Kingsbury, R.; Harsha, H. C.; Nair, B.; Prasad, T. S.; Chauhan, D. S.; Katoch, K.; Katoch, V. M.; Kumar, P.; Chaerkady, R.; Ramachandran, S.; Dash, D.; Pandey, A., Proteogenomic analysis of Mycobacterium tuberculosis by high resolution mass spectrometry. *Mol Cell Proteomics* **2011**, 10, (12), M111 011627.
  75. Jungblut, P. R.; Holzthutter, H. G.; Apweiler, R.; Schluter, H., The speciation of the proteome. *Chem Cent J* **2008**, 2, 16.

76. Schluter, H.; Apweiler, R.; Holzthutter, H. G.; Jungblut, P. R., Finding one's way in proteomics: a protein species nomenclature. *Chem Cent J* **2009**, 3, 11.
77. Low, T. Y.; van Heesch, S.; van den Toorn, H.; Giansanti, P.; Cristobal, A.; Toonen, P.; Schafer, S.; Hubner, N.; van Breukelen, B.; Mohammed, S.; Cuppen, E.; Heck, A. J.; Guryev, V., Quantitative and qualitative proteome characteristics extracted from in-depth integrated genomics and proteomics analysis. *Cell Rep* **2013**, 5, (5), 1469-78.
78. Sassetti, C. M.; Boyd, D. H.; Rubin, E. J., Genes required for mycobacterial growth defined by high density mutagenesis. *Mol Microbiol* **2003**, 48, (1), 77-84.
79. Griffin, J. E.; Gawronski, J. D.; Dejesus, M. A.; Ioerger, T. R.; Akerley, B. J.; Sassetti, C. M., High-resolution phenotypic profiling defines genes essential for mycobacterial growth and cholesterol catabolism. *PLoS Pathog* **2011**, 7, (9), e1002251.
80. Camacho, L. R.; Ensergueix, D.; Perez, E.; Gicquel, B.; Guilhot, C., Identification of a virulence gene cluster of *Mycobacterium tuberculosis* by signature-tagged transposon mutagenesis. *Mol Microbiol* **1999**, 34, (2), 257-67.
81. Domenech, P.; Reed, M. B.; Barry, C. E., 3rd, Contribution of the *Mycobacterium tuberculosis* MmpL protein family to virulence and drug resistance. *Infect Immun* **2005**, 73, (6), 3492-501.
82. Wells, R. M.; Jones, C. M.; Xi, Z.; Speer, A.; Danilchanka, O.; Doornbos, K. S.; Sun, P.; Wu, F.; Tian, C.; Niederweis, M., Discovery of a siderophore export system essential for virulence of *Mycobacterium tuberculosis*. *PLoS Pathog* **2013**, 9, (1), e1003120.
83. de Knecht, G. J.; Bruning, O.; ten Kate, M. T.; de Jong, M.; van Belkum, A.; Endtz, H. P.; Breit, T. M.; Bakker-Woudenberg, I. A.; de Steenwinkel, J. E., Rifampicin-induced transcriptome response in rifampicin-resistant *Mycobacterium tuberculosis*. *Tuberculosis (Edinb)* **2013**, 93, (1), 96-101.
84. Triccas, J. A.; Berthet, F. X.; Pelicic, V.; Gicquel, B., Use of fluorescence induction and sucrose counterselection to identify *Mycobacterium tuberculosis* genes expressed within host cells. *Microbiology* **1999**, 145 ( Pt 10), 2923-30.
85. Rengarajan, J.; Bloom, B. R.; Rubin, E. J., Genome-wide requirements for *Mycobacterium tuberculosis* adaptation and survival in macrophages. *Proc Natl Acad Sci U S A* **2005**, 102, (23), 8327-32.
86. Cereda, A.; Carpen, A.; Picariello, G.; Tedeschi, G.; Pagani, S., The lack of rhodanese RhdA affects the sensitivity of *Azotobacter vinelandii* to oxidative events. *Biochem J* **2009**, 418, (1), 135-43.
87. Bifani, P. J. P., B.B.;Kapur, V.;Stockbauer, K.;Pan, X.;Lutfey M.L.;Moghazeh S.L.;Eisner, W.;Daniel T.M.;Kaplan, M.H.;Crawford, J.T.;Musser, B.N.;Kreiswirth, B.N., Origin and interstate spread of a New York multidrug-resistant *Mycobacterium tuberculosis* clone family. *The Journal of the American Medical Association* **1996**, 275, (6), 6.
88. Constant, P.; Perez, E.; Malaga, W.; Laneelle, M. A.; Saurel, O.; Daffe, M.; Guilhot, C., Role of the *pks15/1* gene in the biosynthesis of phenolglycolipids in the *Mycobacterium tuberculosis* complex. Evidence that all strains synthesize glycosylated p-hydroxybenzoic methyl esters and that strains devoid of phenolglycolipids harbor a frameshift mutation in the *pks15/1* gene. *J Biol Chem* **2002**, 277, (41), 38148-58.

89. Reed, M. B.; Domenech, P.; Manca, C.; Su, H.; Barczak, A. K.; Kreiswirth, B. N.; Kaplan, G.; Barry, C. E., 3rd, A glycolipid of hypervirulent tuberculosis strains that inhibits the innate immune response. *Nature* **2004**, 431, (7004), 84-7.
90. Reed, M. B.; Gagneux, S.; Deriemer, K.; Small, P. M.; Barry, C. E., 3rd, The W-Beijing lineage of *Mycobacterium tuberculosis* overproduces triglycerides and has the DosR dormancy regulon constitutively upregulated. *J Bacteriol* **2007**, 189, (7), 2583-9.
91. Pasca, M. R.; Guglielame, P.; Arcesi, F.; Bellinzoni, M.; De Rossi, E.; Riccardi, G., Rv2686c-Rv2687c-Rv2688c, an ABC fluoroquinolone efflux pump in *Mycobacterium tuberculosis*. *Antimicrob Agents Chemother* **2004**, 48, (8), 3175-8.
92. Duong, D. A.; Nguyen, T. H.; Nguyen, T. N.; Dai, V. H.; Dang, T. M.; Vo, S. K.; Do, D. A.; Nguyen, V. V.; Nguyen, H. D.; Dinh, N. S.; Farrar, J.; Caws, M., Beijing genotype of *Mycobacterium tuberculosis* is significantly associated with high-level fluoroquinolone resistance in Vietnam. *Antimicrob Agents Chemother* **2009**, 53, (11), 4835-9.
93. J.C., O., VENNY. An interactive tool for comparing lists with Venn Diagrams. **2007**.



## Supplementary files

### TABLES

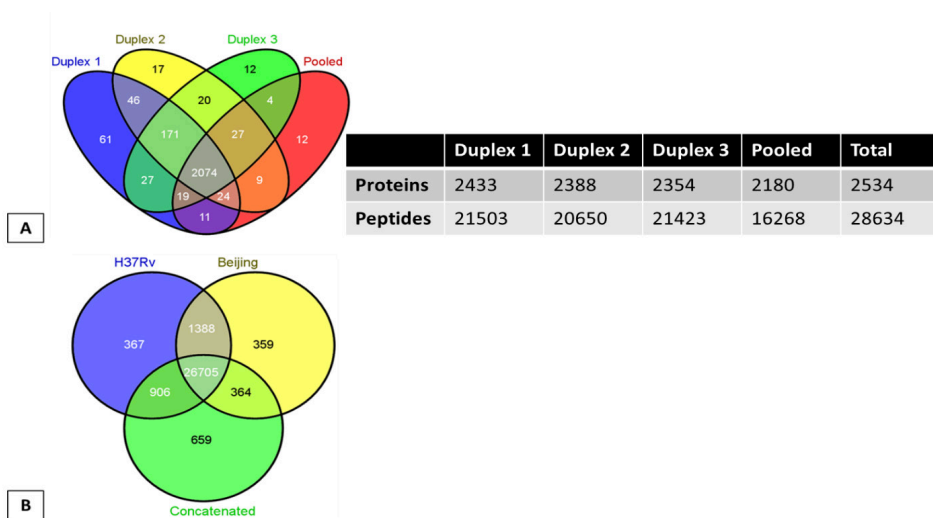
**Supporting Information Table S1:** Peptides identified by a H37Rv, Beijing NITR203 or concatenated database. This table can be downloaded on the website of the journal: <http://www.mcponline.org/content/13/10/2632/suppl/DC1>

**Supporting Information Table S2:** Proteins identified. This table can be downloaded on the website of the journal: <http://www.mcponline.org/content/13/10/2632/suppl/DC1>

**Supporting Information Table S3:** Proteins that were identified as significantly different abundant. This table can be downloaded on the website of the journal: <http://www.mcponline.org/content/13/10/2632/suppl/DC1>

**Supporting Information Table S4:** Comparison of proteins that were previously reported to be more abundant in Hypo-/Hyper-virulent Beijing strains. This table can be downloaded on the website of the journal: <http://www.mcponline.org/content/13/10/2632/suppl/DC1>





**SUPPORTING INFORMATION FIGURE S2:** Venn diagrams (93) showing the overlap between

**A)** The proteins identified in the pooled approach and the three individual approaches

Pooled: Ancient Beijing strains: NLA000017583, NLA1010701604, NLA1010200230, NLA1010501814, and NLA1019801252 versus modern Beijing strains: NLA1010700873, NLA1011100782, NLA1019401707, NLA1019401709, NLA1019402019

Duplex 1: Ancient Beijing: NLA000017583 versus modern Beijing: NLA1010700873

Duplex 2: Ancient Beijing: NLA1010200230 versus modern Beijing: NLA109401709

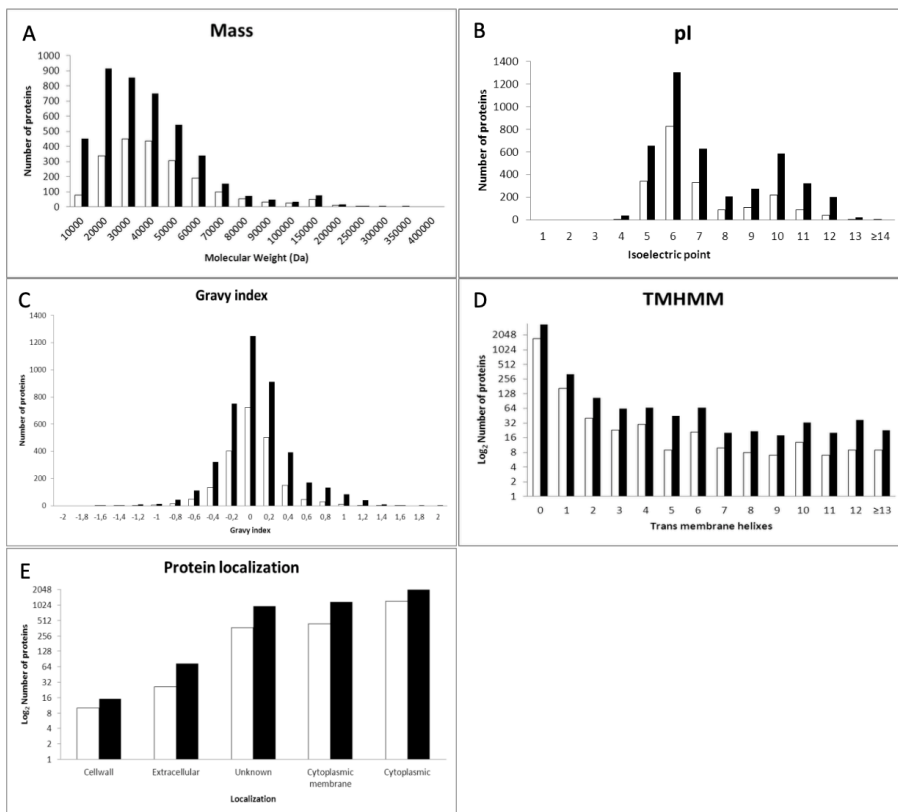
Duplex 3: Ancient Beijing: NLA1019801252 versus modern Beijing: NLA101100782

**B)** Peptides identified with three different databases (30748 peptides in total)

*M. tuberculosis* H37Rv = FASTA database derived from genomic sequence of *M. tuberculosis* H37Rv(51)

*M. tuberculosis* Beijing = FASTA database derived from genomic sequence of *M. tuberculosis* Beijing NITR203(52)

Concatenated = concatenated FASTA database derived from both *M. tuberculosis* H37Rv and *M. tuberculosis* Beijing NITR203 made using MSMSpddb(50)



**SUPPORTING INFORMATION FIGURE S3:** General physiochemical properties and localization of the observed (white bars) and theoretical proteome (filled black bars).

**A-C)** Physiochemical characteristic of *M. tuberculosis* Beijing proteome and our concatenated database.  
**D-E)** Protein localization and number of predicted transmembrane helices for each of the proteins present in our dataset and the concatenated database.(55, 56)



Mechanisms of phenotypic rifampicin tolerance in  
*Mycobacterium tuberculosis* Beijing genotype strain  
B0/W148 revealed by proteomics

Jeroen de Keijzer<sup>1\*</sup>, Arnout Mulder<sup>2</sup>, Jessica de Beer<sup>2</sup>, Arnoud H. de Ru<sup>1</sup>,  
Peter A. van Veelen<sup>1#</sup>, Dick van Soolingen<sup>2,3#</sup>

<sup>1</sup> Department of Immunohematology and Blood Transfusion, Leiden University Medical Center (LUMC), Leiden,  
2300 RC, The Netherlands

<sup>2</sup> Tuberculosis Reference Laboratory, National Institute for Public Health and the Environment (RIVM),  
Bilthoven, <sup>3</sup>720 BA, The Netherlands

<sup>3</sup> Departments of Pulmonary Diseases and Medical Microbiology, Radboud University Medical Center,  
Nijmegen, 6500 HB, The Netherlands

# PAV and DvS share senior authorship

## Abstract

The “successful” Russian clone B0/W148 of *Mycobacterium tuberculosis* Beijing is well known for its capacity to develop antibiotic resistance. During treatment, resistant mutants can occur that have inheritable resistance to specific antibiotics. Next to mutations, *M. tuberculosis* has several mechanisms that increase their tolerance to a variety of antibiotics. Insights in the phenotypic mechanisms that contribute to drug tolerance will increase our understanding of how antibiotic resistance develops in *M. tuberculosis*.

In this study, we examined the (phospho)proteome dynamics in *M. tuberculosis* Beijing strain B0/W148 when exposed to a high dose of rifampicin; one of the most potent first-line antibiotics. A total of 2,534 proteins and 191 phosphorylation sites were identified, and revealed the differential regulation of DosR regulon proteins, which are necessary for the development of a dormant phenotype that is less susceptible to antibiotics. By examining independent phenotypic markers of dormancy, we show that persisters of *in vitro* rifampicin exposure entered a metabolically hypoactive state, which yields rifampicin and other antibiotics largely ineffective. These new insights in the role of protein regulation and post-translational modifications during the initial phase of rifampicin treatment reveals a shortcoming in the anti-tuberculosis regimen that is administered to 8-9 million individuals annually.

## Introduction

Tuberculosis (TB), caused by *Mycobacterium tuberculosis*, is one of the most devastating infectious diseases. Currently, 8-9 million new TB cases and 1.5 million deaths to this disease are recorded annually.<sup>(1)</sup>

The *M. tuberculosis* complex can be delineated into six lineages, which differ in their worldwide distribution, capacity to cause and spread active disease, and correlation with resistance.<sup>(2-4)</sup> The in 1995 described 'Beijing' genotype is among the most frequently studied *M. tuberculosis* lineages due to its remarkable dominance in Asia, the former Soviet Union, parts of Europe and South Africa.<sup>(5-8)</sup> Based on the available genetic markers, the Beijing genotype was reported to be genetically highly conserved, which is associated to active and recent spread.<sup>(5-8)</sup> Throughout several geographic areas, but specifically in Eastern-Europe,<sup>(9)</sup> Beijing strains were found to correlate with (multi and extensively) drug resistance, treatment failure, relapses after treatment and transmission of antibiotic resistant TB.<sup>(6, 7, 9-11)</sup> In line with the spread and prevalence of the *M. tuberculosis* Beijing strains, resistance against anti-TB drugs is a major problem in China, South Africa, Eastern Europe; especially the former Soviet Union States.<sup>(9, 12-17)</sup>

In Russia, half of the *M. tuberculosis* isolates belong to the Beijing family, of which one-fourth belongs to the highly clonal Beijing B0/W148 cluster.<sup>(18)</sup> Compared to other Beijing isolates, members of the Beijing B0/W148 genotype display an increased virulence in macrophage infection models,<sup>(19)</sup> a stronger correlation with multidrug resistance,<sup>(18, 20-22)</sup> and an increased transmissibility.<sup>(22, 23)</sup>

Standard treatment regimens of TB includes rifampicin, one of the cornerstones of anti-TB treatment, which targets the mycobacterial RNA-polymerase. The survival of *M. tuberculosis* and the relatively high chance of resistance development is, however, favored by the sub-optimal dose that is currently used in a standard TB treatment.<sup>(24-31)</sup> Therefore, trials are organized in Africa to validate the application of significantly higher doses of drugs.<sup>(32)</sup> Under the current treatment regimen mutations can occur in the *rpoB* gene, which alters the structure of the RNA-polymerases  $\beta$ -subunit. Genetic alteration of the *rpoB* gene is responsible for >95% of all the rifampicin resistant cases.<sup>(33)</sup>

Next to the acquisition of DNA mutations associated with resistance, *M. tuberculosis* has a variety of features which can contribute to rifampicin tolerance already during the initial exposure.<sup>(34)</sup> One of the most remarkable features is the hydrophobic cell wall of *M. tuberculosis*, they consist of unusual long-chain fatty acids that surround the mycobacteria and provide a high level of resistance to antibiotics.<sup>(35)</sup>



Intrinsic antibiotic resistance in *M. tuberculosis* is further provided by the slow growth rate of the pathogen. Especially in the metabolically hypoactive, non-replicative dormant state of *M. tuberculosis*, induced by the bacilli to evade the host immune response and survive inside the hostile macrophage environment,<sup>(36)</sup> the pathogens becomes more tolerant to several antibiotics, including rifampicin.<sup>(37-42)</sup> The bacteria are far less susceptible during dormancy because the majority of the currently used anti-TB drugs target processes that are involved in cell growth and division.<sup>(40)</sup> Next to intrinsic antibiotic resistance, there is a wide variety of efflux pumps that can translocate toxic compounds from the cytoplasm back into the external environment.<sup>(43)</sup> In fact, in the proteome of Beijing genotype strains specific efflux pumps have been identified, to pre-exist in higher quantities than other studied *M. tuberculosis* genotypes.<sup>(44)</sup> The proteome of *M. tuberculosis* has been explored by several groups to gain information about genomic annotation, protein subcellular localization, virulence factors, environmental stress responses and the impact of rifampicin resistance conferring mutations.<sup>(44-53)</sup> In this study, we examined the proteome to determine whether a drug susceptible isolate of *M. tuberculosis* Beijing B0/W148 uses any of the above mentioned phenotypic mechanisms to cope with rifampicin induced stress during the initial 24 hrs of drug exposure, i.e. the relative impermeable cell wall, adjustment of the metabolic activity and antibiotic extruding efflux pumps. To this end, we determined the temporal dynamics of the proteome and corresponding Ser/Thr/Tyr phosphorylations of *M. tuberculosis* Beijing strain B0/W148 in response to rifampicin. Thereby, we provide evidence that not only resistance acquired by genomic mutations, but also phenotypic drug tolerance mechanisms contribute to in the increasing problem of rifampicin resistance.

## Materials and Methods

### Mycobacterial culture conditions

*M. tuberculosis* B0/W148 was derived from the reference database of clinical isolates at the National Institute for Public Health and the Environment (RIVM) in Bilthoven, the Netherlands (isolate number NLA001100782). Mycobacterial cells were re-cultured from frozen stocks in 5 ml Tween-Albumin liquid culture broth (Tritium Microbiologie, the Netherlands) at 36°C without shaking until an O.D. of 0.4 AU at 600 nm was reached, as described previously.<sup>(44)</sup> One ml of the pre-culture was transferred to a 250 ml Erlenmeyer flask containing 100 ml Tween-Albumin broth and incubated under shaking conditions at 36°C to provide constant aeration. Once the cultures reached an O.D. of 0.6 AU at 600 nm, representing the mid-log phase, the cells were exposed to rifampicin at a concentration of 16 µg/ml or DMSO. Cells were harvested after 1.5, 3, 6, 15 and 24 hrs of exposure by washing three times with ice-cold PBS (Braun, Germany), in 5 ml Lysis-buffer (4% SDS, 100 mM Tris-HCl, pH 7.6) and heat-killed at 95°C for 10 min. Lysates were stored at -20°C until further usage. Biological duplicates and technical replicates were analyzed for each of the assessed time points.

### Rifampicin susceptibility determination

Susceptibility to rifampicin (Sigma Aldrich, the Netherlands) was determined according to Clinical and Laboratory Standards Institute guidelines,<sup>(54)</sup> using the BACTEC MGIT-960 system (Becton, Dickinson and Co., Franklin Lakes, NJ). Mutations in the rifampicin resistance determining region (RRDR) of *rpoB*, the hotspot for drug resistance, were assessed using the MTBDRplus assay according to the manufacturers' recommendations, as described previously.<sup>(55)</sup>

### Mycobacterial viability and culturability determination

To determine mycobacterial viability and ability to multiply after being exposed to rifampicin, 2 ml of mycobacterial cells were taken from a 100 ml culture with varying concentrations of rifampicin. The cells were washed thoroughly to remove rifampicin from the supernatant and dissolved in 2 ml of PBS. Of this suspension, a 200 µl sample was incubated into mycobacterial growth indicator tubes (MGIT) and the time to detection (TTD) was determined using the BACTEC MGIT-960 system (Becton, Dickinson and Co., Franklin Lakes, USA). The remaining cells were heat-killed at 80°C and the ATP content of mycobacterial cells was assessed using the BacTiter-Glo Microbial Cell Viability Assay (Promega, the Netherlands) following the manufacturers' instructions. Biological duplicates and technical triplicates were analysed.

### Protein sample preparation and dimethylation isotope labeling

Two biological duplicates and two technical replicates were analyzed for each of the assessed time points. Proteins were prepared in parallel as described previously.<sup>(44)</sup> In brief,

mycobacterial cell lysates were mechanically disrupted by bead-beating in a mini bead-beater 16 (BioSpec, USA) for 5 min using glass beads. Thereafter, the cells were cooled down on ice for 5 min and the procedure was repeated twice. The cell lysates were cleaned from cell debris by centrifugation for 1 min at 14,000 g and the supernatant was transferred to another tube. Proteins were digested using the filter aided sample preparation (FASP) method.<sup>(56)</sup> In brief, DTT reduced proteins were loaded on a 30 kDa filter. SDS was removed in three washes with 8M urea. The proteins were carbamidomethylated, and the excess reagent was removed by three additional washes with 8M urea. Proteins were then digested overnight using endoproteinase Lys-C (endoLysC), followed by a four hrs digestion using trypsin at RT. Tryptic peptides were desalted on C18 SepPak columns and on column labeled by dimethylation using the “light-” (+28Da) and “medium-label” (+32Da).<sup>(57)</sup> Quantitative proteomic comparisons were performed between cells that were exposed to either DMSO or rifampicin for the same amount of time. A label swap was performed between the biological replicates. An overview of the labelling strategy can be found in Table S1. A total of 100 µg of labeled peptides were fractionated by fractionated by strong cation exchange (SCX) on a Agilent 1100 system equipped with an in-house packed SCX-column (320 µm ID, 15 cm, polysulfoethyl A 3 µm, Poly LC), run at 4 µl/min. The SCX gradient started for 10 min at 100% solvent A (water/acetonitrile/formic acid; 70/30/0.1), after which a linear gradient reached 100% solvent B (250 mM KCl/acetonitrile/formic acid 70/30/0.1) in 15 min, followed by 100% solvent C (500 mM KCl/acetonitrile/formic acid 70/30/0.1) for 15 min. To clean the column, the gradient was held at 100% solvent C for 5 min. Next the column was washed with 100% solvent A. Fifteen fractions were collected in 1 min intervals, lyophilized and reconstituted in 30 µl (water/acetonitrile/formic acid 95/3/0.1) for nanoLC-MS/MS. Analysis was performed by on-line nano-HPLC MS consisting of a Agilent 1100 gradient HPLC system (Agilent, Waldbronn, Germany), and a LTQ-FT Ultra mass spectrometer (Thermo, Bremen, Germany). Of each fraction 5 µl was injected onto a home-made pre-column (100 µm×15 mm; Reprosil-Pur C18-AQ 3 µm, Dr Maisch, Ammerbuch, Germany) and eluted via a home-made analytical nano-HPLC column (15 cm×50 µm; Reprosil-Pur C18-AQ 3 µm). The gradient was run from 0% to 30% solvent B (10/90/0.1 water/acetonitrile/formic acid) in 10-155 min. The end of the nano-HPLC column was drawn to a tip of 5 µm internal diameter and acted as electrospray needle. Full scan FT-ICR MS spectra were collected from 300-1400 m/z with a resolution of 25,000 at a target value of  $5 \times 10^6$ . Data-dependent CID MS/MS was performed of the five most abundant precursors using a normalized collision energy of 35.0 and an isolation width of 2.0 Th. The minimum signal required to trigger an MS2 scan was set to 500. Charge state screening was enabled to reject the acquisition of MS/MS spectra for singly charged precursor ions. A dynamic exclusion duration of 45 seconds was used.

### Phosphopeptide enrichment

Phosphorylated peptides were enriched using Titansphere (GL Sciences, Japan) affinity material

as previously described.<sup>(58)</sup> In short, micro columns were pre-equilibrated by loading 50 µl of TiO<sub>2</sub> loading buffer twice (80% acetonitrile, 6% trifluoroacetic acid and 50 mg/ml dihydroxybenzoic acid). Dimethylated peptides were suspended in 50 µl of loading buffer and loaded onto the micro columns. The columns were sequentially washed with 50 µl of loading buffer followed by two washes with 50% acetonitrile, 0.1% trifluoroacetic acid. The bound peptides were eluted with 25 µl of 5% ammonia which was directly neutralized with 25 µl of 10% formic acid. The samples were cleaned by solid phase extraction on C18 SepPak columns and analyzed by nanoLC-MS/MS as described above.

### Data interpretation

Peptides and proteins were identified and quantified using MaxQuant 1.4.0.3.<sup>(59)</sup> The false discovery rate (FDR) was set to 0.01 for both proteins and peptides. Minimal peptide length was set to six amino acids. A first search was conducted using 20 ppm precursor tolerance, after which the data was corrected for systematic errors by MaxQuant. This re-calibrated dataset was analyzed with 10 ppm precursor mass tolerance in the MaxQuant main search. The MS/MS spectra search was performed with 0.5 Da tolerance using the Andromeda search engine.<sup>(60)</sup> A total of 262 common contaminants were included in the searches by Andromeda. Trypsin specificity was set as C-terminal to arginine and lysine without proline restriction. A maximum of two missed cleavages was allowed. Variable modifications included N-terminal protein acetylation, methionine oxidation, corresponding dimethyl labels, Asn to Asp & Gln to Glu for deamidated peptides and phospho(STY) for the enriched phosphopeptide fractions. Carbamidomethylation of cysteine was selected as a fixed modification. Proteins identified have a minimal peptide count of two unique peptides. All spectra were matched against a FASTA database of *M. tuberculosis* H37Rv (3996 entries).<sup>(61)</sup> Statistical analysis of the outcomes was performed by Perseus using the significance B test with a Benjamini-Hochberg FDR 5%. Proteins considered to be differentially expressed have at least a 1.5-fold ratio<sup>(62)</sup> and a significance B score ≤0.05. In addition, phosphopeptides required a delta score ≥5, Andromeda score ≥60 and a site localization probability ≥0.75. Over 300 raw data files and the MaxQuant output files, which provide access to all annotated spectra, have been deposited to the ProteomeXchange Consortium via the PRIDE partner repository that can be accessed with the dataset identifier PXD002402.

### In solution Auramine-O/Nile Red dual fluorescent staining

Nile Red and auramine-O staining were performed essentially as described previously with some modifications.<sup>(63)</sup> Mycobacterial cells were washed in ice-cold PBS. Subsequently, the pellet was incubated with Phenolic auramine Solution (Sigma Aldrich, the Netherlands) for 15 minutes. The cells were thoroughly washed with PBS and destained using acidic ethanol for 2 min, followed by thorough washes. After auramine-O staining the cells were incubated in Nile Red

(Sigma Aldrich, the Netherlands) followed by thorough washes with PBS and directly analysed using a Glomax-Multi Jr Single tube MultiMode Reader (Promega, USA) with excitation at 525 nm and emission at 580-640 nm for Nile Red staining and excitation at 460nm and emission at 515-570nm for the auramine-O stain.

### **Fluorescence microscopy**

From a mycobacteria culture in mid-logarithmic phase, 25 µl was mixed with 75 µl of PBS and evenly smeared over the surface of glass slides. The sample was allowed to air dry and 200 µl of 70% ethanol was added to fix the bacteria. The slides were flooded with Phenolic auramine Solution (Sigma Aldrich, the Netherlands) for 15 min without drying. Next, the slides were rinsed with distilled water and the excess liquid was shaken off. The slides were flooded with acidic ethanol to decolorize for 2-3 min and thoroughly washed with water. Subsequently, the slides were flooded with Nile Red (Sigma Aldrich, the Netherlands) and incubated for 15 min, followed by a thorough wash with water. Finally, the slides were flooded with potassium permanganate for 3-4 min and rinsed with water. The slides were air dried in the dark and mounted for fluorescence microscopy. Slides were examined with a Zeiss Axioskop 2 fluorescence microscope with an AxioCam HRc camera and Zeiss Axiovision 4.4 software (Zeiss, Germany).

## Results/discussion

### High tolerance to short-term rifampicin treatment in *M. tuberculosis* Beijing B0/W148

Patients with a drug susceptible variant of *M. tuberculosis* are usually treated with rifampicin, one of the most potent first-line anti-TB drugs that is currently available. Rifampicin is administered once a day at a dose of 600 mg for at least six months. Considering its serum half-life of approximately 3 hrs, only  $\pm 0.5\%$  of the initial serum concentration will remain after 24 hrs of rifampicin intake.<sup>(64)</sup> As a consequence, *M. tuberculosis* will essentially be repeatedly pulsed by rifampicin. The initial response of *M. tuberculosis* in the first hours of antibiotic treatment is thereby presumably essential to cope with rifampicin-induced stress.

The administration of high rifampicin doses of 900 mg a day, instead of the commonly prescribed 600 mg, has already been examined in 1968.<sup>(65)</sup> These studies revealed that daily administration of 900 mg rifampicin results in serum concentrations of 16.2  $\mu\text{g/ml}$  3 hrs after intake. To determine whether *M. tuberculosis* Beijing B0/W148 is capable of surviving high doses of 16  $\mu\text{g/ml}$  rifampicin, we exposed the pathogen to various concentrations of rifampicin for 24 hrs. After 24 hrs of treatment we quantified the intracellular ATP concentrations to assess cell viability; Figure 1. Surprisingly, even doses far above 16  $\mu\text{g/ml}$  were tolerated for 24 hrs. To assure that the cells remained culturable<sup>(66)</sup>, and were not beyond survival, we cultured the cells after 24 hrs of rifampicin exposure in MGIT-tubes without antibiotic pressure; Figure 1. To ascertain that the high levels of antibiotic tolerance were not conferred by a mutation in the *rpoB* gene, the primary target of rifampicin, we performed a MTBDR<sub>plus</sub> assay which did not reveal any mutation after 24 hrs exposure to 16  $\mu\text{g/ml}$  rifampicin. These observations demonstrate that *M. tuberculosis* Beijing strain B0/W148 can survive 24 hrs treatment with 16  $\mu\text{g/ml}$  of rifampicin. Since no mutations were identified that confer high levels of rifampicin tolerance, our data suggest that phenotypic tolerance mechanisms play an important role in the initial response to rifampicin.

### Induction of DosR regulon proteins upon exposure of *M. tuberculosis* Beijing B0/W148 to rifampicin

To determine the initial proteomic response of *M. tuberculosis* Beijing B0/W148 upon rifampicin treatment, we exposed the pathogen to a concentration of 16  $\mu\text{g/ml}$  rifampicin. As described above, this concentration is similar to the serum concentrations that can be reached using high dosages of rifampicin during treatment.<sup>(65)</sup> Furthermore, as presented in Figure 1, a concentration of 16  $\mu\text{g/ml}$  does not yield large numbers of dead cells that can compromise our view on the proteome of this pathogen. After 1.5, 3, 6, 15 and 24 hrs of exposure to either rifampicin, or DMSO as a control, the cells were harvested and processed for proteomic analysis as described in the methods section.

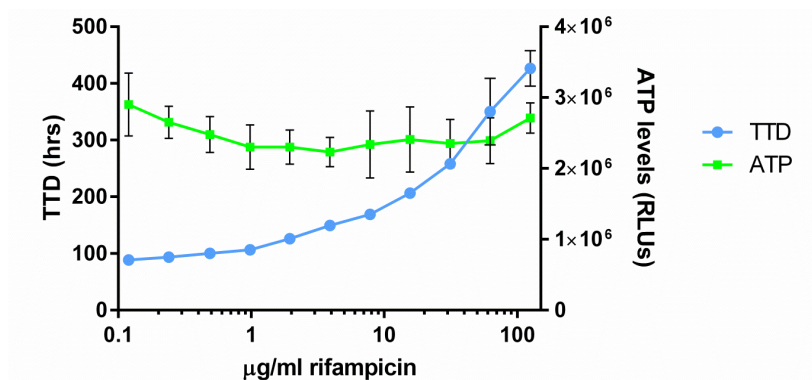


**FIGURE 1:** *M. tuberculosis* Beijing B0/W148 remains culturable after 24 hrs exposure to high concentrations of rifampicin

Viability(ATP) & culturability(TTD) of *M. tuberculosis* Beijing B0/W148 after 24 hrs exposure to rifampicin, after removal of the antibiotic pressure. The culture viability was assessed by quantification of ATP whereas the culturability was determined by inoculating MGIT-tubes with rifampicin treated *M. tuberculosis* in the absence of the drug and measuring the TTD. Biological duplicates and technical triplicates were taken for each of the data points. Error bars represent the standard error of the mean (SEM). Note: the error bars are too small to be visualized for several data points.

We identified and quantified a cumulative number of 30,740 peptides and 2,534 proteins based on at least two unique peptides/proteins, of which 1,828 proteins were quantified at all-time points in both biological replicates; Table S1 & S2. All biological replicates showed a >90% overlap between the proteins identified and quantified. An asymmetrical distribution of protein ratios was observed over time for rifampicin-exposed mycobacteria, i.e. we identified more proteins to be down regulated than up regulated, as an expected consequence of rifampicin dependent RNA-polymerase inhibition; Figure 2 and Figure S1. Since protein stability data for *M. tuberculosis* are not present to date, we cannot state whether proteins are truly down regulated or less abundant due to rifampicin treatment as a result of protein turnover combined with a limited supply of newly synthesized proteins. For example, the relatively rapid decline of Rv3283/sseA could be explained by the predicted relative instability of the protein due to the presence of a, modern Beijing lineage, specific nsNP as we have described previously; Figure S2.<sup>(44, 67)</sup>

Sixty-three proteins were identified to be less abundant after 24 hrs exposure to rifampicin, whereas 10 proteins were up regulated; Table S3. Proteins that were differentially abundant upon 24 hrs of rifampicin treatment were categorized based on their function;<sup>(68)</sup> Figure S3. None of the categories showed to be significantly over- or underrepresented after Chi-square analysis.

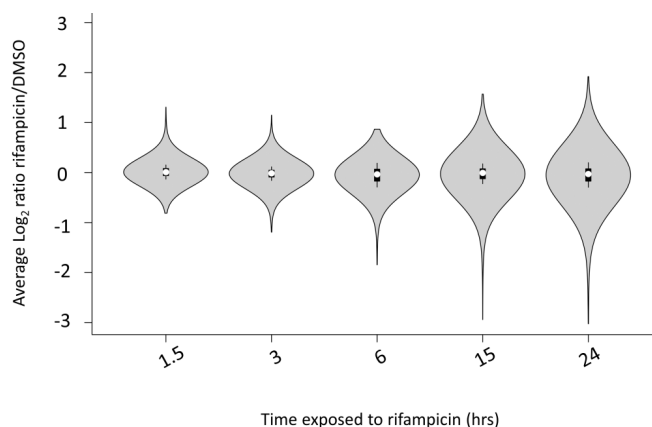


**FIGURE 2: Asymmetrical distribution of protein ratios upon treatment of *M. tuberculosis* Beijing B0/W148 with rifampicin**

A violin-plot(110) representing the average  $\text{Log}_2$  ratio of 1,828 proteins that were quantified at each of the time points analyzed.

Of the 10 proteins that were more abundant upon 24 hrs of rifampicin treatment, six belonged to the DosR dormancy regulon.<sup>(69)</sup> In total, we identified and quantified 23 members of this regulon at all time-points in each of the biological duplicates. The temporal abundance dynamics of 17 of these 23 proteins followed a similar trend; Figure S4.

Most notably is the differential abundance of *Rv2031c/hspX/acr*, which was particularly up regulated within the first 24 hrs of rifampicin treatment. It is known that *Rv2031c/hspX/acr* is one of the earliest and strongest induced DosR genes.<sup>(51, 69, 70)</sup> Furthermore, in a mouse model the *Rv2031c/hspX/acr* knock-out strain showed an increased susceptibility to anti-TB drugs compared to wild-type strains, once treatment was started 3 weeks after infection so dormancy could be established.<sup>(71)</sup>

It has often been speculated that the dormant state of *M. tuberculosis*, which can be induced by the DosR regulon, plays an important role in tolerance towards antibiotics during treatment.<sup>(40, 71-75)</sup> It is however important to note that the induction of dormancy has so far only been observed for environmental stimuli and that this has not been reported for anti-TB drugs in *M. tuberculosis*. A majority of the currently available anti-TB drugs target processes involved in cell growth and division, which can explain why these drugs work less well against metabolically hypoactive, non-replicating mycobacterial cells.<sup>(40)</sup> Next to the lowered effectiveness of antibiotics in metabolically hypoactive mycobacterial cells, it has also been reported that mycobacteria alter their cell envelope during dormancy, which reduces the accumulation of antibiotics.<sup>(76)</sup>



The induction of the DosR regulon proteins upon rifampicin exposure might represent a mechanism of *M. tuberculosis* Beijing B0/W148 to circumvent antibiotic induced stress. However, even though dormancy can be beneficial for *M. tuberculosis* to overcome antibiotic stress, induction of the DosR regulon is not the only and primary mechanism for antibiotic tolerance in the mouse infection models.<sup>(77)</sup> Therefore, we also assessed the abundance of other proteins that could contribute to a more drug tolerable phenotype.

### A POTENTIAL ROLE FOR EFFLUX PUMPS IN RIFAMPICIN TOLERANCE

Other proteins that can play a major role in tolerance and development of antibiotic resistance are antibiotic extruding efflux pumps. A broad variety of these pumps has been identified and can contribute to the active secretion of different types of antibiotics in *M. tuberculosis*.<sup>(43)</sup> In the case of rifampicin, it has been mentioned that the level of drug tolerance can even be defined by the activity of efflux pumps.<sup>(34)</sup> We determined whether any of the efflux pumps that have previously been demonstrated to be induced by rifampicin on the mRNA level or any other of the previously listed efflux pumps<sup>(43)</sup> are differentially regulated upon rifampicin treatment in *M. tuberculosis* B0/W148.

In our dataset of 1,828 proteins we quantified 12 of the previously listed 31 efflux pumps, including Rv1747 & Rv1002c, which were reported to be involved in the response to rifampicin.<sup>(34)</sup> However, none of these efflux pumps showed to be differentially abundant after up to 24 hrs of rifampicin treatment; Table S1.

As we previously proposed, efflux pumps might pre-exist at higher levels of activity in several modern Beijing strains, including the modern Beijing strain B0/W148 used in this study.<sup>(44)</sup> The fact that none of these efflux pumps are differentially regulated does, therefore, not necessarily indicate that efflux mediated rifampicin tolerance does not play a role in *M. tuberculosis* Beijing B0/W148. When we examined the B0/W148 cluster specific nsSNPs that were reported previously regarding their possible influence on protein expression,<sup>(78)</sup> we identified two efflux pump coding genes to possess a nsSNP that can affect the function or stability of these proteins; Rv1877&Rv3728. Taken together, on the basis of our data we can neither exclude, nor include efflux pumps to play an important role in rifampicin tolerance in Beijing B0/W148. However, based on the proteins that we identified to be differentially regulated it seems that the synthesis of DosR regulated proteins is prioritized by the pathogen.

### RIFAMPICIN INDUCED CHANGES IN PROTEIN PHOSPHORYLATION

Reversible phosphorylation is a major regulatory modification which allows both eukaryotic and prokaryotic cells to sense and respond to their environment. In *M. tuberculosis*, the existence of phosphorylation on Ser, Thr, and recently also Tyr has been described, although the function and regulation of specific phosphorylation sites is lacking.<sup>(79-81)</sup> Therefore, we performed a large-

scale quantitative study to investigate the role of Ser/Thr/Tyr phosphorylation in *M. tuberculosis* in response to rifampicin.

In this study, we identified a cumulative number of 191 phosphorylation sites corresponding to 180 phosphopeptides, which mapped to 132 unique proteins; Table S4. Approximately 93% of the identified phosphopeptides contained a single phosphorylated residue, whereas 7% contained two phosphorylation sites; Figure S5. This might be due to the use of TiO<sub>2</sub>, which has a preference for monophosphorylated peptides.<sup>(82)</sup> The observed ratio Ser/Thr/Tyr was 22/76/2. This confirms that phosphorylation in *M. tuberculosis* is biased towards Threonine,<sup>(79)</sup> whereas phospho-Serine is predominant in eukaryotes, *Bacillus subtilis*, *Escherichia coli* and *Pseudomonas* species.<sup>(58, 83-87)</sup>

We observed that phosphorylation of Rv2187, Rv2534, Rv2986c and Rv3458c changed over time, independent of their respective protein kinetics; Figure 3. To confirm the identity of these phosphopeptides we compared the fragmentation spectra with those acquired from synthetic peptides; Figure S6A-H.

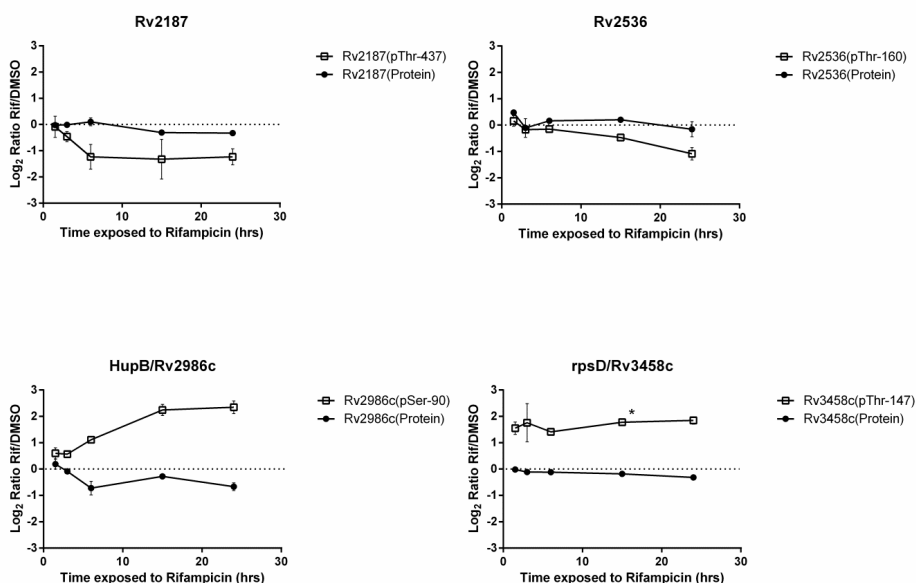


**FIGURE 3: Protein and phosphorylation dynamics during rifampicin exposure.**

Protein (black filled dots) and phosphorylation (white squares) dynamics of Rv2187(Thr-437), Rv2536(Thr-160), Rv2986c(Ser-90) and Rv3458c(Thr-147) during rifampicin exposure. Error bars represent the SEM. \*Was identified in a single biological replicate for T=15hr. Note: the error bars are too small to be displayed for several data points.

The phosphorylation on both Rv2187 & Rv2536 was observed to be down regulated during rifampicin treatment. Rv2187 & Rv2536 have been reported to be differentially regulated upon treatment with erythromycin and streptomycin.<sup>(88)</sup> Both streptomycin and erythromycin are translational inhibitors, whereas rifampicin is known to be a transcriptional inhibitor. As transcription and translation are both essential for protein synthesis we hypothesize that the differential phosphorylation of Rv2187 & Rv2536 is involved in a general response to inhibitors of protein synthesis.

HupB/Rv2986c was the first histone-like protein to be described in *M. tuberculosis* and is capable of binding mycobacterial DNA.<sup>(89)</sup> In this study, we demonstrate that HupB/Rv2986c is increasingly phosphorylated on Ser-90 upon rifampicin treatment; Figure 3. In the presence of iron, HupB/Rv2986c binds the mbtB/Rv2383c promoter.<sup>(90)</sup> Thereby, HupB/Rv2986c, also known as iron-regulated protein (Irep-28),<sup>(91)</sup> can positively regulate the biosynthesis of siderophores which are necessary for the uptake of iron by mycobacteria. We previously established a connection between the success of Beijing strains and the uptake of iron by siderophores.<sup>(44)</sup> Secretion of siderophores is carried out by either Rv0450c/MmpL4, together with Rv0451c/MmpS4, or Rv0677c/MmpS5 together with Rv0676c/MmpL5 in *M. tuberculosis*.<sup>(92)</sup> It is known that modern Beijing strains contain a unique nsSNP in Rv0676c/MmpL5 and consistently over-express Rv0450c/MmpL4.<sup>(44, 93)</sup> The increasing phosphorylation of HupB/Rv2986c fits the overall picture that iron metabolism plays a role in the success of *M. tuberculosis* Beijing. Finally, iron-sequestration has previously been linked to antibiotic tolerance, as the growth inhibitory effects of rifampicin is slightly reversible in the presence of high concentrations of iron and the concentration of siderophores increases in the presence of rifampicin.<sup>(94)</sup> In line with the induction of the dormancy regulon, it has been proposed that *M. tuberculosis* attempts to increase iron-storages for long periods of dormancy.<sup>(95)</sup>

Next to the role of HupB/Rv2946c in the storage of iron and its possible role in dormancy, we also observed increased levels of phosphorylated rpsD/Rv3458c. Similar to HupB/Rv2946c, rpsD/Rv3458c is important to cope with high levels of iron.<sup>(96)</sup> Finally, rpsD/Rv3458c is induced when *M. tuberculosis* enters stationary phase.<sup>(97)</sup>

### **Rifampicin induces a more dormant phenotype in *M. tuberculosis* Beijing B0/W148**

The differential regulation of DosR regulon proteins and the increased phosphorylation of HupB/Rv2986c & rpsD/Rv3458c both point towards a role for dormancy during rifampicin exposure. Previous studies have identified host and environmental factors that can induce dormancy in *M. tuberculosis*.<sup>(39, 98)</sup> However, our (phospho)proteomic data suggest that a drug, rifampicin, itself, can induce dormancy, which would be a completely novel stimulus for the induction of dormancy. The confirmation of this observation would be of direct clinical relevance, since

modern day antibiotic susceptibility testing assays focus on the growth inhibitory concentration of drugs. However, these methods do not take into account that growth can be brought to a halt due to the induction of dormancy. As a consequence, the capability of strains to survive high levels of rifampicin due to dormancy will not be noticed using standard drug susceptibility testing protocols.

The increased abundance of DosR proteins is a strong indication that the pathogen transitioned to a dormant phenotype upon exposure to rifampicin. However, the regulation of DosR proteins is not sufficient to conclude that the cell will enter a non-replicative dormant state. To independently confirm the induction of dormancy upon rifampicin treatment we examined long term persisters of rifampicin treatment, e.g. cells that remained viable after a week of rifampicin treatment. The accumulation of intracytoplasmic lipid inclusions, as indicated by Nile Red, the loss of acid fastness as measured by Auramine-O, the arrest of bacterial multiplication (OD<sub>600nm</sub>, TTD) and the decrease in ATP levels are considered to be hallmarks of dormancy, and were therefore previously assessed in rifampicin-treated *M. tuberculosis*.<sup>(39, 63, 99, 100)</sup>

Treatment of *M. tuberculosis* Beijing B0/W148 with rifampicin brought the growth to a halt, as assessed by optical density; Figure S7A. As examined by the MGIT-assay, culturable cells remained. Striking is the fact that the MIC of 0,0625 µg/ml observed in this study is, even after seven days exposure, not sterilizing. When we increased the MIC 256-fold to 16 µg/ml and exposed the mycobacteria for seven days, we could still detect viable and culturable cells that did not contain a mutation in *rpoB*, which is a strong indication for phenotypic antibiotic tolerance.

If *M. tuberculosis* truly enters dormancy, it would not only bring replication to a halt, but also the concentration of ATP is reported to be 5-fold lowered in the Wayne dormancy model.<sup>(101)</sup> In our approach, we observed a ±10-fold reduction in ATP after a seven-day long treatment with ≥ 0.25 µg/ml rifampicin; Figure S7C. These results strengthen our hypothesis that rifampicin treatment induces dormancy in this strain. The witnessed 10-fold reduction in ATP-levels during rifampicin treatment is not lethal for *M. tuberculosis*. A further reduction of these ATP-levels can be achieved with the use of bedaquiline, which will eventually be fatal for dormant mycobacteria.<sup>(102, 103)</sup>

To further confirm that a dormant phenotype is established by *M. tuberculosis* Beijing B0/W148, we examined the loss of acid-fast staining and accumulation of Nile Red-staining lipid droplets, a well-studied phenotype of dormancy in *M. tuberculosis*.<sup>(39, 63, 99, 100)</sup> Similar to the ATP concentrations determined, there was no dose-response observed in the Nile Red/Auramine stain for rifampicin concentrations ≥ 0.25 µg/ml; Figure S7D. The relative increase of lipid bodies

supports our hypothesis that dormancy is indeed induced upon exposure to rifampicin in this particular pathogen.

Interestingly, actively dividing, mid-logarithmic mycobacterial cells of *M. tuberculosis* Beijing B0/W148 already retained Nile Red; Figure 4. This pre-existent dormant phenotype in the examined *M. tuberculosis* W-Beijing strain adds to a previous study that reported increased levels of triglycerides and elevated levels of mRNA for DosR regulon genes within this specific genotype.<sup>(104)</sup> Therefore, it seems that *M. tuberculosis* W-Beijing strains can more easily enter a phase of dormancy once it encounters stress factors. Moreover, a less complicated transition to dormancy could explain why Beijing strains are more tolerant to transient drug treatment than *M. tuberculosis* H37Ra and East African-Indian strains.<sup>(105)</sup>

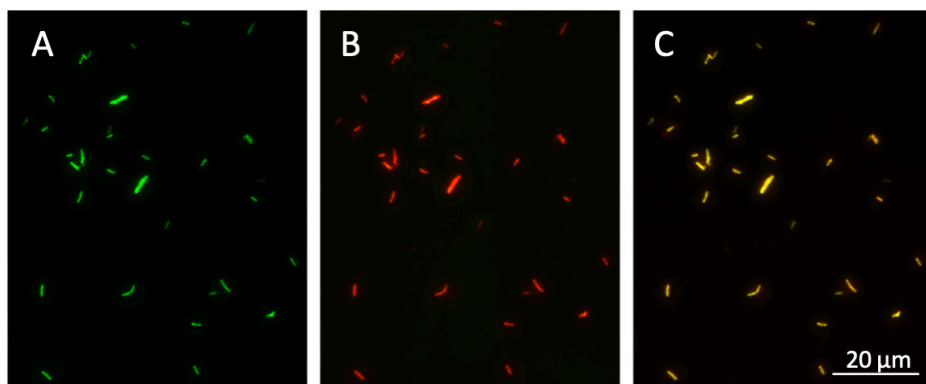


**FIGURE 4: Pre-existence of a dormant phenotype in *M. tuberculosis* Beijing B0/W148.**

A) Acid-fast Auramine-O staining of *M. tuberculosis* Beijing B0/W148.

B) Nile Red staining of intracellular lipid droplets in *M. tuberculosis* Beijing B0/W148.

C) Overlay of Auramine and Nile Red staining shows the pre-existence of a dormant phenotype in all *M. tuberculosis* B0/W148 cells.

Taken together, our study provides evidence that a clinically relevant dose of rifampicin is not sufficient to kill these Beijing genotype mycobacteria, even at high concentrations. Instead, a dormant phenotype is established upon treatment. Metabolic shutdown, as part of dormancy, severely hampers the success of antibiotic treatment for this pathogen and it is questionable whether higher dosage of rifampicin will overcome this effect. The induction of dormancy by *M. tuberculosis* Beijing B0/W148 might thereby be a successful route to cope with antibiotic pressure.

The observation that not only environmentally induced stress, but also drug induced stress can lead to dormancy suggest that the DosR-regulon functions as a general stress response mechanism. This hypothesis is further strengthened by a previous study which showed the induction of DosR proteins upon bedaquiline exposure.<sup>(103)</sup> Therefore this findings might be extended to other (first-line) antibiotics.

The correlation between an established dormant phenotype and antibiotic tolerance is well accepted, but it remains speculative how dormancy can contribute to the development of a rifampicin resistant genotype. It has long been assumed that rifampicin resistance occurs spontaneously due to chromosomal mutations.<sup>(106)</sup> Surprisingly, the mutation rates of *M. tuberculosis* are similar during active and latent disease in a macaques model.<sup>(107)</sup> These mutation rates were similar to those identified by sequencing of human isolates.<sup>(108)</sup> Since the *M. tuberculosis* mutation rate per-time is similar between active and latent disease, *rpoB* mutations can be acquired during prolonged periods of dormancy, a phase that could last for years in which the pathogen is highly tolerant to antibiotics.<sup>(109)</sup>

## Conclusions

Modern, state of the art molecular diagnostics focus on the identification of genotypic markers of antibiotic resistance. In this study we demonstrated that the initial high rifampicin tolerance of the successful Russian *M. tuberculosis* Beijing B0/W148 strain is not acquired due to a mutation in the *rpoB* gene. Instead, the outcome of our (phospho)proteomic- and cellular studies show that phenotypic drug tolerance, caused by the induction of dormancy, plays an important role in *M. tuberculosis* Beijing B0/W148 during the initial phase of rifampicin exposure. Knowledge of the phenotypic mechanisms operative in *M. tuberculosis* will contribute to a more effective form of treatment for the 8-9 million individuals that receive anti-TB therapy annually.

## References

1. WHO, Global tuberculosis report 2013. . **2013**.
2. Schurch, A. C.; van Soolingen, D., DNA fingerprinting of *Mycobacterium tuberculosis*: from phage typing to whole-genome sequencing. *Infect Genet Evol* **2012**, 12, (4), 602-9.
3. Brosch, R.; Gordon, S. V.; Marmiesse, M.; Brodin, P.; Buchrieser, C.; Eiglmeier, K.; Garnier, T.; Gutierrez, C.; Hewinson, G.; Kremer, K.; Parsons, L. M.; Pym, A. S.; Samper, S.; van Soolingen, D.; Cole, S. T., A new evolutionary scenario for the *Mycobacterium tuberculosis* complex. *Proc Natl Acad Sci U S A* **2002**, 99, (6), 3684-9.
4. Hershberg, R.; Lipatov, M.; Small, P. M.; Sheffer, H.; Niemann, S.; Homolka, S.; Roach, J. C.; Kremer, K.; Petrov, D. A.; Feldman, M. W.; Gagneux, S., High functional diversity in *Mycobacterium tuberculosis* driven by genetic drift and human demography. *PLoS Biol* **2008**, 6, (12), e311.
5. van Soolingen, D.; Qian, L.; de Haas, P. E.; Douglas, J. T.; Traore, H.; Portaels, F.; Qing, H. Z.; Enkhsaikan, D.; Nymadawa, P.; van Embden, J. D., Predominance of a single genotype of *Mycobacterium tuberculosis* in countries of east Asia. *J Clin Microbiol* **1995**, 33, (12), 3234-8.
6. Glynn, J. R.; Whiteley, J.; Bifani, P. J.; Kremer, K.; van Soolingen, D., Worldwide occurrence of Beijing/W strains of *Mycobacterium tuberculosis*: a systematic review. *Emerg Infect Dis* **2002**, 8, (8), 843-9.
7. Parwati, I.; Alisjahbana, B.; Apriani, L.; Soetikno, R. D.; Ottenhoff, T. H.; van der Zanden, A. G.; van der Meer, J.; van Soolingen, D.; van Crevel, R., *Mycobacterium tuberculosis* Beijing genotype is an independent risk factor for tuberculosis treatment failure in Indonesia. *J Infect Dis* **2010**, 201, (4), 553-7.
8. Kremer, K.; Glynn, J. R.; Lillebaek, T.; Niemann, S.; Kurepina, N. E.; Kreiswirth, B. N.; Bifani, P. J.; van Soolingen, D., Definition of the Beijing/W lineage of *Mycobacterium tuberculosis* on the basis of genetic markers. *J Clin Microbiol* **2004**, 42, (9), 4040-9.
9. Devaux, I.; Kremer, K.; Heersma, H.; Van Soolingen, D., Clusters of multidrug-resistant *Mycobacterium tuberculosis* cases, Europe. *Emerg Infect Dis* **2009**, 15, (7), 1052-60.
10. Buu, T. N.; Huyen, M. N.; Lan, N. T.; Quy, H. T.; Hen, N. V.; Zignol, M.; Borgdorff, M. W.; Cobelens, F. G.; van Soolingen, D., The Beijing genotype is associated with young age and multidrug-resistant tuberculosis in rural Vietnam. *Int J Tuberc Lung Dis* **2009**, 13, (7), 900-6.
11. Buu, T. N.; van Soolingen, D.; Huyen, M. N.; Lan, N. T.; Quy, H. T.; Tiemersma, E. W.; Kremer, K.; Borgdorff, M. W.; Cobelens, F. G., Increased transmission of *Mycobacterium tuberculosis* Beijing genotype strains associated with resistance to streptomycin: a population-based study. *PLoS One* **2012**, 7, (8), e42323.
12. Dong, H.; Shi, L.; Zhao, X.; Sang, B.; Lv, B.; Liu, Z.; Wan, K., Genetic diversity of *Mycobacterium tuberculosis* isolates from Tibetans in Tibet, China. *PLoS One* **2012**, 7, (3), e33904.
13. Yu, Q.; Su, Y.; Lu, B.; Ma, Y.; Zhao, X.; Yang, X.; Dong, H.; Liu, Y.; Lian, L.; Wan, L.; Wu, Y.; Wan, K., Genetic diversity of *Mycobacterium tuberculosis* isolates from Inner Mongolia, China. *PLoS One* **2013**, 8, (5), e57660.
14. Casali, N.; Nikolayevskyy, V.; Balabanova, Y.; Ignatyeva, O.; Kontsevaya, I.; Harris, S. R.; Bentley, S. D.;

- Parkhill, J.; Nejentsev, S.; Hoffner, S. E.; Horstmann, R. D.; Brown, T.; Drobniewski, F., Microevolution of extensively drug-resistant tuberculosis in Russia. *Genome Res* **2012**, 22, (4), 735-45.
15. Johnson, R.; Warren, R. M.; van der Spuy, G. D.; Gey van Pittius, N. C.; Theron, D.; Streicher, E. M.; Bosman, M.; Coetzee, G. J.; van Helden, P. D.; Victor, T. C., Drug-resistant tuberculosis epidemic in the Western Cape driven by a virulent Beijing genotype strain. *Int J Tuberc Lung Dis* **2010**, 14, (1), 119-21.
  16. European Concerted Action on New Generation Genetic, M.; Techniques for the, E.; Control of, T., Beijing/W genotype Mycobacterium tuberculosis and drug resistance. *Emerg Infect Dis* **2006**, 12, (5), 736-43.
  17. Devaux, I.; Manissero, D.; Fernandez de la Hoz, K.; Kremer, K.; van Soolingen, D.; Euro, T. B. n., Surveillance of extensively drug-resistant tuberculosis in Europe, 2003-2007. *Euro Surveill* **2010**, 15, (11).
  18. Mokrousov, I., Insights into the origin, emergence, and current spread of a successful Russian clone of Mycobacterium tuberculosis. *Clin Microbiol Rev* **2013**, 26, (2), 342-60.
  19. Lasunskaja, E.; Ribeiro, S. C.; Manicheva, O.; Gomes, L. L.; Suffys, P. N.; Mokrousov, I.; Ferrazoli, L.; Andrade, M. R.; Kritski, A.; Otten, T.; Kipnis, T. L.; da Silva, W. D.; Vishnevsky, B.; Oliveira, M. M.; Gomes, H. M.; Baptista, I. F.; Narvskaia, O., Emerging multidrug resistant Mycobacterium tuberculosis strains of the Beijing genotype circulating in Russia express a pattern of biological properties associated with enhanced virulence. *Microbes Infect* **2010**, 12, (6), 467-75.
  20. Marttila, H. J.; Soini, H.; Eerola, E.; Vyshnevskaya, E.; Vyshnevskiy, B. I.; Otten, T. F.; Vasilyef, A. V.; Viljanen, M. K., A Ser315Thr substitution in KatG is predominant in genetically heterogeneous multidrug-resistant Mycobacterium tuberculosis isolates originating from the St. Petersburg area in Russia. *Antimicrob Agents Chemother* **1998**, 42, (9), 2443-5.
  21. Dubiley, S.; Ignatova, A.; Mukhina, T.; Nizova, A.; Blagodatskikh, S.; Stepanshina, V.; Shemyakin, I., Molecular epidemiology of tuberculosis in the Tula area, Central Russia, before the introduction of the Directly Observed Therapy Strategy. *Clin Microbiol Infect* **2010**, 16, (9), 1421-6.
  22. Pardini, M.; Niemann, S.; Varaine, F.; Iona, E.; Meacci, F.; Orru, G.; Yesilkaya, H.; Jarosz, T.; Andrew, P.; Barer, M.; Checchi, F.; Rinder, H.; Orefici, G.; Rusch-Gerdes, S.; Fattorini, L.; Oggioni, M. R.; Bonnet, M., Characteristics of drug-resistant tuberculosis in Abkhazia (Georgia), a high-prevalence area in Eastern Europe. *Tuberculosis (Edinb)* **2009**, 89, (4), 317-24.
  23. Narvskaia, O.; Otten, T.; Limeschenko, E.; Sapozhnikova, N.; Graschenkova, O.; Steklova, L.; Nikonova, A.; Filipenko, M. L.; Mokrousov, I.; Vyshnevskiy, B., Nosocomial outbreak of multidrug-resistant tuberculosis caused by a strain of Mycobacterium tuberculosis W-Beijing family in St. Petersburg, Russia. *Eur J Clin Microbiol Infect Dis* **2002**, 21, (8), 596-602.
  24. de Steenwinkel, J. E.; Aarnoutse, R. E.; de Knecht, G. J.; ten Kate, M. T.; Teulen, M.; Verbrugh, H. A.; Boeree, M. J.; van Soolingen, D.; Bakker-Woudenberg, I. A., Optimization of the rifampin dosage to improve the therapeutic efficacy in tuberculosis treatment using a murine model. *Am J Respir Crit Care Med* **2013**, 187, (10), 1127-34.
  25. Steingart, K. R.; Jotblad, S.; Robsky, K.; Deck, D.; Hopewell, P. C.; Huang, D.; Nahid, P., Higher-dose



rifampin for the treatment of pulmonary tuberculosis: a systematic review. *Int J Tuberc Lung Dis* **2011**, 15, (3), 305-16.

26. Mitchison, D. A., Role of individual drugs in the chemotherapy of tuberculosis. *Int J Tuberc Lung Dis* **2000**, 4, (9), 796-806.
27. Jayaram, R.; Gaonkar, S.; Kaur, P.; Suresh, B. L.; Mahesh, B. N.; Jayashree, R.; Nandi, V.; Bharat, S.; Shandil, R. K.; Kantharaj, E.; Balasubramanian, V., Pharmacokinetics-pharmacodynamics of rifampin in an aerosol infection model of tuberculosis. *Antimicrob Agents Chemother* **2003**, 47, (7), 2118-24.
28. Diacon, A. H.; Patientia, R. F.; Venter, A.; van Helden, P. D.; Smith, P. J.; McIlleron, H.; Maritz, J. S.; Donald, P. R., Early bactericidal activity of high-dose rifampin in patients with pulmonary tuberculosis evidenced by positive sputum smears. *Antimicrob Agents Chemother* **2007**, 51, (8), 2994-6.
29. Ruslami, R.; Nijland, H. M.; Alisjahbana, B.; Parwati, I.; van Crevel, R.; Aarnoutse, R. E., Pharmacokinetics and tolerability of a higher rifampin dose versus the standard dose in pulmonary tuberculosis patients. *Antimicrob Agents Chemother* **2007**, 51, (7), 2546-51.
30. Ruslami, R.; Ganiem, A. R.; Dian, S.; Apriani, L.; Achmad, T. H.; van der Ven, A. J.; Borm, G.; Aarnoutse, R. E.; van Crevel, R., Intensified regimen containing rifampicin and moxifloxacin for tuberculous meningitis: an open-label, randomised controlled phase 2 trial. *Lancet Infect Dis* **2013**, 13, (1), 27-35.
31. Rosenthal, I. M.; Tasneen, R.; Peloquin, C. A.; Zhang, M.; Almeida, D.; Mdluli, K. E.; Karakousis, P. C.; Grosset, J. H.; Nuermberger, E. L., Dose-ranging comparison of rifampin and rifapentine in two pathologically distinct murine models of tuberculosis. *Antimicrob Agents Chemother* **2012**, 56, (8), 4331-40.
32. Boeree, M. J.; Diacon, A. H.; Dawson, R.; Narunsky, K.; du Bois, J.; Venter, A.; Phillips, P. P.; Gillespie, S. H.; McHugh, T. D.; Hoelscher, M.; Heinrich, N.; Rehal, S.; van Soolingen, D.; van Ingen, J.; Magis-Escurra, C.; Burger, D.; Plemper van Balen, G.; Aarnoutse, R. E.; Pan, A. C., A dose-ranging trial to optimize the dose of rifampin in the treatment of tuberculosis. *Am J Respir Crit Care Med* **2015**, 191, (9), 1058-65.
33. Somoskovi, A.; Parsons, L. M.; Salfinger, M., The molecular basis of resistance to isoniazid, rifampin, and pyrazinamide in *Mycobacterium tuberculosis*. *Respir Res* **2001**, 2, (3), 164-8.
34. Louw, G. E.; Warren, R. M.; Gey van Pittius, N. C.; Leon, R.; Jimenez, A.; Hernandez-Pando, R.; McEvoy, C. R.; Grobbelaar, M.; Murray, M.; van Helden, P. D.; Victor, T. C., Rifampicin reduces susceptibility to ofloxacin in rifampicin-resistant *Mycobacterium tuberculosis* through efflux. *Am J Respir Crit Care Med* **2011**, 184, (2), 269-76.
35. Daffe, M.; Draper, P., The envelope layers of mycobacteria with reference to their pathogenicity. *Adv Microb Physiol* **1998**, 39, 131-203.
36. Wayne, L. G.; Sohaskey, C. D., Nonreplicating persistence of mycobacterium tuberculosis. *Annu Rev Microbiol* **2001**, 55, 139-63.
37. Xie, Z.; Siddiqi, N.; Rubin, E. J., Differential antibiotic susceptibilities of starved *Mycobacterium tuberculosis* isolates. *Antimicrob Agents Chemother* **2005**, 49, (11), 4778-80.
38. de Steenwinkel, J. E.; de Knecht, G. J.; ten Kate, M. T.; van Belkum, A.; Verbrugh, H. A.; Kremer, K.; van Soolingen, D.; Bakker-Woudenberg, I. A., Time-kill kinetics of anti-tuberculosis drugs, and emergence

- of resistance, in relation to metabolic activity of *Mycobacterium tuberculosis*. *J Antimicrob Chemother* **2010**, 65, (12), 2582-9.
39. Deb, C.; Lee, C. M.; Dubey, V. S.; Daniel, J.; Abomoelak, B.; Sirakova, T. D.; Pawar, S.; Rogers, L.; Kolattukudy, P. E., A novel in vitro multiple-stress dormancy model for *Mycobacterium tuberculosis* generates a lipid-loaded, drug-tolerant, dormant pathogen. *PLoS One* **2009**, 4, (6), e6077.
  40. Gomez, J. E.; McKinney, J. D., M. tuberculosis persistence, latency, and drug tolerance. *Tuberculosis (Edinb)* **2004**, 84, (1-2), 29-44.
  41. Zahrt, T. C., Molecular mechanisms regulating persistent *Mycobacterium tuberculosis* infection. *Microbes Infect* **2003**, 5, (2), 159-67.
  42. Kapoor, N.; Pawar, S.; Sirakova, T. D.; Deb, C.; Warren, W. L.; Kolattukudy, P. E., Human granuloma in vitro model, for TB dormancy and resuscitation. *PLoS One* **2013**, 8, (1), e53657.
  43. Louw, G. E.; Warren, R. M.; Gey van Pittius, N. C.; McEvoy, C. R.; Van Helden, P. D.; Victor, T. C., A balancing act: efflux/influx in mycobacterial drug resistance. *Antimicrob Agents Chemother* **2009**, 53, (8), 3181-9.
  44. de Keijzer, J.; de Haas, P. E.; de Ru, A. H.; van Veelen, P. A.; van Soolingen, D., Disclosure of selective advantages in the 'modern' sublineage of the *Mycobacterium tuberculosis* Beijing genotype family by quantitative proteomics. *Mol Cell Proteomics* **2014**.
  45. de Souza, G. A.; Fortuin, S.; Aguilar, D.; Pando, R. H.; McEvoy, C. R.; van Helden, P. D.; Koehler, C. J.; Thiede, B.; Warren, R. M.; Wiker, H. G., Using a label-free proteomics method to identify differentially abundant proteins in closely related hypo- and hypervirulent clinical *Mycobacterium tuberculosis* Beijing isolates. *Mol Cell Proteomics* **2010**, 9, (11), 2414-23.
  46. de Souza, G. A.; Arntzen, M. O.; Fortuin, S.; Schurch, A. C.; Malen, H.; McEvoy, C. R.; van Soolingen, D.; Thiede, B.; Warren, R. M.; Wiker, H. G., Proteogenomic analysis of polymorphisms and gene annotation divergences in prokaryotes using a clustered mass spectrometry-friendly database. *Mol Cell Proteomics* **2011**, 10, (1), M110 002527.
  47. Malen, H.; Pathak, S.; Softeland, T.; de Souza, G. A.; Wiker, H. G., Definition of novel cell envelope associated proteins in Triton X-114 extracts of *Mycobacterium tuberculosis* H37Rv. *BMC Microbiol* **2010**, 10, 132.
  48. de Souza, G. A.; Malen, H.; Softeland, T.; Saelensminde, G.; Prasad, S.; Jonassen, I.; Wiker, H. G., High accuracy mass spectrometry analysis as a tool to verify and improve gene annotation using *Mycobacterium tuberculosis* as an example. *BMC Genomics* **2008**, 9, 316.
  49. Yu, Y.; Jin, D.; Hu, S.; Zhang, Y.; Zheng, X.; Zheng, J.; Liao, M.; Chen, X.; Graner, M.; Liu, H.; Jin, Q., A novel tuberculosis antigen identified from human tuberculosis granulomas. *Mol Cell Proteomics* **2015**, 14, (4), 1093-103.
  50. Albrethsen, J.; Agner, J.; Piersma, S. R.; Hojrup, P.; Pham, T. V.; Weldingh, K.; Jimenez, C. R.; Andersen, P.; Rosenkrands, I., Proteomic profiling of *Mycobacterium tuberculosis* identifies nutrient-starvation-responsive toxin-antitoxin systems. *Mol Cell Proteomics* **2013**, 12, (5), 1180-91.
  51. Gopinath, V.; Raghunandan, S.; Gomez, R. L.; Jose, L.; Surendran, A.; Ramachandran, R.; Pushparajan,

- A. R.; Mundayoor, S.; Jaleel, A.; Kumar, R. A., Profiling the proteome of *Mycobacterium tuberculosis* during dormancy and reactivation. *Mol Cell Proteomics* **2015**.
52. Bisson, G. P.; Mehaffy, C.; Broeckling, C.; Prenni, J.; Rifat, D.; Lun, D. S.; Burgos, M.; Weissman, D.; Karakousis, P. C.; Dobos, K., Upregulation of the phthiocerol dimycocerosate biosynthetic pathway by rifampin-resistant, *rpoB* mutant *Mycobacterium tuberculosis*. *J Bacteriol* **2012**, 194, (23), 6441-52.
  53. Singh, A.; Gopinath, K.; Sharma, P.; Bisht, D.; Sharma, P.; Singh, N.; Singh, S., Comparative proteomic analysis of sequential isolates of *Mycobacterium tuberculosis* from a patient with pulmonary tuberculosis turning from drug sensitive to multidrug resistant. *Indian J Med Res* **2015**, 141, (1), 27-45.
  54. Woods, G. L.; Brown-Elliott, B. A.; Desmond, E. P.; Hall, G. S.; Heifets, L.; Pfyffer, G. E.; Ridderhof, J. C.; Wallace, R. J.; Warren, N. G.; Witebsky, F. G., Susceptibility Testing of *Mycobacteria*, *Nocardiae*, and Other Aerobic Actinomycetes; Approved Standard, second edition. *Clinical and Laboratory Standards Institute* **2011**.
  55. Huyen, M. N.; Tiemersma, E. W.; Lan, N. T.; Cobelens, F. G.; Dung, N. H.; Sy, D. N.; Buu, T. N.; Kremer, K.; Hang, P. T.; Caws, M.; O'Brien, R.; van Soolingen, D., Validation of the GenoType MTBDRplus assay for diagnosis of multidrug resistant tuberculosis in South Vietnam. *BMC Infect Dis* **2010**, 10, 149.
  56. Wisniewski, J. R.; Zougman, A.; Nagaraj, N.; Mann, M., Universal sample preparation method for proteome analysis. *Nat Methods* **2009**, 6, (5), 359-62.
  57. Boersema, P. J.; Raijmakers, R.; Lemeer, S.; Mohammed, S.; Heck, A. J., Multiplex peptide stable isotope dimethyl labeling for quantitative proteomics. *Nat Protoc* **2009**, 4, (4), 484-94.
  58. Zhou, H.; Low, T. Y.; Hennrich, M. L.; van der Toorn, H.; Schwend, T.; Zou, H.; Mohammed, S.; Heck, A. J., Enhancing the identification of phosphopeptides from putative basophilic kinase substrates using Ti (IV) based IMAC enrichment. *Mol Cell Proteomics* **2011**, 10, (10), M110 006452.
  59. Cox, J.; Mann, M., MaxQuant enables high peptide identification rates, individualized p.p.b.-range mass accuracies and proteome-wide protein quantification. *Nat Biotechnol* **2008**, 26, (12), 1367-72.
  60. Cox, J.; Neuhauser, N.; Michalski, A.; Scheltema, R. A.; Olsen, J. V.; Mann, M., Andromeda: a peptide search engine integrated into the MaxQuant environment. *J Proteome Res* **2011**, 10, (4), 1794-805.
  61. Cole, S. T.; Brosch, R.; Parkhill, J.; Garnier, T.; Churcher, C.; Harris, D.; Gordon, S. V.; Eiglmeier, K.; Gas, S.; Barry, C. E., 3rd; Tekaia, F.; Badcock, K.; Basham, D.; Brown, D.; Chillingworth, T.; Connor, R.; Davies, R.; Devlin, K.; Feltwell, T.; Gentles, S.; Hamlin, N.; Holroyd, S.; Hornsby, T.; Jagels, K.; Krogh, A.; McLean, J.; Moule, S.; Murphy, L.; Oliver, K.; Osborne, J.; Quail, M. A.; Rajandream, M. A.; Rogers, J.; Rutter, S.; Seeger, K.; Skelton, J.; Squares, R.; Squares, S.; Sulston, J. E.; Taylor, K.; Whitehead, S.; Barrell, B. G., Deciphering the biology of *Mycobacterium tuberculosis* from the complete genome sequence. *Nature* **1998**, 393, (6685), 537-44.
  62. Mann, M.; Kelleher, N. L., Precision proteomics: the case for high resolution and high mass accuracy. *Proc Natl Acad Sci U S A* **2008**, 105, (47), 18132-8.
  63. Garton, N. J.; Christensen, H.; Minnikin, D. E.; Adegbola, R. A.; Barer, M. R., Intracellular lipophilic inclusions of mycobacteria in vitro and in sputum. *Microbiology* **2002**, 148, (Pt 10), 2951-8.
  64. Acocella, G., Clinical pharmacokinetics of rifampicin. *Clin Pharmacokinet* **1978**, 3, (2), 108-27.

65. Constans, P.; Saint-Paul, M.; Morin, Y.; Bonnaud, G.; Bariety, M., [Rifampicin: initial study of plasma levels during prolonged treatment of pulmonary tuberculosis patients]. *Rev Tuberc Pneumol (Paris)* **1968**, 32, (8), 991-1006.
66. Davis, C., Enumeration of probiotic strains: Review of culture-dependent and alternative techniques to quantify viable bacteria. *J Microbiol Methods* **2014**, 103C, 9-17.
67. Schurch, A. C.; Kremer, K.; Hendriks, A. C.; Freyee, B.; McEvoy, C. R.; van Crevel, R.; Boeree, M. J.; van Helden, P.; Warren, R. M.; Siezen, R. J.; van Soolingen, D., SNP/RD typing of Mycobacterium tuberculosis Beijing strains reveals local and worldwide disseminated clonal complexes. *PLoS One* **2011**, 6, (12), e28365.
68. Doerks, T.; van Noort, V.; Minguéz, P.; Bork, P., Annotation of the M. tuberculosis hypothetical orfeome: adding functional information to more than half of the uncharacterized proteins. *PLoS One* **2012**, 7, (4), e34302.
69. Chauhan, S.; Sharma, D.; Singh, A.; Surolia, A.; Tyagi, J. S., Comprehensive insights into Mycobacterium tuberculosis DevR (DosR) regulon activation switch. *Nucleic Acids Res* **2011**, 39, (17), 7400-14.
70. Schubert, O. T.; Mouritsen, J.; Ludwig, C.; Rost, H. L.; Rosenberger, G.; Arthur, P. K.; Claassen, M.; Campbell, D. S.; Sun, Z.; Farrah, T.; Gengenbacher, M.; Maiolica, A.; Kaufmann, S. H.; Moritz, R. L.; Aebersold, R., The Mtb proteome library: a resource of assays to quantify the complete proteome of Mycobacterium tuberculosis. *Cell Host Microbe* **2013**, 13, (5), 602-12.
71. Hu, Y.; Liu, A.; Menendez, M. C.; Garcia, M. J.; Oravcova, K.; Gillespie, S. H.; Davies, G. R.; Mitchison, D. A.; Coates, A. R., HspX knock-out in Mycobacterium tuberculosis leads to shorter antibiotic treatment and lower relapse rate in a mouse model--a potential novel therapeutic target. *Tuberculosis (Edinb)* **2015**, 95, (1), 31-6.
72. Wallis, R. S.; Patil, S.; Cheon, S. H.; Edmonds, K.; Phillips, M.; Perkins, M. D.; Joloba, M.; Namale, A.; Johnson, J. L.; Teixeira, L.; Dietze, R.; Siddiqi, S.; Mugerwa, R. D.; Eisenach, K.; Ellner, J. J., Drug tolerance in Mycobacterium tuberculosis. *Antimicrob Agents Chemother* **1999**, 43, (11), 2600-6.
73. Wallis, R. S.; Palaci, M.; Eisenach, K., Persistence, not resistance, is the cause of loss of isoniazid effect. *J Infect Dis* **2007**, 195, (12), 1870-1; author reply 1872-3.
74. Dick, T., Dormant tubercle bacilli: the key to more effective TB chemotherapy? *J Antimicrob Chemother* **2001**, 47, (1), 117-8.
75. Warner, D. F.; Mizrahi, V., Tuberculosis chemotherapy: the influence of bacillary stress and damage response pathways on drug efficacy. *Clin Microbiol Rev* **2006**, 19, (3), 558-70.
76. Sarathy, J.; Dartois, V.; Dick, T.; Gengenbacher, M., Reduced drug uptake in phenotypically resistant nutrient-starved nonreplicating Mycobacterium tuberculosis. *Antimicrob Agents Chemother* **2013**, 57, (4), 1648-53.
77. Bartek, I. L.; Rutherford, R.; Gruppo, V.; Morton, R. A.; Morris, R. P.; Klein, M. R.; Visconti, K. C.; Ryan, G. J.; Schoolnik, G. K.; Lenaerts, A.; Voskuil, M. I., The DosR regulon of M. tuberculosis and antibacterial tolerance. *Tuberculosis (Edinb)* **2009**, 89, (4), 310-6.
78. Shitikov, E. A.; Bespyatykh, J. A.; Ischenko, D. S.; Alexeev, D. G.; Karpova, I. Y.; Kostryukova, E. S.; Isaeva,

- Y. D.; Nosova, E. Y.; Mokrousov, I. V.; Vyazovaya, A. A.; Narvskaya, O. V.; Vishnevsky, B. I.; Otten, T. F.; Zhuravlev, V. Y.; Yablonsky, P. K.; Ilina, E. N.; Govorun, V. M., Unusual large-scale chromosomal rearrangements in *Mycobacterium tuberculosis* Beijing B0/W148 cluster isolates. *PLoS One* **2014**, *9*, (1), e84971.
79. Prisic, S.; Dankwa, S.; Schwartz, D.; Chou, M. F.; Locasale, J. W.; Kang, C. M.; Bemis, G.; Church, G. M.; Steen, H.; Husson, R. N., Extensive phosphorylation with overlapping specificity by *Mycobacterium tuberculosis* serine/threonine protein kinases. *Proc Natl Acad Sci U S A* **2010**, *107*, (16), 7521-6.
  80. Kusebauch, U.; Ortega, C.; Ollodart, A.; Rogers, R. S.; Sherman, D. R.; Moritz, R. L.; Grundner, C., *Mycobacterium tuberculosis* supports protein tyrosine phosphorylation. *Proc Natl Acad Sci U S A* **2014**, *111*, (25), 9265-70.
  81. Fortuin, S.; Tomazella, G. G.; Nagaraj, N.; Sampson, S. L.; Gey van Pittius, N. C.; Soares, N. C.; Wiker, H. G.; de Souza, G. A.; Warren, R. M., Phosphoproteomics analysis of a clinical *Mycobacterium tuberculosis* Beijing isolate: expanding the mycobacterial phosphoproteome catalog. *Front Microbiol* **2015**, *6*, 6.
  82. Thingholm, T. E.; Jensen, O. N.; Robinson, P. J.; Larsen, M. R., SIMAC (sequential elution from IMAC), a phosphoproteomics strategy for the rapid separation of monophosphorylated from multiply phosphorylated peptides. *Mol Cell Proteomics* **2008**, *7*, (4), 661-71.
  83. Ubersax, J. A.; Ferrell, J. E., Jr., Mechanisms of specificity in protein phosphorylation. *Nat Rev Mol Cell Biol* **2007**, *8*, (7), 530-41.
  84. Soufi, B.; Gnad, F.; Jensen, P. R.; Petranovic, D.; Mann, M.; Mijakovic, I.; Macek, B., The Ser/Thr/Tyr phosphoproteome of *Lactococcus lactis* IL1403 reveals multiply phosphorylated proteins. *Proteomics* **2008**, *8*, (17), 3486-93.
  85. Macek, B.; Mijakovic, I.; Olsen, J. V.; Gnad, F.; Kumar, C.; Jensen, P. R.; Mann, M., The serine/threonine/tyrosine phosphoproteome of the model bacterium *Bacillus subtilis*. *Mol Cell Proteomics* **2007**, *6*, (4), 697-707.
  86. Macek, B.; Gnad, F.; Soufi, B.; Kumar, C.; Olsen, J. V.; Mijakovic, I.; Mann, M., Phosphoproteome analysis of *E. coli* reveals evolutionary conservation of bacterial Ser/Thr/Tyr phosphorylation. *Mol Cell Proteomics* **2008**, *7*, (2), 299-307.
  87. Ravichandran, A.; Sugiyama, N.; Tomita, M.; Swarup, S.; Ishihama, Y., Ser/Thr/Tyr phosphoproteome analysis of pathogenic and non-pathogenic *Pseudomonas* species. *Proteomics* **2009**, *9*, (10), 2764-75.
  88. Morris, R. P.; Nguyen, L.; Gatfield, J.; Visconti, K.; Nguyen, K.; Schnappinger, D.; Ehrh, S.; Liu, Y.; Heifets, L.; Pieters, J.; Schoolnik, G.; Thompson, C. J., Ancestral antibiotic resistance in *Mycobacterium tuberculosis*. *Proc Natl Acad Sci U S A* **2005**, *102*, (34), 12200-5.
  89. Prabhakar, S.; Annapurna, P. S.; Jain, N. K.; Dey, A. B.; Tyagi, J. S.; Prasad, H. K., Identification of an immunogenic histone-like protein (HLPMT) of *Mycobacterium tuberculosis*. *Tuber Lung Dis* **1998**, *79*, (1), 43-53.
  90. Pandey, S. D.; Choudhury, M.; Yousuf, S.; Wheeler, P. R.; Gordon, S. V.; Ranjan, A.; Sritharan, M., Iron-regulated protein HupB of *Mycobacterium tuberculosis* positively regulates siderophore biosynthesis

- and is essential for growth in macrophages. *J Bacteriol* **2014**, 196, (10), 1853-65.
91. Yeruva, V. C.; Duggirala, S.; Lakshmi, V.; Kolarich, D.; Altmann, F.; Sritharan, M., Identification and characterization of a major cell wall-associated iron-regulated envelope protein (Irep-28) in *Mycobacterium tuberculosis*. *Clin Vaccine Immunol* **2006**, 13, (10), 1137-42.
  92. Wells, R. M.; Jones, C. M.; Xi, Z.; Speer, A.; Danilchanka, O.; Doornbos, K. S.; Sun, P.; Wu, F.; Tian, C.; Niederweis, M., Discovery of a siderophore export system essential for virulence of *Mycobacterium tuberculosis*. *PLoS Pathog* **2013**, 9, (1), e1003120.
  93. Schurch, A. C.; Kremer, K.; Warren, R. M.; Hung, N. V.; Zhao, Y.; Wan, K.; Boeree, M. J.; Siezen, R. J.; Smith, N. H.; van Soolingen, D., Mutations in the regulatory network underlie the recent clonal expansion of a dominant subclone of the *Mycobacterium tuberculosis* Beijing genotype. *Infect Genet Evol* **2011**, 11, (3), 587-97.
  94. Raghu, B.; Sarma, G. R.; Venkatesan, P., Effect of anti-tuberculosis drugs on the iron-sequestration mechanisms of mycobacteria. *Indian J Pathol Microbiol* **1995**, 38, (3), 287-92.
  95. Voskuil, M. I.; Visconti, K. C.; Schoolnik, G. K., *Mycobacterium tuberculosis* gene expression during adaptation to stationary phase and low-oxygen dormancy. *Tuberculosis (Edinb)* **2004**, 84, (3-4), 218-27.
  96. Rao, P. K.; Rodriguez, G. M.; Smith, I.; Li, Q., Protein dynamics in iron-starved *Mycobacterium tuberculosis* revealed by turnover and abundance measurement using hybrid-linear ion trap-Fourier transform mass spectrometry. *Anal Chem* **2008**, 80, (18), 6860-9.
  97. Hampshire, T.; Soneji, S.; Bacon, J.; James, B. W.; Hinds, J.; Laing, K.; Stabler, R. A.; Marsh, P. D.; Butcher, P. D., Stationary phase gene expression of *Mycobacterium tuberculosis* following a progressive nutrient depletion: a model for persistent organisms? *Tuberculosis (Edinb)* **2004**, 84, (3-4), 228-38.
  98. Wayne, L. G., In Vitro Model of Hypoxically Induced Nonreplicating Persistence of *Mycobacterium tuberculosis*. *Methods Mol Med* **2001**, 54, 247-69.
  99. Seiler, P.; Ulrichs, T.; Bandermann, S.; Pradl, L.; Jorg, S.; Krenn, V.; Morawietz, L.; Kaufmann, S. H.; Aichele, P., Cell-wall alterations as an attribute of *Mycobacterium tuberculosis* in latent infection. *J Infect Dis* **2003**, 188, (9), 1326-31.
  100. Daniel, J.; Maamar, H.; Deb, C.; Sirakova, T. D.; Kolattukudy, P. E., *Mycobacterium tuberculosis* uses host triacylglycerol to accumulate lipid droplets and acquires a dormancy-like phenotype in lipid-loaded macrophages. *PLoS Pathog* **2011**, 7, (6), e1002093.
  101. Rao, S. P.; Alonso, S.; Rand, L.; Dick, T.; Pethe, K., The protonmotive force is required for maintaining ATP homeostasis and viability of hypoxic, nonreplicating *Mycobacterium tuberculosis*. *Proc Natl Acad Sci U S A* **2008**, 105, (33), 11945-50.
  102. Koul, A.; Vranckx, L.; Dendouga, N.; Balemans, W.; Van den Wyngaert, I.; Vergauwen, K.; Gohlmann, H. W.; Willebrords, R.; Poncelet, A.; Guillemont, J.; Bald, D.; Andries, K., Diarylquinolines are bactericidal for dormant mycobacteria as a result of disturbed ATP homeostasis. *J Biol Chem* **2008**, 283, (37), 25273-80.
  103. Koul, A.; Vranckx, L.; Dhar, N.; Gohlmann, H. W.; Ozdemir, E.; Neefs, J. M.; Schulz, M.; Lu, P.; Mortz, E.; McKinney, J. D.; Andries, K.; Bald, D., Delayed bactericidal response of *Mycobacterium tuberculosis* to

bedaquiline involves remodelling of bacterial metabolism. *Nat Commun* **2014**, 5, 3369.

104. Reed, M. B.; Gagneux, S.; Deriemer, K.; Small, P. M.; Barry, C. E., 3rd, The W-Beijing lineage of *Mycobacterium tuberculosis* overproduces triglycerides and has the DosR dormancy regulon constitutively upregulated. *J Bacteriol* **2007**, 189, (7), 2583-9.
105. den Hertog, A. L.; Menting, S.; van Soolingen, D.; Anthony, R. M., *Mycobacterium tuberculosis* Beijing genotype resistance to transient rifampin exposure. *Emerg Infect Dis* **2014**, 20, (11), 1932-3.
106. McGrath, M.; Gey van Pittius, N. C.; van Helden, P. D.; Warren, R. M.; Warner, D. F., Mutation rate and the emergence of drug resistance in *Mycobacterium tuberculosis*. *J Antimicrob Chemother* **2014**, 69, (2), 292-302.
107. Ford, C. B.; Lin, P. L.; Chase, M. R.; Shah, R. R.; Iartchouk, O.; Galagan, J.; Mohaideen, N.; Ioegeer, T. R.; Sacchetti, J. C.; Lipsitch, M.; Flynn, J. L.; Fortune, S. M., Use of whole genome sequencing to estimate the mutation rate of *Mycobacterium tuberculosis* during latent infection. *Nat Genet* **2011**, 43, (5), 482-6.
108. Ford, C. B.; Shah, R. R.; Maeda, M. K.; Gagneux, S.; Murray, M. B.; Cohen, T.; Johnston, J. C.; Gardy, J.; Lipsitch, M.; Fortune, S. M., *Mycobacterium tuberculosis* mutation rate estimates from different lineages predict substantial differences in the emergence of drug-resistant tuberculosis. *Nat Genet* **2013**, 45, (7), 784-90.
109. Flynn, J. L.; Chan, J., Tuberculosis: latency and reactivation. *Infect Immun* **2001**, 69, (7), 4195-201.
110. Spitzer, M.; Wildenhain, J.; Rappsilber, J.; Tyers, M., BoxPlotR: a web tool for generation of box plots. *Nat Methods* **2014**, 11, (2), 121-2.

## Supporting information

**SUPPORTING INFORMATION TABLE S1:** Overview of the proteins identified in all of the samples analyzed.

This table can be downloaded on the website of the journal: <https://pubs.acs.org/doi/suppl/10.1021/acs.jproteome.5b01073>

**SUPPORTING INFORMATION TABLE S2:** Overview of all the peptides identified. This table can be

downloaded on the website of the journal: <https://pubs.acs.org/doi/suppl/10.1021/acs.jproteome.5b01073>

**SUPPORTING INFORMATION TABLE S3:** Proteins identified to be differentially regulated after 24 h of

rifampicin treatment. This table can be downloaded on the website of the journal: <https://pubs.acs.org/doi/suppl/10.1021/acs.jproteome.5b01073>

**SUPPORTING INFORMATION TABLE S4:** Overview of the phosphopeptides and phosphoproteins identified.

This table can be downloaded on the website of the journal: <https://pubs.acs.org/doi/suppl/10.1021/acs.jproteome.5b01073>



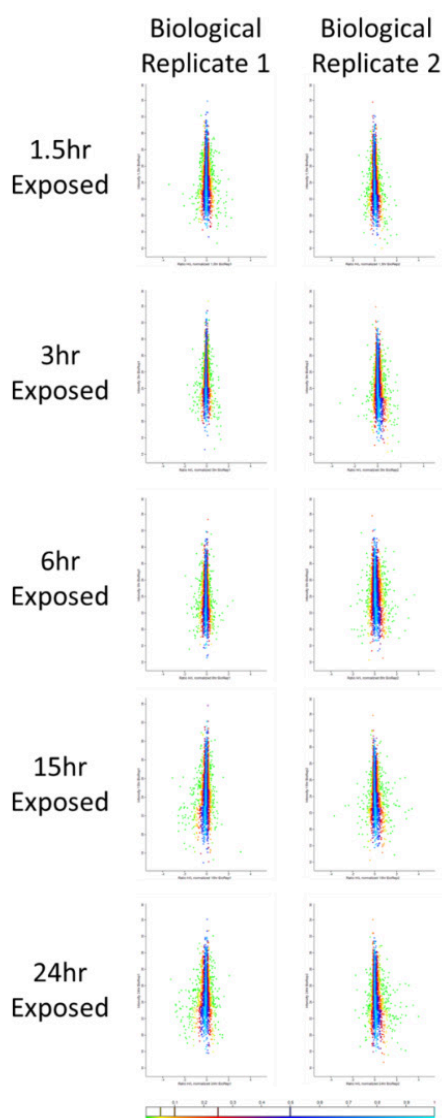


**FIGURE S1:** Protein ratio distribution comparison in rifampicin exposed *M. tuberculosis* Beijing B0/W148. Normalized Log2 transformed protein ratio's plotted against the summed Log2 protein intensity for both biological replicates. The peptides derived from rifampicin exposed mycobacteria was provided with a “medium”-label in biological replicate 1 and a “light”-label in biological replicate 2. Data points are coloured based on their significance B values. Turquoise is >0.5, blue >0.25, red >0.1, yellow >0.05 and green <0.05. Note: a label swap was performed between both biological replicates.

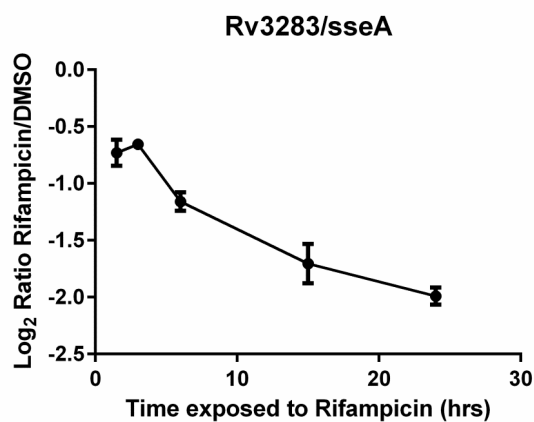


**FIGURE S2:** Abundance kinetics of Rv3283/sseA during rifampicin exposure. Error bars represent SEM.

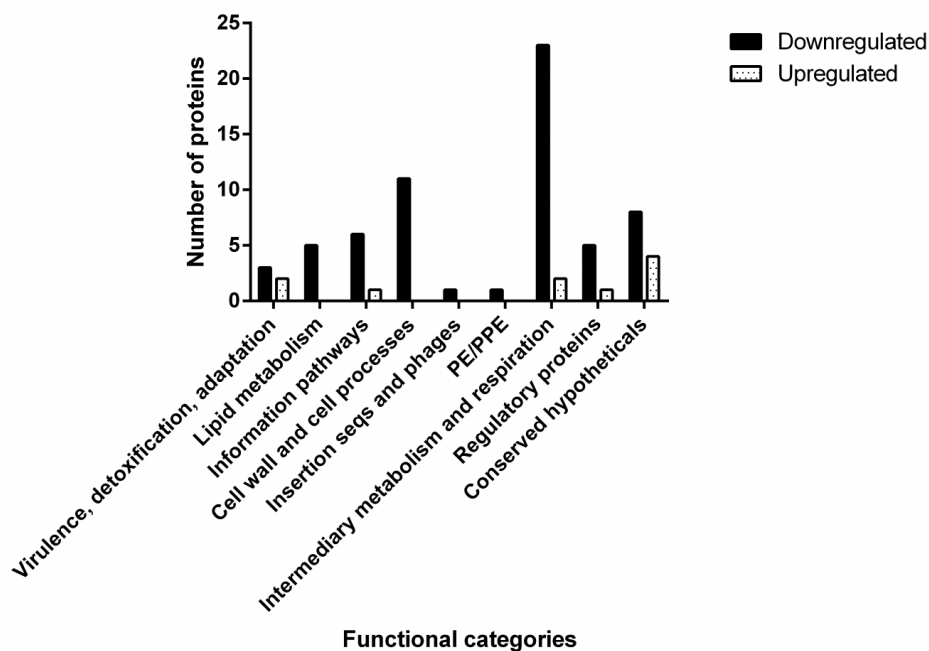


**FIGURE S3:** Proteins significantly down regulated or upregulated after 24 hr of rifampicin treatment. None of the functional categories(68) showed to be significantly over/underrepresented after Chi-square analysis.

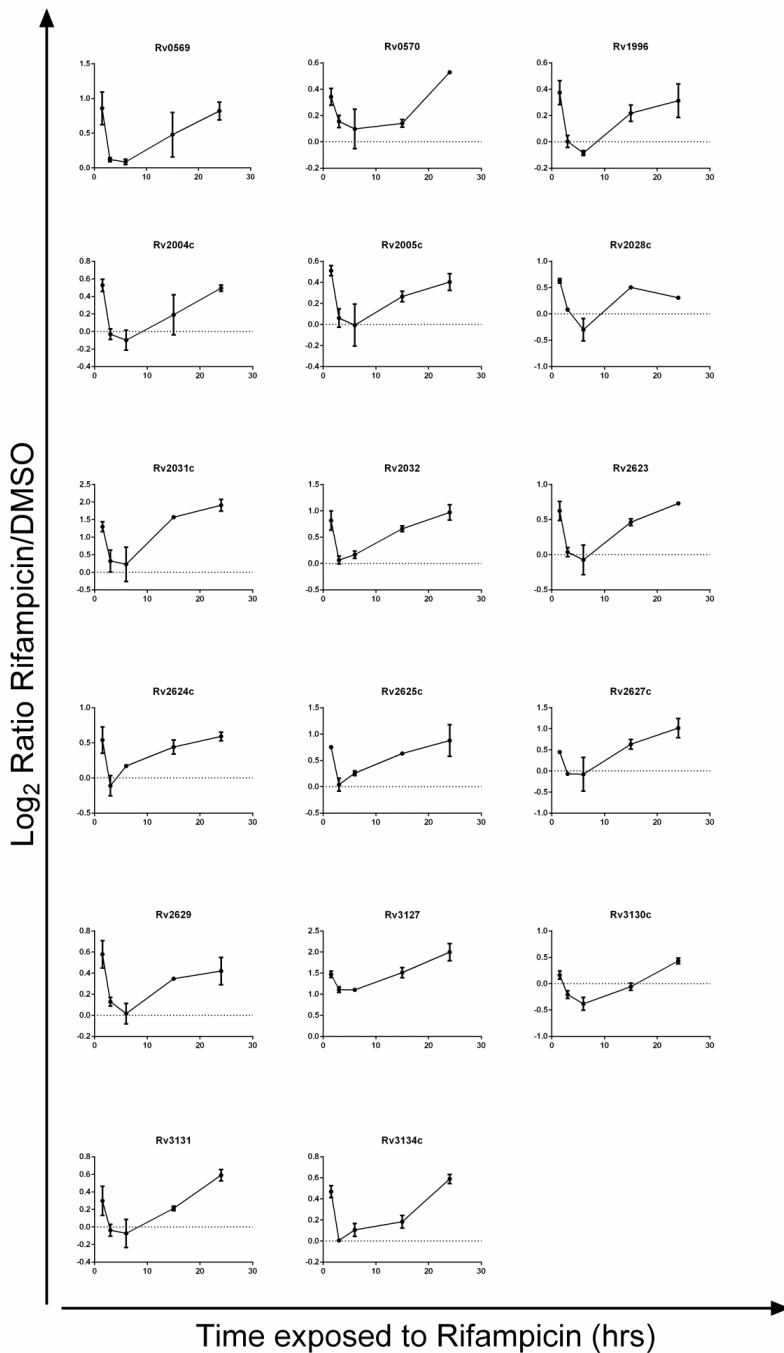


**FIGURE S4:** Differential regulation of DosR regulon proteins upon rifampicin exposure. Error bars represent SEM.

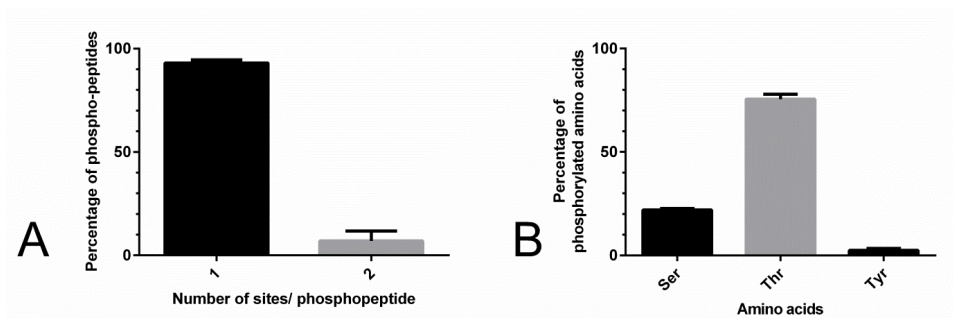
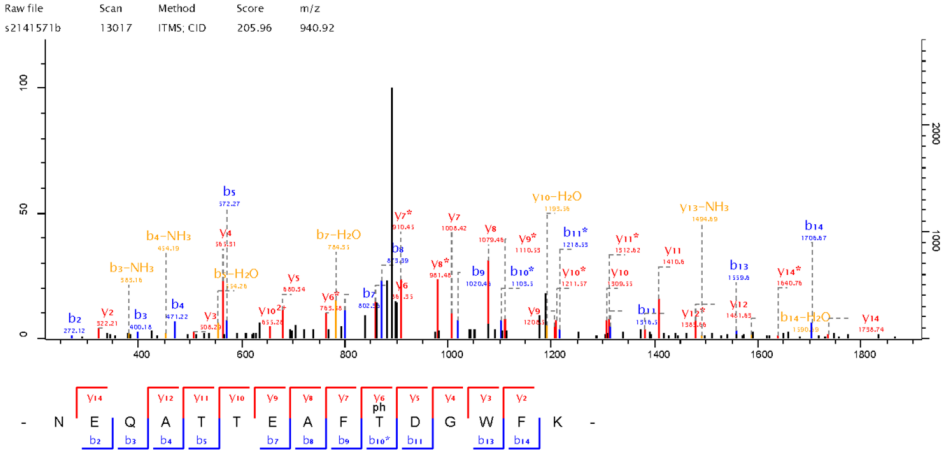
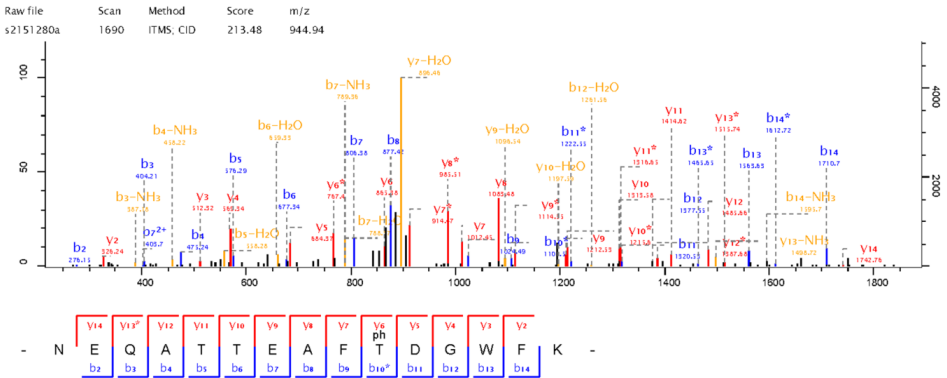


**FIGURE S5:** Percentage of phosphosites identified per phosphopeptide(A) and the percentage of Ser/Thr/Tyr phosphorylation. Error bars represent SEM.

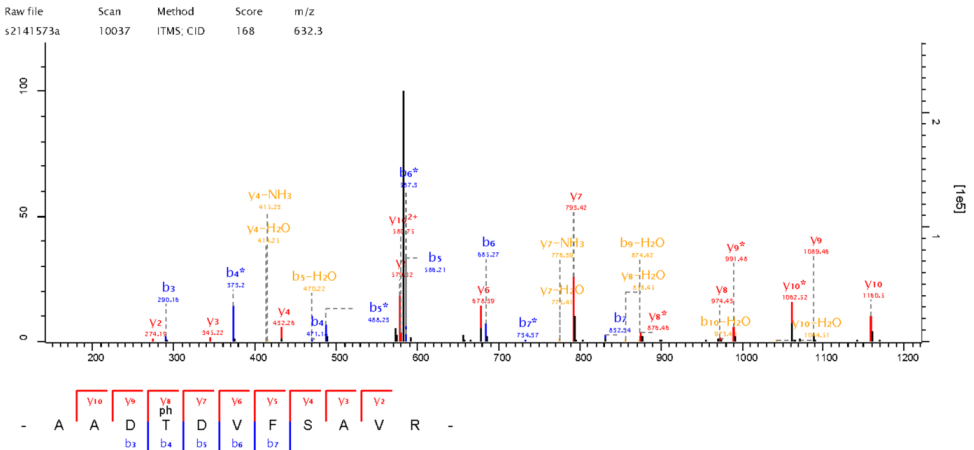
### A: MS/MS-spectrum of the phosphopeptide of Rv2187(Thr-437)



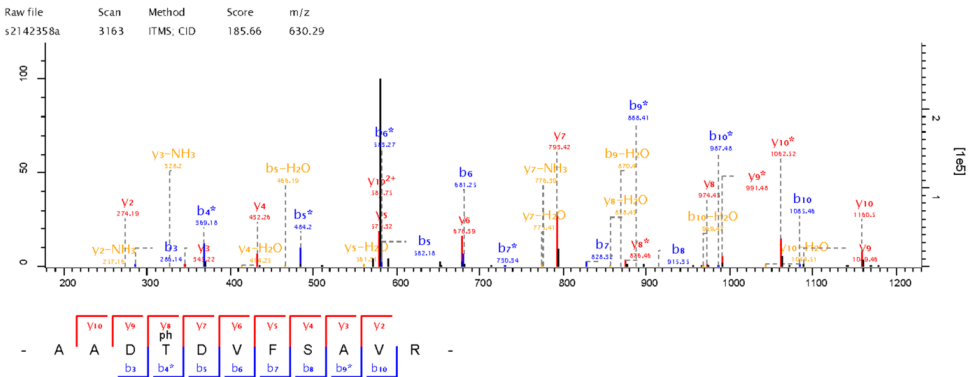
### B: MS/MS-spectrum of the synthetic phosphopeptide for Rv2187(Thr-437)



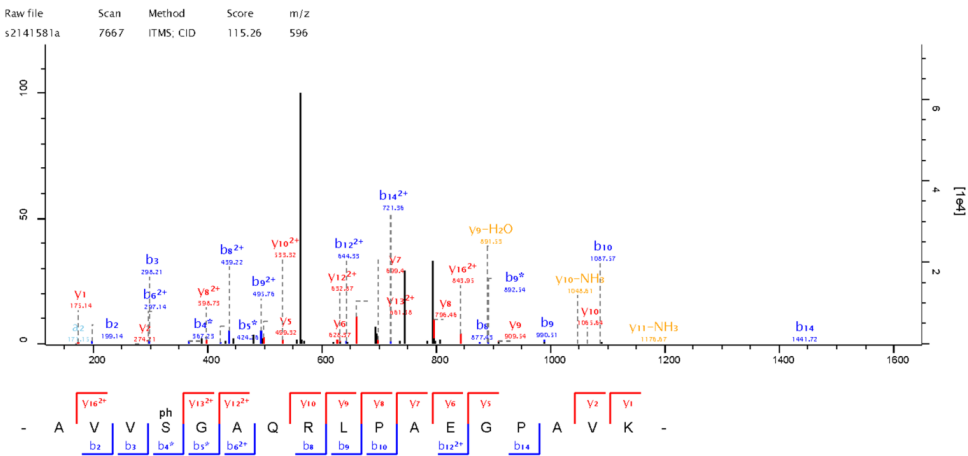
### C: MS/MS-spectrum of the phosphopeptide of Rv2536(Thr-160)



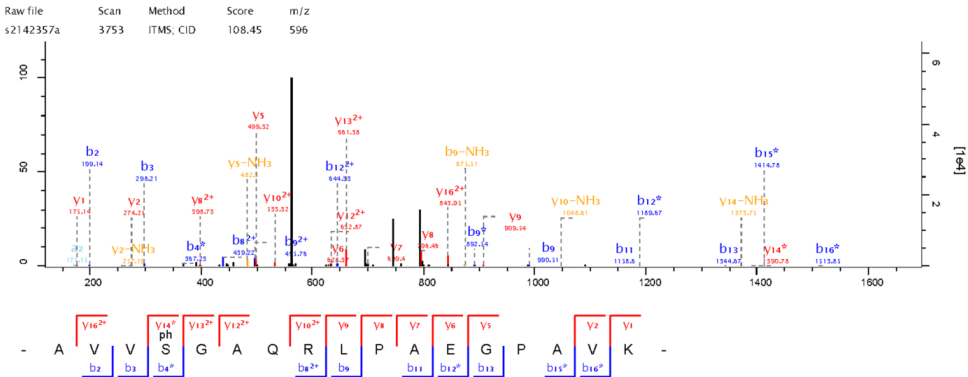
D: MS/MS-spectrum of the synthetic phosphopeptide for Rv2536(Thr-160)



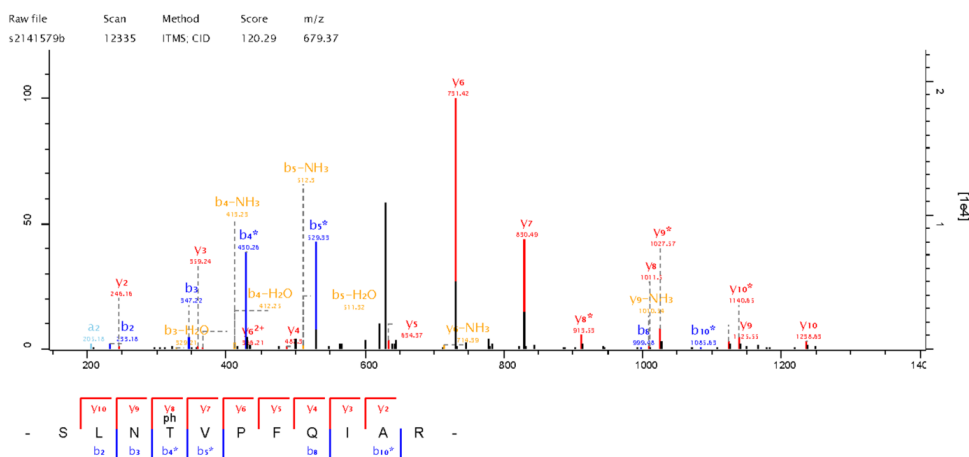
E: MS/MS-spectrum of the phosphopeptide of Rv2986c(Ser-90)



F: MS/MS-spectrum of the synthetic phosphopeptide for Rv2986c(Ser-90)



### G: MS/MS-spectrum of the phosphopeptide of Rv3458c(Thr-147)



### H: MS/MS-spectrum of the synthetic phosphopeptide for Rv3458c(Thr-147)

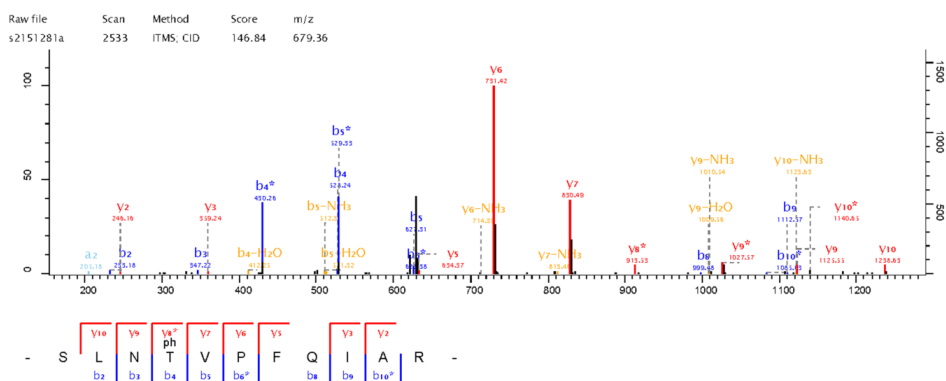


**FIGURE S6:** MS/MS-spectra of selected phosphopeptides

- A) MS/MS-spectrum of the phosphopeptide of Rv2187(Thr-437)
- B) MS/MS-spectrum of the synthetic phosphopeptide for Rv2187(Thr-437)
- C) MS/MS-spectrum of the phosphopeptide of Rv2536(Thr-160)
- D) MS/MS-spectrum of the synthetic phosphopeptide for Rv2536(Thr-160)
- E) MS/MS-spectrum of the phosphopeptide of Rv2986c(Ser-90)
- F) MS/MS-spectrum of the synthetic phosphopeptide for Rv2986c(Ser-90)
- G) MS/MS-spectrum of the phosphopeptide of Rv3458c(Thr-147)
- H) MS/MS-spectrum of the synthetic phosphopeptide for Rv3458c(Thr-147)

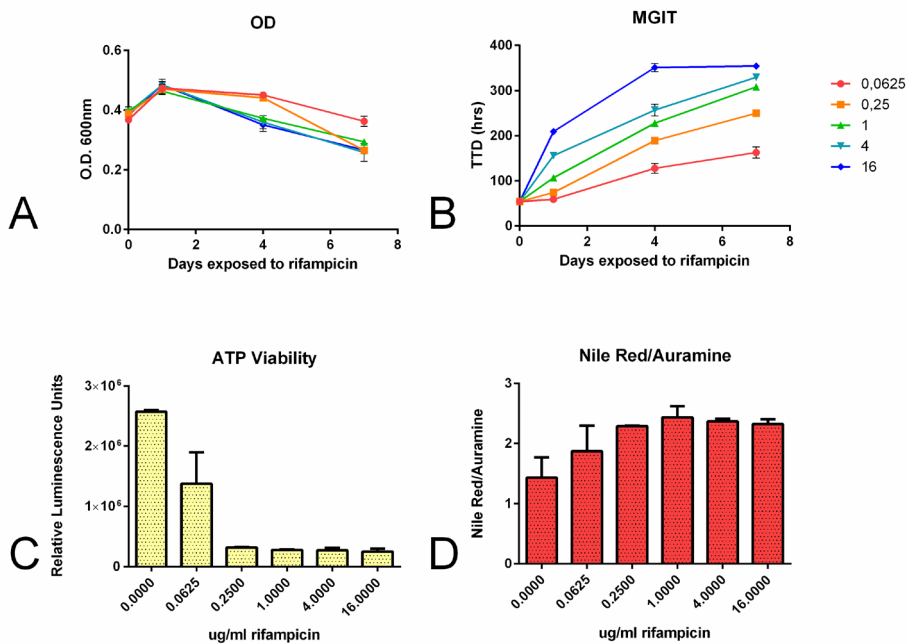


**FIGURE S7:** Development of a dormant phenotype upon rifampicin treatment. Error bars represent the SEM. The concentrations are reported in  $\mu\text{g/ml}$ .

- A) The optical density measured at 600nm.
- B) The time till detection (TTD) determined after 0,1,4 and 7 days of rifampicin treatment.
- C) Viability of the cells was assessed by determination of the concentration of ATP after treatment with different concentrations of rifampicin for 7 days.
- D) The normalized Nile Red/Auramine ratio after 7 days of treatment with multiple concentrations of rifampicin.





Parallel reaction monitoring of clinical *Mycobacterium tuberculosis* lineages reveals pre-existent markers of rifampicin tolerance in the emerging Beijing lineage

Jeroen de Keijzer<sup>1\*</sup>, Arnout Mulder<sup>2</sup>, Arnoud H. de Ru<sup>1,3</sup>,  
Dick van Soolingen<sup>2,4#</sup>, Peter A. van Veelen<sup>1,3#</sup>

<sup>1</sup> Department of Immunohematology and Blood Transfusion, Leiden University Medical Center (LUMC), Leiden, 2300 RC, the Netherlands

<sup>2</sup> Tuberculosis Reference Laboratory, National Institute for Public Health and the Environment (RIVM), Bilthoven, 3720 BA, the Netherlands

<sup>3</sup> Center for Proteomics and Metabolomics, Leiden University Medical Center (LUMC), Leiden, 2300 RC, the Netherlands

<sup>4</sup> Departments of Pulmonary Diseases and Medical Microbiology, Radboud University Medical Center, Nijmegen, 6500 HB, the Netherlands

#PAvV and DvS share senior authorship

## Abstract

The spread of multidrug resistant *Mycobacterium tuberculosis* is one of the major challenges in tuberculosis control. In Eurasia, the spread of multidrug resistant tuberculosis is driven by the *M. tuberculosis* Beijing genotype. In this study, we examined whether selective advantages are present in the proteome of Beijing isolates that contribute to the emergence of this genotype. To this end, we compared the proteome of *M. tuberculosis* Beijing to that of *M. tuberculosis* H37Rv, both in the presence and absence of the first-line antibiotic rifampicin. During rifampicin exposure, both *M. tuberculosis* genotypes express proteins belonging to the DosR dormancy regulon, which induces a metabolically hypoactive-, drug tolerant phenotype. However, these markers of rifampicin tolerance were already more abundant in the *M. tuberculosis* Beijing isolate prior to drug exposure. To determine whether the *a priori* high abundance of specific proteins contribute to the formation of antibiotic resistance in *M. tuberculosis* Beijing, we quantified the abundance of 33 selected proteins in 27 clinical isolates from the five most common *M. tuberculosis* lineages using parallel reaction monitoring. The observed pre-existing high abundance of dormancy proteins in Beijing strains provides an evolutionary advantage that allow these strains to persist for prolonged periods during rifampicin treatment.

## Introduction

*Mycobacterium tuberculosis* has recently been declared the most important worldwide cause of death by a single infectious disease.<sup>(1)</sup> In 2014 tuberculosis (TB) caused the death of 890,000 men, 480,000 women and 140,000 children.<sup>(1)</sup> Of major concern is the spread of multidrug resistant tuberculosis (MDR-TB), a form of TB that is resistant to at least rifampicin and isoniazid, the cornerstones in anti-TB treatment. In Eurasia, the dissemination of MDR-TB is largely attributable to the *M. tuberculosis* Beijing genotype.<sup>(2, 3)</sup>

Strains of the *M. tuberculosis* Beijing lineage seem to possess selective advantages to acquire rifampicin resistance,<sup>(4-7)</sup> to circumvent BCG-vaccine induced immunity<sup>(8-10)</sup> and hyper-transmissibility compared to other *M. tuberculosis* lineages.<sup>(11-14)</sup> Not surprisingly, the *M. tuberculosis* Beijing genotype is correlated with (multi)drug resistance, hyper-virulence and relapses after curative treatment in many geographical areas.<sup>(15-20)</sup>

Although it is well accepted that *M. tuberculosis* Beijing manifests itself differently from other *M. tuberculosis* lineages regarding transmission, drug resistance and virulence, there is some discrepancy between the various studies published. This heterogeneity is partly attributable to differences between *M. tuberculosis* sub-lineages in the Beijing genotype family.<sup>(21)</sup> Phylogenetically, the Beijing genotype can be delineated into the more “ancient” or atypical and the more “modern” or typical Beijing sub-lineage. However, both sub-lineages are genetically highly similar.<sup>(22, 23)</sup> In fact, only 31 non synonymous single nucleotide polymorphisms (nsSNP) have been identified that discriminate both sub-lineages.<sup>(24)</sup> Although genetically similar, the degree of genetic conservation is much higher within the typical Beijing sub-lineage, which suggests that these strains acquired selective advantages over atypical Beijing strains in relatively recent years.<sup>(24)</sup> This hypothesis is further strengthened by the fact that it is mainly the modern typical Beijing sub-lineage that is associated with (multi)drug resistance and the ability to spread and cause disease.<sup>(25)</sup> Currently, there is no unequivocal model that can clarify the evolutionary success of *M. tuberculosis* (typical) Beijing strains.<sup>(26)</sup> However, the key to the evolutionary success of *M. tuberculosis* (typical) Beijing might be traced within the proteomic composition of strains in this lineage.

Over a decade ago, a two-dimensional gel electrophoresis approach was used to identify proteins that are differentially abundant in *M. tuberculosis* Beijing, a second “non-Beijing” clinical isolate, and *M. tuberculosis* H37Rv, a frequently studied mycobacterial laboratory strain.<sup>(27)</sup> One protein was identified to be more abundant in *M. tuberculosis* Beijing (Rv2031c/hspX), whereas three other proteins were identified to be less abundant (Rv0440/GroEL2, Rv0934/PstS1 and Rv1860/47kDa). In a recent study, we quantitatively compared the proteomes of

typical with that of atypical Beijing strains, in which we found that Beijing sub-lineages are extremely conserved in terms of protein abundance.<sup>(28)</sup> In fact, the two proteomes were so similar that we could only identify two proteins to be differentially regulated between both sub-lineages; Rv0450c/mmpL4 and Rv3283/sseA. Subsequently, when we examined the initial response of a typical Beijing isolate to rifampicin, we found the so-called DosR dormancy regulon to be induced within 24 hrs after treatment.<sup>(29)</sup> The DosR dormancy regulon induces a non-replicative, metabolically inactive and drug tolerant mycobacterial phenotype which may severely compromise treatment efficacy.<sup>(30)</sup> We demonstrated that dormancy can be actively induced by the pathogen to protect itself from toxic compounds, whereas it was previously only known that environmental factors can induce dormancy.<sup>(31, 32)</sup> If *M. tuberculosis* Beijing strains possess an increased ability to induce dormancy upon exposure to rifampicin, this could possibly reflect the mechanism through which Beijing genotype bacteria developed a higher tolerance to antibiotics within patients, which consequently leads to a longer persistence, development of resistance and higher relapse rates even after curative treatment. However, the induction of the dormancy regulon upon rifampicin exposure has so far only been demonstrated in *M. tuberculosis* Beijing.

Therefore, we here address the question of what proteins typify the proteome of *M. tuberculosis* Beijing and what proteins contribute to the emergence of drug-resistant *M. tuberculosis* Beijing. To this end, we used a data-dependent acquisition (DDA) approach to compare the proteome of the *M. tuberculosis* Beijing B0/W-148, which resembles the “successful” Russian typical Beijing strain,<sup>(33)</sup> with the proteome of the *M. tuberculosis* laboratory-strain H37Rv, both with and without exposure to rifampicin. Based on the proteins quantified by DDA proteomics, we made a selection of 33 proteins and examined their abundance using parallel reaction monitoring (PRM) in multiple lineages of well characterized clinical *M. tuberculosis* isolates; typical Beijing, atypical Beijing, East-African Indian (EAI), Haarlem and Central Asian Strain (CAS) lineages.

Following this approach, we provide a thorough inter-lineage comparison of protein abundance in well characterized *M. tuberculosis* genotypes. The results presented in this manuscript show that proteins required to circumvent rifampicin-induced killing are already highly abundant in strains of the *M. tuberculosis* Beijing genotype, prior to drug exposure.

## Materials & Methods

### Culture conditions

Mycobacterial cells were re-cultured from frozen stocks in 5 ml Tween-Albumin liquid culture broth (Tritium Microbiologie, the Netherlands) at 36°C to an O.D. of 0.4 AU at 600 nm, as described previously.<sup>(28)</sup> One ml of this pre-culture was transferred to a 250 ml Erlenmeyer flask containing 100 ml Tween-Albumin broth and incubated under constant rotation at 36°C to provide aeration. Once the cultures reached an O.D. of 0.6 AU at 600 nm, representing the mid-log phase, the cells were exposed to 1 µg/ml rifampicin (Sigma Aldrich, the Netherlands) or DMSO as a control. Cells were harvested after 24 hrs of incubation and washed three times with ice-cold PBS (Braun, Germany), the resulting pellet was suspended in 5 ml Lysis-buffer (4% SDS, 100 mM Tris-HCl, pH 7.6) and heat-killed at 95°C for 10 min. Lysates were stored at -20°C until further usage. Biological duplicates were grown, processed and analyzed in parallel.

### Rifampicin susceptibility determination

To exclude the selection of rifampicin resistant mycobacteria we analysed the rifampicin resistance determining region (RRDR) of *rpoB*, the hotspot for drug resistance, for presence of mutations using the MTBDR<sub>plus</sub> assay according to the manufacturers' recommendations, as described previously.<sup>(34)</sup> Phenotypic rifampicin susceptibility, as determined by the minimal inhibitory concentration (MIC), was determined according to Clinical and Laboratory Standards Institute guidelines,<sup>(35)</sup> using the BACTEC MGIT-960 system (Becton, Dickinson and Co., Franklin Lakes, NJ).

### Sample preparation

Protein digests were prepared as described previously.<sup>(28)</sup> In brief, mycobacterial cell lysates were mechanically disrupted by bead-beating in a mini bead-beater 16 (BioSpec, USA) after which the lysates were transferred to a fresh tube. Proteins in the lysate were digested using the filter aided sample preparation (FASP) method, including reduction, removal of SDS by urea and carbamidomethylation of cysteines.<sup>(36)</sup> The tryptic digest was desalted on C18 SepPak columns (Waters Corporation, Massachusetts, USA) and on column labeled by dimethylation.<sup>(37)</sup> Samples analyzed by data dependent acquisition (DDA) were fractionated into 15 fractions by strong cation exchange (SCX) on a Agilent 1100 system equipped with an in-house packed SCX-column (320 µm ID, 15 cm, polysulfoethyl A 3 µm, Poly LC, Columbia, USA), run at 4 µl/min. The SCX gradient started for 10 min at 100% solvent A (water/acetonitrile/formic acid; 70/30/0.1), after which a linear gradient reached 100% solvent B (250 mM KCl/acetonitrile/formic acid 70/30/0.1) in 15 min, followed by 100% solvent C (500 mM KCl/acetonitrile/formic acid 70/30/0.1) for 15 min. To clean the column, the gradient was held at 100% solvent C for 5 min. Next, the column was washed with 100% solvent A. Fifteen fractions were collected in 1

min intervals, lyophilized and reconstituted in 30  $\mu$ l (water/acetonitrile/formic acid 95/3/0.1) for nanoLC-MS/MS.

### Data acquisition

Samples prepared for DDA analysis were analyzed on a nanoLC-MS/MS system consisting of an Easy nLC 1000 gradient HPLC system (Thermo scientific, Bremen, Germany), and a Q-Exactive mass spectrometer (Thermo scientific, Bremen, Germany). SCX fractions were injected onto an in-house packed precolumn (100  $\mu$ m  $\times$  15 mm; Reprosil-Pur C18-AQ 3  $\mu$ m, Dr. Maisch, Germany) and eluted via a homemade analytical nano-HPLC column (15 cm  $\times$  50  $\mu$ m; Reprosil-Pur C18-AQ 3  $\mu$ m). The gradient was run from 0% to 30% solvent B (10/90/0.1 water/acetonitrile/formic acid) in 120 min. A tip of  $\sim$ 5  $\mu$ m was drawn at the end of the nano-HPLC which acted as the electrospray needle of the MS source. The Q-Exactive mass spectrometer was operated in top10-mode. Parameters were; resolution 70,000 at an AGC target value of 3e6, a maximum fill time of 20 ms (full scan), and resolution 17,500 at an AGC target value of 1e5 with a maximum fill time of 60 ms for MS/MS. For PRM analysis the Q-Exactive mass spectrometer was operated in PRM-mode: a cycle comprised one full scan and ten transitions. Full scans were acquired at 17,500 resolution, and AGC target value of 3e6, a maximum fill time of 20 ms. Tandem mass spectra were acquired with a resolution of 35,000 at an AGC target value of 2e5 and a maximum fill time of 128 ms. The isolation window was set at 1.5  $m/z$ .

### Data dependent acquisition data processing

Peptides and proteins were identified and quantified using MaxQuant 1.4.0.3.<sup>(38)</sup> The false discovery rate (FDR) was set to 0.01 for both proteins and peptides. The first search was conducted using 10 ppm, while the main search was performed with 4.5 ppm using the Andromeda search engine.<sup>(39)</sup> MS/MS spectra were searched using 20 mmu mass tolerance. A total of 262 common contaminants were included in the searches by Andromeda. Trypsin specificity was set as C-terminal to arginine and lysine without proline restriction. A maximum of two missed cleavages was allowed. Variable modifications included N-terminal protein acetylation, methionine oxidation, and corresponding dimethyl labels. Carbamidomethylation of cysteine was selected as a fixed modification. A minimal unique peptide count of two was used for protein identification. All spectra were matched against a FASTA database of *M. tuberculosis* reference strain H37Rv (3996 entries).<sup>(40)</sup> Statistical analysis of the outcomes was performed by Perseus using the significance B test with a Benjamini-Hochberg FDR 5%.<sup>(39)</sup> Proteins considered to be differentially abundant have significance B score of  $\leq$ 0.05. Principal component analysis and the generation of a heat map based on the protein ratios was performed in Perseus.<sup>(39)</sup> The RAW data files and the MaxQuant output files, which provide access to all annotated spectra, have been deposited to the ProteomeXchange Consortium via the PRIDE partner repository that can be accessed with the dataset identifier PXD003474.

### Parallel reaction monitoring data analysis

PRM data analysis and data integration was performed in Skyline 3.1.0.7382.<sup>(41)</sup>

Quantitative analysis was performed using synthetic stable isotopically labelled (SIL) peptides that were dimethylated (+36Da). Ten fmol per peptide was injected together with 500 ng dimethylated (+28Da) tryptic digest. The intensity rank order and chromatographic elution of the transitions were required to match those of a synthetic standard for each peptides measured. Summed peak areas from the selected peptide transitions were compared to that of the SIL peptide. Statistical evaluation of the outcomes was performed using a one-way ANOVA with *post hoc* Dunnet test to compare the mean of all lineages with the mean of the typical Beijing genotype. All RAW-files and the corresponding Skyline files have been deposited to the ProteomeXchange Consortium via the PRIDE partner repository that can be accessed with the dataset identifier PXD003474.

### Molecular characterization of *M. tuberculosis* isolates

*M. tuberculosis* isolates were derived from the reference database of clinical isolates at the National Institute for Public Health and the Environment (RIVM) in Bilthoven, the Netherlands. The genotypes of the selected isolates were determined as described previously.<sup>(42)</sup> Phylogenetic relationships between the different strains were analysed using mycobacterial interspersed repeat units (MIRU) 24-loci variable number of tandem repeats (VNTR) typing with a few minor modifications.<sup>(42)</sup> The in-house VNTR method is based on the protocol of the MIRU-VNTR typing manual with minor modifications: the amount of DNA polymerase used was 0.75 units per multiplex PCR, and the initial concentration of labelled primers was increased to 8  $\mu$ M for locus 2165 and locus 2163b. The amplicon sizes were determined by using the automated ABI 3730 DNA analyser (Applied Biosystems, California, USA).



# Results and discussion

## M. tuberculosis isolates reveal a large diversity in proteome composition

Members of the *M. tuberculosis* Beijing genotype differ from other *M. tuberculosis* strains in terms of transmission, virulence and capacity to develop antibiotic resistance.<sup>(11, 15-20)</sup> To determine whether the relative proteomic composition of *M. tuberculosis* Beijing contributes to these phenomena, we compared the proteome of *M. tuberculosis* Beijing B0/W148, a typical Beijing strain, with the proteome of *M. tuberculosis* reference strain H37Rv, both in the presence and absence of rifampicin; Figure 1A & B.

A total of 2,903 unique proteins were identified of which 2,429 proteins were relatively quantified against the internal control in each of the analyses, based on at least two unique peptides per protein; Figure 1C & Table S1, S2. A high reproducibility was observed between the biological replicates (Pearson  $r > 0.9$ ), which shows that the technical and biological reproducibility is high and that the detected differentially abundant proteins reflect true heterogeneity in the proteomic composition of both lineages; Figure S1 & Figure S2.

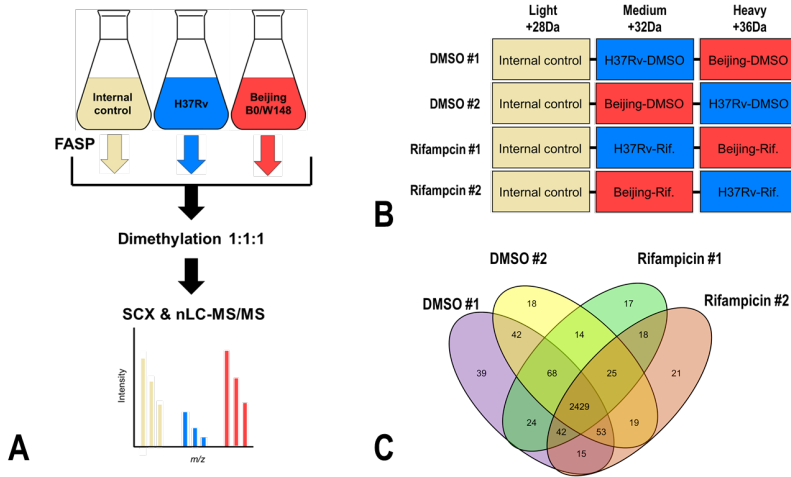


**FIGURE 1:** Quantitative proteome analysis of rifampicin treated *M. tuberculosis* lineages.

A) In-depth proteome analysis was performed by parallel processing of the samples using the FASP procedure.<sup>(36)</sup> After trypsin digestion the samples were labelled by dimethylation and mixed in a 1:1:1 ratio.<sup>(37)</sup> The resulting peptides were fractionated using SCX chromatography and analysed by high-resolution nanoLC-MS/MS.

B) Experimental design for the proteomic analysis of *M. tuberculosis* lineages with and without 24 hrs of rifampicin treatment. A label-swap was performed between biological replicates.

C) Venn diagram of the number of proteins quantified in the different conditions examined.

A clear segregation between both *M. tuberculosis* lineages and antibiotic treatment was found using principal component analysis; Figure 2A. Similarly, hierarchical clustering of these samples showed that the inter-lineage variation is much more profound than the variation introduced by exposure to a bactericidal dose of rifampicin; Figure 2B. Due to the substantial inter-lineage variation we first focussed on the proteins that were differentially regulated between *M. tuberculosis* Beijing and *M. tuberculosis* H37Rv after 24hr of DMSO treatment.

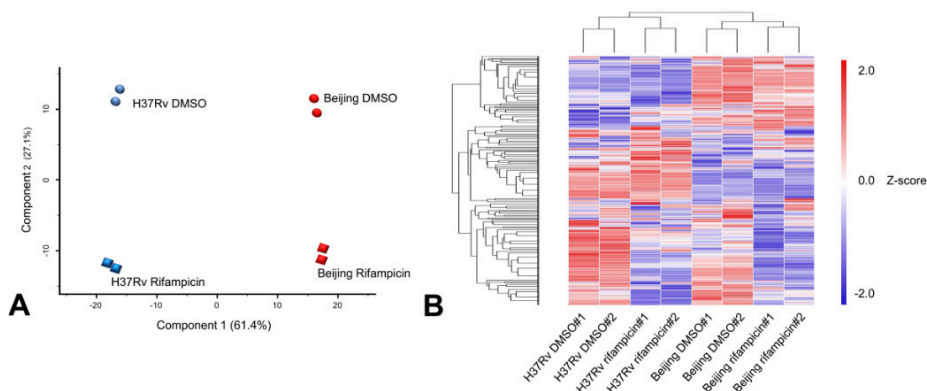


**FIGURE 2:** Characterization of the relative proteomic variation between *M. tuberculosis* typical Beijing and *M. tuberculosis* H37Rv.

A) Principal component analysis of the log<sub>2</sub>-transformed abundance changes of the 2429 proteins that were quantified in both genotypes in both conditions tested.

B) Protein ratios were log<sub>2</sub>-transformed and z-score normalized. The different samples in the columns were hierarchically clustered and rows containing quantified proteins entries were clustered by k-means.

### PhoPR and DosR regulon proteins differ in abundance between the Beijing- and the H37Rv strain

In our proteomic DDA dataset of 2,429 proteins, we identified a total of 287 proteins to be more abundant in the *M. tuberculosis* typical Beijing strain compared to H37Rv; Table S1. Among the proteins we identified to be more abundant in the typical Beijing lineage was Rv2031c/hspX, a protein that has previously been identified to be more abundant in a clinical isolate of *M. tuberculosis* Beijing.<sup>(27)</sup> In that same study, three other proteins were identified to be less abundant in that specific *M. tuberculosis* Beijing isolate compared to H37Rv; Rv0440/GroEL2, Rv0934/PstS1 and Rv1860/47kDa. Although all three proteins were present in our dataset, none of these proteins was less abundant in *M. tuberculosis* Beijing; Table S1. This discrepancy is possibly caused by the genomic variation in H37Rv strains that are maintained in different mycobacterial research laboratories.<sup>(43)</sup>

One regulon of which we found the proteins to be more abundant in the *M. tuberculosis* Beijing strain is the DosR dormancy regulon; Table S3. The DosR regulon in the pathogen is necessary to enter a latent, non-replicative state for prolonged periods of time up to decades.<sup>(44)</sup> This latent, metabolically hypoactive dormant state makes the pathogen highly tolerant to drugs, since most antibiotics inhibit active metabolic processes.<sup>(45)</sup> Diverse stimuli, including nitric oxide, acidity, nutrient deprivation and hypoxia can induce this dormant phenotype.<sup>(46-49)</sup> Next to these environmental stimuli, we have recently shown that an active duplicating clinical typical Beijing strain develops a dormant phenotype during exposure to rifampicin.<sup>(29)</sup> In addition, by knocking-out the dormancy protein Rv2031c/hspX, *M. tuberculosis* becomes more susceptible for rifampicin and relapses less often after treatment with anti-TB drugs, compared to wild-type strains.<sup>(50)</sup>

We identified a total of 23 DosR regulon proteins, of which ten proteins were significantly more abundant in the *M. tuberculosis* typical Beijing strain analysed; Table S3. Previous mRNA analysis of five selected DosR genes demonstrated that *M. tuberculosis* Beijing strains maintain higher levels of these DosR gene transcripts than non-Beijing strains.<sup>(51)</sup> From these five proteins, we could confirm the increased abundance of Rv2031c/hspX, Rv3133c/devR and Rv3130c/tgs1 in a direct comparison with the H37Rv strain.

The second regulon we identified to be enriched for differentially abundant proteins is the PhoPR regulon; Figure 3.<sup>(52)</sup> Especially PhoPR regulated proteins involved in lipid metabolism were found to be more abundant in the proteome of *M. tuberculosis* H37Rv. The virulence of PhoPR knock-outs is impaired to such an extent that *M. tuberculosis* PhoPR mutants are considered safe enough to be used as vaccine strains.<sup>(53, 54)</sup> The differential abundance of PhoPR proteins might reflect a not yet explored mechanism of *M. tuberculosis* Beijing related to a distinct virulent phenotype. Regarding rifampicin susceptibility, PhoPR knock-outs display a MIC similar to that of wildtype *M. tuberculosis*, indicating that PhoPR does not directly contribute to drug tolerance.<sup>(54)</sup>

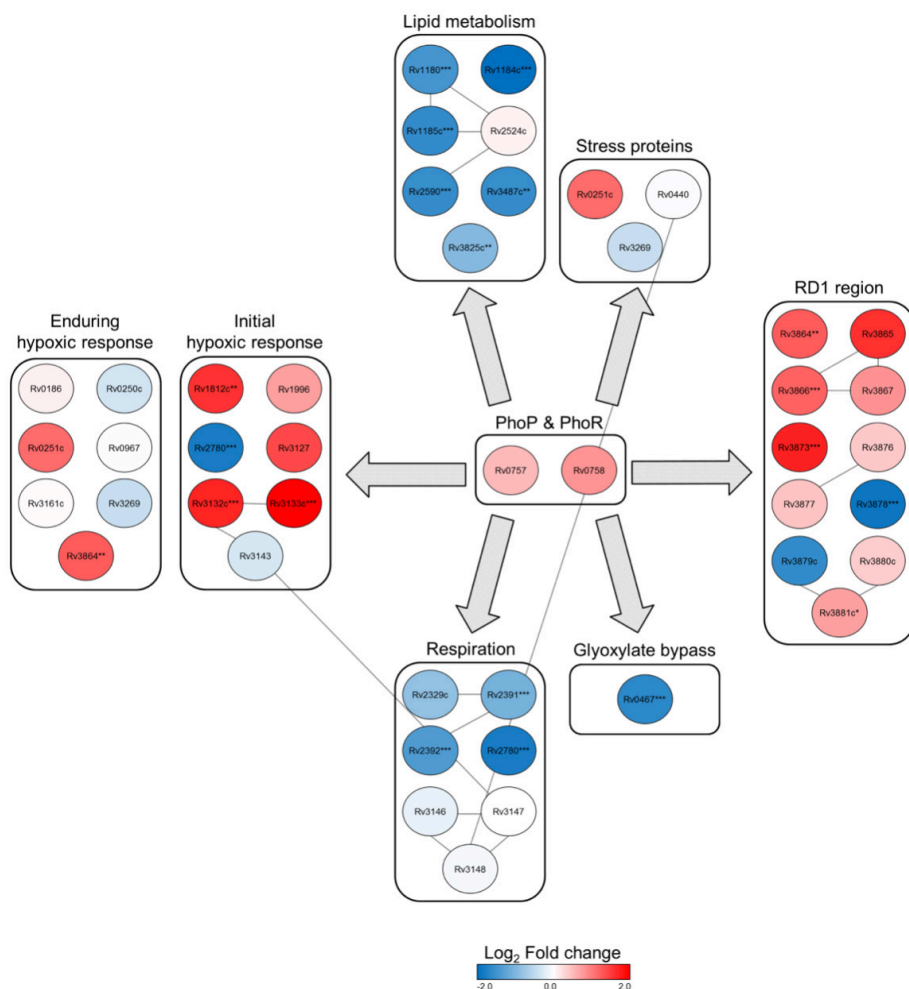


**FIGURE 3:** The PhoPR regulon network. PhoPR regulated genes that are related to intracellular survival and virulence are visualized and grouped by function as described previously.(52) The selected proteins of the PhoPR network are coloured by their fold change, proteins in red are more abundant in *M. tuberculosis* typical Beijing whereas red coloured proteins were identified to be less abundant in *M. tuberculosis* typical Beijing compared to H37Rv. The significance of the proteins, as determined with the significance B-test, is presented as follows: \* <0.05, \*\* <0.01, \*\*\*<0.001. Grey lines correspond to protein-protein interactions as reported in the STRING database, with a minimal confidence of 0.7.(66)

### **Dormancy proteins are induced by *M. tuberculosis* H37Rv and Beijing after exposure to rifampicin**

When we compared the proteomes of both *M. tuberculosis* genotypes after exposure to rifampicin, we observed a shared response to the antibiotic; Table S1. Rv1942c/mazF5 was the

strongest induced protein in both lineages. The DosR regulon associated proteins Rv2031c/hspX and, to a lesser extent, RV2032/acg, were more abundant in both lineages after exposure; Figure S2. Thereby, we show that the induction of DosR proteins upon rifampicin exposure is shared by multiple *M. tuberculosis* lineages. However, the observed absolute increase of Rv2031c/hspX induced by rifampicin was more than three-fold higher in the *M. tuberculosis* typical Beijing strain than in H37Rv; Figure S3.

The increased abundance and stronger induction of DosR regulon proteins in *M. tuberculosis* typical Beijing, compared to H37Rv, possibly reflects an increased ability of Beijing strains to swiftly develop a dormant phenotype when stressed. This potentially more rapid transition to dormancy will make the pathogen less susceptible to rifampicin, thus providing a prolonged period for the selection of mutants, which will reduce the efficacy of this drug to sterilize tissues containing bacteria. It is thereby conceivable this will lead to more relapses after curative treatment.

Furthermore, the observation that environmental factors and rifampicin can induce dormancy proteins, suggests that the DosR-regulon is induced as part of a general stress response.<sup>(31)</sup> The increased abundance and stronger induction of DosR regulon proteins might therefore provide a selective advantage to multiple (first-line) antibiotics.

Taken together, the outcomes of our proteomic study demonstrate that both *M. tuberculosis* typical Beijing and H37Rv induce DosR proteins as a response to rifampicin-induced stress, however, the base-line level of these proteins is higher in Beijing genotype strains. This observation suggests that the *a priori* high abundance of DosR proteins contributes to the “success” of *M. tuberculosis* typical Beijing. However, strain H37Rv is, although considered virulent, a laboratory strain. Therefore, we cannot state whether the differences in proteomic composition reflect differences between *M. tuberculosis* typical Beijing and all other clinical strains.

### **M. tuberculosis typical Beijing proteome signature**

To extend our DDA derived findings to a larger cohort of *M. tuberculosis* isolates of different genotypes, we designed a large-scale PRM assay with spiked-in SIL peptides. Based on our DDA proteomic dataset and the available literature, we made a selection of 33 proteins, including PhoPR proteins, DosR proteins, the antigens esxA/B/W and efflux pumps, that potentially contribute to the success of *M. tuberculosis* Beijing lineage. For a list of the proteins and peptides selected and the corresponding rationale for selection, see Table S4. The selection of appropriate proteotypic peptides for PRM was performed either manually, based on the

DDA data obtained intensity and fragmentation pattern, or from an online repository of *M. tuberculosis* targeted proteomic assays.<sup>(55)</sup> SIL peptides were labelled with a ‘heavy’ dimethyl label (+36Da), whereas the tryptic digest was ‘light’ labelled (+28Da). The selected 33 proteins were monitored by 83 peptides and a total of 348 transitions per isotopic mass label.

The abundance of these 33 proteins was determined in the proteomes of 27 clinical isolates derived from four of the most prevalent *M. tuberculosis* lineages; Figure S4 and Table S5. In addition, we selected members of the atypical Beijing lineage; a sub-lineage genetically closely related to typical Beijing strains, but less conserved.<sup>(24)</sup> The *M. africanum* lineage was excluded as cases are restricted to West-Africa<sup>(56)</sup> and *M. bovis* was excluded as it causes <3% of all pulmonary TB cases worldwide.<sup>(57)</sup>

Protein ratios obtained by PRM showed to be highly reproducible; Figure S5 and Table S6. Two proteins, Rv0450c/mmpL4 and Rv3283/sseA were only identified to be differentially abundant in the *M. tuberculosis* typical Beijing strains; Figure 4 and Figure S6. We have previously described that the abundance of these two proteins differ between typical and atypical Beijing lineages.<sup>(28)</sup> However, in this study we demonstrate that this observation extends to all the other *M. tuberculosis* genotypes examined.

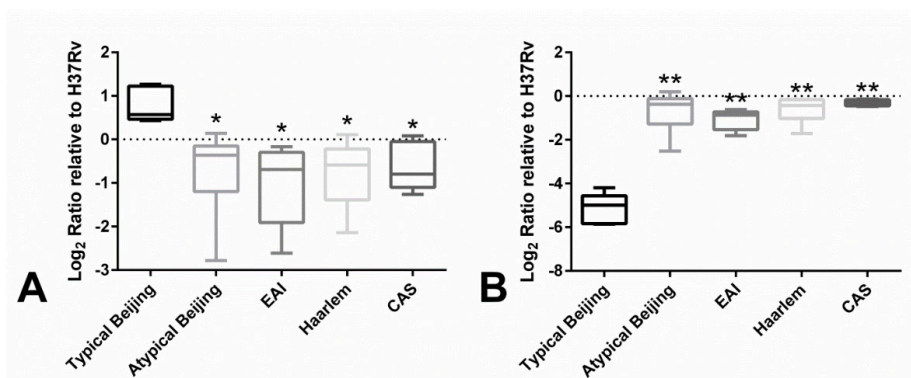


**FIGURE 4:** Proteins identified to be differentially abundant in the typical Beijing sub-lineage. Rv0450c/mmpL4 is more abundant in *M. tuberculosis* typical Beijing (A), whereas Rv3283/sseA is less abundant in the typical Beijing sub-lineage (B). All protein ratios are relative to the protein abundance determined in *M. tuberculosis* H37Rv. The box-plot representation shows the median value of protein abundance (middle bold line), the lower and upper limits of each box representing the first and third quartiles, respectively. Whiskers represent the min/max protein abundance determined (\*P=<0.05, \*\*P=<0.01).

Rv0450c/mmpL4 is generally an essential virulence factor for *M. tuberculosis*, as demonstrated by knock-out experiments.<sup>(58, 59)</sup> Within *M. tuberculosis*, the function of Rv0450c/mmpL4 appears to be complementary to Rv0676c/mmpL5, both secreting iron-scavenging siderophores.<sup>(60)</sup> However, Rv0676c/mmpL5 contains a nsSNP specific to typical Beijing, whereas we here describe that Rv0450c/mmpL4, and not Rv0676c/mmpL5, is more abundant in typical Beijing strains than in any of the other *M. tuberculosis* genotypes examined; Figure 4A and Figure S6A. Both the specific presence of a nsSNP in Rv0676c/mmpL5 of typical Beijing strains and the increased abundance of Rv0450c/mmpL4 indicate a unique role for iron metabolism in typical Beijing strains. In relation to dormancy, *M. tuberculosis* has been suggested to increase iron storages prior to this phase of non-replicating persistence.<sup>(61)</sup> The high abundance of Rv0450c/mmpL4 in *M. tuberculosis* typical Beijing is most likely a pre-existent dormancy related factor within this specific sub-lineage.

Both Rv0450c/mmpL4 and Rv3283/sseA contain a nsSNP specific to *M. tuberculosis* typical Beijing.<sup>(24, 28)</sup> For Rv3283/sseA, a thiosulfate sulfurtransferase, we have previously demonstrated that the typical Beijing specific nsSNP yields the protein unstable.<sup>(28)</sup> As a consequence, we have observed that Rv3283/sseA is less abundant in members of the typical Beijing genotype; Figure 4B and Figure S6B. Generally, the loss of functional proteins in *M. tuberculosis* promotes an attenuated phenotype. However, mycobacteria deficient of a functional Rv3283/sseA show improved growth in an *in vitro* macrophage model.<sup>(62)</sup> Thereby, it is conceivable that the average  $\pm 50$ -fold lower abundance of Rv3283/sseA in typical Beijing strains contributes to the increased virulence of this sub-lineage.

### Regulators of dormancy are more abundant in Beijing strains

One of the regulatory networks of which the protein abundance differed between the typical Beijing and the H37Rv strain was PhoPR, a major virulence regulon within *M. tuberculosis*; Figure 3<sup>(52, 53)</sup> Our PRM data show that the abundance of PhoPR regulated proteins is conserved throughout the various *M. tuberculosis* isolates examined; Figure S7. Thereby, we demonstrate that the abundance of PhoPR differs between clinical isolates and the laboratory reference strain H37Rv. This difference in PhoPR regulon protein abundance between the H37Rv reference and *M. tuberculosis* clinical isolates could be responsible for the described deviant virulence associated characteristics in the H37Rv strain, including the uptake by monocyte-derived-macrophages and early pro-inflammatory cytokine induction.<sup>(63)</sup>

A second regulatory network, of which we identified the proteins to be more abundant in the typical Beijing isolate compared to H37Rv, is the DosR dormancy regulon; Table S3. Of the eight DosR regulon proteins that we quantified in the clinical isolates examined, we identified Rv3132c/devS and Rv3133c/devR, the proteins that compromise the DosR two-component

regulatory system, to be more abundant in both *M. tuberculosis* Beijing sub-lineages; Figure 5 and Figure S8 & S9. Furthermore, the DosR controlled proteins Rv0079, Rv2031c/hspX, Rv2032/acg, Rv2627c, Rv3130c/tgs1 and Rv3131 showed to be less abundant in *M. tuberculosis* CAS than in *M. tuberculosis* typical Beijing; Figure 5 & Figure S8.

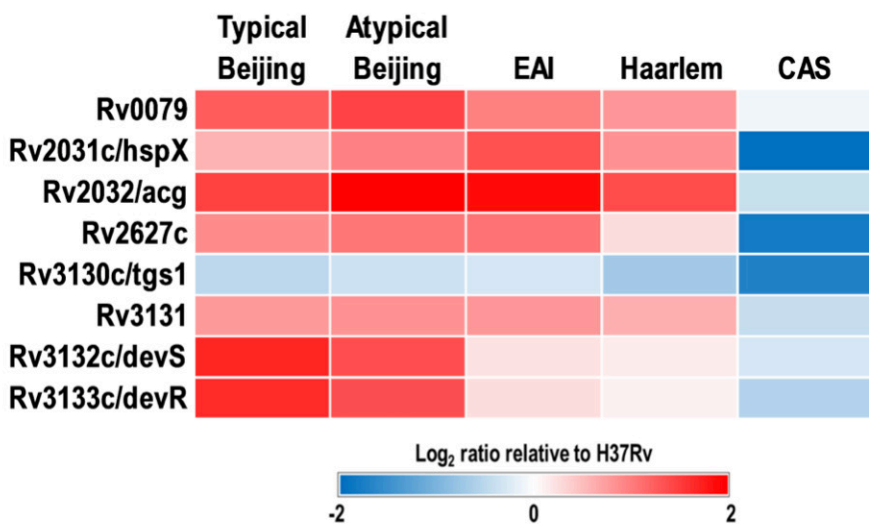


**FIGURE 5:** Heat map of selected differentially regulated DosR proteins quantified by PRM in various *M. tuberculosis* genotypes. The selected proteins were coloured by the average fold change of the genotype, relative to *M. tuberculosis* H37Rv.

Our DDA data demonstrate that dormancy proteins are induced in both the typical Beijing- and the *M. tuberculosis* reference strain H37Rv, showing that this response is shared by multiple members of the *M. tuberculosis* grouping. Based on this observation, combined with our PRM data that demonstrates that *M. tuberculosis* Beijing strains maintain higher levels of the dormancy regulator, we can conclude that early markers of the response to rifampicin are constitutively more abundant in Beijing strains compared to other clinically relevant strains.

*M. tuberculosis* typical Beijing strains contain a specific mutation in Rv2027c/dosT, the sensor part of the two-component dormancy regulatory system.<sup>(64)</sup> The presence of this mutation correlated with the expression of Rv3133c/devR transcripts in the same study. As a consequence, it has been suggested that typical Beijing strains express on average a 12-fold more Rv3133c/devR-mRNA than atypical Beijing strains.<sup>(64)</sup> Our PRM based quantification of Rv3133c/devR



shows that this protein is equally abundant in both typical and atypical Beijing sub-lineages and four-fold more abundant in the Beijing strains examined compared to the other genotypes analysed; Figure 5 and Figure S8. Thereby, we reject the hypothesis that this mutation correlates with differential abundance of Rv3133c/devR on the protein level. However, this finding does not preclude the possibility that the mutation in Rv2027c/dosT plays a (in)direct role in the biology of more modern lineages of *M. tuberculosis* Beijing. In fact, the presence of a typical Beijing specific mutation in the DosR regulon strengthens our hypothesis that there is a unique role in the dormancy pathway in this specific pathogenic sub-lineage.

Bacteria that are capable to establish dormancy during antibiotic treatment, extend their window of opportunity to acquire drug resistance conferring mutations. Moreover, *M. tuberculosis* cells that enter a fully dormant state of non-replicating persistence, maintain the same mutation rate as actively growing cells.<sup>(65)</sup> Therefore, we argue that the constitutive high abundance of DosR, as described specifically for *M. tuberculosis* Beijing strains in this study, contributes to an accelerated development of antibiotic resistance for compounds targeting metabolically active cells.

## Conclusion

In this study, we searched for specific bacterial factors that may account for the epidemiological and *in vitro* phenomena that have been described for the Beijing genotype of *M. tuberculosis*. Our DDA study shows that the typical Beijing- and H37Rv strain both induce DosR dormancy proteins as a shared response to rifampicin exposure. However, we observed that these proteins are more abundant in typical Beijing strains than in the reference strain H37Rv already prior to drug exposure. Subsequent PRM based quantification of these dormancy proteins in multiple, clinically relevant *M. tuberculosis* lineages demonstrated that the regulators of dormancy are more abundant in members of *M. tuberculosis* Beijing genotype than in any of the other lineages examined. The here described pre-existing high abundance of dormancy regulators in Beijing strains can provide these strains an edge over other strains to persist for prolonged periods of time during rifampicin treatment. The identification of this *M. tuberculosis* Beijing specific trait will eventually contribute to improved diagnostics and treatment for the millions of individuals that receive anti-TB therapy annually. Consequently, this finding may contribute to the global management of MDR-TB.

## References

1. Organisation, W. H., Global tuberculosis report 2015. *Geneva* **2015**.
2. Casali, N.; Nikolayevskyy, V.; Balabanova, Y.; Harris, S. R.; Ignatyeva, O.; Kontsevaya, I.; Corander, J.; Bryant, J.; Parkhill, J.; Nejentsev, S.; Horstmann, R. D.; Brown, T.; Drobniewski, F., Evolution and transmission of drug-resistant tuberculosis in a Russian population. *Nat Genet* **2014**, 46, (3), 279-86.
3. Mokrousov, I., Insights into the origin, emergence, and current spread of a successful Russian clone of *Mycobacterium tuberculosis*. *Clin Microbiol Rev* **2013**, 26, (2), 342-60.
4. Ford, C. B.; Shah, R. R.; Maeda, M. K.; Gagneux, S.; Murray, M. B.; Cohen, T.; Johnston, J. C.; Gardy, J.; Lipsitch, M.; Fortune, S. M., *Mycobacterium tuberculosis* mutation rate estimates from different lineages predict substantial differences in the emergence of drug-resistant tuberculosis. *Nat Genet* **2013**, 45, (7), 784-90.
5. Ebrahimi-Rad, M.; Bifani, P.; Martin, C.; Kremer, K.; Samper, S.; Rauzier, J.; Kreiswirth, B.; Blazquez, J.; Jouan, M.; van Soolingen, D.; Gicquel, B., Mutations in putative mutator genes of *Mycobacterium tuberculosis* strains of the W-Beijing family. *Emerg Infect Dis* **2003**, 9, (7), 838-45.
6. de Steenwinkel, J. E.; ten Kate, M. T.; de Knecht, G. J.; Kremer, K.; Aarnoutse, R. E.; Boeree, M. J.; Verbrugh, H. A.; van Soolingen, D.; Bakker-Woudenberg, I. A., Drug susceptibility of *Mycobacterium tuberculosis* Beijing genotype and association with MDR TB. *Emerg Infect Dis* **2012**, 18, (4), 660-3.
7. den Hertog, A. L.; Menting, S.; van Soolingen, D.; Anthony, R. M., *Mycobacterium tuberculosis* Beijing genotype resistance to transient rifampin exposure. *Emerg Infect Dis* **2014**, 20, (11), 1932-3.
8. Kremer, K.; van-der-Werf, M. J.; Au, B. K.; Anh, D. D.; Kam, K. M.; van-Doorn, H. R.; Borgdorff, M. W.; van-Soolingen, D., Vaccine-induced immunity circumvented by typical *Mycobacterium tuberculosis* Beijing strains. *Emerg Infect Dis* **2009**, 15, (2), 335-9.
9. Ordway, D. J.; Shang, S.; Henao-Tamayo, M.; Obregon-Henao, A.; Nold, L.; Caraway, M.; Shanley, C. A.; Basaraba, R. J.; Duncan, C. G.; Orme, I. M., *Mycobacterium bovis* BCG-mediated protection against W-Beijing strains of *Mycobacterium tuberculosis* is diminished concomitant with the emergence of regulatory T cells. *Clin Vaccine Immunol* **2011**, 18, (9), 1527-35.
10. Orme, I. M., Development of new vaccines and drugs for TB: limitations and potential strategic errors. *Future Microbiol* **2011**, 6, (2), 161-77.
11. Buu, T. N.; van Soolingen, D.; Huyen, M. N.; Lan, N. T.; Quy, H. T.; Tiemersma, E. W.; Kremer, K.; Borgdorff, M. W.; Cobelens, F. G., Increased transmission of *Mycobacterium tuberculosis* Beijing genotype strains associated with resistance to streptomycin: a population-based study. *PLoS One* **2012**, 7, (8), e42323.
12. Yang, C.; Luo, T.; Sun, G.; Qiao, K.; Sun, G.; DeRiemer, K.; Mei, J.; Gao, Q., *Mycobacterium tuberculosis* Beijing strains favor transmission but not drug resistance in China. *Clin Infect Dis* **2012**, 55, (9), 1179-87.
13. Wada, T.; Fujihara, S.; Shimouchi, A.; Harada, M.; Ogura, H.; Matsumoto, S.; Hase, A., High transmissibility of the modern Beijing *Mycobacterium tuberculosis* in homeless patients of Japan. *Tuberculosis (Edinb)* **2009**, 89, (4), 252-5.

14. Tounghoussova, O. S.; Mariandyshev, A.; Bjune, G.; Sandven, P.; Caugant, D. A., Molecular epidemiology and drug resistance of *Mycobacterium tuberculosis* isolates in the Archangel prison in Russia: predominance of the W-Beijing clone family. *Clin Infect Dis* **2003**, 37, (5), 665-72.
15. Glynn, J. R.; Whiteley, J.; Bifani, P. J.; Kremer, K.; van Soolingen, D., Worldwide occurrence of Beijing/W strains of *Mycobacterium tuberculosis*: a systematic review. *Emerg Infect Dis* **2002**, 8, (8), 843-9.
16. Parwati, I.; Alisjahbana, B.; Apriani, L.; Soetikno, R. D.; Ottenhoff, T. H.; van der Zanden, A. G.; van der Meer, J.; van Soolingen, D.; van Crevel, R., *Mycobacterium tuberculosis* Beijing genotype is an independent risk factor for tuberculosis treatment failure in Indonesia. *J Infect Dis* **2010**, 201, (4), 553-7.
17. Devaux, I.; Kremer, K.; Heersma, H.; Van Soolingen, D., Clusters of multidrug-resistant *Mycobacterium tuberculosis* cases, Europe. *Emerg Infect Dis* **2009**, 15, (7), 1052-60.
18. Buu, T. N.; Huyen, M. N.; Lan, N. T.; Quy, H. T.; Hen, N. V.; Zignol, M.; Borgdorff, M. W.; Cobelens, F. G.; van Soolingen, D., The Beijing genotype is associated with young age and multidrug-resistant tuberculosis in rural Vietnam. *Int J Tuberc Lung Dis* **2009**, 13, (7), 900-6.
19. Drobniewski, F.; Balabanova, Y.; Nikolayevsky, V.; Ruddy, M.; Kuznetsov, S.; Zakharova, S.; Melentyev, A.; Fedorin, I., Drug-resistant tuberculosis, clinical virulence, and the dominance of the Beijing strain family in Russia. *JAMA* **2005**, 293, (22), 2726-31.
20. European Concerted Action on New Generation Genetic, M.; Techniques for the, E.; Control of, T., Beijing/W genotype *Mycobacterium tuberculosis* and drug resistance. *Emerg Infect Dis* **2006**, 12, (5), 736-43.
21. Kato-Maeda, M.; Shanley, C. A.; Ackart, D.; Jarlsberg, L. G.; Shang, S.; Obregon-Henao, A.; Harton, M.; Basaraba, R. J.; Henao-Tamayo, M.; Barrozo, J. C.; Rose, J.; Kawamura, L. M.; Coscolla, M.; Fofanov, V. Y.; Koshinsky, H.; Gagneux, S.; Hopewell, P. C.; Ordway, D. J.; Orme, I. M., Beijing sublineages of *Mycobacterium tuberculosis* differ in pathogenicity in the guinea pig. *Clin Vaccine Immunol* **2012**, 19, (8), 1227-37.
22. Mokrousov, I.; Narvskaya, O.; Otten, T.; Vyazovaya, A.; Limeschenko, E.; Steklova, L.; Vyshnevskiy, B., Phylogenetic reconstruction within *Mycobacterium tuberculosis* Beijing genotype in northwestern Russia. *Res Microbiol* **2002**, 153, (10), 629-37.
23. Tsolaki, A. G.; Gagneux, S.; Pym, A. S.; Goguet de la Salmoniere, Y. O.; Kreiswirth, B. N.; Van Soolingen, D.; Small, P. M., Genomic deletions classify the Beijing/W strains as a distinct genetic lineage of *Mycobacterium tuberculosis*. *J Clin Microbiol* **2005**, 43, (7), 3185-91.
24. Schurch, A. C.; Kremer, K.; Warren, R. M.; Hung, N. V.; Zhao, Y.; Wan, K.; Boeree, M. J.; Siezen, R. J.; Smith, N. H.; van Soolingen, D., Mutations in the regulatory network underlie the recent clonal expansion of a dominant subclone of the *Mycobacterium tuberculosis* Beijing genotype. *Infect Genet Evol* **2011**, 11, (3), 587-97.
25. Hanekom, M.; van der Spuy, G. D.; Streicher, E.; Ndabambi, S. L.; McEvoy, C. R.; Kidd, M.; Beyers, N.; Victor, T. C.; van Helden, P. D.; Warren, R. M., A recently evolved sublineage of the *Mycobacterium tuberculosis* Beijing strain family is associated with an increased ability to spread and cause disease. *J*

*Clin Microbiol* **2007**, 45, (5), 1483-90.

26. Parwati, I.; van Crevel, R.; van Soolingen, D., Possible underlying mechanisms for successful emergence of the Mycobacterium tuberculosis Beijing genotype strains. *Lancet Infect Dis* **2010**, 10, (2), 103-11.
27. Pheiffer, C.; Betts, J. C.; Flynn, H. R.; Lukey, P. T.; van Helden, P., Protein expression by a Beijing strain differs from that of another clinical isolate and Mycobacterium tuberculosis H37Rv. *Microbiology* **2005**, 151, (Pt 4), 1139-50.
28. de Keijzer, J.; de Haas, P. E.; de Ru, A. H.; van Veelen, P. A.; van Soolingen, D., Disclosure of selective advantages in the 'modern' sublineage of the Mycobacterium tuberculosis Beijing genotype family by quantitative proteomics. *Mol Cell Proteomics* **2014**.
29. de Keijzer, J.; Mulder, A.; de Beer, J.; de Ru, A. H.; van Veelen, P. A.; van Soolingen, D., Mechanisms of Phenotypic Rifampicin Tolerance in Mycobacterium tuberculosis Beijing Genotype Strain B0/W148 Revealed by Proteomics. *J Proteome Res* **2016**, 15, (4), 1194-204.
30. Gomez, J. E.; McKinney, J. D., M. tuberculosis persistence, latency, and drug tolerance. *Tuberculosis (Edinb)* **2004**, 84, (1-2), 29-44.
31. Deb, C.; Lee, C. M.; Dubey, V. S.; Daniel, J.; Abomoelak, B.; Sirakova, T. D.; Pawar, S.; Rogers, L.; Kolattukudy, P. E., A novel in vitro multiple-stress dormancy model for Mycobacterium tuberculosis generates a lipid-loaded, drug-tolerant, dormant pathogen. *PLoS One* **2009**, 4, (6), e6077.
32. Wayne, L. G., In Vitro Model of Hypoxically Induced Nonreplicating Persistence of Mycobacterium tuberculosis. *Methods Mol Med* **2001**, 54, 247-69.
33. Mokrousov, I.; Narvskaya, O.; Vyazovaya, A.; Otten, T.; Jiao, W. W.; Gomes, L. L.; Suffys, P. N.; Shen, A. D.; Vishnevsky, B., Russian "successful" clone B0/W148 of Mycobacterium tuberculosis Beijing genotype: a multiplex PCR assay for rapid detection and global screening. *J Clin Microbiol* **2012**, 50, (11), 3757-9.
34. Huyen, M. N.; Tiemersma, E. W.; Lan, N. T.; Cobelens, F. G.; Dung, N. H.; Sy, D. N.; Buu, T. N.; Kremer, K.; Hang, P. T.; Caws, M.; O'Brien, R.; van Soolingen, D., Validation of the GenoType MTBDRplus assay for diagnosis of multidrug resistant tuberculosis in South Vietnam. *BMC Infect Dis* **2010**, 10, 149.
35. Woods, G. L.; Brown-Elliott, B. A.; Desmond, E. P.; Hall, G. S.; Heifets, L.; Pfyffer, G. E.; Ridderhof, J. C.; Wallace, R. J.; Warren, N. G.; Witebsky, F. G., Susceptibility Testing of Mycobacteria, Nocardiae, and Other Aerobic Actinomycetes; Approved Standard, second edition. *Clinical and Laboratory Standards Institute* **2011**.
36. Wisniewski, J. R.; Zougman, A.; Nagaraj, N.; Mann, M., Universal sample preparation method for proteome analysis. *Nat Methods* **2009**, 6, (5), 359-62.
37. Boersema, P. J.; Raijmakers, R.; Lemeer, S.; Mohammed, S.; Heck, A. J., Multiplex peptide stable isotope dimethyl labeling for quantitative proteomics. *Nat Protoc* **2009**, 4, (4), 484-94.
38. Cox, J.; Mann, M., MaxQuant enables high peptide identification rates, individualized p.p.b.-range mass accuracies and proteome-wide protein quantification. *Nat Biotechnol* **2008**, 26, (12), 1367-72.
39. Cox, J.; Neuhauser, N.; Michalski, A.; Scheltema, R. A.; Olsen, J. V.; Mann, M., Andromeda: a peptide search engine integrated into the MaxQuant environment. *J Proteome Res* **2011**, 10, (4), 1794-805.
40. Cole, S. T.; Brosch, R.; Parkhill, J.; Garnier, T.; Churcher, C.; Harris, D.; Gordon, S. V.; Eiglmeier, K.; Gas,

- S.; Barry, C. E., 3rd; Tekaia, F.; Badcock, K.; Basham, D.; Brown, D.; Chillingworth, T.; Connor, R.; Davies, R.; Devlin, K.; Feltwell, T.; Gentles, S.; Hamlin, N.; Holroyd, S.; Hornsby, T.; Jagels, K.; Krogh, A.; McLean, J.; Moule, S.; Murphy, L.; Oliver, K.; Osborne, J.; Quail, M. A.; Rajandream, M. A.; Rogers, J.; Rutter, S.; Seeger, K.; Skelton, J.; Squares, R.; Squares, S.; Sulston, J. E.; Taylor, K.; Whitehead, S.; Barrell, B. G., Deciphering the biology of *Mycobacterium tuberculosis* from the complete genome sequence. *Nature* **1998**, 393, (6685), 537-44.
41. MacLean, B.; Tomazela, D. M.; Shulman, N.; Chambers, M.; Finney, G. L.; Frewen, B.; Kern, R.; Tabb, D. L.; Liebler, D. C.; MacCoss, M. J., Skyline: an open source document editor for creating and analyzing targeted proteomics experiments. *Bioinformatics* **2010**, 26, (7), 966-8.
  42. Bergval, I.; Sengstake, S.; Brankova, N.; Levterova, V.; Abadia, E.; Tadumaze, N.; Bablishvili, N.; Akhalaia, M.; Tuin, K.; Schuitema, A.; Panaiotov, S.; Bachiyska, E.; Kantardjiev, T.; de Zwaan, R.; Schurch, A.; van Soolingen, D.; van 't Hoog, A.; Cobelens, F.; Aspindzelashvili, R.; Sola, C.; Klatser, P.; Anthony, R., Combined species identification, genotyping, and drug resistance detection of *Mycobacterium tuberculosis* cultures by MLPA on a bead-based array. *PLoS One* **2012**, 7, (8), e43240.
  43. Ioerger, T. R.; Feng, Y.; Ganesula, K.; Chen, X.; Dobos, K. M.; Fortune, S.; Jacobs, W. R., Jr.; Mizrahi, V.; Parish, T.; Rubin, E.; Sasseti, C.; Sacchetti, J. C., Variation among genome sequences of H37Rv strains of *Mycobacterium tuberculosis* from multiple laboratories. *J Bacteriol* **2010**, 192, (14), 3645-53.
  44. Flynn, J. L.; Chan, J., Tuberculosis: latency and reactivation. *Infect Immun* **2001**, 69, (7), 4195-201.
  45. Evangelopoulos, D.; da Fonseca, J. D.; Waddell, S. J., Understanding anti-tuberculosis drug efficacy: rethinking bacterial populations and how we model them. *Int J Infect Dis* **2015**, 32, 76-80.
  46. Wayne, L. G.; Sohaskey, C. D., Nonreplicating persistence of mycobacterium tuberculosis. *Annu Rev Microbiol* **2001**, 55, 139-63.
  47. Voskuil, M. I.; Schnappinger, D.; Visconti, K. C.; Harrell, M. I.; Dolganov, G. M.; Sherman, D. R.; Schoolnik, G. K., Inhibition of respiration by nitric oxide induces a *Mycobacterium tuberculosis* dormancy program. *J Exp Med* **2003**, 198, (5), 705-13.
  48. Schnappinger, D.; Ehrt, S.; Voskuil, M. I.; Liu, Y.; Mangan, J. A.; Monahan, I. M.; Dolganov, G.; Efron, B.; Butcher, P. D.; Nathan, C.; Schoolnik, G. K., Transcriptional Adaptation of *Mycobacterium tuberculosis* within Macrophages: Insights into the Phagosomal Environment. *J Exp Med* **2003**, 198, (5), 693-704.
  49. Betts, J. C.; Lukey, P. T.; Robb, L. C.; McAdam, R. A.; Duncan, K., Evaluation of a nutrient starvation model of *Mycobacterium tuberculosis* persistence by gene and protein expression profiling. *Mol Microbiol* **2002**, 43, (3), 717-31.
  50. Hu, Y.; Liu, A.; Menendez, M. C.; Garcia, M. J.; Oravcova, K.; Gillespie, S. H.; Davies, G. R.; Mitchison, D. A.; Coates, A. R., HspX knock-out in *Mycobacterium tuberculosis* leads to shorter antibiotic treatment and lower relapse rate in a mouse model—a potential novel therapeutic target. *Tuberculosis (Edinb)* **2015**, 95, (1), 31-6.
  51. Reed, M. B.; Gagneux, S.; Deriemer, K.; Small, P. M.; Barry, C. E., 3rd, The W-Beijing lineage of *Mycobacterium tuberculosis* overproduces triglycerides and has the DosR dormancy regulon constitutively upregulated. *J Bacteriol* **2007**, 189, (7), 2583-9.

52. Gonzalo-Asensio, J.; Mostowy, S.; Harders-Westerveen, J.; Huygen, K.; Hernandez-Pando, R.; Thole, J.; Behr, M.; Gicquel, B.; Martin, C., PhoP: a missing piece in the intricate puzzle of *Mycobacterium tuberculosis* virulence. *PLoS One* **2008**, 3, (10), e3496.
53. Walters, S. B.; Dubnau, E.; Kolesnikova, I.; Laval, F.; Daffe, M.; Smith, I., The *Mycobacterium tuberculosis* PhoPR two-component system regulates genes essential for virulence and complex lipid biosynthesis. *Mol Microbiol* **2006**, 60, (2), 312-30.
54. Cardona, P. J.; Asensio, J. G.; Arbues, A.; Otal, I.; Lafoz, C.; Gil, O.; Caceres, N.; Ausina, V.; Gicquel, B.; Martin, C., Extended safety studies of the attenuated live tuberculosis vaccine SO2 based on phoP mutant. *Vaccine* **2009**, 27, (18), 2499-505.
55. Schubert, O. T.; Mouritsen, J.; Ludwig, C.; Rost, H. L.; Rosenberger, G.; Arthur, P. K.; Claassen, M.; Campbell, D. S.; Sun, Z.; Farrah, T.; Gengenbacher, M.; Maiolica, A.; Kaufmann, S. H.; Moritz, R. L.; Aebersold, R., The Mtb proteome library: a resource of assays to quantify the complete proteome of *Mycobacterium tuberculosis*. *Cell Host Microbe* **2013**, 13, (5), 602-12.
56. de Jong, B. C.; Antonio, M.; Gagneux, S., *Mycobacterium africanum*--review of an important cause of human tuberculosis in West Africa. *PLoS Negl Trop Dis* **2010**, 4, (9), e744.
57. Muller, B.; Durr, S.; Alonso, S.; Hattendorf, J.; Laisse, C. J.; Parsons, S. D.; van Helden, P. D.; Zinsstag, J., Zoonotic *Mycobacterium bovis*-induced tuberculosis in humans. *Emerg Infect Dis* **2013**, 19, (6), 899-908.
58. Camacho, L. R.; Ensergueix, D.; Perez, E.; Gicquel, B.; Guilhot, C., Identification of a virulence gene cluster of *Mycobacterium tuberculosis* by signature-tagged transposon mutagenesis. *Mol Microbiol* **1999**, 34, (2), 257-67.
59. Domenech, P.; Reed, M. B.; Barry, C. E., 3rd, Contribution of the *Mycobacterium tuberculosis* MmpL protein family to virulence and drug resistance. *Infect Immun* **2005**, 73, (6), 3492-501.
60. Wells, R. M.; Jones, C. M.; Xi, Z.; Speer, A.; Danilchanka, O.; Doornbos, K. S.; Sun, P.; Wu, F.; Tian, C.; Niederweis, M., Discovery of a siderophore export system essential for virulence of *Mycobacterium tuberculosis*. *PLoS Pathog* **2013**, 9, (1), e1003120.
61. Voskuil, M. I.; Visconti, K. C.; Schoolnik, G. K., *Mycobacterium tuberculosis* gene expression during adaptation to stationary phase and low-oxygen dormancy. *Tuberculosis (Edinb)* **2004**, 84, (3-4), 218-27.
62. Triccas, J. A.; Berthet, F. X.; Pelicic, V.; Gicquel, B., Use of fluorescence induction and sucrose counterselection to identify *Mycobacterium tuberculosis* genes expressed within host cells. *Microbiology* **1999**, 145 ( Pt 10), 2923-30.
63. Sarkar, R.; Lenders, L.; Wilkinson, K. A.; Wilkinson, R. J.; Nicol, M. P., Modern lineages of *Mycobacterium tuberculosis* exhibit lineage-specific patterns of growth and cytokine induction in human monocyte-derived macrophages. *PLoS One* **2012**, 7, (8), e43170.
64. Fallow, A.; Domenech, P.; Reed, M. B., Strains of the East Asian (W/Beijing) lineage of *Mycobacterium tuberculosis* are DosS/DosT-DosR two-component regulatory system natural mutants. *J Bacteriol* **2010**, 192, (8), 2228-38.

65. Ford, C. B.; Lin, P. L.; Chase, M. R.; Shah, R. R.; Iartchouk, O.; Galagan, J.; Mohaideen, N.; Iøerger, T. R.; Sacchettini, J. C.; Lipsitch, M.; Flynn, J. L.; Fortune, S. M., Use of whole genome sequencing to estimate the mutation rate of *Mycobacterium tuberculosis* during latent infection. *Nat Genet* **2011**, 43, (5), 482-6.
66. Szklarczyk, D.; Franceschini, A.; Wyder, S.; Forslund, K.; Heller, D.; Huerta-Cepas, J.; Simonovic, M.; Roth, A.; Santos, A.; Tsafou, K. P.; Kuhn, M.; Bork, P.; Jensen, L. J.; von Mering, C., STRING v10: protein-protein interaction networks, integrated over the tree of life. *Nucleic Acids Res* **2015**, 43, (Database issue), D447-52.

## Supporting information

**SUPPORTING INFORMATION TABLE S1:** Overview of the protein identified and quantified in both biological replicates. This table can be downloaded on the website of the journal:

<https://www.sciencedirect.com/science/article/pii/S1874391916303992?via%3Dihub>

**SUPPORTING INFORMATION TABLE S2:** Overview of the peptides identified and quantified in both biological replicates. This table can be downloaded on the website of the journal:

<https://www.sciencedirect.com/science/article/pii/S1874391916303992?via%3Dihub>

**SUPPORTING INFORMATION TABLE S3:** Overview of the dosR regulon proteins identified with their corresponding ratio and significance B score.

Accession number	Gene name	Beijing/H37Rv DMSO#1 Ratio	Beijing/H37Rv DMSO#1 Sig. B	Beijing/H37Rv DMSO#2 Ratio	Beijing/H37Rv DMSO#1 Sig. B
Rv0079	Rv0079	4,906	0,000	5,150	0,000
Rv0081	Rv0081	2,169	0,010	1,391	0,368
Rv0569	Rv0569	1,517	0,195	1,380	0,382
Rv0570	nrdZ	1,505	0,202	1,381	0,381
Rv0571c	Rv0571c	1,161	0,545	1,415	0,300
Rv1812c	Rv1812c	1,717	0,003	1,920	0,003
Rv1996	Rv1996	1,727	0,014	1,695	0,047
Rv1998c	Rv1998c	0,915	0,956	1,209	0,638
Rv2004c	Rv2004c	1,248	0,404	1,266	0,542
Rv2006	otsB1	1,068	0,734	1,136	0,795
Rv2028c	Rv2028c	1,323	0,352	1,281	0,518
Rv2031c	hspX	9,206	0,000	5,090	0,000
Rv2032	acg	4,798	0,000	8,121	0,000
Rv2623	TB31.7	1,484	0,031	1,690	0,019
Rv2624c	Rv2624c	1,085	0,696	1,341	0,432
Rv2627c	Rv2627c	2,559	0,007	2,759	0,003
Rv2629	Rv2629	1,553	0,126	1,570	0,161
Rv3130c	tgs1	4,919	0,000	2,608	0,005
Rv3131	Rv3131	2,300	0,016	2,047	0,037
Rv3132c	devS	3,294	0,000	3,612	0,000
Rv3133c	devR	3,994	0,000	4,587	0,000
Rv3134c	Rv3134c	1,509	0,200	1,597	0,187
Rv3137	Rv3137	0,998	0,971	0,952	0,677

**SUPPORTING INFORMATION TABLE S4:** Overview of the proteins and their corresponding peptides selected for parallel reaction monitoring. This table can be downloaded on the website of the journal:



<https://www.sciencedirect.com/science/article/pii/S1874391916303992?via%3Dihub>

**SUPPORTING INFORMATION TABLE S5:** Overview of the clinical isolates of *Mycobacterium tuberculosis* analysed by parallel reaction monitoring. This table can be downloaded on the website of the journal:

<https://www.sciencedirect.com/science/article/pii/S1874391916303992?via%3Dihub>

**SUPPORTING INFORMATION TABLE S6:** Overview of the protein ratios, relative to *M. tuberculosis* H37Rv, determined by parallel reaction monitoring. This table can be downloaded on the website of the journal:

<https://www.sciencedirect.com/science/article/pii/S1874391916303992?via%3Dihub>

## FIGURES

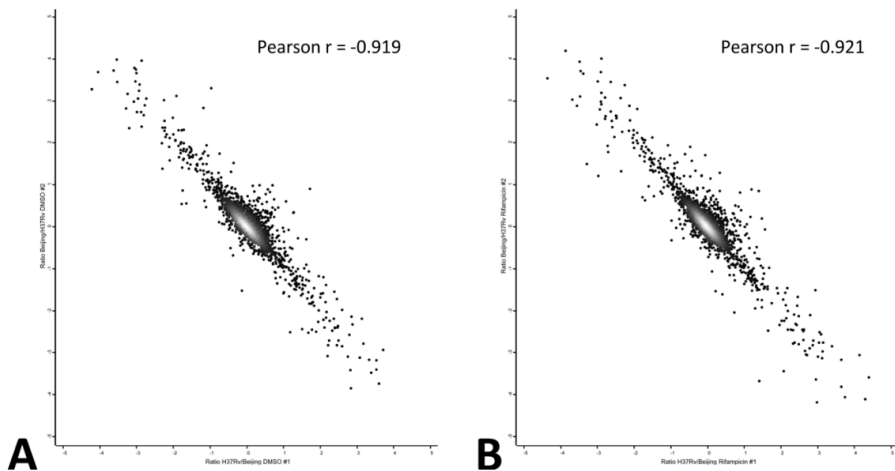


**FIGURE S1:** Density plot of the reproducibility between biological replicates. Biological variability was analysed by quantitative comparison of the protein abundances between both biological replicates after 24hrs treatment with DMSO (A) or rifampicin (B).

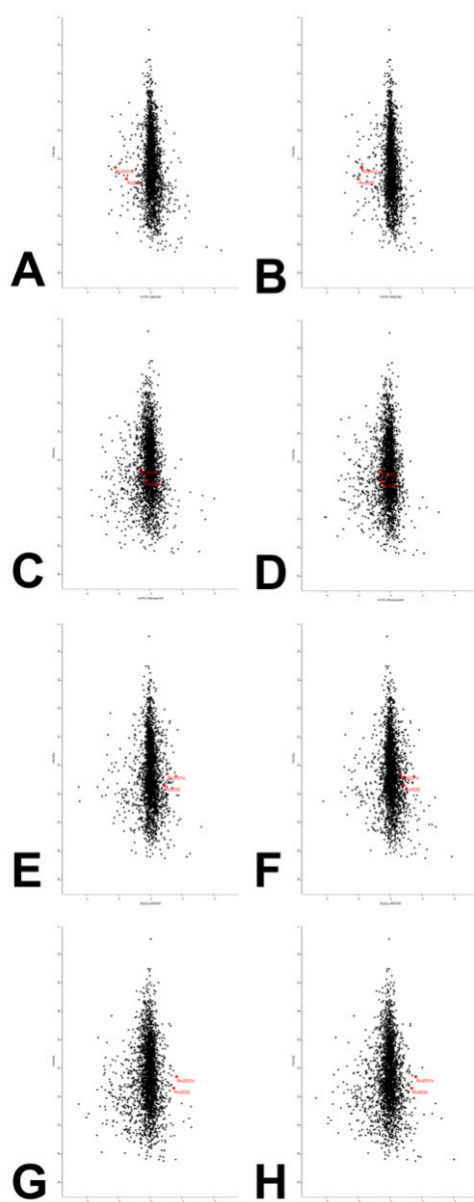


**FIGURE S2:** Scatterplot of protein ratios compared to the internal control for *M. tuberculosis* H37Rv with DMSO (A&B) or rifampicin (C&D) treatment and for *M. tuberculosis* typical Beijing with DMSO (E&F) or rifampicin (G&H) treatment. The protein intensity is plotted on the y-axis and the ratio relative to the internal control is plotted on the x-axis. The dormancy proteins Rv2031c/hspX and Rv2032/acg are highlighted in red.

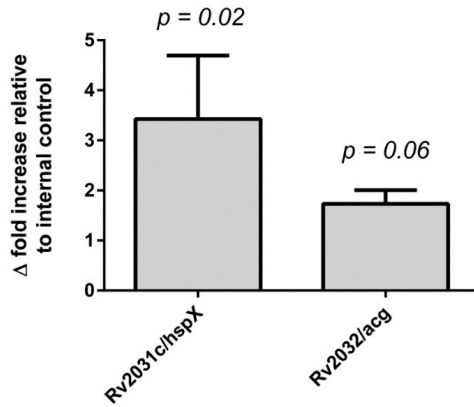


**FIGURE S3:** Delta fold-change induction of Rv2031c/hspX and Rv2032/acg relative to the internal control. The delta fold change was calculated using the following formula:

$$\frac{(\text{fold change Beijing rifampicin to internal control}) - (\text{fold change Beijing DMSO to internal control})}{(\text{fold change H37Rv rifampicin to internal control}) - (\text{fold change H37Rv DMSO to internal control})}$$

P-values were determined between the fold change induced by rifampicin treatment using an unpaired t-test.

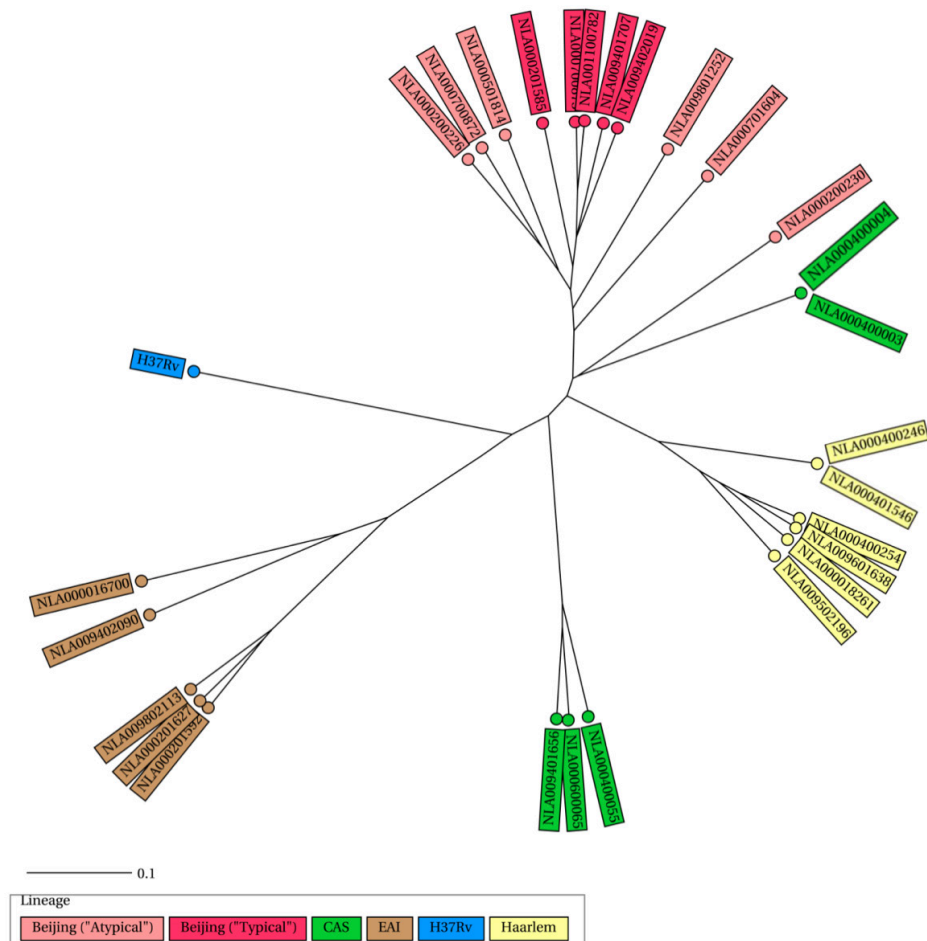


**FIGURE S4:** Phylogenetic relations between the clinical isolates analysed by PRM. A radial UPGMA tree based was constructed based on the copy numbers of 24 MIRU-VNTR loci in our selection of *M. tuberculosis* clinical isolates; typical Beijing (n=5), atypical Beijing (n=6), EAI (n=5), Haarlem (n=6) and CAS (n=5). The tree was calculated using the MIRU-VNTRplus server.

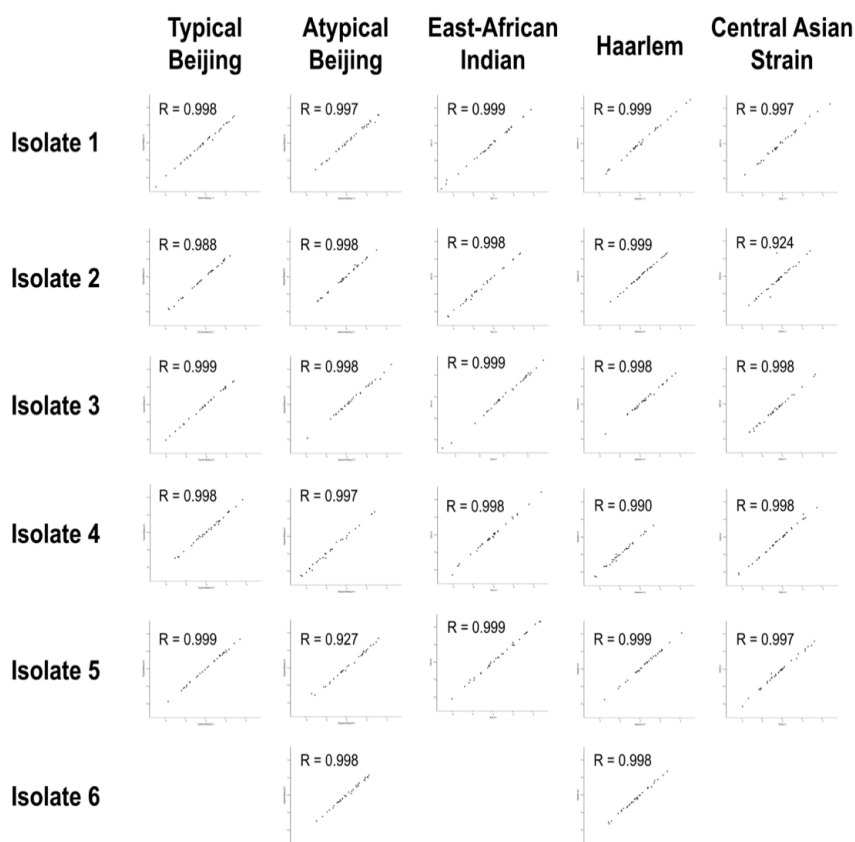


**Figure S5:** Scatter plot of the reproducibility between technical replicates. Biological variability was analysed by quantitative comparison of the protein ratios between both technical replicates.

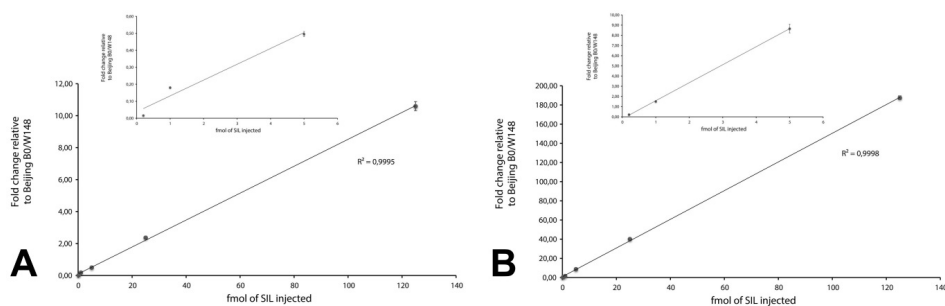


**FIGURE S6:** Calibration curve of protein ratios derived after injection of a five-fold dilution series of SIL peptides (+36Da) in a complete proteome matrix derived from *M. tuberculosis* Beijing B0/W148 (500ng). The derived protein ratios for Rv0450c/mmpL4(A) and Rv3283/sseA(B) in the clinical isolates examined are within the linear range of the calibration curve.

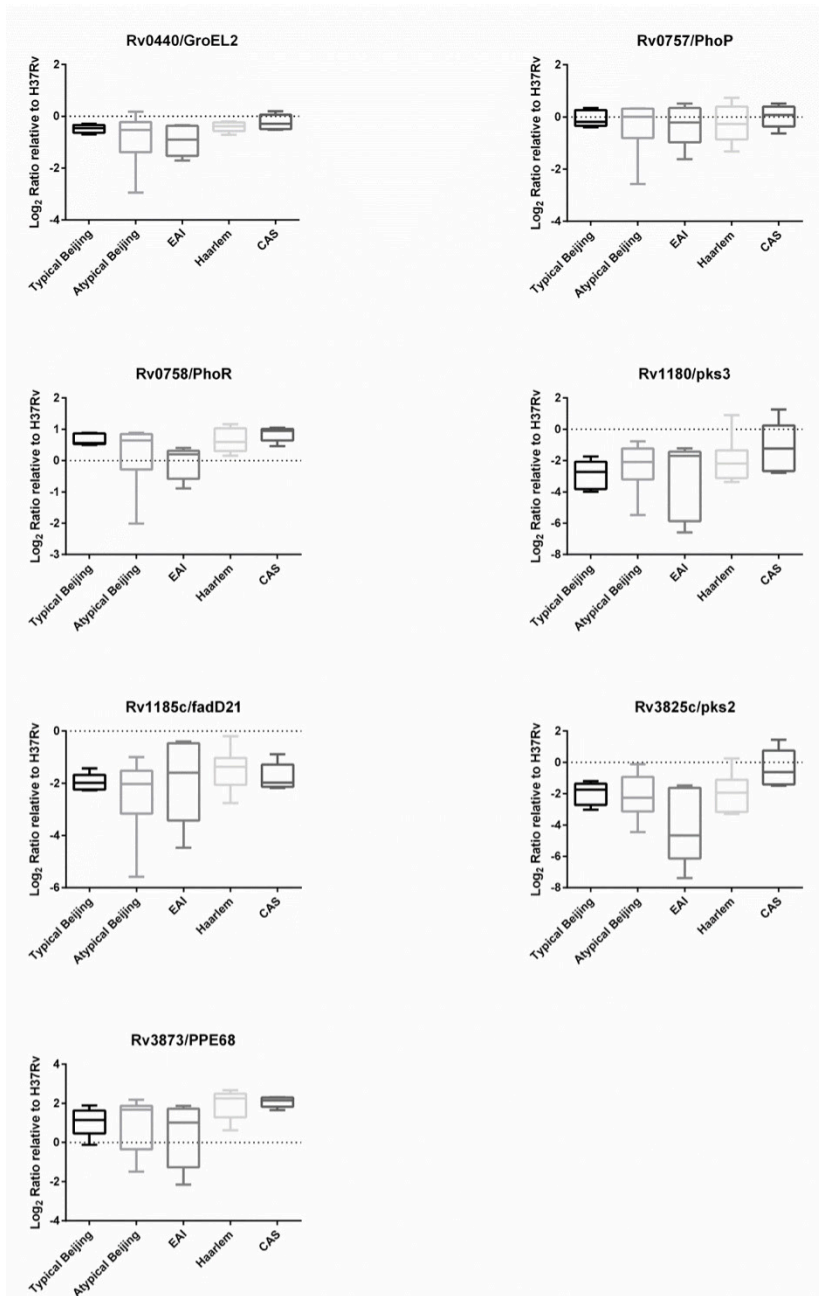


**FIGURE S7:** Quantification of selected PhoPR regulon interaction network proteins in five *M. tuberculosis* genotypes. The significance of the protein fold-change compared to *M. tuberculosis* Typical Beijing, but none of the proteins ratios deviated significantly.

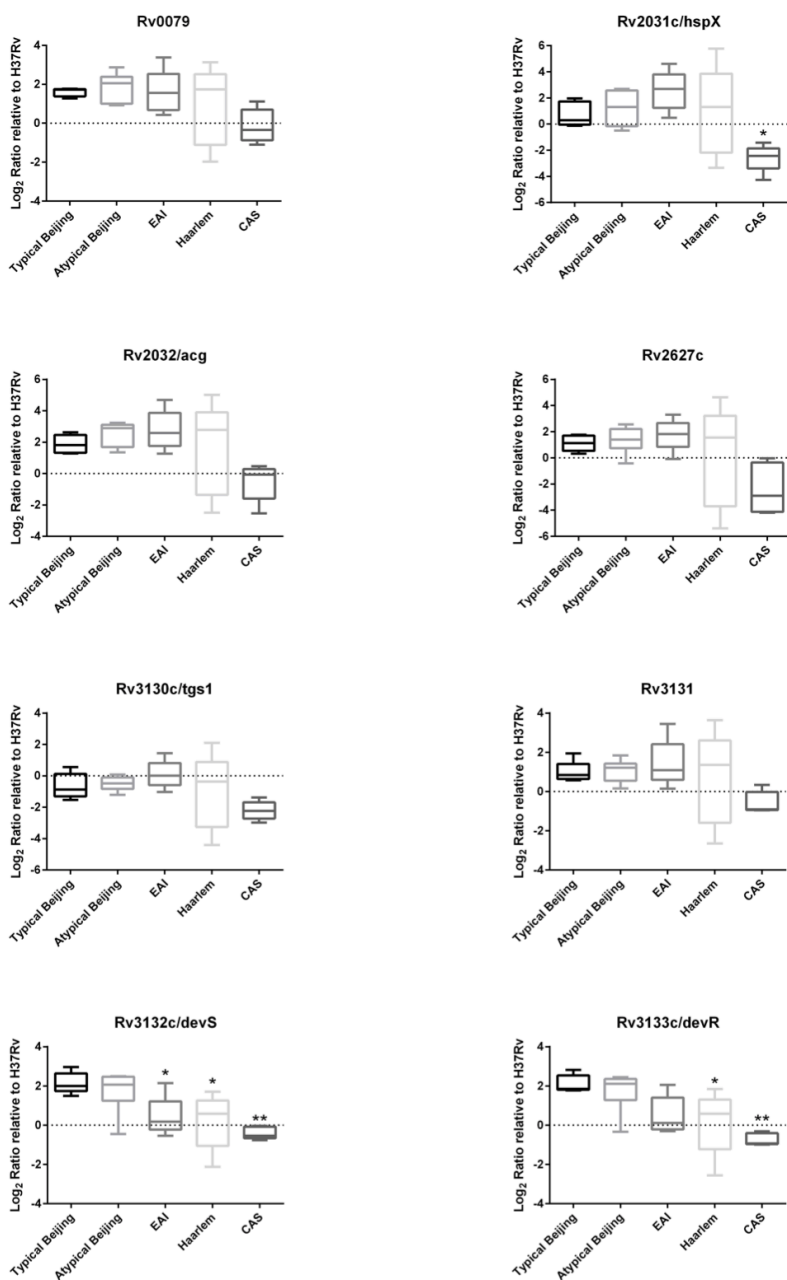


**FIGURE S8:** Quantification of selected dosR dormancy regulon proteins in five *M. tuberculosis* genotypes. The significance of the protein fold-change compared to *M. tuberculosis* typical Beijing is presented as follows: \* <0.05, \*\* <0.01.

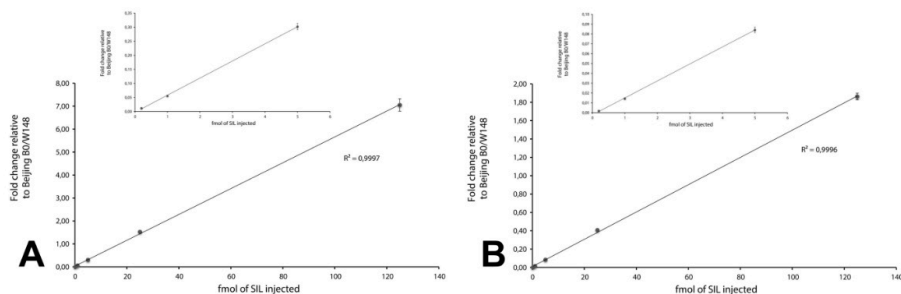


**FIGURE S9:** calibration curve of protein ratios derived after injection of a five-fold dilution series of heavy labelled peptides (+36Da) in a complete proteome matrix derived from *M. tuberculosis* Beijing B0/W148 (500ng). The derived protein ratios for Rv3132c/devS(A) and Rv3133c/devR(B) in the clinical isolates examined are within the linear range of the calibration curve.





## Thioridazine alters the cell envelope permeability of *Mycobacterium tuberculosis*

Jeroen de Keijzer<sup>1\*</sup>, Arnout Mulder<sup>2</sup>, Petra E. W. de Haas<sup>2</sup>, Arnoud H. de Ru<sup>1</sup>, Evy M. Heerkens<sup>3</sup>,  
Leonard Amaral<sup>4</sup>, Dick van Soolingen<sup>2,5#</sup>, Peter A. van Veelen<sup>1#</sup>

<sup>1</sup> *Department of Immunohematology and Blood Transfusion, Leiden University Medical Centre (LUMC), Leiden,  
2300 RC, The Netherlands*

<sup>2</sup> *Tuberculosis Reference Laboratory, National Institute for Public Health and the Environment (RIVM),  
Bilthoven, 3720 BA, The Netherlands*

<sup>3</sup> *Diagnostic Laboratory for Infectious Diseases and Perinatal Screening, National Institute for Public Health  
and the Environment (RIVM), Bilthoven, 3720 BA, The Netherlands*

<sup>4</sup> *Travel Medicine of the CMDT, Institute of Hygiene and Tropical Medicine, Universidade Nova de Lisboa,  
Lisboa, 1349-008, Portugal*

<sup>5</sup> *Departments of Pulmonary Diseases and Medical Microbiology, Radboud University Medical Centre,  
Nijmegen, 6500 HB, The Netherlands*

<sup>#</sup> DvS and PAvV share senior authorship

## Abstract

The increasing occurrence of multidrug resistant tuberculosis exerts a major burden on treatment of this infectious disease. Thioridazine, previously used as a neuroleptic, is active against extensively drug resistant tuberculosis when added to other second and third line antibiotics. By quantitatively studying the proteome of thioridazine treated *Mycobacterium tuberculosis*, we discovered the differential abundance of several proteins that are involved in the maintenance of the cell envelope permeability barrier. By assessing the accumulation of fluorescent dyes in mycobacterial cells over time, we demonstrate that long term drug exposure of *M. tuberculosis* indeed increased the cell envelope permeability. The results of the current study demonstrate that thioridazine induced an increase in cell envelope permeability, and thereby the enhanced uptake of compounds. These results serve as a novel explanation to the previously reported synergistic effects between thioridazine and other anti-tuberculosis drugs. This new insight in the working mechanism of this anti-tuberculosis compound could open novel perspectives of future drug administration regimens in combinational therapy.

## Introduction

*Mycobacterium tuberculosis*, the causative agent of tuberculosis (TB), is one of the most successful pathogens worldwide. Currently, 8-9 million TB cases and close to 1.5 million deaths due to *M. tuberculosis* are recorded annually.<sup>(1)</sup>

A major obstacle in the control of TB is the emergence of multidrug resistant TB (MDR-TB), i.e. *M. tuberculosis* strains that are resistant to at least rifampicin and isoniazid, two of the most potent drugs used in anti-TB regimens. In 2013, 3.7% of all new TB cases were reported as MDR-TB, but this is most likely an under estimation.<sup>(2)</sup> Alarmingly, the reported levels of MDR-TB are around 20% for patients previously treated for TB.<sup>(2)</sup> Moreover, there is a progression of MDR-TB towards extensively drug resistant TB (XDR-TB), which, in addition to resistance for isoniazid and rifampicin, also involves resistance to any of the fluoroquinolones and at least one aminoglycoside.<sup>(3)</sup> Finally, the term totally drug resistant TB (TDR-TB) has been introduced to describe resistance against all known TB drugs available at a particular setting. The existence of MDR-TB, XDR-TB and TDR-TB underlines that there is an urgent need for new effective anti-TB compounds.

Thioridazine (THZ), a compound belonging to the class of phenothiazines, is a drug that has previously been used to treat psychotic disorders such as schizophrenia.<sup>(4)</sup> Over fifteen years ago the *in vitro* effect of THZ on the respiration of *M. tuberculosis* has been reported.<sup>(5)</sup> The current increase in the frequency of MDR-TB infections and increased level of resistance against anti-TB drugs has renewed the interest in phenothiazines and their anti-mycobacterial properties.<sup>(6)</sup> In mouse models, a clear positive effect on the killing of *M. tuberculosis* was noticed when THZ was used alone<sup>(7)</sup> or added to other drugs in treatment regimen.<sup>(8)</sup> Despite the promising reports of anti-TB treatment with THZ, it should be noted that the anti-mycobacterial effects of THZ, also in combination with other antibiotics, vary between published animal model based studies.<sup>(9),(10),(11),(12)</sup> Nevertheless, in a clinical setting, THZ has been used for therapy of 17 XDR-TB patients in Buenos Aires, Argentina with remarkable success.<sup>(13)</sup> As shown by this latter study and others, THZ does not produce significant negative side effects when patients are monitored for possible cardiac effects during treatment.<sup>(14)</sup>

Three mechanisms have been proposed to explain the mode of action of phenothiazines: 1) accumulation of phenothiazines in macrophages and lung homogenate to concentrations that are equal to those which are bactericidal *in vitro* together with the promotion of intracellular killing by macrophages,<sup>(15),(16),(17),(10)</sup> 2) potential inhibition of antibiotic extruding efflux pumps that might be over-expressed in MDR-TB infections<sup>(18),(19),(20),(21)</sup> and which can be experimentally upregulated by exposure to increasing concentrations of anti-TB drugs such as isoniazid<sup>(20, 22)</sup>

and 3) direct *in vitro* killing of *M. tuberculosis*.<sup>(23),(24)</sup>

Efflux pumps that possess the ability to transport antibiotics across the cell envelope are thought to play a major role in the development of drug tolerance next to genomic mutations.<sup>(25)</sup> Moreover, an increased abundance of efflux pumps can stimulate the accumulation of resistance mutations, by enhancing drug tolerance for prolonged time periods.<sup>(26)</sup> The genome of *M. tuberculosis* encodes for several efflux pumps that may contribute to the development of drug resistance<sup>(27)</sup> and these have been suggested to be inhibited by phenothiazines.<sup>(20)</sup> Thus, the use of an efflux pump inhibitor in combination with other antibiotics can prevent the development of efflux pump induced antibiotic resistance and even result in an enhanced activity of other antibiotics. Indeed, synergistic effects between THZ and the first-line antibiotics rifampicin and isoniazid have been reported, as well as synergism between THZ and the anti-mycobacterial drug streptomycin.<sup>(10),(20),(28)</sup>

Notably, rifampicin and isoniazid best target replicating, metabolically active cells.<sup>(29),(30),(31),(32),(33),(34)</sup> To the contrary, THZ also displays bactericidal activity against starved cells.<sup>(29)</sup> Furthermore, THZ monotherapy could cure both drug susceptible and MDR-TB in a mouse model and *in vitro*.<sup>(8, 24)</sup> Both observations demonstrate that THZ is not only able to inhibit efflux pumps, but also show that THZ can be bactericidal.

To get an understanding of the molecular mechanisms used by *M. tuberculosis* to manage THZ induced cell stress, we quantitatively studied the proteome of *M. tuberculosis in vitro* with and without the continuous presence of THZ. We report the differential abundance of several proteins and protein clusters upon THZ treatment, which are involved in the maintenance of the cells permeability barrier. In addition, we demonstrate that long-term treatment of *M. tuberculosis* with THZ alters the mycobacterial plasma membrane composition and increases the cell envelope permeability, which influences the uptake of anti-mycobacterial compounds. In addition to the suggested function of THZ as efflux pump inhibitor, we herewith present data that offers a novel explanation to the previously reported synergistic effects between THZ and other anti-tuberculosis drugs.

## Material and Methods

### Mycobacterial culture conditions

*M. tuberculosis* H37Rv was re-cultured from frozen stocks in 5 ml Tween-Albumin liquid culture broth (Tritium Microbiologie, the Netherlands) at 36°C without shaking until an O.D. at 600 nm of 0.4 AU was reached. Of the mycobacterial pre-culture, 1 ml was transferred to a 250 ml Erlenmeyer flask containing 100 ml Tween-Albumin broth, with 0, 4, 6 and 8 mg/l THZ, and incubated under shaking conditions at 36°C with constant aeration; see Figure S1a. A >100-fold dilution of the pre-culture to prevent the inclusion of death cells for proteomic analysis. The mycobacteria used for proteome analyses were continuously treated with 6 mg/l THZ. Once these cultures reached an O.D. at 600 nm of 0.6 AU, representing the mid-log phase, the cells were washed three times with ice cold PBS, dissolved in 5 ml Lysis-buffer (4% SDS, 100 mM Tris-HCl, pH 7.6) and heat-killed at 95°C for 10 min. Lysates were stored at -20°C until further usage.

### Thermostability of thioridazine

The thermostability of THZ, over the culture period of approximately two weeks, was assessed by pre-incubating culture flasks containing 6 mg/l THZ for 21 days at 37°C prior to inoculation with *M. tuberculosis*. We compared the growth curves of this pre-incubated culture broth with that of freshly prepared culture broth containing 6 mg/l THZ; see Figure S1b. The resemblance between the obtained growth curves indicates that the growth rate of *M. tuberculosis* is similar in media containing THZ that is freshly prepared to media containing THZ that was pre-incubated at 37°C for 21 days. This demonstrates that THZ is thermostable on the time-scale of our experiments, and maintained the majority of its activity over the examined culture period.

### Proteome analysis

Cells were processed as described previously.<sup>(35)</sup> In brief, heat inactivated cells for proteomic experiments were mechanically lysed by bead-beating in a mini bead-beater 16 (BioSpec, USA) for 5 min using glass beads. Thereafter, the cells were cooled down on ice for 5 min after which the procedure was repeated twice. The cell lysates were cleared from cell debris by centrifugation for 1 min at 14,000 g and the supernatant was transferred to a fresh tube. Proteins were digested using the filter aided sample preparation (FASP) method. In brief, 100 µg of DTT reduced proteins was loaded on a 30 kDa filter. SDS was removed in three washes with 8 M urea. The proteins were carbamidomethylated, and the excess reagent was removed by three additional washes with 8 M urea. Proteins were then digested overnight using endoproteinase Lys-C (endoLysC), followed by a four hr digestion using trypsin at RT. The tryptic protein digest was desalted on C18 SepPak columns and labelled by reductive amination. A label swap was performed between biological replicates to prevent any experimental bias. A total 100 µg of labeled peptides were fractionated by strong cation exchange (SCX) on an Agilent 1100 system

equipped with an in-house packed SCX-column (320  $\mu\text{m}$  ID, 15 cm, polysulfoethyl A 3  $\mu\text{m}$ , Poly LC), run at 4  $\mu\text{l}/\text{min}$ . The gradient started with a 10 min run at 100% solvent A 70/30/0.1 (water/acetonitrile/formic acid), after which a linear gradient reached 100% solvent B (250 mM KCl, 30% acetonitrile, 0.1% formic acid) in 15 min, followed by 100 % solvent C (500 mM KCl, 30% acetonitrile 0.1% formic acid) in the following 15 min. The gradient was held at 100 % solvent C for 5 min, then switched back to 100 % solvent A. Fifteen fractions were collected in 1 min intervals, lyophilized and reconstituted in 30  $\mu\text{l}$  95/3/0.1 (water/acetonitrile/formic acid). Dissolved fractions were analyzed by on-line nano-HPLC MS with a system consisting of a Agilent 1100 gradient HPLC system (Agilent, Waldbronn, Germany) as described previously,<sup>(35)</sup> coupled to a LTQ-FT Ultra mass spectrometer (Thermo, Bremen, Germany). Five  $\mu\text{l}$  of each fraction was injected onto a home-made pre-column (100  $\mu\text{m}\times 15\text{ mm}$ ; Reprosil-Pur C18-AQ 3  $\mu\text{m}$ , Dr Maisch, Ammerbuch, Germany) and eluted via a home-made analytical nano-HPLC column (50  $\mu\text{m}\times 15\text{ cm}$ ; Reprosil-Pur C18-AQ 3  $\mu\text{m}$ ). The gradient was run from 0 to 30% solvent B (10/90/0.1 water/acetonitrile/formic acid) in 10-155 min. A tip of approximately 5  $\mu\text{m}$  was drawn at the tip of the nano-HPLC column to act as electrospray needle. Full scan mass spectra were acquired in the FT-ICR with a resolution of 25,000 at a target value of  $5\times 10^6$ . The five most intense ions were selected and fragmented in the linear ion trap using collision-induced dissociation at a target value of 10,000. Peptide and protein identification and quantitation was accomplished using MaxQuant 1.4.0.3, as described previously.<sup>(35)</sup> In brief, the false discovery rate (FDR) was set to 0.01. Minimal peptide length was set to 6 amino acids. The first search was performed using 20 ppm, while the main search was conducted with 10 ppm. Search of MS/MS spectra was performed with 0.6 Da using the Andromeda search engine. Both the first search and the main search were carried out against a database of *M. tuberculosis* H37Rv (3,996 entries). In total, 262 common contaminants were included in the searches by Andromeda. Enzyme specificity was set as C-terminal to arginine and lysine without proline restriction. A maximum of two missed cleavages was allowed. Variable modifications included N-terminal protein acetylation, methionine oxidation and corresponding dimethyl labels. Carbamidomethylation of cysteine was selected as a fixed modification. Proteins considered for quantification required a cumulative peptide count of two, including both unique and razor peptides. A maximum heavy/light variability of 150% was allowed. Proteins identified by site, which matched against the reverse database or were identified as a contamination, were excluded for further analysis. Statistical analysis of the outcomes was performed by Perseus using the significance B test with a Benjamini-Hochberg FDR 5%. The raw data files and the MaxQuant output files have deposited to the ProteomeXchange Consortium via the PRIDE partner repository with the dataset identifier PXD001208.

### Cell envelope permeability assay

The accumulation of Sytox Orange (Life Technologies, USA), Nile Red (Sigma-Aldrich, the

Netherlands) and ethidium bromide (Sigma-Aldrich, the Netherlands) was determined essentially as described previously.<sup>(36)</sup> In brief, *M. tuberculosis* H37Rv was grown to an O.D. 600 nm of 0.6 AU, washed three times with PBS, and resuspended in Tween-Albumine culture broth (Tritium Microbiologie, the Netherlands) to an O.D. 600 nm of 0.3 AU. Of this cell suspension 500 µl was inserted into a sealed cuvette. Sytox Orange and ethidium bromide were added to final concentration of 100 nM and 6 µM respectively. In addition, the efflux pump inhibitor reserpine<sup>(37)</sup> (Sigma-Aldrich, the Netherlands) was added to a final concentration of 100 µg/ml in selected samples. The cell suspensions were incubated at 36°C with occasional mixing for 60 min. The accumulation of dyes was determined by fluorescence using a Glomax-Multi Jr Single tube MultiMode Reader (Promega, USA) with an excitation of 525 nm and emission of 580-640 nm. The outcomes of the assay were evaluated using a paired t-test.

### **Analysis of phospholipid derived fatty acids**

*M. tuberculosis* H37Rv was cultured as described above, while constantly being exposed to 6 mg/l THZ. Preparation and analysis of fatty acid derived methyl ester (FAME) according to the manufacturers instruction (Sherlock 6.1 Microbial Identification System, MIDI, USA). In brief, cells were washed with ice-cold PBS and resuspended in 1 ml of 15% (w/v) NaOH in 50% (v/v) aqueous methanol. This suspension was then incubated for 30 min in a water bath set at 100°C. The saponified samples were allowed to cool to RT in cold water, acidified and methylated by the addition of 2 ml reagents consisting out of 54% 6 M HCl and 46% aqueous methanol, followed by a 10 min incubation in a water bath set at 80 °C. The samples were cooled by handshaking the sample tubes in ice-cold water. The methylated fatty acids were extracted with 1.25 ml of 50% methyl-tert butyl ether in hexane. The suspensions were allowed to mix for 10 min using end-over-end rotation. The upper phase was washed with 3 ml of 0.3 M NaOH plus 2.2 M NaCl after which the FAMES were transferred into a gas chromatography sample vial for analysis. Separation of FAMES was performed using a HP6890 gas chromatograph (Hewlett Packard, USA) with a fused-silica capillary column (25 m × 0.2 mm) cross-linked with 5% phenylmethyl silicone. The operating parameters were set and controlled automatically by the Sherlock 6.1 computer program (MIDI Inc., USA). Identification of peaks and assessment of column performance was achieved using a calibration standard mix (Microbial ID1200-A) containing nC9 – nC20 saturated and 2- and 3-hydroxy fatty acids. Peak areas were determined after careful excision of the selected peaks and weighing it on an analytical balance. The outcomes were evaluated using a paired t-test.

### **Lipid analysis**

50 ml of mycobacteria were grown in the presence or absence of 6 mg/l of THZ until the cultures reached mid-logarithmic phase. Cells were washed three times with ice-cold PBS and resuspended in methanol–0.3% NaCl (aqueous) (10:1). Apolar lipids were extracted twice with



petroleum ether (bp. 60-80°C) as described previously.(38) Lipid extracts were dried under a stream of nitrogen and weighted. 60 µg of apolar lipid extract, and a PDIM standard (obtained through BEI Resources, NIAID, NIH: Mycobacterium tuberculosis, Strain H37Rv, Purified Phthiocerol Dimycocerosate (PDIM), NR-20328 were spotted onto silica gel 60 thin-layer chromatography (TLC) plates (Merck Millipore, Germany), which was then developed three times in petroleum ether-ethyl acetate (98:2). PDIM was visualized using 5% phosphomolybdic acid in ethanol and gentle heating using a heat gun.

## Results

### Culture considerations and proteome analysis

To obtain a reliable model of protein abundance within THZ exposed *M. tuberculosis* cells, a strongly diluted pre-culture was started, which was treated continuously with THZ until the growth reached mid-logarithmic phase. To determine the maximum dosage of THZ that allows the growth of *M. tuberculosis* under the described culture conditions, we inoculated *M. tuberculosis* in the presence of 0, 4, 6 and 8 mg/l THZ; see Figure S1a. THZ partially inhibited the growth of *M. tuberculosis* up to a concentration of 6 mg/l THZ. Exposure of *M. tuberculosis* to 8 mg/l of THZ did not allow for any growth of *M. tuberculosis* within the examined culture period of 24 days. It should be noted that concentrations of 6 mg/l THZ are not clinically achievable within serum. However, compared to the serum concentration THZ is >30-fold concentrated within lungs and alveolar macrophages.<sup>(10)</sup> As a consequence, it had been demonstrated that clinically achievable serum concentrations of 0.5-1 mg/l and even 0.1 mg/l of THZ can kill intracellular *M. tuberculosis*.<sup>(16)</sup> A concentration of 6 mg/l THZ, as used in our model, fits well within this clinically relevant range. All cells were cultured, with or without 6 mg/l THZ, to mid-logarithmic phase, harvested and processed according to the protocol outlined in Figure 1a. Proteins were isolated, digested, and the obtained peptides were dimethylated, fractionated using SCX chromatography and analyzed by nanoLC-MS/MS. A total of 15 SCX fractions were analyzed twice. Two biological replicates were analyzed using this approach.

We recently reported how this method yields an unbiased view of the *M. tuberculosis* proteome.<sup>(35)</sup> The cumulative number of unique proteins that was identified and quantified, based on at least two peptides was 2,479; see Figure 1b. A total of 2,241 proteins were identified in both experiments, corresponding to an overlap of approximately 95% between the biological replicates, which is typically achieved in shotgun proteomics when nearly full proteome coverage is reached. The obtained quantification values of the 2,241 proteins that have been identified in both biological replicates showed a high correlation; see Figure 1c.

### Overview of *M. tuberculosis* protein abundance after long-term in vitro thioridazine exposure

To get an overview of proteins that are differentially abundant due to the influence of THZ, we applied strict quantification criteria to our dataset of 2,241 proteins that were identified in both biological replicates, as described in the method section. A total of 59 proteins was identified to be at least two-fold more abundant and 30 proteins to be at least two-fold less abundant upon continuous THZ exposure both with a significance B value  $\leq 0.05$ ; see Table S1 and Figure S2. We classified the differentially abundant proteins according to functional categories as given by Tuberculist; see Figure 2. Thirty-seven proteins that were categorized to be involved in 'intermediary metabolism and respiration' were shown to be differentially abundant. Previous

studies already described that phenothiazines inhibit aerobic respiration of *M. tuberculosis* in a NADH-dependent manner.<sup>(39)</sup> Using InterPro we identified a total of seven proteins with an NAD(P)-binding domain to be two-fold more abundant upon treatment with THZ; see Table S1.

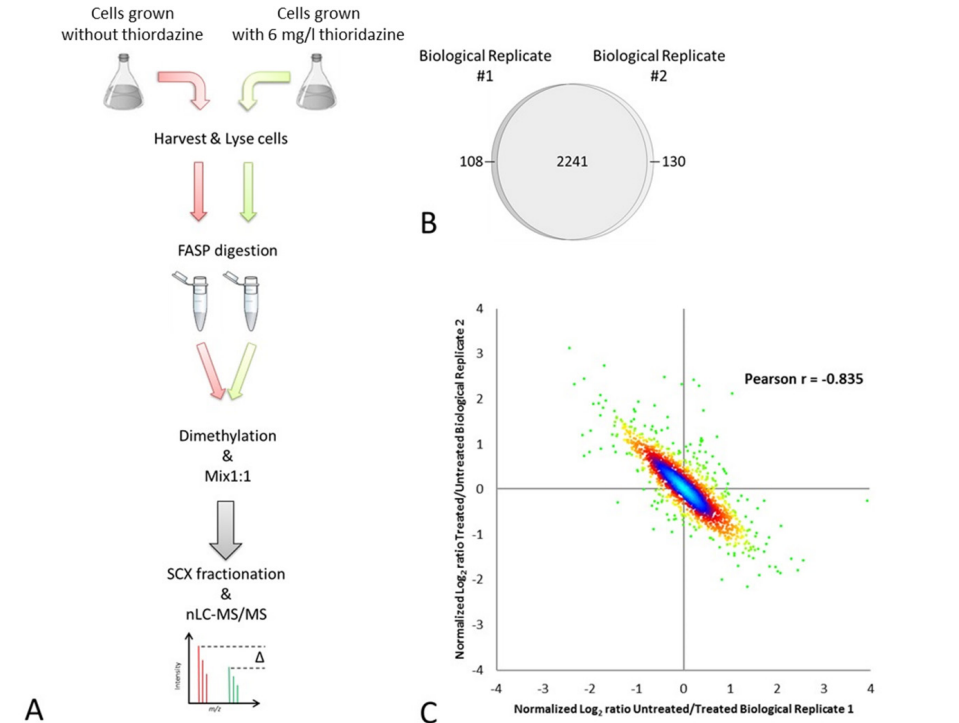


**FIGURE 1. Proteomic approach to identify differentially regulated proteins in *M. tuberculosis* with and without continuous thioridazine treatment**

**A:** Schematic design of the experimental approach used in this study. Cells were cultured and processed in parallel until dimethylation of the protein digest. In short, *M. tuberculosis* H37Rv was cultured in the presence or absence of THZ until mid-logarithmic phase was reached. Harvesting of the cells was performed by centrifugation following three washes with ice-cold PBS. The cells were mechanically lysed using bead-beating followed by protein digestion using the FASP procedure. Protein digests were provided with a dimethyl mass label, combined and fractionated using SCX. Fifteen fractions were taken, lyophilized and analyzed by LC-MS/MS.

**B:** Venn diagram representing the proteins that have been quantified in Biological Replicate 1 and 2. A cumulative number of 2,479 proteins were quantified, of which 2,241 were quantified in both analyses.

**C:** Comparison of 2,241 normalized protein ratios that were determined in both biological replicates. Proteins were colored using a density gradient. The correlation between biological replicates is presented by the Pearson  $r$  (-0.835). Note: A label swap was performed between both biological replicates.

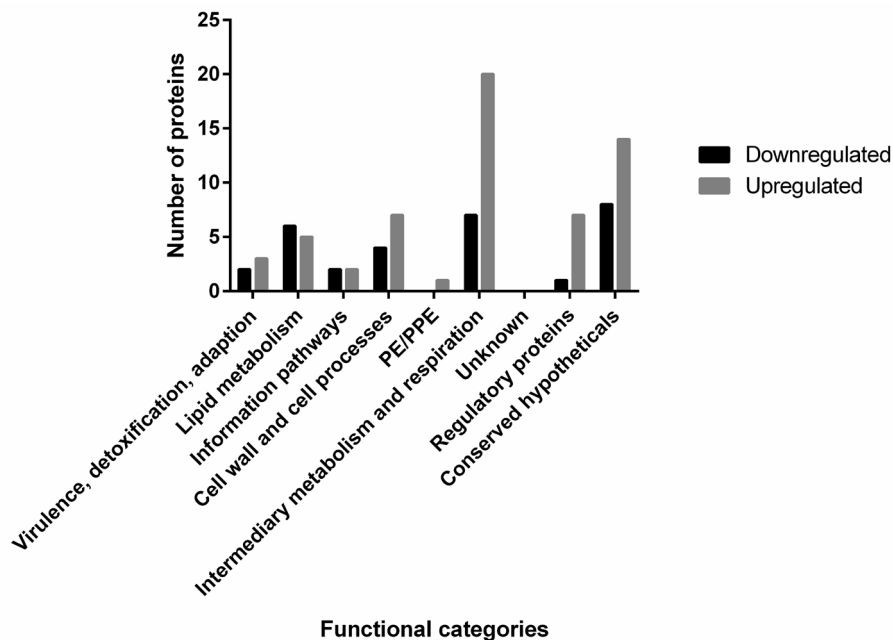


**FIGURE 2. Functional categorization of proteins that are differentially regulated upon thioridazine exposure *in vitro***

Proteins that were either less (Black filled bars) or more (grey bars) abundant in THZ treated cells compared to the control cells were categorized based on their function as given by Tuberculist. None of the functional categories showed to be significantly enriched after Chi-square analyses.

The potential inhibition of antibiotic extruding efflux pumps by THZ has been studied repeatedly.<sup>(18-21)</sup> In this study we have identified and quantified 15 of the 31 previously listed antibiotic efflux pumps,<sup>(40)</sup> but none of these efflux pumps was observed to be more abundant due to long-term THZ exposure; see Table S2.

Here we examined the proteome of *M. tuberculosis* after continuous exposure to THZ, whereas as a previous transcriptomic study focused on the short, initial response after one, two, four and six hours of exposure THZ.<sup>(23)</sup> A direct comparison of our proteomic dataset with the previously reported transcriptomic dataset is difficult due the fact that there is not necessarily a correlation between the expression of mRNA and the abundance of a protein in *M. tuberculosis*.<sup>(41)</sup> Nevertheless, we were able to confirm the differential expression of seven out of ten gene transcripts that were previously reported to be induced at one, two, four and six hrs after THZ treatment, including Rv2710/sigB and the *mce4*/ Rv3492c-Rv3501c locus; see Table S3. Moreover, 21 out of 59 proteins that we have observed to be two-fold more abundant were

also identified by transcriptomics to be upregulated on at least a single time point. Similarly, 12 out of 30 proteins that we have observed to be two-fold less abundant were also identified by transcriptomics to be downregulated on at least a single time point. Taken together, more than 35% of the proteins that we have identified to be differentially abundant using proteomics were previously also identified by transcriptomics, despite the variability's between both study designs.

### **Differential abundance of proteins involved in maintaining the cell envelope permeability barrier**

Mycobacteria are known for their unique cell wall, typified by mycolic acids which are unusually long-chain fatty acids.<sup>(42)</sup> This unique mycolic acid bilayer forms an efficient impermeable barrier that protects the bacteria from hostile environments, see Abdallah *et al.* for a comprehensive overview of the mycobacterial cell envelope.<sup>(43)</sup> Using our proteomic approach, we witnessed the differential abundance of two protein clusters that are involved in the maintenance of the cell envelope permeability barrier upon long-term THZ treatment of *M. tuberculosis*. A lipid family that retained special attention over the years is phthiocerol dimycocerosates (PDIM). These C83-103 long lipids alter the plasma membrane of host cells,<sup>(44)</sup> protect the pathogen from nitric oxide,<sup>(45),(46)</sup> modulate the early innate immune response<sup>(45),(46),(47)</sup> and lower the cell envelope permeability.<sup>(48),(36)</sup>

Fourteen proteins are located in the biosynthetic locus of PDIM/Rv2928-Rv2942 and Rv2940c; see Figure 3a. Seven of these proteins displayed an upward trend in our dataset upon continuous THZ exposure of *M. tuberculosis*. The increased abundance of multiple proteins in the PDIM synthesis locus suggests that THZ treated cells need to put in extra effort to maintain normal levels of PDIM in the cell envelope, which prevents the cell envelope from becoming too permeable; see Figure S3. Another protein, Rv2190c, which is involved in cell envelope maintenance and alteration of PDIM levels, was less abundant in THZ treated *M. tuberculosis* cells.<sup>(49)</sup>

A second cluster of proteins that we observed to be differentially abundant under THZ pressure was the *mce4* operon, as also described on the mRNA level for short-term treated *M. tuberculosis*; see Figure 3b.<sup>(23)</sup> The *mce4* operon is involved in the uptake of cholesterol, an essential nutrient for *M. tuberculosis* during chronic infection, and thereby an essential virulence factor for *M. tuberculosis*.<sup>(50)</sup> Similar to PDIM, the accumulation of cholesterol is known to play a role in the mycobacterial cell envelope permeability as the build-up of cholesterol increases the cell envelope permeability for rifampin in *M. tuberculosis*.<sup>(51)</sup> The lower abundance of *mce4* will lower the uptake of cholesterol by *M. tuberculosis*, which could lead to a decrease of the cell envelope permeability.

In line with the differential abundance of the PDIM and *mce4* locus, which leads to a decrease

in cell envelope permeability, Rv0516c was identified to be threefold less abundant upon continuous THZ treatment. Genetic disruption of Rv0516c increases the osmotic resistance in *M. tuberculosis* and enhances the bacterial tolerance to vancomycin, which affects cell envelope synthesis.<sup>(52)</sup>

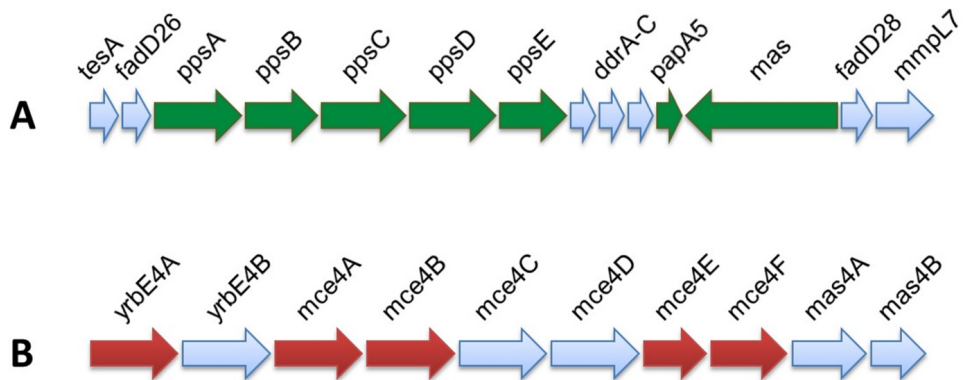


**FIGURE 3. Differential regulation of the PDIM biosynthetic/*mce4* cholesterol uptake locus in thioridazine exposed *M. tuberculosis***

A: Open reading frame of the genes involved in the synthesis PDIM are represented by the arrows. The proteins that we identified to be approximately two-fold more abundant under THZ pressure in the PDIM biosynthetic locus are highlighted in green.

B: Arrows represent the open reading frames of the genes involved in the uptake of cholesterol. The proteins that were less abundant under the continuous pressure of THZ are highlighted in red.

Finally, Rv0129c/Antigen 85c was found to be threefold more abundant in *M. tuberculosis* strains that were continuously treated with THZ. Inactivation of Antigen 85c results in a 40% decrease of cell wall bound mycolate.<sup>(53)</sup> As a consequence of the decreased mycolate content in the mycobacterial cell envelope, the permeability towards both the hydrophobic molecule chenodeoxycholate and the hydrophilic compound glycerol increases.<sup>(53)</sup> The increased abundance of Antigen 85c might therefore lead to a decrease in cell envelope permeability. Although mycobacteria possess an efficient permeability barrier, when properly maintained, the intrusion of hydrophilic antibiotics may take place via porins.<sup>(54)</sup> Porins are proteins in bacterial outer membranes that enable the non-specific influx of hydrophilic solutes.<sup>(55)</sup> OmpATb/ Rv0899 is the most well-known pore forming protein of *M. tuberculosis*. However, THZ treatment did not influence the abundance of this protein; see Table S1. In contrast, the outer membrane channel protein, Rv1698, was observed to be approximately two-fold more abundant in our THZ treated mycobacterial cells. It was reported that a *M. tuberculosis* strain harboring a mutated

Rv1698 gene, accumulated 100-fold more copper than wild-type *M. tuberculosis*.<sup>(56)</sup> The increased abundance of Rv1698 upon THZ treatment might therefore be a necessity to prevent the accumulation of copper when the cell envelope of *M. tuberculosis* becomes compromised. In summary; we have identified a total of 16 proteins to be differentially abundant upon THZ treatment that contribute to a decrease in cell envelope permeability. We hypothesize that the proteins in the PDIM synthesis locus, *mce4* locus, Rv0516c, Rv1698 and Antigen 85c are differentially regulated upon long term exposure of *M. tuberculosis* to THZ to counteract THZ induced cell envelope damage. This hypothesis is supported by electron microscopy images published earlier, which clearly show that the cell envelope of *M. tuberculosis* becomes damaged after four hours of THZ treatment.<sup>(23)</sup>

### **The effect of thioridazine treatment on the plasma membrane of *M. tuberculosis***

A recently proposed mechanism of THZ, that was supported by a computer-simulation study, is that THZ interacts with lipid-bilayers in bacteria, which causes significant membrane thinning.<sup>(57)</sup> This novel insight is in line with previous studies that also showed how THZ and other phenothiazines interact with negatively charged phospholipids in erythrocytes,<sup>(58)</sup> partitions in lipid-bilayers and the outer and inner membranes of mitochondria.<sup>(59)</sup> The induced damage to the mycobacterial cell envelope upon THZ treatment as suggested by the proteomic data in this study, in light of the latter cited studies, supports the model in which THZ interacts with the bacterial plasma membrane. This interaction of THZ with the plasma membrane of *M. tuberculosis* could lead to a more permeable cell envelope which results in a faster accumulation of antibiotics. To determine whether THZ alters the composition of the mycobacterial phospholipid bilayer, we examined the phospholipid-derived fatty acids (PLFA) of both continuously THZ treated and untreated *M. tuberculosis*. Although a direct effect of THZ on proteins involved in fatty acid metabolism has been suggested, this was not reflected in our proteomic dataset.<sup>(60)</sup> Examination of the PLFA profiles derived from continuously THZ treated *M. tuberculosis* and untreated *M. tuberculosis* cells, we revealed a significant increase in the proportion of tuberculostearic acid (10Me-C18:0) in THZ treated cells; see Figure 4. An increase of tuberculostearic acid has previously been observed in an ethambutol tolerant strain, when compared to an ethambutol susceptible strain.<sup>(61)</sup> Ethambutol is known to increase the cell envelope permeability towards rifampicin in multiple mycobacterial species<sup>(62)</sup>, it therefore might be that the increased proportion of tuberculostearic acid is a response of the mycobacteria towards drug-induced cell envelope permeability stress.

Tuberculostearic acid is produced by mycobacteria through the methylation of phospholipid esterified oleic acid, with S-adenosyl methionine as methyl donor followed by a reduction with NADPH as a cofactor.<sup>(63)</sup> Interestingly, an increase of NAD(P)H has been described for THZ treated *M. tuberculosis*.<sup>(64)</sup> Furthermore, as mentioned above, we observed a two-fold increased level

for seven proteins with an NAD(P)-binding domain; see Table S1.

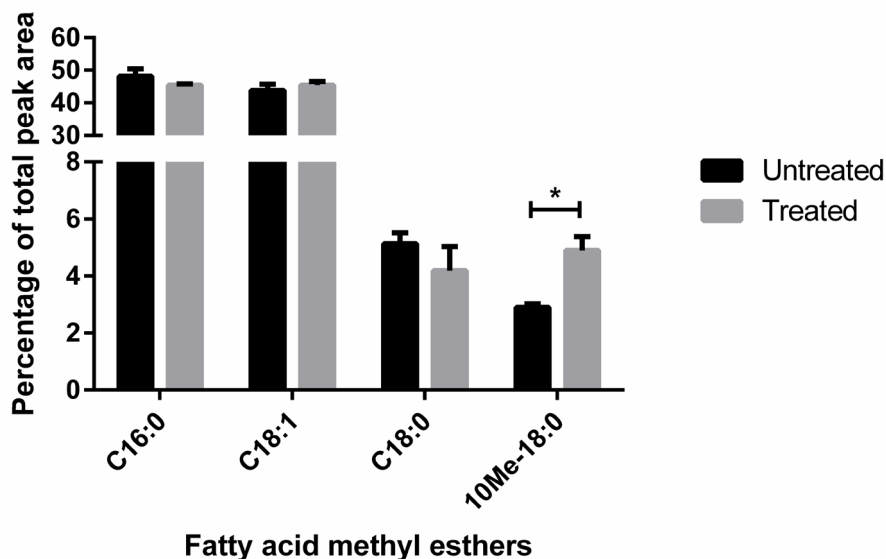


**FIGURE 4. A larger proportion of tuberculostearic acid is present in thioridazine exposed *M. tuberculosis*.** Phospholipid-derived fatty acids of untreated *M. tuberculosis* cells (black bars) and THZ treated cells (grey bars) were analyzed. The composition is given as the average percentage of total integrated chromatographic areas. Error bars represent the mean  $\pm$  SEM of the average peak area for each of the independent biological triplicates. \*  $P \leq 0.05$

#### Alteration of the mycobacterial cell envelope permeability upon long-term thioridazine treatment

To determine whether the cell envelope permeability of *M. tuberculosis* is increased upon continuous THZ treatment as hypothesized in our study, we used fluorescence spectrophotometry to measure the accumulation of several fluorescent compounds over a one hour time period. Similar experimental approaches were previously performed using ethidium bromide to determine the efflux pump activity of bacteria.<sup>(21),(65),(66),(67),(68)</sup>

However, it is not possible to determine the impact of THZ on the efflux pump inhibition solely by measuring the accumulation of ethidium bromide, as the total accumulation of ethidium bromide is dependent on both efflux pump activity and cell envelope permeability/influx. Therefore, we needed to analyze the accumulation of ethidium bromide alongside another membrane permeable fluorescent dye that does not act as a substrate for efflux pumps. Sytox



Orange, is known as a membrane permeable fluorophore, that, similarly to ethidium bromide, emits fluorescence once it intercalates with mycobacterial DNA. In contrast to ethidium bromide, Sytox Orange has, to our knowledge, not been used as an efflux pump substrate in *M. tuberculosis*. To assure that Sytox Orange is not susceptible to efflux we monitored the accumulation of Sytox Orange and ethidium bromide in the presence and absence of the efflux pump inhibitor reserpine. As presented in Figure 5, ethidium bromide is accumulated to higher levels in the presence of the efflux pump inhibitor reserpine<sup>(37)</sup> and THZ, whereas increased accumulation of Sytox Orange was solely observed in the presence of THZ. Thus the data indicates that Sytox Orange does not act as an efflux pump substrate.

The combination of ethidium bromide and Sytox Orange provides a better understanding of cell envelope permeability than the sole usage of ethidium bromide. Since both fluorescent compounds were accumulated to higher levels in continuously THZ treated mycobacterial cells, compared to untreated cells, the data supports our hypothesis that THZ is able to increase the permeability of the mycobacterial cell envelope.

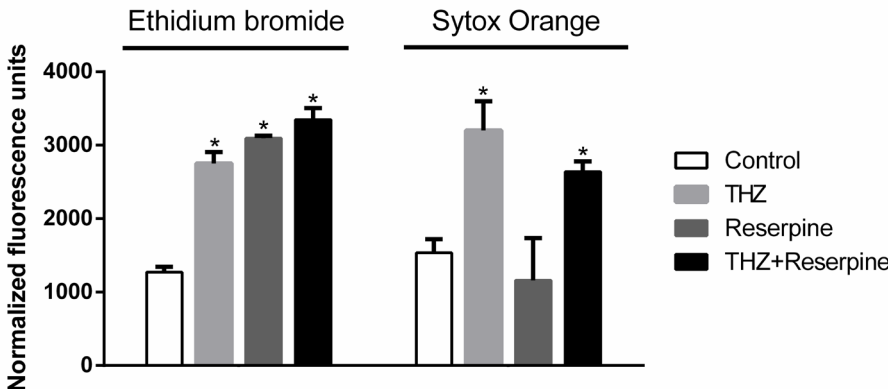


**FIGURE 5. Ethidium bromide and Sytox Orange accumulate faster in thioridazine treated *M. tuberculosis*.** Untreated *M. tuberculosis* cells (white filled bars), THZ treated cells (light grey bars), reserpine treated cells (dark grey bars) and THZ+reserpine treated cells (black bars) were assessed for the accumulation of ethidium bromide and Sytox Orange by fluorescent spectrophotometry. Independent biological duplicates were taken and samples were analyzed in duplicate. Error bars represent the mean  $\pm$  SD of the average normalized fluorescence units for each biological replicate. Significant differences in accumulation compared to the untreated control group were calculated using two-tailed paired Student's t-tests. P-values<0.05 were considered to be significant and are indicated with (\*).

## Discussion

The accumulation of antibiotics inside a bacterial cell is crucial for successful treatment. Efflux pumps provide an intrinsic mechanism in several bacteria that allows the active secretion of drugs.<sup>(69)</sup> As a result, less of the anti-bacterial compound will be present within the bacteria. The inhibition of efflux pumps is a promising development, as inhibition of efflux pumps has been shown to increase the drug susceptibility of *M. tuberculosis*.<sup>(40)</sup>

Treatment of *M. tuberculosis* with THZ results in an increased susceptibility of the pathogen towards rifampicin, isoniazid and streptomycin.<sup>(9, 10, 20, 28, 70)</sup> Furthermore, ethidium bromide, a common substrate for efflux pumps, accumulates faster in THZ treated mycobacteria.<sup>(21)</sup> Therefore, it has been suggested that THZ inhibited efflux pumps, which leads to an increase of intracellular drug accumulation that could explain the synergistic effects between THZ and other antibiotics. Based on the data obtained in the current study we propose an alternative molecular mechanism that connects the outcomes of several other studies.

Using a proteomic approach, we demonstrated the differential abundance of 16 proteins that are known to fulfill a function in the maintenance of the mycobacterial cell envelope. These observations support a previous study that demonstrated THZ induced cell envelope damage.<sup>(23)</sup> In fact, we confirmed the differential of SigB on the protein level, that was previously reported to be induced on the mRNA level in the response to THZ.<sup>(23)</sup> More importantly, our proteomic data points to several molecular processes that might be utilized by *M. tuberculosis* to compensate for THZ induced cell envelope damage. Further studies are warranted to elucidate the role of these proteins in response to THZ stress that might be caused by a direct interaction of THZ with the plasma membrane of *M. tuberculosis*.<sup>(57)</sup> There is no experimental evidence that THZ binds to the plasma membrane of *M. tuberculosis*. However, in our study we demonstrate that the composition of the mycobacterial plasma membrane is altered upon long-term exposure to THZ; see Figure 4.

Based on the proteomic response of *M. tuberculosis* to THZ we hypothesized that THZ compromises the mycobacterial cell envelope, which allows for rapid accumulation of several antibiotics. To support this hypothesis we performed a fluorescent spectrophotometry based accumulation assay. To this end, we have selected two fluorophores with unique properties; ethidium bromide and Sytox Orange. Ethidium bromide was used to monitor both cell envelope permeability and efflux pump activity, whereas we demonstrated that the accumulation of Sytox Orange is solely dependent on cell permeability; see Figure 5. Using this experimental setup we demonstrated that THZ treated cells accumulate more Sytox Orange and ethidium bromide than untreated cells, which supports our hypothesis that the cell envelope of *M. tuberculosis*

becomes more permeable after THZ treatment; see Figure 5.

Synergistic effects between antibiotics, due to alteration of the cell envelope permeability, have previously been observed for ethambutol, which increases the accumulation of rifampicin in multiple mycobacteria: *M. aurum*, *M. smegmatis* and *M. tuberculosis*.<sup>(62)</sup> In addition, it has also been shown in *M. marinum* that the susceptibility towards multiple antibiotics increases once the cell envelope permeability was significantly increased.<sup>(36, 71)</sup> The THZ induced cell envelope permeability could explain the synergistic effects between THZ and other drugs in *M. tuberculosis* as described previously.<sup>(9, 10, 20, 28, 70)</sup>

The exceptional cell envelope of *M. tuberculosis* provides the pathogen with an intrinsic form of antibiotic tolerance.<sup>(43)</sup> By permeabilizing the cell envelope antibiotics can more readily enter the cell and accumulate to a bactericidal concentration. In fact, due to the increased permeability of the cell envelope to old drugs and new anti-tuberculosis antibiotics, not only would the old drug(s) be restored to an effective therapeutic level, the dose levels of new but toxic anti-tubercular compounds may be significantly reduced.

Regarding the accumulation of ethidium bromide, we did not observe a synergistic effect when we combined THZ with the efflux pump inhibitor reserpine, at the concentrations and timespan examined; see Figure 5. However, the observation that Sytox Orange accumulates to higher levels in THZ treated cells than reserpine treated cells demonstrates that there is a role for cell envelope permeabilizing agents next to efflux pump inhibitors. As demonstrated, some compounds only accumulate to high intracellular levels through the induction of cell permeability.

In the here described model we demonstrate that THZ induces cell envelope permeability. The corresponding proteomic data revealed that proteins involved in the synthesis of PDIM and uptake of cholesterol are differentially abundant during THZ treatment. Similarly, we demonstrated that the relative content of tuberculostearic acid increases in the plasma membrane upon exposure to THZ. Both the differential abundance of these proteins and the alteration of the plasma membrane composition can play a vital role to counter act the THZ induced cell envelope permeability. The extent to which these changes contribute to THZ tolerance in *M. tuberculosis* requires further assessment.

The increase in cell envelope permeability upon THZ treatment is an alternative explanation for the synergistic effects of THZ with other antibiotics that has so far only been attributed to the inhibition of efflux pumps. Nevertheless, there remain two conceivable hypotheses in which THZ inhibits mycobacterial efflux pumps. First, the THZ induced cell envelope permeability might

reduce the proton motive force, which indirectly inhibits efflux pumps by denying its source of energy.<sup>(72),(73),(74)</sup> Secondly, the THZ induced alteration of the phospholipid bilayer might also result in a membrane-mediated inhibition of efflux pumps by THZ as suggested previously.<sup>(57)</sup> It is important to note that both the indirect inhibition of efflux pumps and an increase of cell envelope permeability can contribute to a more rapid accumulation of antibiotic compounds in the cell. Cell envelope influencing agents like THZ may therefore increase the efficacy of other drugs significantly.

Finally, permeabilization of the cell envelope could lead to the loss of metabolites, ions and thereby the loss of, for example, the proton motive force which will ultimately lead to cell death. Thereby, the permeabilization of the mycobacterial cell envelope by THZ could also explain why THZ is active against metabolically inactive cells.<sup>(29)</sup>

## Conclusion

By analysing the proteome of THZ treated *M. tuberculosis* cells we observed the differential abundance of 16 proteins that are involved in the maintenance of the mycobacterial permeability barrier. We further demonstrated that long-term THZ treatment yields a relatively permeable *M. tuberculosis* cell envelope. Finally, we also showed how the plasma membrane composition of *M. tuberculosis* is altered under the influence of THZ. This renewed insight in the working mechanism of THZ offers a better understanding on the molecular basis of this promising new antibiotic, which will hopefully result in a more efficient use of this drug, possibly in combination with other efflux pump inhibitors.

## References

1. Eurosurveillance editorial, t., WHO publishes Global tuberculosis report 2013. *Euro Surveill* **2013**, 18, (43).
2. WHO, Multidrug-resistant tuberculosis (MDR-TB) 2013 Update. Factsheet. Available at: [http://www.who.int/tb/challenges/mdr/MDR\\_TB\\_FactSheet.pdf](http://www.who.int/tb/challenges/mdr/MDR_TB_FactSheet.pdf) **2013**, (Accessed: 16 January 2015).
3. Centers for Disease, C.; Prevention, Plan to combat extensively drug-resistant tuberculosis: recommendations of the Federal Tuberculosis Task Force. *MMWR Recomm Rep* **2009**, 58, (RR-3), 1-43.
4. Thanacoody, H. K., Thioridazine: resurrection as an antimicrobial agent? *Br J Clin Pharmacol* **2007**, 64, (5), 566-74.
5. Amaral, L.; Kristiansen, J. E.; Abebe, L. S.; Millett, W., Inhibition of the respiration of multi-drug resistant clinical isolates of *Mycobacterium tuberculosis* by thioridazine: potential use for initial therapy of freshly diagnosed tuberculosis. *J Antimicrob Chemother* **1996**, 38, (6), 1049-53.
6. Amaral, L.; Kristiansen, J. E.; Viveiros, M.; Atouguia, J., Activity of phenothiazines against antibiotic-resistant *Mycobacterium tuberculosis*: a review supporting further studies that may elucidate the potential use of thioridazine as anti-tuberculosis therapy. *J Antimicrob Chemother* **2001**, 47, (5), 505-11.
7. Martins, M.; Viveiros, M.; Kristiansen, J. E.; Molnar, J.; Amaral, L., The curative activity of thioridazine on mice infected with *Mycobacterium tuberculosis*. *In Vivo* **2007**, 21, (5), 771-5.
8. van Soolingen, D.; Hernandez-Pando, R.; Orozco, H.; Aguilar, D.; Magis-Escurra, C.; Amaral, L.; van Ingen, J.; Boeree, M. J., The antipsychotic thioridazine shows promising therapeutic activity in a mouse model of multidrug-resistant tuberculosis. *PLoS One* **2010**, 5, (9).
9. de Knecht, G. J.; ten Kate, M. T.; van Soolingen, D.; Aarnoutse, R.; Boeree, M. J.; Bakker-Woudenberg, I. A.; de Steenwinkel, J. E., Enhancement of in vitro activity of tuberculosis drugs by addition of thioridazine is not reflected by improved in vivo therapeutic efficacy. *Tuberculosis (Edinb)* **2014**, 94, (6), 701-7.
10. Dutta, N. K.; Pinn, M. L.; Karakousis, P. C., Reduced Emergence of Isoniazid Resistance with Concurrent Use of Thioridazine against Acute Murine Tuberculosis. *Antimicrob Agents Chemother* **2014**, 58, (7), 4048-4053.
11. Dutta, N. K.; Pinn, M. L.; Karakousis, P. C., Sterilizing activity of thioridazine in combination with the first-line regimen against acute murine tuberculosis. *Antimicrob Agents Chemother* **2014**, 58, (9), 5567-9.
12. Dutta, N. K.; Pinn, M. L.; Zhao, M.; Rudek, M. A.; Karakousis, P. C., Thioridazine lacks bactericidal activity in an animal model of extracellular tuberculosis. *J Antimicrob Chemother* **2013**, 68, (6), 1327-30.
13. Amaral, L.; Boeree, M. J.; Gillespie, S. H.; Udwadia, Z. F.; van Soolingen, D., Thioridazine cures extensively drug-resistant tuberculosis (XDR-TB) and the need for global trials is now! *Int J Antimicrob Agents* **2010**, 35, (6), 524-6.

14. Udhwadia, Z. F.; Sen, T.; Pinto, L. M., Safety and efficacy of thioridazine as salvage therapy in Indian patients with XDR-TB. *Recent Pat Antiinfect Drug Discov* **2011**, 6, (2), 88-91.
15. Crowle, A. J.; Douvas, G. S.; May, M. H., Chlorpromazine: a drug potentially useful for treating mycobacterial infections. *Chemotherapy* **1992**, 38, (6), 410-9.
16. Ordway, D.; Viveiros, M.; Leandro, C.; Bettencourt, R.; Almeida, J.; Martins, M.; Kristiansen, J. E.; Molnar, J.; Amaral, L., Clinical concentrations of thioridazine kill intracellular multidrug-resistant *Mycobacterium tuberculosis*. *Antimicrob Agents Chemother* **2003**, 47, (3), 917-22.
17. Martins, M.; Viveiros, M.; Ramos, J.; Couto, I.; Molnar, J.; Boeree, M.; Amaral, L., SILA 421, an inhibitor of efflux pumps of cancer cells, enhances the killing of intracellular extensively drug-resistant tuberculosis (XDR-TB). *Int J Antimicrob Agents* **2009**, 33, (5), 479-82.
18. Rodrigues, L.; Ainsa, J. A.; Amaral, L.; Viveiros, M., Inhibition of drug efflux in mycobacteria with phenothiazines and other putative efflux inhibitors. *Recent Pat Antiinfect Drug Discov* **2011**, 6, (2), 118-27.
19. Viveiros, M.; Leandro, C.; Amaral, L., Mycobacterial efflux pumps and chemotherapeutic implications. *Int J Antimicrob Agents* **2003**, 22, (3), 274-8.
20. Machado, D.; Couto, I.; Perdigao, J.; Rodrigues, L.; Portugal, I.; Baptista, P.; Veigas, B.; Amaral, L.; Viveiros, M., Contribution of efflux to the emergence of isoniazid and multidrug resistance in *Mycobacterium tuberculosis*. *PLoS One* **2012**, 7, (4), e34538.
21. Rodrigues, L.; Wagner, D.; Viveiros, M.; Sampaio, D.; Couto, I.; Vavra, M.; Kern, W. V.; Amaral, L., Thioridazine and chlorpromazine inhibition of ethidium bromide efflux in *Mycobacterium avium* and *Mycobacterium smegmatis*. *J Antimicrob Chemother* **2008**, 61, (5), 1076-82.
22. Viveiros, M.; Martins, M.; Rodrigues, L.; Machado, D.; Couto, I.; Ainsa, J.; Amaral, L., Inhibitors of mycobacterial efflux pumps as potential boosters for anti-tubercular drugs. *Expert Rev Anti Infect Ther* **2012**, 10, (9), 983-98.
23. Dutta, N. K.; Mehra, S.; Kaushal, D., A *Mycobacterium tuberculosis* sigma factor network responds to cell-envelope damage by the promising anti-mycobacterial thioridazine. *PLoS One* **2010**, 5, (4), e10069.
24. van Ingen, J.; van der Laan, T.; Amaral, L.; Dekhuijzen, R.; Boeree, M. J.; van Soolingen, D., In vitro activity of thioridazine against mycobacteria. *Int J Antimicrob Agents* **2009**, 34, (2), 190-1.
25. Amaral, L.; Fanning, S.; Pages, J. M., Efflux pumps of gram-negative bacteria: genetic responses to stress and the modulation of their activity by pH, inhibitors, and phenothiazines. *Adv Enzymol Relat Areas Mol Biol* **2011**, 77, 61-108.
26. Martins, A.; Iversen, C.; Rodrigues, L.; Spengler, G.; Ramos, J.; Kern, W. V.; Couto, I.; Viveiros, M.; Fanning, S.; Pages, J. M.; Amaral, L., An AcrAB-mediated multidrug-resistant phenotype is maintained following restoration of wild-type activities by efflux pump genes and their regulators. *Int J Antimicrob Agents* **2009**, 34, (6), 602-4.
27. da Silva, P. E.; Von Groll, A.; Martin, A.; Palomino, J. C., Efflux as a mechanism for drug resistance in *Mycobacterium tuberculosis*. *FEMS Immunol Med Microbiol*. **2011**, 63, (1), 1-9.
28. Viveiros, M.; Amaral, L., Enhancement of antibiotic activity against poly-drug resistant *Mycobacterium*

tuberculosis by phenothiazines. *Int J Antimicrob Agents* **2001**, 17, (3), 225-8.

29. Xie, Z.; Siddiqi, N.; Rubin, E. J., Differential antibiotic susceptibilities of starved *Mycobacterium tuberculosis* isolates. *Antimicrob Agents Chemother* **2005**, 49, (11), 4778-80.
30. de Steenwinkel, J. E.; de Knecht, G. J.; ten Kate, M. T.; van Belkum, A.; Verbrugh, H. A.; Kremer, K.; van Soolingen, D.; Bakker-Woudenberg, I. A., Time-kill kinetics of anti-tuberculosis drugs, and emergence of resistance, in relation to metabolic activity of *Mycobacterium tuberculosis*. *J Antimicrob Chemother* **2010**, 65, (12), 2582-9.
31. Deb, C.; Lee, C. M.; Dubey, V. S.; Daniel, J.; Abomoelak, B.; Sirakova, T. D.; Pawar, S.; Rogers, L.; Kolattukudy, P. E., A novel in vitro multiple-stress dormancy model for *Mycobacterium tuberculosis* generates a lipid-loaded, drug-tolerant, dormant pathogen. *PLoS One* **2009**, 4, (6), e6077.
32. Gomez, J. E.; McKinney, J. D., *M. tuberculosis* persistence, latency, and drug tolerance. *Tuberculosis (Edinb)* **2004**, 84, (1-2), 29-44.
33. Zahrt, T. C., Molecular mechanisms regulating persistent *Mycobacterium tuberculosis* infection. *Microbes Infect* **2003**, 5, (2), 159-67.
34. Kapoor, N.; Pawar, S.; Sirakova, T. D.; Deb, C.; Warren, W. L.; Kolattukudy, P. E., Human granuloma in vitro model, for TB dormancy and resuscitation. *PLoS One* **2013**, 8, (1), e53657.
35. de Keijzer, J.; de Haas, P. E.; de Ru, A. H.; van Veelen, P. A.; van Soolingen, D., Disclosure of selective advantages in the 'modern' sublineage of the *Mycobacterium tuberculosis* Beijing genotype family by quantitative proteomics. *Mol Cell Proteomics* **2014**.
36. Yu, J.; Tran, V.; Li, M.; Huang, X.; Niu, C.; Wang, D.; Zhu, J.; Wang, J.; Gao, Q.; Liu, J., Both phthiocerol dimycocerosates and phenolic glycolipids are required for virulence of *Mycobacterium marinum*. *Infect Immun* **2012**, 80, (4), 1381-9.
37. Li, G.; Zhang, J.; Guo, Q.; Jiang, Y.; Wei, J.; Zhao, L. L.; Zhao, X.; Lu, J.; Wan, K., Efflux pump gene expression in multidrug-resistant *Mycobacterium tuberculosis* clinical isolates. *PLoS One* **2015**, 10, (2), e0119013.
38. Slayden, R. A.; Barry, C. E., 3rd, Analysis of the Lipids of *Mycobacterium tuberculosis*. *Methods Mol Med* **2001**, 54, 229-45.
39. Yano, T.; Li, L. S.; Weinstein, E.; Teh, J. S.; Rubin, H., Steady-state kinetics and inhibitory action of antitubercular phenothiazines on *mycobacterium tuberculosis* type-II NADH-menaquinone oxidoreductase (NDH-2). *J Biol Chem* **2006**, 281, (17), 11456-63.
40. Louw, G. E.; Warren, R. M.; Gey van Pittius, N. C.; McEvoy, C. R.; Van Helden, P. D.; Victor, T. C., A balancing act: efflux/influx in mycobacterial drug resistance. *Antimicrob Agents Chemother* **2009**, 53, (8), 3181-9.
41. Cortes, T.; Schubert, O. T.; Rose, G.; Arnvig, K. B.; Comas, I.; Aebbersold, R.; Young, D. B., Genome-wide mapping of transcriptional start sites defines an extensive leaderless transcriptome in *Mycobacterium tuberculosis*. *Cell Rep* **2013**, 5, (4), 1121-31.
42. Daffe, M.; Draper, P., The envelope layers of mycobacteria with reference to their pathogenicity. *Adv Microb Physiol* **1998**, 39, 131-203.

43. Abdallah, A. M.; Gey van Pittius, N. C.; Champion, P. A.; Cox, J.; Luirink, J.; Vandenbroucke-Grauls, C. M.; Appelmek, B. J.; Bitter, W., Type VII secretion--mycobacteria show the way. *Nat Rev Microbiol* **2007**, 5, (11), 883-91.
44. Astarie-Dequeker, C.; Le Guyader, L.; Malaga, W.; Seaphanh, F. K.; Chalut, C.; Lopez, A.; Guilhot, C., Phthiocerol dimycocerosates of *M. tuberculosis* participate in macrophage invasion by inducing changes in the organization of plasma membrane lipids. *PLoS Pathog* **2009**, 5, (2), e1000289.
45. Rousseau, C.; Winter, N.; Pivert, E.; Bordat, Y.; Neyrolles, O.; Ave, P.; Huerre, M.; Gicquel, B.; Jackson, M., Production of phthiocerol dimycocerosates protects *Mycobacterium tuberculosis* from the cidal activity of reactive nitrogen intermediates produced by macrophages and modulates the early immune response to infection. *Cell Microbiol* **2004**, 6, (3), 277-87.
46. Murry, J. P.; Pandey, A. K.; Sassetti, C. M.; Rubin, E. J., Phthiocerol dimycocerosate transport is required for resisting interferon-gamma-independent immunity. *J Infect Dis* **2009**, 200, (5), 774-82.
47. Goren, M. B.; Brokl, O.; Schaefer, W. B., Lipids of putative relevance to virulence in *Mycobacterium tuberculosis*: phthiocerol dimycocerosate and the attenuation indicator lipid. *Infect Immun* **1974**, 9, (1), 150-8.
48. Camacho, L. R.; Constant, P.; Raynaud, C.; Laneelle, M. A.; Triccas, J. A.; Gicquel, B.; Daffe, M.; Guilhot, C., Analysis of the phthiocerol dimycocerosate locus of *Mycobacterium tuberculosis*. Evidence that this lipid is involved in the cell wall permeability barrier. *J Biol Chem* **2001**, 276, (23), 19845-54.
49. Parthasarathy, G.; Lun, S.; Guo, H.; Ammerman, N. C.; Geiman, D. E.; Bishai, W. R., Rv2190c, an NlpC/P60 family protein, is required for full virulence of *Mycobacterium tuberculosis*. *PLoS One* **2012**, 7, (8), e43429.
50. Pandey, A. K.; Sassetti, C. M., Mycobacterial persistence requires the utilization of host cholesterol. *Proc Natl Acad Sci U S A* **2008**, 105, (11), 4376-80.
51. Brzostek, A.; Pawelczyk, J.; Rumijowska-Galewicz, A.; Dziadek, B.; Dziadek, J., *Mycobacterium tuberculosis* is able to accumulate and utilize cholesterol. *J Bacteriol* **2009**, 191, (21), 6584-91.
52. Hatzios, S. K.; Baer, C. E.; Rustad, T. R.; Siegrist, M. S.; Pang, J. M.; Ortega, C.; Alber, T.; Grundner, C.; Sherman, D. R.; Bertozzi, C. R., Osmosensory signaling in *Mycobacterium tuberculosis* mediated by a eukaryotic-like Ser/Thr protein kinase. *Proc Natl Acad Sci U S A* **2013**, 110, (52), E5069-77.
53. Jackson, M.; Raynaud, C.; Laneelle, M. A.; Guilhot, C.; Laurent-Winter, C.; Ensergueix, D.; Gicquel, B.; Daffe, M., Inactivation of the antigen 85C gene profoundly affects the mycolate content and alters the permeability of the *Mycobacterium tuberculosis* cell envelope. *Mol Microbiol* **1999**, 31, (5), 1573-87.
54. Rodrigues, L.; Ramos, J.; Couto, I.; Amaral, L.; Viveiros, M., Ethidium bromide transport across *Mycobacterium smegmatis* cell-wall: correlation with antibiotic resistance. *BMC Microbiol* **2011**, 11, 35.
55. Nikaido, H., Molecular basis of bacterial outer membrane permeability revisited. *Microbiol Mol Biol Rev* **2003**, 67, (4), 593-656.
56. Wolschendorf, F.; Ackart, D.; Shrestha, T. B.; Hascall-Dove, L.; Nolan, S.; Lamichhane, G.; Wang, Y.; Bossmann, S. H.; Basaraba, R. J.; Niederweis, M., Copper resistance is essential for virulence of



Mycobacterium tuberculosis. *Proc Natl Acad Sci U S A* **2011**, 108, (4), 1621-6.

57. Kopec, W.; Khandelia, H., Reinforcing the membrane-mediated mechanism of action of the anti-tuberculosis candidate drug thioridazine with molecular simulations. *J Comput Aided Mol Des* **2014**, 28, (2), 123-34.
58. Hendrich, A. B.; Lichacz, K.; Burek, A.; Michalak, K., Thioridazine induces erythrocyte stomatocytosis due to interactions with negatively charged lipids. *Cell Mol Biol Lett* **2002**, 7, (4), 1081-6.
59. Rodrigues, T.; Santos, A. C.; Pigoso, A. A.; Mingatto, F. E.; Uyemura, S. A.; Curti, C., Thioridazine interacts with the membrane of mitochondria acquiring antioxidant activity toward apoptosis--potentially implicated mechanisms. *Br J Pharmacol* **2002**, 136, (1), 136-42.
60. Dutta, N. K.; Mazumdar, K.; Dastidar, S. G.; Karakousis, P. C.; Amaral, L., New patentable use of an old neuroleptic compound thioridazine to combat tuberculosis: a gene regulation perspective. *Recent Pat Antiinfect Drug Discov* **2011**, 6, (2), 128-38.
61. Sareen, M.; Khuller, G. K., Effect of ethambutol on the phospholipids of ethambutol susceptible and resistant strains of Mycobacterium smegmatis ATCC 607. *Indian J Biochem Biophys* **1990**, 27, (1), 39-42.
62. Piddock, L. J.; Williams, K. J.; Ricci, V., Accumulation of rifampicin by Mycobacterium aurum, Mycobacterium smegmatis and Mycobacterium tuberculosis. *J Antimicrob Chemother* **2000**, 45, (2), 159-65.
63. Akamatsu, Y.; Law, J. H., Enzymatic alkylenation of phospholipid fatty acid chains by extracts of Mycobacterium phlei. *J Biol Chem* **1970**, 245, (4), 701-8.
64. Rao, S. P.; Alonso, S.; Rand, L.; Dick, T.; Pethe, K., The protonmotive force is required for maintaining ATP homeostasis and viability of hypoxic, nonreplicating Mycobacterium tuberculosis. *Proc Natl Acad Sci U S A* **2008**, 105, (33), 11945-50.
65. Martins, M.; Santos, B.; Martins, A.; Viveiros, M.; Couto, I.; Cruz, A.; Pages, J. M.; Molnar, J.; Fanning, S.; Amaral, L.; Management Committee, M.; of Cost, B.; European Commission/European Science, F., An instrument-free method for the demonstration of efflux pump activity of bacteria. *In Vivo* **2006**, 20, (5), 657-64.
66. Viveiros, M.; Martins, A.; Paixao, L.; Rodrigues, L.; Martins, M.; Couto, I.; Fahnrich, E.; Kern, W. V.; Amaral, L., Demonstration of intrinsic efflux activity of Escherichia coli K-12 AG100 by an automated ethidium bromide method. *Int J Antimicrob Agents* **2008**, 31, (5), 458-62.
67. Viveiros, M.; Rodrigues, L.; Martins, M.; Couto, I.; Spengler, G.; Martins, A.; Amaral, L., Evaluation of efflux activity of bacteria by a semi-automated fluorometric system. *Methods Mol Biol* **2010**, 642, 159-72.
68. Sharples, D.; Brown, J. R., Correlation of the base specificity of DNA--intercalating ligands with their physico-chemical properties. *FEBS Lett* **1976**, 69, (1), 37-40.
69. Webber, M. A.; Piddock, L. J., The importance of efflux pumps in bacterial antibiotic resistance. *J Antimicrob Chemother* **2003**, 51, (1), 9-11.
70. Amaral, L.; Viveiros, M., Why thioridazine in combination with antibiotics cures extensively drug-

- resistant *Mycobacterium tuberculosis* infections. *Int J Antimicrob Agents* **2012**, 39, (5), 376-80.
71. Chavadi, S. S.; Edupuganti, U. R.; Vergnolle, O.; Fatima, I.; Singh, S. M.; Soll, C. E.; Quadri, L. E., Inactivation of *tesA* reduces cell wall lipid production and increases drug susceptibility in mycobacteria. *J Biol Chem* **2011**, 286, (28), 24616-25.
  72. Amaral, L.; Cerca, P.; Spengler, G.; Machado, L.; Martins, A.; Couto, I.; Viveiros, M.; Fanning, S.; Pages, J. M., Ethidium bromide efflux by *Salmonella*: modulation by metabolic energy, pH, ions and phenothiazines. *Int J Antimicrob Agents* **2011**, 38, (2), 140-5.
  73. Martins, A.; Spengler, G.; Rodrigues, L.; Viveiros, M.; Ramos, J.; Martins, M.; Couto, I.; Fanning, S.; Pages, J. M.; Bolla, J. M.; Molnar, J.; Amaral, L., pH Modulation of efflux pump activity of multi-drug resistant *Escherichia coli*: protection during its passage and eventual colonization of the colon. *PLoS One* **2009**, 4, (8), e6656.
  74. Cruz, T. S.; Faria, P. A.; Santana, D. P.; Ferreira, J. C.; Oliveira, V.; Nascimento, O. R.; Cerchiaro, G.; Curti, C.; Nantes, I. L.; Rodrigues, T., On the mechanisms of phenothiazine-induced mitochondrial permeability transition: Thiol oxidation, strict  $\text{Ca}^{2+}$  dependence, and cyt c release. *Biochem Pharmacol* **2010**, 80, (8), 1284-95.

## Supporting information

**Supporting Information Table S1.** Table showing the identified and quantified proteins in both biological replicates with additional information. This table can be downloaded on the website of the journal: <https://pubs.acs.org/doi/suppl/10.1021/acs.jproteome.5b01037>

**Supporting Information Table S2.** Table showing the identified drug efflux pumps with their corresponding drug targets. This table can be downloaded on the website of the journal: <https://pubs.acs.org/doi/suppl/10.1021/acs.jproteome.5b01037>

**Supporting Information Table S3.** Table showing a comparison between gene transcript expression data derived from short-term THZ-treated *M. tuberculosis* reported previously (23) and the identified protein abundance ratios in the reported proteomic data set. This table can be downloaded on the website of the journal: <https://pubs.acs.org/doi/suppl/10.1021/acs.jproteome.5b01037>

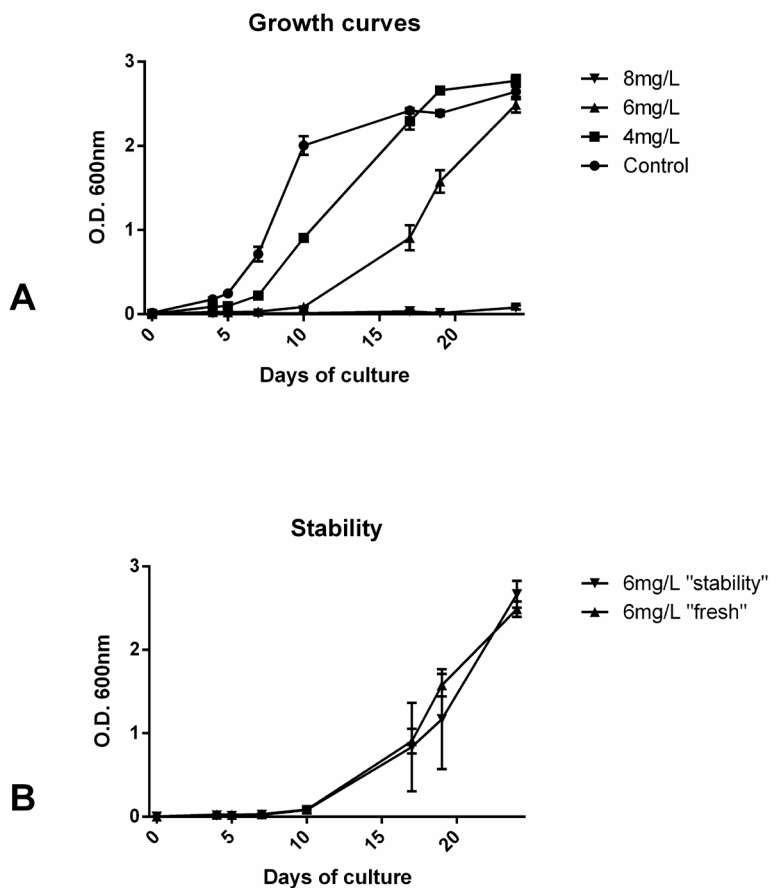


**FIGURE S1.** Growth patterns of *M. tuberculosis* H37Rv treated with thioridazine.

(A) Exposure of *M. tuberculosis* to 0(control), 4, 6 & 8 mg/L thioridazine.

(B) Growth curves of media containing 6 mg/L thioridazine media that has been pre-incubated for 21 days at 37°C (stability) and media containing 6 mg/L that has freshly been prepared.

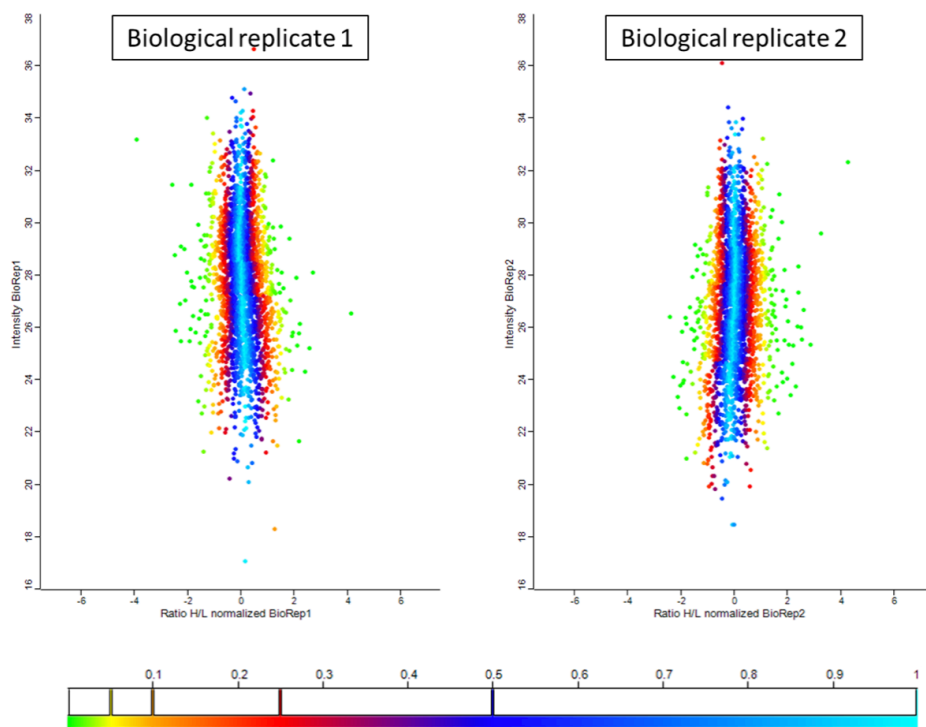


**FIGURE S2.** protein ratio distribution comparison of thioridazine treated and untreated *M. tuberculosis* H37Rv. Normalized Log2 transformed protein ratio's plotted against the summed Log2 peptide intensity for both biological replicates. Data points are colored based on their significance B values. Turquoise is >0.5, blue >0.25, red >0.1, yellow >0.05 and green <0.05. Note: a label swap was performed between both biological replicates.

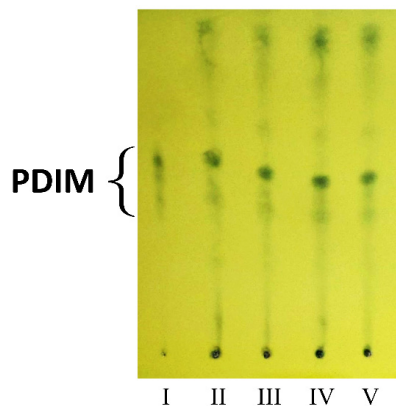


**FIGURE S3.** Thin Layer Chromatohraphy analysis of phthiocerol dimycocerosate(PDIM) abundance in *M. tuberculosis* H37Rv. Apolar lipids were extracted, analysed on silica gel TLC plates and three times developed in petroleum ether:ethyl acetate (98:2). I: a spot of PDIM standard, II/III: spots of untreated *M. tuberculosis* H37Rv, IV/V: spots of thioridazine treated *M. tuberculosis*.



Identification of phylogenetic relationships  
in the *Mycobacterium* genus by direct  
comparison of shared spectral content

Jeroen de Keijzer<sup>1#</sup>, Suzanne J. van der Plas-Duivesteijn<sup>2</sup>, Arnout Mulder<sup>3</sup>, Rina de Zwaan<sup>3</sup>, Arnoud H. de Ru<sup>2</sup>, Peter A. van Veelen<sup>2</sup>, Dick van Soolingen<sup>3,4</sup>, Magnus Palmblad<sup>2</sup>

*Department of Immunohematology and Blood Transfusion, Leiden University Medical Centre (LUMC), Leiden, 2300 RC, The Netherlands*

*Center for Proteomics and Metabolomics, Leiden University Medical Centre (LUMC), Leiden, 2300 RC, The Netherlands*

*Tuberculosis Reference Laboratory, National Institute for Public Health and the Environment (RIVM), Bilthoven, 3720 BA, The Netherlands*

*Departments of Pulmonary Diseases and Medical Microbiology, Radboud University Medical Centre, Nijmegen, 6500 HB, The Netherlands*



## Abstract

The degree of pathogenicity and antibiotic susceptibility differs greatly between species of the *Mycobacterium* genus. Correct identification of mycobacteria is therefore a necessity to discriminate harmless mycobacteria from clinically relevant species. To overcome limitations of current phenotypic and molecular identification methods, we examined the potential of tandem mass spectrometry to identify species and determine phylogenetic relationships between various mycobacteria. Mass spectrometry data were acquired using a standard proteomics configuration, after which the shared spectral content between samples was determined. The resulting phylogenetic tree was constructed out of 11 species that were represented by 29 unique isolates, and *Escherichia coli* as an outgroup. Comparison of the species-level clustering with the conventional mycobacterial identification methods based on 16S rRNA and *rpoB* sequencing showed the increased discriminatory power of the here described technique. Thereby, we demonstrate that the number of shared tandem mass spectra can be used as a direct measure of phylogenetic relatedness. Furthermore, this method does not require any prior knowledge of the sample or the availability of genomic information, which makes it applicable to virtually any organism.

## Introduction

*Mycobacterium tuberculosis*, the causative agent of tuberculosis, is the best known member of the *Mycobacterium* genus. Next to the *M. tuberculosis* complex, the genus consists of more than 140 so called nontuberculous mycobacterial (NTM) species and this number is still growing.

<sup>(1)</sup> Approximately 25 non-tuberculous mycobacteria, previously also referred to as 'atypical mycobacteria' or 'mycobacteria other than tuberculosis' (MOTT), are potentially pathogenic to either humans or animals.<sup>(1, 2)</sup>

The correct identification and classification of clinical mycobacterial isolates is important for proper diagnosis, treatment and epidemiological surveillance of mycobacteria.<sup>(3)</sup> A variety of molecular and phenotypic methods is available for the identification of *M. tuberculosis* complex sub-groupings and NTM species, yet each of these methods has its own limitations.<sup>(4)</sup>

Traditional biochemical and phenotypic assays that were utilized for the identification of mycobacteria were replaced by molecular diagnostics. 16S rRNA gene sequencing was introduced in the early 1990's as the gold standard to determine phylogenetic relationships between a variety of micro-organisms, including mycobacteria.<sup>(5)</sup> However, 16S rRNA sequencing lacks the required resolution to discriminate between some groupings of NTM, especially for rapid growing species.<sup>(6, 7)</sup>

Sequencing of the *rpoB* gene might be more suitable to study phylogenetic relationships between NTMs, compared to sequencing of 16S rRNA genes.<sup>(8, 9)</sup> *RpoB* sequencing can be more discriminative than 16S rRNA sequencing, but is still prone to misidentifications, presumably due to horizontal gene transfer events.<sup>(10)</sup> Furthermore, identification of species using *rpoB* sequencing is limited due to the absence of sequence data for the less frequent encountered NTM in the GenBank database.<sup>(9)</sup>

Despite the above mentioned limitations, single gene based molecular identification is widely accepted and generally applied to study phylogenetic relationships between mycobacteria. In addition, the analysis of clinical specimens using matrix assisted laser desorption ionization time-of-flight (MALDI-TOF) technology is gaining popularity due to the minimal turnaround time, ease of sample preparation and low cost per sample.<sup>(11, 12)</sup> This phenotypic identification method compares proteome compositions to discriminate between species.<sup>(13)</sup> However, the MALDI-TOF approach is not able to discriminate all (sub)species and does not provide interpretable spectral information.<sup>(12, 14, 15)</sup> Since spectra are solely acquired from molecules within the range of 2-20 kDa, identification is largely dependent on a limited number of features that mainly consist of the generally well conserved ribosomal proteins.<sup>(16)</sup> Since these methods fully rely on a small number of nucleotides or protein sequences, they can readily oversimplify the species

phylogeny. Therefore, it remains challenging to identify mycobacteria and re-construct their phylogeny with a single, straightforward, affordable, non-targeted assay.

LC-MS/MS analysis of an entire bacterial proteome or selected proteins can be used for the identification of micro-organisms, as reviewed recently.<sup>(17)</sup> In these approaches, proteins are proteolytically digested and the resulting peptide are separated by HPLC. The peptides eluting from the HPLC are ionized, detected and fragmented for analysis. Identification of the peptides is subsequently established by matching the obtained tandem-MS spectra against theoretical fragment data. There are several advantages to LC-MS/MS analysis of bacteria as the method provides detailed information that could reveal minor differences between species while only using inexpensive consumables for the preparation of samples.<sup>(18, 19)</sup> However, correct identification of species requires the presence of fully annotated databases, which is to date still limiting.<sup>(18)</sup>

We previously demonstrated that phylogenetic relationships between primates can be established using a direct pairwise analysis of tandem mass spectra derived from trypsinized serum samples.<sup>(20)</sup> One of the promising features of this approach is that it functions independently of genomic information. Furthermore, following standard proteomics procedures, one can readily acquire thousands of tandem mass spectra that all serve as features to discriminate between species and construct a phylogenetic tree. Similar approaches have already successfully been used for the authentication of commercial fish products<sup>(21)</sup> and tick blood meals derived from vertebrate species.<sup>(22)</sup>

In this study, we further examined the potential of tandem mass spectrometry for the identification of mycobacterial species, both of NTM as the closely related *M. tuberculosis* complex (sub)species. By comparing the shared spectral content between various species, we demonstrate that phylogenetic relationships can be revealed with this technique and that closely related species can be discriminated without prior knowledge or information of the organism to be analysed.

## Materials and Methods

### Mycobacterial culture conditions

The following mycobacterial species, derived from clinical isolates, were cultured in mycobacterial growth indicator tubes (MGIT) and incubated until positive growth was detected using the BACTEC MGIT 960 (Becton Dickinson, USA): *Mycobacterium gordonae*, *Mycobacterium szulgai*, *Mycobacterium kansasii*, *Mycobacterium avium*, *Mycobacterium malmoense*, *Mycobacterium marinum*, *Mycobacterium tuberculosis*, *Mycobacterium bovis*, *Mycobacterium canettii*, *Mycobacterium abscessus* and *Mycobacterium fortuitum*. Each of these species was represented by two or three unique, clinically derived, isolates. Approximately 0.2 ml was inoculated onto 7H10 medium agar plates (Tritium Microbiologie B.V., the Netherlands) and incubated at 36 °C until colony formation was visible, except for *M. marinum* isolates, which were incubated at 30 °C. A 1-µl inoculation loop full of mycobacterial biomass, collected from one to three colonies, was transferred to 0.5 ml of lysis-buffer (4% SDS, 100mM Tris-HCl) and heat-inactivated at 100 °C for 15 minutes. Cell lysates were frozen at -70 °C until further usage. Biological duplicates were taken from each isolate.

### Molecular diagnostics

Authenticity of the NTM samples was determined using INNO-LiPA Mycobacteria v2 (Fujirebio, Belgium) with additional partial 16S rRNA sequencing for *M. szulgai* and the *M. tuberculosis* complex samples was identified with the GenoType MTBC method (Hain Lifescience, Germany) with additional variable number tandem repeat (VNTR) typing for *M. canettii*.<sup>(23)</sup>

Partial 16S rRNA and *rpoB* sequencing were performed as described previously.<sup>(9)</sup> In brief, 16S rRNA gene sequence analysis started from *E. coli* position 28 (479 bp, including the hypervariable regions A and B).<sup>(5, 24)</sup> Partial sequencing of the *rpoB* gene was performed using previously published primers.<sup>(25)</sup> Analyses of the 16S rRNA and *rpoB* gene sequences was performed using Bionumerics version 7.5 software (Applied Math, Belgium). Phylogenetic trees constructed using the Unweighted Pair-Group Method with Arithmetic Mean (UPGMA) distance calculation.

### Protein sample preparation

Samples were essentially processed as described previously.<sup>(26)</sup> Briefly, mycobacterial cell lysates were mechanically disrupted by bead-beating in a mini bead-beater 16 (BioSpec, USA) for 5 min using glass beads of 0.4-0.6 mm (Sartorius, Germany). Thereafter, the cells were cooled on ice for 5 min and further disrupted by two more rounds of bead-beating. The cell lysates were separated from cell debris by centrifugation for 1 min at 14,000xg and the supernatant was transferred to another tube. Proteins were digested using the filter aided sample preparation (FASP) method.<sup>(27)</sup> DTT reduced proteins were loaded on a 30 kDa filter. SDS was removed in three washes with 8M urea. The proteins were carbamidomethylated, and the excess reagent

was removed by three additional washes with 8M urea. Proteins were then digested overnight using endoproteinase Lys-C (endoLysC), followed by a four hrs digestion using trypsin at RT. Tryptic peptides were desalted on C18 SepPak columns (Waters, USA) and dissolved at 125 ng/ $\mu$ l for LC-MS/MS analysis.<sup>(28)</sup>

### Liquid chromatography- tandem mass spectrometry Q-Exactive

Samples were analysed on a nanoLC-MS/MS system consisting of an Easy nLC 1000 gradient HPLC system (Thermo scientific, Bremen, Germany) that was coupled to a Q-Exactive mass spectrometer (Thermo scientific, Bremen, Germany). SCX fractions were injected onto an in-house packed precolumn (100  $\mu$ m  $\times$  15 mm; Reprosil-Pur C18-AQ 3  $\mu$ m, Dr. Maisch, Germany) and eluted via a homemade analytical nano-HPLC column (15 cm  $\times$  50  $\mu$ m; Reprosil-Pur C18-AQ 3  $\mu$ m). The gradient was run from 0% to 30% solvent B (10/90/0.1 water/acetonitrile/formic acid) in 10 minutes. A tip with a  $\sim$ 5  $\mu$ m internal diameter was drawn at the end of the nano-HPLC which acted as the electrospray needle of the MS source. The Q-Exactive mass spectrometer was operated in top10-mode. Parameter settings were; resolution 70,000 at an AGC target value of 3e6, a maximum fill time of 20 ms (full scan), and resolution 17,500 at an AGC target value of 1e6 with a maximum fill time of 80 ms for MS/MS. The RAW data files have been deposited to the ProteomeXchange Consortium via the PRIDE partner repository and can be accessed with the dataset identifier PXD003488.

### Spectral annotation using Proteome Discoverer

Peptides and proteins were identified and quantified using Proteome Discoverer 1.4 (Thermo scientific, Bremen, Germany) using the SEQUEST HT algorithm. The false discovery rate (FDR) was set to 0.01 using Percolator.<sup>(29)</sup> The precursor tolerance was set 10 ppm, while MS/MS spectra were searched using 20 mmu mass tolerance. Trypsin specificity was set as C-terminal to arginine and lysine without proline restriction. A maximum of two missed cleavages was allowed. Methionine oxidation was selected as variable modification. Carbamidomethylation of cysteine was selected as a fixed modification. All spectra were matched against a FASTA database of *M. tuberculosis* reference strain H37Rv (3,996 entries), and a database composed out of common contaminants (116 entries). The Proteome Discoverer output files, which provide access to all annotated spectra, have been deposited to the ProteomeXchange Consortium via the PRIDE partner repository that can be accessed with the dataset identifier PXD003488.

### Molecular phylogenetics using compareMS2

The Q-Exactive raw files were converted into Mascot Generic Format (mgf) files using Proteome Discoverer 1.4. The similarity between mgf-files was determined using compareMS2.<sup>(20)</sup> Pairwise comparisons between tandem mass spectra was performed by compareMS2 for precursors differing less than 0.01 Th and recorded within 600 scans from each other. Spectra were

considered to be shared between samples when compareMS2 calculated a dot product larger than 0.8., which corresponds to a false discovery rate of approximately 1%.<sup>(30)</sup> The fraction of dot product above 0.8 was loaded into a distance matrix that was exported in the MEGA format.

<sup>(31)</sup> Phylogenetic trees were constructed using UPGMA algorithm.

## Results & discussion

### Sampled features of the mycobacterial proteome

Mycobacteria were cultured on solid media and processed as outlined in Figure 1. The data acquired for all species, biological replicates and technical replicates were of similar quality, based on visual inspection of the total ion chromatograms and number of tandem mass spectra; supplemental Figure 1. Each dataset consists out of roughly 2,500 tandem mass spectra, which all serve as features to discriminate between the various species. Spectra acquired from the well-annotated *M. tuberculosis* H37Rv<sup>(32, 33)</sup> were interpreted using the SEQUEST HT algorithm in Proteome Discoverer. The peptides identified were derived from 578 to 630 unique proteins. In contrast to the MALDI-TOF based technology, in which only proteins in the mass range of 2-20 kDa are sampled,<sup>(13)</sup> we also identified proteins larger than 20 kDa proteins; supplemental Figure 2a. The inclusion of a protein digestion step in the here reported method enabled acquisition of tandem mass spectra from both small and large proteins. The ability to acquire features that are derived from the entire mass range of the proteome is likely to result in enhanced discriminatory power compared to the limited mass range sampled by the MALDI-TOF approach.

Mass spectra were acquired using a top 10 data dependent acquisition (DDA) approach, which automatically selects the ten most intense peptides for fragmentation. As expected, our short, 10 min DDA method showed a strong preference for highly abundant proteins; supplemental Figure 2b.<sup>(34)</sup> This bias for high abundant proteins is advantageous as the identification of abundant proteins requires less sensitivity and allows for reproducible sampling between different untargeted LC-MS/MS runs using DDA approaches.

### Discriminatory power of CompareMS2 compared to 16S rRNA and rpoB sequencing

CompareMS2 software was used to determine the number of shared tandem mass spectra between the various samples analysed.<sup>(20)</sup> CompareMS2 pairs tandem mass spectra generates a similarity score between two spectra, which is expressed as a dot product; Figure 2. Tandem mass spectra with a dot product greater than 0.8 were considered to be shared between species. The number of shared tandem mass spectra between the various samples was converted into a distance matrix to generate a phylogenetic tree; supplemental Figure 3A&B. The approach described here discriminates between the rapid growing mycobacteria; *M. fortuitum* and *M. abscessus*, and slow growing mycobacteria. Furthermore, all NTMs analysed clustered on the species level. Moreover, there was very limited variation between the biological and technical replicates analysed. The position of *M. malmoeense* in the vertical dimension differs between both technical replicates. However, the calculated distance from *M. malmoeense* to either *M. marinum* or *M. avium* in the horizontal dimension is comparable in both technical replicates.

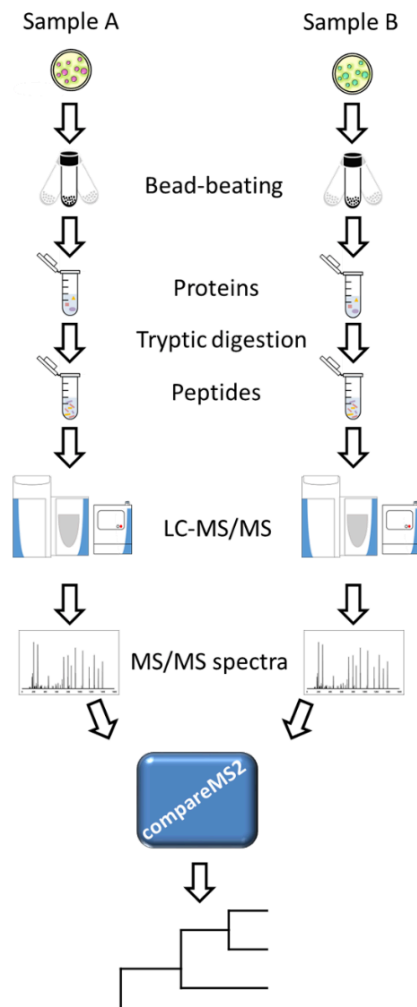


**FIGURE 1.** Experimental design. Mycobacteria were cultured on solid agar until colonies were observed. Colonies were dissolved in 4% SDS and heat-killed. The cells were mechanically lysed by bead-beating, after which the proteins were digested using the FASP procedure.<sup>(27)</sup> Spectra of intact peptide and tandem mass spectra of fragmented peptides were acquired on a Q-Exactive mass spectrometer after which the percentage of shared tandem mass spectra between datasets was calculated using compareMS2.<sup>(20)</sup>

Compared to 16S rRNA and *rpoB* sequencing, we observed that our approach is the only assay than can sufficiently discriminate between the *M. tuberculosis* complex members *M. bovis*, *M. canettii* and *M. tuberculosis* while it is also capable to discriminate between various NTMs; supplemental Figures 3C&D. Similarly, the MALDI-TOF method is only able to identify members



of the *M. tuberculosis* complex on the complex level, but lacks the discriminatory power to separate individual members at the species level.<sup>(12)</sup>

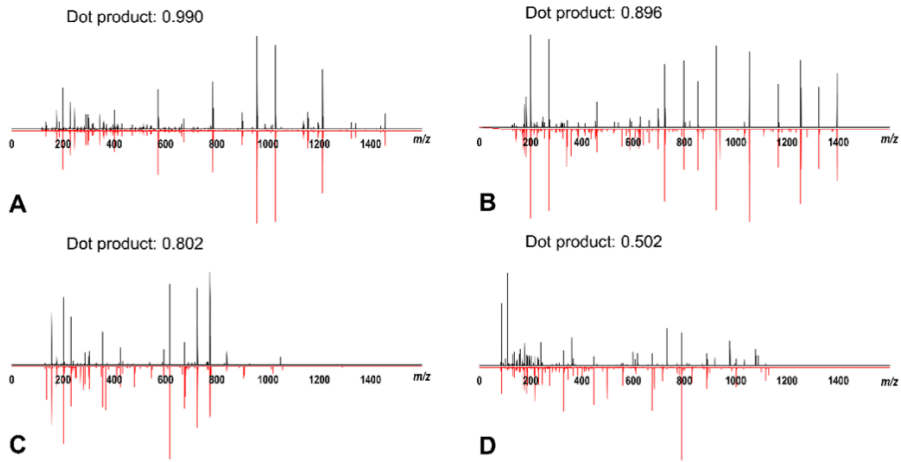


**FIGURE 2:** Mirror plots of two tandem mass spectra derived from *M. tuberculosis* (black, top) and *M. marinum* (red, bottom). The similarity between spectra was calculated using SpectraST 5.0, and reported as a dot product.<sup>(37)</sup> Spectra with dot product close to 1.0 are almost indistinguishable (A&B). Spectra with a dot product of 0.8 are still recognizably similar (C). Spectra with a dot product well below 0.8 are not considered to be shared or considered to originate from the same precursor peptide (D).

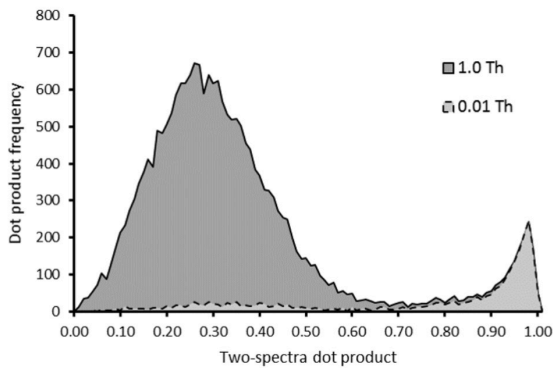


**FIGURE 3:** *In silico* analyses of the two-spectra dot product distribution between two *M. tuberculosis* H37Rv biological replicates with different precursor mass tolerances. Both the high- and low-resolution datasets follow the same distribution when a dot product greater than 0.8 is used as a cut-off, indicating that low-resolution mass spectrometers can be used to study and reconstruct phylogenetic relationships.

### The effect of instrument resolution

CompareMS2 uses the precursor mass of a peptide to compare their corresponding tandem mass spectra pairwise. In our case, compareMS2 only processed tandem mass spectra of which the precursor differed less than 0.01 Th. The usage of high resolution, high accuracy mass is becoming more prevalent in the field of proteomics. High resolution instruments offer considerable advantages for the analysis of proteomic samples of increased complexity, but this high quality data comes with a price tag.<sup>(35)</sup> To examine the added benefits of a high resolution precursor scan for the identification of mycobacterial species by shared spectral content, we analysed our high resolution data with less resolution *in silico*.

To investigate the impact of mass measurement accuracy, we modified two MGF files derived from biological replicates of *M. tuberculosis* H37Rv using Gaussian distributed random numbers from <http://random.org> with zero mean and a standard deviation of 0.5 Th. These Gaussian randomised MGF files were processed with compareMS2 using a precursor mass tolerance of 1.0 Th; a mass precision that is readily achieved with a more affordable ion trap mass spectrometer. The original high resolution MGF files were processed with a 0.01 Th precursor mass tolerance. For both datasets we used a fragment mass bin size of 0.2 Th.

The relative wide precursor mass tolerance of 1.0 Th did result in more low scoring two-spectra dot products, i.e. tandem mass spectra that score lower than 0.8; Figure 3. However, both the high- and low resolution data follow the same distribution when a dot product of 0.8 was used as a cut-off.

Reconstruction of the phylogeny using either 0.01 Th or 1.0 Th precursor mass tolerance did not affect clustering, since solely the spectra pairs with a dot product greater than 0.8 were used for clustering; supplemental Figure 4. This observation underlines the robustness of the method, but also indicates that more affordable low resolution mass spectrometers can be used to examine the species' phylogeny in a reliable way.<sup>(36)</sup> This hypothesis is strengthened by a previous study that demonstrated the power of spectral matching for the identification of commercial (processed) fish products on a low resolution ion trap.<sup>(21)</sup>

It should be noted that both the identification of fish products, as well as the identification of mycobacterial species was performed without any filtering of the data or optimization of the processing workflow. Thereby, the method shows to be inherently robust. In addition, the described methodology functions without any prior knowledge of the sample, thereby circumventing the need of organism specific consumables such as primers, which are required for molecular diagnostic assays. Therefore, we anticipate that the method is directly transferable to other organisms.

## Conclusion

To date, the identification of NTM and species within the *M. tuberculosis* complex has been limited to specialized laboratories that often rely on a variety of molecular assays. This study demonstrates a straightforward and rapid proteome-based method that can differentiate between closely-related mycobacterial species and even construct phylogenetic relationships. Compared to other MS-based phenotypic typing approaches, this method brings the following advantages: it requires no prior knowledge of the organism to be analysed (e.g. specific primers), the method can be transferred to virtually all (micro-)organisms, all acquired tandem mass spectra can be used for clustering and identification, the acquisition of tandem mass spectra can be performed on both high and low resolution instrumentation, and the method can easily be implemented in a typical proteomics laboratory.

## References

1. van Ingen, J., Diagnosis of nontuberculous mycobacterial infections. *Semin Respir Crit Care Med* **2013**, 34, (1), 103-9.
2. Johnson, M. M.; Odell, J. A., Nontuberculous mycobacterial pulmonary infections. *J Thorac Dis* **2014**, 6, (3), 210-20.
3. Li, W.; Raoult, D.; Fournier, P. E., Bacterial strain typing in the genomic era. *FEMS Microbiol Rev* **2009**, 33, (5), 892-916.
4. Jagielski, T.; van Ingen, J.; Rastogi, N.; Dziadek, J.; Mazur, P. K.; Bielecki, J., Current methods in the molecular typing of *Mycobacterium tuberculosis* and other mycobacteria. *Biomed Res Int* **2014**, 2014, 645802.
5. Springer, B.; Bottger, E. C.; Kirschner, P.; Wallace, R. J., Jr., Phylogeny of the *Mycobacterium chelonae*-like organism based on partial sequencing of the 16S rRNA gene and proposal of *Mycobacterium mucogenicum* sp. nov. *Int J Syst Bacteriol* **1995**, 45, (2), 262-7.
6. Tortoli, E., Phylogeny of the genus *Mycobacterium*: many doubts, few certainties. *Infect Genet Evol* **2012**, 12, (4), 827-31.
7. Turenne, C. Y.; Tschetter, L.; Wolfe, J.; Kabani, A., Necessity of quality-controlled 16S rRNA gene sequence databases: identifying nontuberculous *Mycobacterium* species. *J Clin Microbiol* **2001**, 39, (10), 3637-48.
8. Ben Salah, I.; Adekambi, T.; Raoult, D.; Drancourt, M., rpoB sequence-based identification of *Mycobacterium avium* complex species. *Microbiology* **2008**, 154, (Pt 12), 3715-23.
9. de Zwaan, R.; van Ingen, J.; van Soolingen, D., Utility of rpoB gene sequencing for identification of nontuberculous mycobacteria in the Netherlands. *J Clin Microbiol* **2014**, 52, (7), 2544-51.
10. Macheras, E.; Roux, A. L.; Bastian, S.; Leao, S. C.; Palaci, M.; Sivadon-Tardy, V.; Gutierrez, C.; Richter, E.; Rusch-Gerdes, S.; Pfyffer, G.; Bodmer, T.; Cambau, E.; Gaillard, J. L.; Heym, B., Multilocus sequence analysis and rpoB sequencing of *Mycobacterium abscessus* (sensu lato) strains. *J Clin Microbiol* **2011**, 49, (2), 491-9.
11. Sauer, S.; Freiwald, A.; Maier, T.; Kube, M.; Reinhardt, R.; Kostrzewa, M.; Geider, K., Classification and identification of bacteria by mass spectrometry and computational analysis. *PLoS One* **2008**, 3, (7), e2843.
12. Saleeb, P. G.; Drake, S. K.; Murray, P. R.; Zelazny, A. M., Identification of mycobacteria in solid-culture media by matrix-assisted laser desorption ionization-time of flight mass spectrometry. *J Clin Microbiol* **2011**, 49, (5), 1790-4.
13. Mather, C. A.; Rivera, S. F.; Butler-Wu, S. M., Comparison of the Bruker Biotyper and Vitek MS matrix-assisted laser desorption ionization-time of flight mass spectrometry systems for identification of mycobacteria using simplified protein extraction protocols. *J Clin Microbiol* **2014**, 52, (1), 130-8.
14. Lotz, A.; Ferroni, A.; Beretti, J. L.; Dauphin, B.; Carboneille, E.; Guet-Revillet, H.; Veziris, N.; Heym, B.; Jarlier, V.; Gaillard, J. L.; Pierre-Audigier, C.; Frapy, E.; Berche, P.; Nassif, X.; Bille, E., Rapid identification

of mycobacterial whole cells in solid and liquid culture media by matrix-assisted laser desorption ionization-time of flight mass spectrometry. *J Clin Microbiol* **2010**, 48, (12), 4481-6.

15. Leao, S. C.; Tortoli, E.; Viana-Niero, C.; Ueki, S. Y.; Lima, K. V.; Lopes, M. L.; Yubero, J.; Menendez, M. C.; Garcia, M. J., Characterization of mycobacteria from a major Brazilian outbreak suggests that revision of the taxonomic status of members of the *Mycobacterium chelonae*-*M. abscessus* group is needed. *J Clin Microbiol* **2009**, 47, (9), 2691-8.
16. Clark, A. E.; Kaleta, E. J.; Arora, A.; Wolk, D. M., Matrix-assisted laser desorption ionization-time of flight mass spectrometry: a fundamental shift in the routine practice of clinical microbiology. *Clin Microbiol Rev* **2013**, 26, (3), 547-603.
17. Cheng, K.; Chui, H.; Domish, L.; Hernandez, D.; Wang, G., Recent development of mass spectrometry and proteomics applications in identification and typing of bacteria. *Proteomics Clin Appl* **2016**, 10, (4), 346-57.
18. Kooken, J.; Fox, K.; Fox, A.; Altomare, D.; Creek, K.; Wunschel, D.; Pajares-Merino, S.; Martinez-Ballesteros, I.; Garaizar, J.; Oyarzabal, O.; Samadpour, M., Reprint of "Identification of staphylococcal species based on variations in protein sequences (mass spectrometry) and DNA sequence (sodA microarray)". *Mol Cell Probes* **2014**, 28, (2-3), 73-82.
19. Paul, C. J.; Twine, S. M.; Tam, K. J.; Mullen, J. A.; Kelly, J. F.; Austin, J. W.; Logan, S. M., Flagellin diversity in *Clostridium botulinum* groups I and II: a new strategy for strain identification. *Appl Environ Microbiol* **2007**, 73, (9), 2963-75.
20. Palmblad, M.; Deelder, A. M., Molecular phylogenetics by direct comparison of tandem mass spectra. *Rapid Commun Mass Spectrom* **2012**, 26, (7), 728-32.
21. Wulff, T.; Nielsen, M. E.; Deelder, A. M.; Jessen, F.; Palmblad, M., Authentication of fish products by large-scale comparison of tandem mass spectra. *J Proteome Res* **2013**, 12, (11), 5253-9.
22. Onder, O.; Shao, W.; Kemps, B. D.; Lam, H.; Brisson, D., Identifying sources of tick blood meals using unidentified tandem mass spectral libraries. *Nat Commun* **2013**, 4, 1746.
23. Supply, P.; Allix, C.; Lesjean, S.; Cardoso-Oelemann, M.; Rusch-Gerdes, S.; Willery, E.; Savine, E.; de Haas, P.; van Deutekom, H.; Roring, S.; Bifani, P.; Kurepina, N.; Kreiswirth, B.; Sola, C.; Rastogi, N.; Vatin, V.; Gutierrez, M. C.; Fauville, M.; Niemann, S.; Skuce, R.; Kremer, K.; Locht, C.; van Soolingen, D., Proposal for standardization of optimized mycobacterial interspersed repetitive unit-variable-number tandem repeat typing of *Mycobacterium tuberculosis*. *J Clin Microbiol* **2006**, 44, (12), 4498-510.
24. Reischl, U.; Feldmann, K.; Naumann, L.; Gaugler, B. J.; Ninet, B.; Hirschel, B.; Emler, S., 16S rRNA sequence diversity in *Mycobacterium celatum* strains caused by presence of two different copies of 16S rRNA gene. *J Clin Microbiol* **1998**, 36, (6), 1761-4.
25. Adekambi, T.; Colson, P.; Drancourt, M., rpoB-based identification of nonpigmented and late-pigmenting rapidly growing mycobacteria. *J Clin Microbiol* **2003**, 41, (12), 5699-708.
26. de Keijzer, J.; de Haas, P. E.; de Ru, A. H.; van Veelen, P. A.; van Soolingen, D., Disclosure of selective advantages in the 'modern' sublineage of the *Mycobacterium tuberculosis* Beijing genotype family by quantitative proteomics. *Mol Cell Proteomics* **2014**.

27. Wisniewski, J. R.; Zougman, A.; Nagaraj, N.; Mann, M., Universal sample preparation method for proteome analysis. *Nat Methods* **2009**, 6, (5), 359-62.
28. Boersema, P. J.; Raijmakers, R.; Lemeer, S.; Mohammed, S.; Heck, A. J., Multiplex peptide stable isotope dimethyl labeling for quantitative proteomics. *Nat Protoc* **2009**, 4, (4), 484-94.
29. Kall, L.; Canterbury, J. D.; Weston, J.; Noble, W. S.; MacCoss, M. J., Semi-supervised learning for peptide identification from shotgun proteomics datasets. *Nat Methods* **2007**, 4, (11), 923-5.
30. Lam, H.; Deutsch, E. W.; Eddes, J. S.; Eng, J. K.; King, N.; Stein, S. E.; Aebersold, R., Development and validation of a spectral library searching method for peptide identification from MS/MS. *Proteomics* **2007**, 7, (5), 655-67.
31. Tamura, K.; Peterson, D.; Peterson, N.; Stecher, G.; Nei, M.; Kumar, S., MEGA5: molecular evolutionary genetics analysis using maximum likelihood, evolutionary distance, and maximum parsimony methods. *Mol Biol Evol* **2011**, 28, (10), 2731-9.
32. Kelkar, D. S.; Kumar, D.; Kumar, P.; Balakrishnan, L.; Muthusamy, B.; Yadav, A. K.; Shrivastava, P.; Marimuthu, A.; Anand, S.; Sundaram, H.; Kingsbury, R.; Harsha, H. C.; Nair, B.; Prasad, T. S.; Chauhan, D. S.; Katoch, K.; Katoch, V. M.; Kumar, P.; Chaerkady, R.; Ramachandran, S.; Dash, D.; Pandey, A., Proteogenomic analysis of Mycobacterium tuberculosis by high resolution mass spectrometry. *Mol Cell Proteomics* **2011**, 10, (12), M111 011627.
33. de Souza, G. A.; Arntzen, M. O.; Fortuin, S.; Schurch, A. C.; Malen, H.; McEvoy, C. R.; van Soolingen, D.; Thiede, B.; Warren, R. M.; Wiker, H. G., Proteogenomic analysis of polymorphisms and gene annotation divergences in prokaryotes using a clustered mass spectrometry-friendly database. *Mol Cell Proteomics* **2011**, 10, (1), M110 002527.
34. Schubert, O. T.; Mouritsen, J.; Ludwig, C.; Rost, H. L.; Rosenberger, G.; Arthur, P. K.; Claassen, M.; Campbell, D. S.; Sun, Z.; Farrah, T.; Gengenbacher, M.; Maiolica, A.; Kaufmann, S. H.; Moritz, R. L.; Aebersold, R., The Mtb proteome library: a resource of assays to quantify the complete proteome of Mycobacterium tuberculosis. *Cell Host Microbe* **2013**, 13, (5), 602-12.
35. Mann, M.; Kelleher, N. L., Precision proteomics: the case for high resolution and high mass accuracy. *Proc Natl Acad Sci U S A* **2008**, 105, (47), 18132-8.
36. Nessen, M. A.; van der Zwaan, D. J.; Grevers, S.; Dalebout, H.; Staats, M.; Kok, E.; Palmblad, M., Authentication of Closely Related Fish and Derived Fish Products Using Tandem Mass Spectrometry and Spectral Library Matching. *J Agric Food Chem* **2016**, 64, (18), 3669-77.
37. Lam, H.; Deutsch, E. W.; Aebersold, R., Artificial decoy spectral libraries for false discovery rate estimation in spectral library searching in proteomics. *J Proteome Res* **2010**, 9, (1), 605-10.

# Supporting information

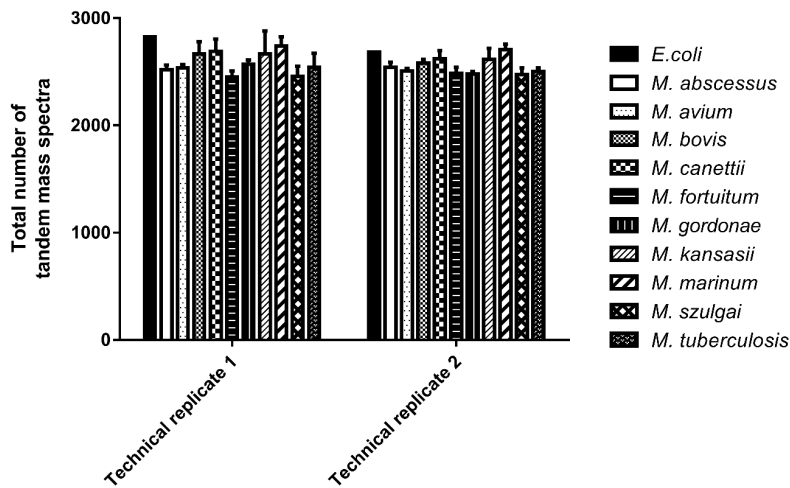


**FIGURE S1:** total number of mass spectra acquired on the Q-Exactive for each of the species analysed. Error bars represent the standard deviation of biological variation within the grouped species.

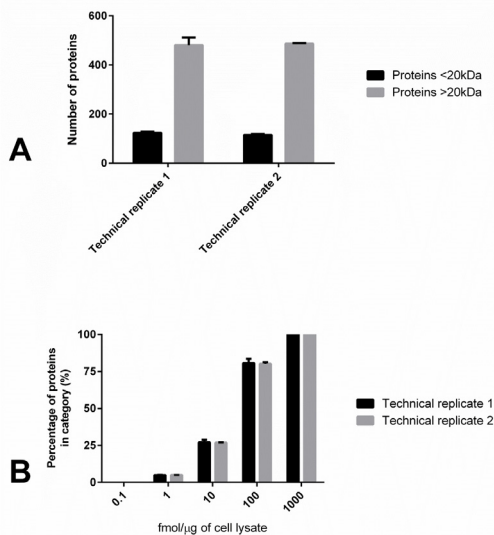


**FIGURE S2:** The spectra acquired for *M. tuberculosis* H37Rv were searched using the SEQUEST HT peptide search engine. Proteins that were molecular weight (A) and the estimated abundance (Schubert et al., 2013) (B) compared to complete the *M. tuberculosis* H37Rv proteome. (Cole et al., 1998) Error bars represent the standard deviation between biological replicates.

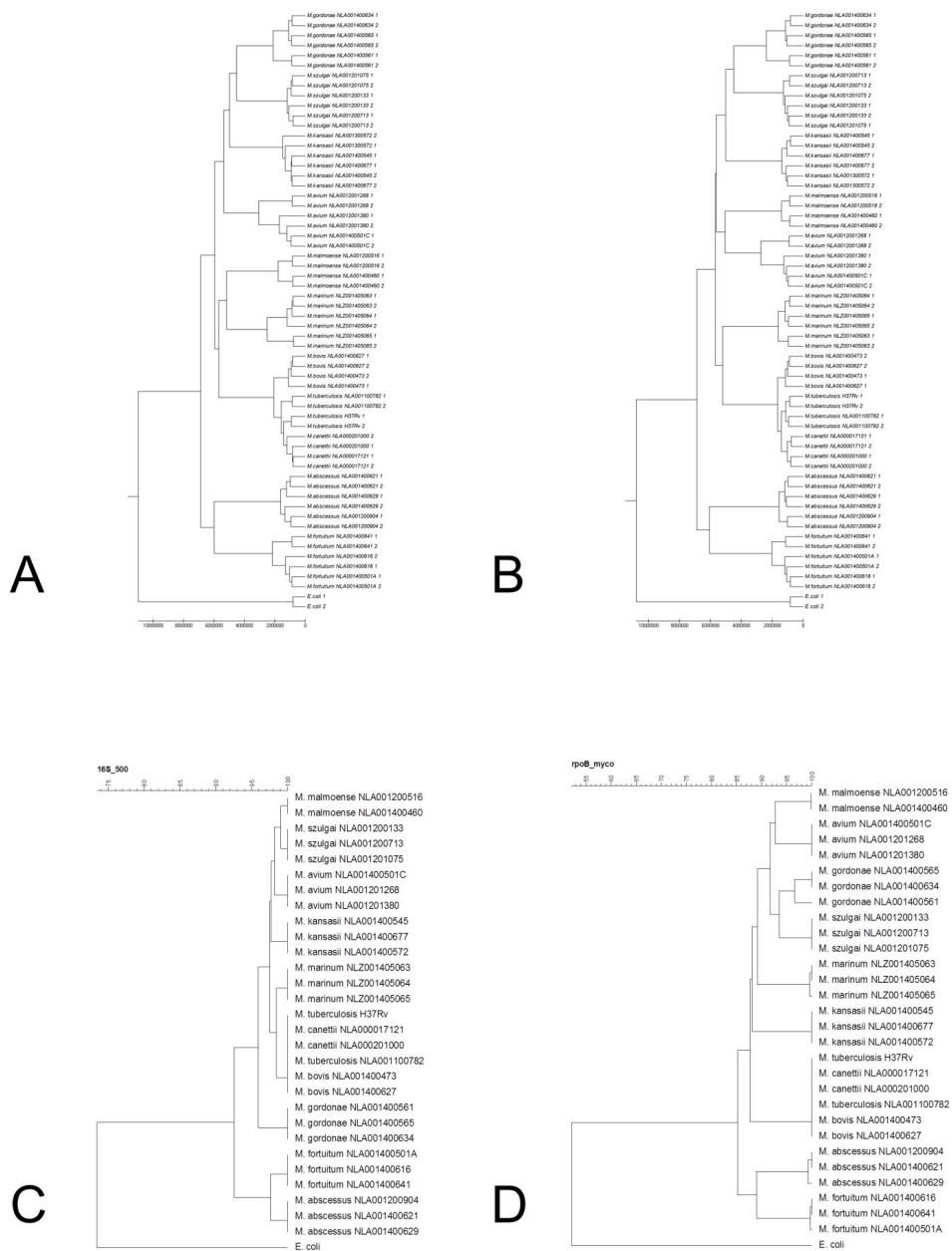


**FIGURE S3:** Phylogenetic trees of selected mycobacteria were established using compareMS2 (Palmbiad and Deelder, 2012) Two technical replicates were analysed (A&B) and compared with 16S rRNA (C) and rpoB (D) sequencing.



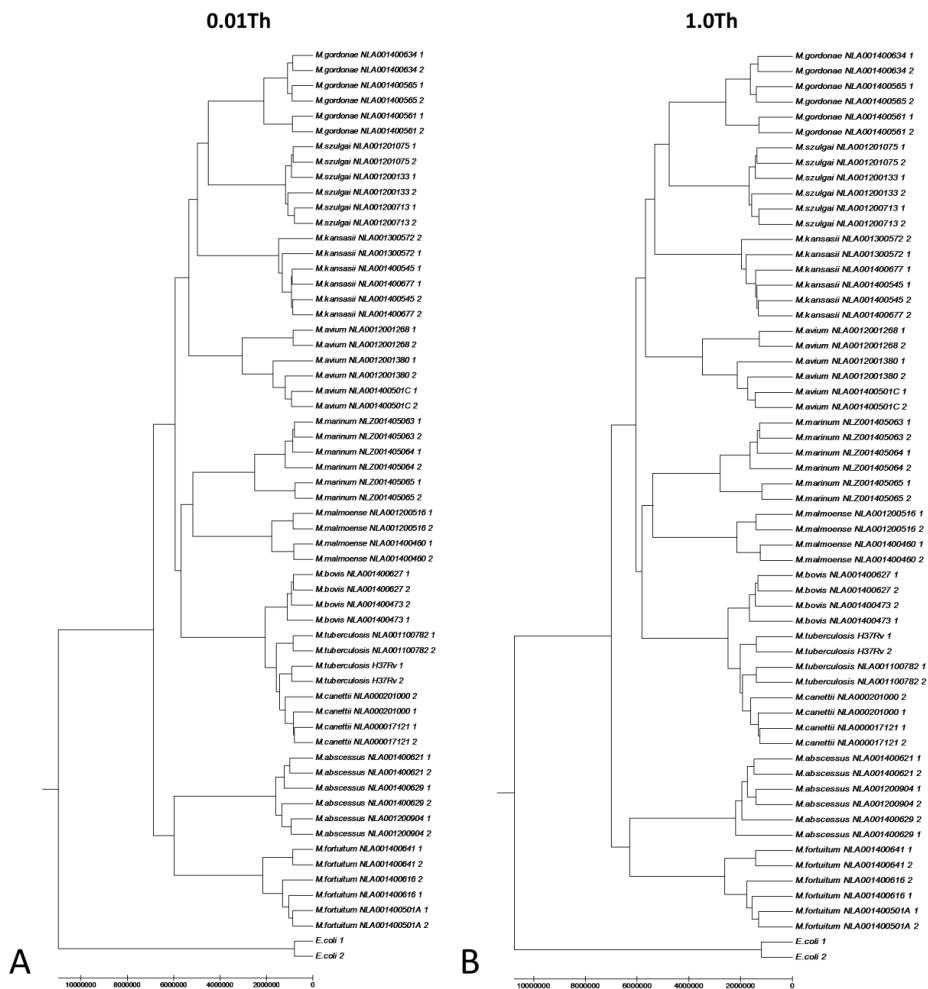


**FIGURE S4:** Phylogenetic tree constructed out of 11 *Mycobacterium* species, represented by 29 unique isolates, and *E. coli* using the UPGMA hierarchical clustering method on approximately 2000 tandem mass spectra that were acquired on the Q-Exactive for each of sample, in biological duplicates. The trees were constructed using compareMS2 with either 0.01 Th (A) and 1.0 Th (B) precursor mass tolerance. The distances were calculated using the formula:  $\#(\text{spectra})/\#(\text{spectra}|\text{dot}>0.8)$





## General discussion

## General Discussion

The ongoing spread of (multi-)drug resistant *Mycobacterium tuberculosis* presents a major burden on the management of tuberculosis (TB).<sup>(1)</sup> Early detection of drug resistance or drug tolerance can be essential to minimize the spread of resistant strains. Furthermore, a better knowledge of interstrain variation, mechanisms of action of anti-TB drugs and mycobacterial drug tolerance will facilitate the development of improved diagnostic assays, new drug targets and novel drug treatment strategies. In this thesis, we made use of mass spectrometry-based proteomics as an unbiased hypothesis generating tool to study protein regulation in *M. tuberculosis* in relation to the development and transmission of drug resistance. The (major) novel findings described in this thesis are summarized and discussed in this Chapter; Box 1.

### **BOX 1: Summary of novel findings described in this thesis.**

In this thesis, we examined to what extent regulation of the *M. tuberculosis* proteome contributes to drug tolerance, a (sub-)lineage specific phenotype and the anti-TB mechanism of antibiotics. The main findings are listed below:

- Chapter 2 & 4 a gap is bridged between the *M. tuberculosis* Beijing sub-lineages genotype and phenotype by identifying the differential abundance of Rv0450c/MmpL4 and Rv3283/sseA in modern Beijing strains relative to other clinically relevant *M. tuberculosis* lineages.
- In Chapter 3 it is demonstrated that the DosR dormancy regulon is actively induced by *M. tuberculosis* Beijing B0/W148 upon rifampicin treatment. Furthermore, it is demonstrated that the *M. tuberculosis* Beijing B0/W148 strain displays a pre-dormant phenotype prior to rifampicin treatment.
- In Chapter 4 it is demonstrated that next to *M. tuberculosis* Beijing B0/W148, also *M. tuberculosis* H37Rv induces the dormancy regulon upon rifampicin treatment. Additionally, it is shown that the proteinaceous regulators of dormancy are a priori more abundant in *M. tuberculosis* Beijing strains compared to other clinically relevant *M. tuberculosis* strains.
- In Chapter 5 a novel mechanism of action for the potential new antibiotic thioridazine is described.
- In Chapter 6 we demonstrate that phylogenetic relationships between closely related mycobacteria and *M. tuberculosis* strains can be reconstructed based on their phenotype using tandem mass spectrometry.

## Proteomic analysis of *M. tuberculosis*

In order to establish a comprehensive, representable proteomic view of *M. tuberculosis* using mass spectrometry, mycobacterial proteins need to be extracted from the cell. Reproducible, unbiased extraction of an entire mycobacterial proteome is hampered by the thick, lipid-rich cell wall surrounding mycobacteria.<sup>(2, 3)</sup> To obtain a representative extract of the mycobacterial proteome, we made use of a chemical disruption, using sodium dodecyl sulfate, combined with heat treatment and mechanical disruption by means of bead-beating. Based on the identified recovered proteins, we demonstrate that this procedure yields a reproducible extraction of the mycobacterial proteome without a bias towards a protein's physiochemical properties and cellular localization (**Chapter 2**).

The proteomic coverage in a proteomics experiment is dependent on several variables, including pre-fractionation of the proteome and the type of mass spectrometer used. Within this thesis, we made use of a Thermo Scientific LTQ-FT Ultra hybrid mass spectrometer and a Thermo Scientific Q-Exactive quadrupole orbitrap mass spectrometer. As expected, the Q-Exactive outperformed the LTQ-FT Ultra in total number of identified proteins; Table 1. The Q-Exactive is a newer generation of mass spectrometer, that can generate more high resolution mass spectra per second, which resulted in more peptide identifications and ultimately more protein identifications.

In the proteomic dataset generated with the Q-Exactive mass spectrometer, we reproducibly quantified a total of 2,429 proteins with  $\geq 2$  peptides per protein and a 1% false discovery rate (**Chapter 4**). Thereby, this proteomic dataset covers  $\pm 60\%$  of all proteins theoretically present in *M. tuberculosis* and  $\pm 80\%$  of the expressed proteome reported to date.<sup>(4-6)</sup> Considering that we analyzed a homogenous culture of *M. tuberculosis* cells that was in mid-logarithmic growth phase, we assume that for example stationary growth phase specific proteins were likely to be absent, or in quantities too low to be detected.<sup>(7)</sup>

The comprehensive, unbiased proteome-wide quantifications performed in this thesis were obtained after pre-fractionation of the digested proteome to decrease complexity and thereby increase proteomic coverage. However, with the availability of new bioinformatic tools and even faster scanning mass spectrometers, pre-fractionation of mycobacterial protein digests can possibly be omitted. One novel powerful approach to study unfractionated proteomes is the data-independent acquisition (DIA) method SWATH (Sequential Window Acquisition of all Theoretical Mass Spectra).<sup>(8)</sup>

Analysis of the *M. tuberculosis* proteome using SWATH allowed for the quantification of up to

2,458 proteins in a single LC-MS/MS run on a Sciex TripleTOF 5600 mass spectrometer.<sup>(6)</sup> Using SWATH, *M. tuberculosis* proteomes can be quantitatively studied with a high-throughput, but SWATH also has several disadvantages. A major drawback of SWATH assays is that the method is not compatible with conventional proteomic database search algorithms. The generation of a SWATH assay specific proteomics library requires a major investment. For the generation of the *M. tuberculosis* SWATH library, a total of 17,463 peptides were selected, synthesized and analyzed by data-dependent acquisition (DDA) on a TripleTOF 5600 mass spectrometer.<sup>(5, 6)</sup> The resulting tandem mass spectra were compiled into a SWATH assay library. Albeit very powerful, this SWATH library resource is only of use for researchers that have access to a TripleTOF mass analyzer or other mass spectrometers that produce peptide fragmentation patterns similar to the curated tandem mass spectra stored in the SWATH library.

Due to the limitations of DIA/SWATH analysis, DDA remains to be an attractive alternative. Even more than DIA, DDA analysis of complex samples relies on the acquisition speed of the mass analyzer. The ongoing development of mass spectrometers continues to lead to new mass spectrometers with increased resolution and acquisition speed. For example, with the introduction of the Thermo Scientific Orbitrap Fusion mass analyser, comprehensive analysis of the *Saccharomyces cerevisiae* proteome could be achieved using a single 95 minute analysis.<sup>(9)</sup> Considering the fact that the *S. cerevisiae* proteome consists of 6,100 theoretical proteins, compared to *M. tuberculosis* producing 4,000 proteins, and the fact that the dynamic range of the proteome in *S. cerevisiae* is an order of magnitude larger than that of *M. tuberculosis*, we can conclude that the observable proteome of *S. cerevisiae* is more complex than that of *M. tuberculosis*.<sup>(5, 10, 11)</sup> Therefore, we would anticipate that comprehensive DDA proteomic analysis of *M. tuberculosis* can be achieved within 95 minutes using the latest generation of mass spectrometers.

Despite the ongoing development of mass spectrometers, the current, state-of-the-art, equipment is sufficiently powerful to comprehensively study the proteome of *M. tuberculosis* and address scientific questions. The development and implementation of new mass spectrometers with increased resolution and acquisition speed will be of limited added value to the *M. tuberculosis* proteomics research field that performs bottom-up proteomic analysis, i.e. faster mass spectrometer will mainly allow for a higher sample throughput. However, the development of novel fragmentation techniques, that are orthogonal to the commonly used fragmentation method collision induced dissociation, will be of more interest as the characterization of (semi-) intact proteins and post-translational modifications become increasingly important.<sup>(12-14)</sup>

In the cell, proteins can engage into highly specific interactions that affect the cellular phenotype. With the hardware available to identify and quantify these proteins within a reasonable

timeframe, the generated mass spectrometry data should be analyzed to add biological meaning to data and generate new hypotheses. Proteomic analysis is heavily dependent on downstream software solutions, both for the identification & quantification of proteins and interpretation of the large datasets generated. The functional interpretation of quantitative proteomic datasets can be performed using pathway and protein-protein interaction analysis. Pathway analysis refers to a type of data analysis that aims to identify (de)activated biological pathways typically including; signalling pathways, gene regulatory pathways and metabolic pathways.<sup>(15)</sup> The interpretation of proteomic datasets by either network or pathway analysis requires prior information of the proteins of interest, such as protein-protein interactions, a proteins cellular localization and its molecular function. For well-studied organisms, this type of data can be derived from well curated scientific publications.

Regarding the functional assignment of the proteins present in *M. tuberculosis*, relatively little pre-existing functional biological information is present. This is well illustrated by the functional categorization of the *M. tuberculosis* proteome as performed by Tuberculist, a regularly updated database of *M. tuberculosis* proteins, where a quarter of the proteome is categorized as hypothetical.<sup>(16)</sup> Despite the, mainly bioinformatic, attempts to assign these hypothetical proteins to a molecular function, specific functional information is limited for most of the *M. tuberculosis* proteome.<sup>(17)</sup> More information on this aspect will improve the functional biological interpretation of new and previously published proteomic datasets, and thereby further advance our understanding of cellular processes in *M. tuberculosis*. Now that the analytical hardware reached a level of maturity that is sufficient for the rapid, comprehensive study of *M. tuberculosis* proteomes, it is highly conceivable that the availability of protein functionality data will become the next bottleneck at the frontier of *M. tuberculosis* proteomics.

**TABLE 1:** Overview of the proteomics analyses performed and proteins identified in this thesis. Proteins identified contain  $\geq 2$  peptides/ protein and 1% False Discover Rate (FDR).

Chapter	<i>M. tuberculosis</i> Strains	Multiplex	SCX fractions	Bio./Tech. duplicate	Total no. of fractions analysed	Mass analyzer	Total no. of proteins identified
2	Atypical and Typical Beijing	2	3 x 15	No/ Yes	90	LTQ-FTICR Ultra	2392
3	Typical Beijing	2	5 x 15	Yes/ Yes	300	LTQ-FTICR Ultra	2534
4	Typical Beijing & H37Rv	3	2 x 15	Yes/ Yes	60	Q-Exactive	2903
5	H37Rv	2	1 x 15	Yes/ Yes	30	LTQ-FTICR Ultra	2479



## Metabolic reprogramming of *M. tuberculosis* in response to rifampicin treatment

*M. tuberculosis* has a wide variety of molecular tools that can increase the cells' tolerance to drugs and thereby prevent rapid drug induced killing of the pathogen (**Chapter 1**). In this thesis, we set out to identify the mechanisms that come to play in *M. tuberculosis* during the initial 24 hrs of rifampicin exposure (**Chapter 3 & Chapter 4**). As described in **Chapter 3**, we reasoned that short-term exposure of the pathogen to rifampicin will yield a more accurate representation of the *in vivo* situation than long-term rifampicin exposure due to the short half-life time of rifampicin *in vivo*.<sup>(18)</sup>

Although we aimed to identify the molecular tools that contribute to the development of rifampicin resistance, we did not study rifampicin resistant strains. Strains that have acquired a rifampicin resistance conferring mutation will no longer be susceptible to the drug. As a consequence, it is not to be expected that a rifampicin resistant mutant will regulate stress induced proteins or any of the molecular tools that provide drug tolerance when the cells are exposed to rifampicin. Therefore, we reasoned that the physiology and proteome of a drug resistant strain will not provide information on the proteins required to develop an enduring drug tolerant phenotype.

Rifampicin targets *rpoB*, an enzyme whose RNA polymerase activity is required for the synthesis of proteins.<sup>(19, 20)</sup> However, in this thesis we demonstrated that despite the presence of high levels of rifampicin, *M. tuberculosis* still manages to regulate the abundance of proteins in the initial 24 hrs after the start of rifampicin exposure. Strikingly, when we exposed *M. tuberculosis* Beijing B0/W148 to 16 µg/ml of rifampicin for 24 hrs, we did observe the increased abundance of DosR dormancy proteins (**Chapter 3**). Using DosR proteins, *M. tuberculosis* can enter a metabolically hypoactive latent state where the pathogen is less susceptible to antibiotics which act as inhibitors of active cellular or metabolic processes.<sup>(21)</sup> In this thesis, we did not only describe the proteomic changes induced by rifampicin exposure, but using cellular assays, we demonstrated that, following the induction of DosR dormancy proteins, rifampicin exposed cells develop a more dormant phenotype (**Chapter 3**).

To determine whether this response is shared by other *M. tuberculosis* strains, we also exposed *M. tuberculosis* H37Rv, a laboratory *M. tuberculosis* strain, to rifampicin (**Chapter 4**). Similar to the results obtained after exposure of *M. tuberculosis* Beijing B0/W148 to rifampicin, we found that *M. tuberculosis* H37Rv also induces dormancy proteins as a response to rifampicin treatment. Thereby, the outcomes of this thesis suggest that transition to dormancy, as a response to rifampicin induced stress, is conserved throughout various *M. tuberculosis*

genotypes, although this may be more pronounced in genotypes such as the Beijing family, that is often associated with the spread of drug resistant TB.<sup>(22-28)</sup>

If rifampicin treatment induces the transition into a dormant phenotype, it will eventually make the pathogen less susceptible to a variety of antibiotics, since the mechanism of action of most drugs share the requirement for growth or active metabolism.<sup>(21)</sup> The increased tolerance of the pathogen during dormancy will lead to extended survival times of the cells during treatment, but the pathogen can still be killed by antibiotics. However, dormant *M. tuberculosis* cells maintain the same mutation rate as actively growing cells.<sup>(29)</sup> Thereby, dormancy increases the window of opportunity of the pathogen to establish a drug resistant genotype, which can ultimately result in relapses of drug resistant *M. tuberculosis*.

The dramatic effects of drug induced dormancy are not limited to the *in vivo* situation. *In vitro*, drug susceptibility testing aims to determine the growth inhibitory concentrations of antibiotics, known as the minimal inhibitory concentration (MIC). Since mycobacterial growth in a known concentration of a given antibiotic is the only measure of these assays, it cannot diagnose a situation in which growth is actively inhibited by the pathogen to prevent killing. As a consequence, the read-out of the assay does provide the tester with a growth limiting concentration of the antibiotic examined, but it does not provide a measure of antibiotic tolerance. Therefore, the currently available drug susceptibility testing is not capable of diagnosing bacteria more prone to escape treatment and develop drug resistance.

As an alternative to MIC testing, it has been suggested to supplement current microbial drug susceptibility testing with minimum duration for killing (MDK) testing.<sup>(30)</sup> The combination of MIC and MDK values can be very powerful to determine mycobacterial tolerance to specific drugs and combinatorial therapy. However, the time required to perform both MIC and MDK testing for slow growing *M. tuberculosis* cells would significantly increase diagnostic turnaround times. Ideally, in the future, the abundance of phenotypic markers of drug tolerance, as the DosR proteins identified in this thesis, can be rapidly monitored to provide a quantitative measure of drug tolerance.

Finally, it is known that a wide variety of stimuli can induce dormancy, including nitric oxide, acidity, nutrient deprivation and hypoxia.<sup>(31-34)</sup> Therefore, we hypothesized that the observed DosR regulated metabolic reprogramming can be part of a general stress response for *M. tuberculosis* (**Chapter 3 & Chapter 4**). In support of this hypothesis, it was recently reported that the DosR protein Rv0081 is involved in the mycobacterial response to isoniazid, rifampicin, moxifloxacin, mefloquine and bedaquiline.<sup>(35)</sup> Thereby, it is conceivable that not only rifampicin, but also other antibiotics can induce a more dormant phenotype in *M. tuberculosis*, indicating

that the impact of the findings presented in this thesis can have a much broader impact than we can foresee with our current knowledge.

## The regulators of dormancy are more abundant in the emerging *M. tuberculosis* Beijing genotype

In **Chapter 3**, we demonstrated that *M. tuberculosis* Beijing B0/W148 is actively inducing a more dormant phenotype as a mechanism to circumvent killing by rifampicin. Furthermore, in **Chapter 4** we observed a similar response to rifampicin in *M. tuberculosis* H37Rv. In addition, we also observed that out of the 23 identified DosR regulon proteins, ten were significantly more abundant prior to drug exposure in *M. tuberculosis* Beijing B0/W148 than *M. tuberculosis* H37Rv (**Chapter 4**). Finally, we found that the *M. tuberculosis* Beijing B0/W148 cultures possess a highly homogenous, close to dormant, phenotype (**Chapter 3**). To determine whether the *a priori* high abundance of DosR proteins is a Beijing specific trait, we examined the abundance of eight DosR proteins in five of the globally most prevalent *M. tuberculosis* (sub-)lineages; atypical Beijing, typical Beijing, East-African Indian, Haarlem and Central Asian strains (**Chapter 4**). Strikingly, we observed that the proteinaceous regulators of dormancy, Rv3132c/devS and Rv3133c/devR, are more abundant in the *M. tuberculosis* Beijing genotype than in any of the other clinically relevant *M. tuberculosis* lineages examined.

In **Chapter 4**, we demonstrated that *M. tuberculosis* Beijing B0/W148 induces three-fold more copies of the DosR protein Rv2031c/hspX within the initial 24 hrs of rifampicin exposure than H37Rv. This observation is an indication that *M. tuberculosis* Beijing B0/W148 transitions faster to dormancy than *M. tuberculosis* H37Rv. It is tempting to assume that the quantity of DosR proteins is a direct reflection of a pathogen's potential to switch to a fully dormant state. However, this conclusion can only be drawn based on cellular assays, where the induction of dormancy, and phenotypic markers of dormancy, correlate with the quantity of DosR proteins present. Nevertheless, in **Chapter 3** we did demonstrate that *M. tuberculosis* Beijing strains possess a pre-existent dormant phenotype during logarithmic growth, indicating that the cells are always prepared to enter a fully dormant state.

The *a priori* high abundance of DosR proteins that are required for the response to rifampicin and pre-existing dormant phenotype in *M. tuberculosis* Beijing, provide a potential advantage over other strains to establish an enduring drug tolerant phenotype. Therefore, we reasoned that part of the success of *M. tuberculosis* Beijing strains might be attributable to the constant high abundance of dormancy proteins. As the abundance of DosR proteins is conserved in the *M. tuberculosis* Beijing lineage, it is plausible that phenotype associated drug tolerance is

conserved throughout entire *M. tuberculosis* genotypes. In the case of *M. tuberculosis* Beijing it has been demonstrated that this specific genotype is more tolerant to rifampicin, which correlates with the specific pre-dormant phenotype we described in this thesis.<sup>(22, 23)</sup>

It should be noted that the results in this thesis are obtained in an *in vitro* model of *M. tuberculosis*. Although the here described results impact *in vitro* *M. tuberculosis* drug susceptibility testing, the *in vivo* impact and validity of these findings remain to be examined. However, the dormancy regulon has been pinpointed in this thesis as a key factor in drug tolerance and hence most likely in resistance development. Using targeted proteomic approaches, these proteins can potentially be quantified in patient sputum or in an *in vivo* *M. tuberculosis* infection model.

Finally, in view of the importance of DosR for mycobacterial persistence and the findings presented in this thesis, it can be concluded that DosR proteins are promising drug targets.<sup>(36, 37)</sup> It could be speculated that if novel drugs designed to target the DosR dormancy regulon and prevent the pathogen from entering dormancy, TB treatment times can potentially be reduced due to synergism with other antibiotics and even MIC-testing can improve with regard to forecasting drug tolerance.<sup>(35)</sup>

## ***M. tuberculosis* Beijing sublineages specific traits**

In **Chapter 2** & **Chapter 4**, we demonstrated that the abundance of DosR proteins is conserved between the more ancient “atypical” Beijing and more modern “typical” Beijing strains. Nevertheless, both sublineages differ in their capacity to cause and spread active disease, leading to global prevalence of the typical Beijing strain, except for Japan.<sup>(38-40)</sup> Therefore, we hypothesized that there are selective advantages present in the more modern typical Beijing strain, which resulted in the dominance of this sublineage over other *M. tuberculosis* strains (**Chapter 2**).

Genetically, the atypical and typical Beijing strains are highly related, with a mere total of 31 non-synonymous single nucleotide polymorphisms (nsSNPs) that separate the two sublineages.<sup>(41)</sup> Since the genome of *M. tuberculosis* can be seen as the blueprint for the proteome of the organism, it could be that the polymorphisms present in the genome can be displayed in the proteome.

By systematically comparing the proteomes of well characterized *M. tuberculosis* Beijing sublineages, we identified four proteins to be differentially abundant between typical and atypical Beijing strains: Rv0450c/MmpL4, Rv1269c, Rv3137, and Rv3283/sseA. By analysing enzymatic activity and the expression of mRNA of these genes in a large cohort of 29 clinically

derived Beijing strains, we could confirm the differential regulation of Rv0450c/MmpL4 and Rv3283/sseA in the *M. tuberculosis* Beijing sublineages (**Chapter 2**). In **Chapter 4** we further compared the abundance of Rv0450c/MmpL4 and Rv3283/sseA in five clinically prevalent *M. tuberculosis* genotypes and found that Rv0450c/MmpL4 is always highly abundant in *M. tuberculosis* typical Beijing, whereas Rv3283/sseA is always less abundant in typical Beijing strains, relative to all other *M. tuberculosis* (sub-)lineages examined.

For Rv3283/sseA, we were able to bridge the observed typical Beijing specific proteomic phenotype with the typical Beijing specific genotype. It is known that typical Beijing strains possess a typical Beijing specific nsSNP in Rv3283/sseA.<sup>(41)</sup> In **Chapter 2**, we described how this nsSNP impacts protein stability, and as result, we demonstrate in **Chapter 3** that once protein production is inhibited by the presence of rifampicin, the abundance of Rv3283/sseA rapidly declines due to the instability of the protein.

The relatively low abundance of Rv3283/sseA in the typical Beijing strains could provide the sub-lineage with an advantage over other genotypes, as a Rv3283/sseA deficiency was reported to promote enhanced growth of *M. tuberculosis* in macrophages relative to wild-type *M. tuberculosis*.<sup>(42)</sup> Thereby, the inheritable differential abundance of Rv3283/sseA in typical Beijing strains presents a potential factor that provides the sublineage with a selective advantage. Regarding Rv0450c/MmpL4, there is no typical Beijing specific nsSNP described in the gene of this protein. However, Rv0450c/MmpL4, together with Rv0451c/MmpS4 or Rv0677c/MmpS5 and Rv0676c/MmpL5, are required for the secretion of iron-scavenging siderophores in *M. tuberculosis*.<sup>(43)</sup> The typical Beijing specific nsSNP present in Rv0676c/MmpL5 does, using the bioinformatic algorithms used in this thesis, not impact the functionality or half-life time of the protein (**Chapter 2**). Nevertheless, considering the shared functionality of Rv0450c/MmpL4 and Rv0676c/MmpL5, it is plausible that increased levels of Rv0450c/MmpL4 are present to compensate for the mutated Rv0676c/MmpL5 in typical Beijing strains. Since both Rv0450c/MmpL4 and Rv0676c/MmpL5 play an important role in mycobacterial iron metabolism, our data suggest a unique role for iron metabolism in typical Beijing strains.

The importance of iron metabolism in *M. tuberculosis* Beijing strains has been stressed before. From the host's perspective, it has been demonstrated that patients with a mutation in SLC11A1/NRAMP1, a divalent transition metal transporter involved in human iron metabolism, have been associated with increased odds of contracting *M. tuberculosis* Beijing.<sup>(44)</sup> Adaption of the mycobacterial iron metabolism to the altered situation in the host is evidence for the co-evolution of *M. tuberculosis* Beijing and humans in the region.

In **Chapter 3**, we found more evidence linking iron metabolism to the success of *M. tuberculosis*

typical Beijing strains. Rv2986c/HupB, also known as iron-regulated protein (Irep-28), was observed to be phosphorylated during rifampicin treatment. Rv2986c/HupB can positively regulate the biosynthesis of siderophores.<sup>(45, 46)</sup> Next to Rv2986c/HupB, we also found Rv3458c/rpsD to be increasingly phosphorylated during initial exposure to rifampicin (**Chapter 3**). Similar to Rv2986c/HupB, Rv3458c/rpsD plays a role in the pathogens iron metabolism.<sup>(47)</sup> Thereby, we were not only the first to link the regulation of post-translational modifications to drug treatment, but also support the correlation between iron metabolism and drug tolerance.  
(48)

Finally, others recently reported that Rv1346/MbtN, an acyl-CoA dehydrogenase that is involved in the production siderophores, was significantly more abundant in the *M. tuberculosis* Beijing strains, compared to the other *M. tuberculosis* lineages examined.<sup>(49)</sup> Eventually, iron metabolism and dormancy are related. *M. tuberculosis* cells that enter dormancy, or a metabolic hypoactive state, attempt to increase their iron storages.<sup>(50, 51)</sup> The link of iron metabolism with dormancy fits our overall, re-occurring, picture that iron metabolism is an important feature of *M. tuberculosis* Beijing strains, especially typical Beijing strains, which requires further investigation.

Dormancy and iron metabolism are potentially related within *M. tuberculosis* Beijing, with even a genomic link between the typical Beijing specific nsSNP in Rv0676c/MmpL5 and iron metabolism (**Chapter 2**). In relation to the typical Beijing genome and dormancy, there is a typical Beijing specific mutation present in the DosR gene Rv2027c/DosT.<sup>(52)</sup> It has been reported that the presence of this mutation correlates with an increased abundance of Rv3133c/devR mRNA, where typical Beijing strains express on average 12-fold more Rv3133c/devR transcripts than atypical Beijing strains. However, both in our comparative proteomic (**Chapter 2**) and parallel reaction monitoring (**Chapter 4**) studies, we did not find this relation on the protein level. Nevertheless, the presence of a typical Beijing specific mutation in a DosR regulon protein strengthens the hypothesis that there is a unique relation between the genotype of typical Beijing strains in relation to dormancy and iron metabolism.

Now that we are bridging the gap between the typical Beijing specific genotype and phenotype, we can supplement molecular differentiation between Beijing sub-lineages using genotypic markers of which we know they more closely reflect a sub-lineage specific phenotype; Rv0676c/MmpL5, Rv2027c/DosT and Rv3283/sseA.

## Thioridazine, the magic bullet for dormant tuberculosis?

Antibiotics are essential for curative treatment of TB patients and prevention of dissemination of the disease. Despite the presence of effective antibiotics, *M. tuberculosis* is increasingly found to be resistant to one or several antibiotics.<sup>(53)</sup> In this thesis, we reasoned that antibiotic tolerance, and thereby resistance, is at least partially caused by dormancy (**Chapter 3 & Chapter 4**). As we described in **Chapter 4**, dormancy is related to the *M. tuberculosis* Beijing genotype and can be induced by anti-TB treatment regimens. Also other factors can induce dormancy, including nitric oxide, acidity, nutrient deprivation and hypoxia.<sup>(31-34)</sup> As a result, *in vivo M. tuberculosis* often transitions itself in its dormant state. Since most antibiotics target replicating metabolically active cells, they lose activity once the cellular metabolism is down regulated. The ideal novel antibiotic would not only target metabolically active cells, but also the dormant forms of *M. tuberculosis*.<sup>(54-58)</sup>

Several phenothiazine neuroleptics, such as thioridazine, exhibit *in vitro* and *in vivo* activity against *M. tuberculosis*.<sup>(59)</sup> Thioridazine has already been successfully used, off-label, in combination with third-line antibiotics for compassionate therapy of patients presenting with extensively drug resistant infections of TB in Buenos Aires.<sup>(60)</sup> In this and other studies, thioridazine has proven to work synergistically with other antibiotics.<sup>(61-63)</sup>

The synergy between thioridazine and other antibiotics has been attributed to the potential inhibition of drug secreting efflux pumps by thioridazine. The inhibition of efflux pumps was thought to increase the accumulation of antibiotics, which could explain the synergy between thioridazine and other drugs.<sup>(64)</sup> However, the inhibition of drug efflux pumps solely does not fully explain the reported bactericidal effects of thioridazine, leaving the mode of action of thioridazine unknown. Using an unbiased proteomic approach, we set out to unravel the molecular mechanism of this potential new anti-TB component by examining the impact of continuous thioridazine exposure on the proteome of *M. tuberculosis* (**Chapter 5**).

Long-term exposure of *M. tuberculosis* to thioridazine requires the drug to be thermostable over a culture period of approximately two weeks. To determine the thermostability of thioridazine, we designed a straightforward, easy to implement, bioassay that demonstrated the stability of thioridazines' anti-TB activity over a period of 21 days (**Chapter 5**).

By analyzing the proteomic composition of thioridazine treated and untreated cells, we discovered that under the influence of thioridazine several proteins, including two large clusters of proteins involved in the maintenance of the cell wall permeability barrier, are differentially regulated. Our study data did not provide evidence for the differential regulation of specific

mycobacterial efflux pumps that are potentially inhibited by thioridazine.

Following our proteomic data that suggested a difference in cell envelope permeability, we assessed the accumulation of fluorescent dyes in *M. tuberculosis* over time. Our findings show that long-term thioridazine exposure of *M. tuberculosis* increased the accumulation of both hydrophilic and hydrophobic fluorescent compounds. Furthermore, using gas chromatography, we demonstrated that treatment of *M. tuberculosis* with thioridazine altered the composition of the mycobacterial plasma membrane, similarly to other cell envelope permeabilizing drugs.<sup>(65)</sup> The observed increase of cell envelope permeability upon thioridazine treatment explains the reported synergistic effects and increased accumulation of other antibiotics when thioridazine was included in multidrug treatment regimens, i.e. drugs can more easily cross the mycobacterial cell envelope after thioridazine treatment. Although the hypothesis that thioridazine treatment leads to higher intercellular drug concentrations has not changed in this study, the more exact knowledge of its mode of action is a step forward and could facilitate further development of this class of drugs for therapy of multidrug resistant pulmonary infections of TB. In fact, due to the increased permeability of the cell envelope after thioridazine exposure, old drugs can be accumulated to an effective therapeutic level, and also the dose levels of new, but toxic, anti-TB compounds may be significantly reduced.

The mechanism of action described for thioridazine in **Chapter 5** does not only explain why thioridazine acts synergistically with other antibiotics, but also serves as a plausible explanation for the effectivity of thioridazine to both metabolically active and hypoactive cells, as thioridazine seems to directly target the cell envelope.<sup>(54, 66)</sup> Despite reported adverse events associated with the usage of thioridazine, the need for novel antibiotics could justify the risk associated with usage of this repurposed drug for the treatment of drug resistant TB.<sup>(67)</sup> However, the development of less toxic, more potent thioridazine analogues, will bring the routine usage of thioridazine closer to the clinic, which could ultimately result in more effective treatment of drug tolerant, dormant and to dormant transitioning *M. tuberculosis*.<sup>(68)</sup>

## Differentiation of mycobacterial species using tandem mass spectrometry

The mycobacterium genus, including *M. tuberculosis*, consists out of more than 140 species.<sup>(69)</sup> The various mycobacterial species cause various diseases, some leading to morbidity and mortality, but not all mycobacteria are of clinical significance, and not all mycobacteria are susceptible to the same antibiotics.<sup>(69, 70)</sup> In order to properly diagnose and treat patients infected with a *Mycobacterium*, the pathogen needs to be correctly identified.<sup>(71)</sup> However, the



occurrence of >140 *Mycobacterium* species, of which some species are genetically very closely related, hampers the routine identification with a single test.

In **Chapter 6**, we demonstrated that using a rapid proteomics-based method, phylogenetic relationships between closely related mycobacterial species can be established by directly comparing tandem mass spectra derived from a proteolytic digest of the mycobacterial proteome. The method brings the following advantages compared to other currently employed mycobacterial typing approaches; prior knowledge of the species to be identified is not required when performing this untargeted assay (e.g. specific primers), the workflow can be applied to virtually all (micro-)organisms, all acquired tandem mass spectra can be used for clustering of species, the acquisition of tandem mass spectra can be performed on both high and low resolution mass spectrometers, and the technique can easily be implemented in a proteomic laboratory. Ideally, the method would not only be capable of species identification as demonstrated in **Chapter 6**, but it would also be able to discriminate between antibiotic susceptible, tolerant and resistant strains. However, since drug resistant bacteria could differ from drug susceptible bacteria by as little as a single mutation, it would be difficult to predict drug resistance using an untargeted method as described in this thesis. Theoretically, a single mutation could alter the physiology of a cell and thereby the proteome, making identification of drug resistant strains a possibility. However, as such data is not available in literature, other approaches should be explored.

As discussed above, current *in vitro* drug susceptibility testing methods often determine the growth inhibitory concentrations of antibiotics, the MIC. Since the outgrowth of the pathogen in a pre-determined drug concentration is the only measure of these assays, it is not possible to identify drug tolerant bacteria which inhibit their own growth to prevent killing as we presented in **Chapter 3 & Chapter 4**. As a consequence, based on the outcomes of these types of drug susceptibility assays, one can solely conclude whether a strain is drug resistant, i.e. drug resistant strains will grow in high concentrations of antibiotics, whereas drug susceptible strains will not be able to grow in the presence of antibiotics. Theoretically, the in **Chapter 6** described mycobacterial typing method can be applied to discriminate between bacterial drug responses, as discussed below.

It is conceivable that rifampicin treatment will not inhibit the production of new proteins in rifampicin resistant strains. Therefore, it is to be expected that the proteome of a rifampicin resistant strain will not change dramatically during rifampicin treatment. In contrast, rifampicin treatment of fully drug susceptible cells will lead to cell death and might eventually even lead to cell lysis, which will result in a proteomic signature that differs from that of drug resistant, viable, cells. Finally, drug tolerant cells that will persist during drug treatment, but

stop growing, will need to adjust their metabolism and thereby their proteome, described in **Chapter 3 & Chapter 4**. As a result, drug susceptible, tolerant and resistant cells are likely to present a different proteome after drug exposure. Therefore, it would be of interest to perform a traditional phenotypic drug susceptibility assay of which the cultures are also analysed using the described compareMS2 method.

If the pathogen is able to grow in the presence of an antibiotic, we can state that the pathogen is drug resistant, as can be determined using current drug susceptibility testing. If there is no growth, the pathogen can be either drug susceptible or drug tolerant. In this situation, the mass spectrometer can be used to determine whether the cells are drug tolerant, based on their proteomic signature. As a control, the bacteria could be transferred to fresh cultured broths without antibiotics, so non-killed, drug tolerant cells can be re-cultured, as also described in **Chapter 3**. However, the re-culture of cells would take significantly longer than the identification of drug tolerant cells using tandem mass spectra. Thereby, phenotypic identification methods, as compareMS2, could shorten the diagnostic turn-around times significantly.

Although the hypothetical situation outlined above could lead to the discrimination of drug tolerant and drug susceptible strains, it is to be expected that in a cultured population both drug tolerant and drug susceptible strains are present due to the heterogeneity of cell cultures, even with highly defined culture conditions.<sup>(72)</sup> However, as recently reported for meat products, the described compareMS2 method is capable to determine the relative composition of a sample containing meat derived from two or more species.<sup>(73)</sup> Thereby, the method has, theoretically, the potential to not only discriminate between closely-related mycobacterial species, but also determine the relative composition of drug susceptible, tolerant or resistant cells present within a single culture.

The limitations and possibilities of the method should be further examined before it can reach its full potential and being considered for routine use in the clinic. However, based on the data presented in **Chapter 6**, we can conclude that the approach has the potential to advance our understanding of phenotypic relationships between mycobacterial species. Furthermore, the principles of this method can provide accurate species identification and could be of help in directing rapid, accurate and effective patient treatment in the future.

## Concluding remarks

The research presented in this thesis has increased our understanding of the mechanisms that provide rifampicin tolerance, the limitations of drug susceptibility testing, inter- and intra-strain

variation in *M. tuberculosis*, thioridazine's mechanism of action and potential new diagnostic methods. The hypotheses generated, tested and confirmed in this thesis were the result of unbiased proteomic approaches that allowed for novel insights into the regulation of the *M. tuberculosis* proteome in well-defined experimental settings. Although we found that the phenotype *M. tuberculosis* Beijing lineage is more equipped to withstand antibiotic treatment, the outcomes of this thesis indicate that if we advance our understanding of the etiology of drug resistance in *M. tuberculosis*, improved treatment strategies and diagnostic methods will be on the horizon.

## References

1. Donald, P. R.; van Helden, P. D., The global burden of tuberculosis--combating drug resistance in difficult times. *N Engl J Med* **2009**, 360, (23), 2393-5.
2. Lanigan, M. D.; Vaughan, J. A.; Shiell, B. J.; Beddome, G. J.; Michalski, W. P., Mycobacterial proteome extraction: comparison of disruption methods. *Proteomics* **2004**, 4, (4), 1094-100.
3. Rabodoarivelo, M. S.; Aerts, M.; Vandamme, P.; Palomino, J. C.; Rasolofo, V.; Martin, A., Optimizing of a protein extraction method for Mycobacterium tuberculosis proteome analysis using mass spectrometry. *J Microbiol Methods* **2016**, 131, 144-147.
4. Kelkar, D. S.; Kumar, D.; Kumar, P.; Balakrishnan, L.; Muthusamy, B.; Yadav, A. K.; Shrivastava, P.; Marimuthu, A.; Anand, S.; Sundaram, H.; Kingsbury, R.; Harsha, H. C.; Nair, B.; Prasad, T. S.; Chauhan, D. S.; Katoch, K.; Katoch, V. M.; Kumar, P.; Chaerkady, R.; Ramachandran, S.; Dash, D.; Pandey, A., Proteogenomic analysis of Mycobacterium tuberculosis by high resolution mass spectrometry. *Mol Cell Proteomics* **2011**, 10, (12), M111 011627.
5. Schubert, O. T.; Mouritsen, J.; Ludwig, C.; Rost, H. L.; Rosenberger, G.; Arthur, P. K.; Claassen, M.; Campbell, D. S.; Sun, Z.; Farrah, T.; Gengenbacher, M.; Maiolica, A.; Kaufmann, S. H.; Moritz, R. L.; Aebersold, R., The Mtb proteome library: a resource of assays to quantify the complete proteome of Mycobacterium tuberculosis. *Cell Host Microbe* **2013**, 13, (5), 602-12.
6. Schubert, O. T.; Ludwig, C.; Kogadeeva, M.; Zimmermann, M.; Rosenberger, G.; Gengenbacher, M.; Gillet, L. C.; Collins, B. C.; Rost, H. L.; Kaufmann, S. H.; Sauer, U.; Aebersold, R., Absolute Proteome Composition and Dynamics during Dormancy and Resuscitation of Mycobacterium tuberculosis. *Cell Host Microbe* **2015**, 18, (1), 96-108.
7. Pfeiffer, C.; Betts, J.; Lukey, P.; van Helden, P., Protein expression in Mycobacterium tuberculosis differs with growth stage and strain type. *Clin Chem Lab Med* **2002**, 40, (9), 869-75.
8. Gillet, L. C.; Navarro, P.; Tate, S.; Rost, H.; Selevsek, N.; Reiter, L.; Bonner, R.; Aebersold, R., Targeted data extraction of the MS/MS spectra generated by data-independent acquisition: a new concept for consistent and accurate proteome analysis. *Mol Cell Proteomics* **2012**, 11, (6), O111 016717.
9. Hebert, A. S.; Richards, A. L.; Bailey, D. J.; Ulbrich, A.; Coughlin, E. E.; Westphall, M. S.; Coon, J. J., The one hour yeast proteome. *Mol Cell Proteomics* **2014**, 13, (1), 339-47.
10. Kumar, A.; Agarwal, S.; Heyman, J. A.; Matson, S.; Heidtman, M.; Piccirillo, S.; Umansky, L.; Drawid, A.; Jansen, R.; Liu, Y.; Cheung, K. H.; Miller, P.; Gerstein, M.; Roeder, G. S.; Snyder, M., Subcellular localization of the yeast proteome. *Genes Dev* **2002**, 16, (6), 707-19.
11. Picotti, P.; Bodenmiller, B.; Mueller, L. N.; Domon, B.; Aebersold, R., Full dynamic range proteome analysis of S. cerevisiae by targeted proteomics. *Cell* **2009**, 138, (4), 795-806.
12. Olsen, J. V.; Mann, M., Status of large-scale analysis of post-translational modifications by mass spectrometry. *Mol Cell Proteomics* **2013**, 12, (12), 3444-52.
13. Brodbelt, J. S., Ion Activation Methods for Peptides and Proteins. *Anal Chem* **2016**, 88, (1), 30-51.
14. Cannon, J. R.; Kluwe, C.; Ellington, A.; Brodbelt, J. S., Characterization of green fluorescent proteins by

193 nm ultraviolet photodissociation mass spectrometry. *Proteomics* **2014**, 14, (10), 1165-73.

15. Wu, X.; Hasan, M. A.; Chen, J. Y., Pathway and network analysis in proteomics. *J Theor Biol* **2014**, 362, 44-52.
16. Lew, J. M.; Kapopoulou, A.; Jones, L. M.; Cole, S. T., TubercuList--10 years after. *Tuberculosis (Edinb)* **2011**, 91, (1), 1-7.
17. Doerks, T.; van Noort, V.; Minguéz, P.; Bork, P., Annotation of the *M. tuberculosis* hypothetical orfeome: adding functional information to more than half of the uncharacterized proteins. *PLoS One* **2012**, 7, (4), e34302.
18. Acocella, G., Clinical pharmacokinetics of rifampicin. *Clin Pharmacokinet* **1978**, 3, (2), 108-27.
19. Taniguchi, H.; Aramaki, H.; Nikaido, Y.; Mizuguchi, Y.; Nakamura, M.; Koga, T.; Yoshida, S., Rifampicin resistance and mutation of the *rpoB* gene in *Mycobacterium tuberculosis*. *FEMS Microbiol Lett* **1996**, 144, (1), 103-8.
20. Floss, H. G.; Yu, T. W., Rifamycin-mode of action, resistance, and biosynthesis. *Chem Rev* **2005**, 105, (2), 621-32.
21. Connolly, L. E.; Edelstein, P. H.; Ramakrishnan, L., Why is long-term therapy required to cure tuberculosis? *PLoS Med* **2007**, 4, (3), e120.
22. den Hertog, A. L.; Menting, S.; van Soolingen, D.; Anthony, R. M., *Mycobacterium tuberculosis* Beijing genotype resistance to transient rifampin exposure. *Emerg Infect Dis* **2014**, 20, (11), 1932-3.
23. de Steenwinkel, J. E.; ten Kate, M. T.; de Knecht, G. J.; Kremer, K.; Aarnoutse, R. E.; Boeree, M. J.; Verbrugh, H. A.; van Soolingen, D.; Bakker-Woudenberg, I. A., Drug susceptibility of *Mycobacterium tuberculosis* Beijing genotype and association with MDR TB. *Emerg Infect Dis* **2012**, 18, (4), 660-3.
24. Devaux, I.; Kremer, K.; Heersma, H.; Van Soolingen, D., Clusters of multidrug-resistant *Mycobacterium tuberculosis* cases, Europe. *Emerg Infect Dis* **2009**, 15, (7), 1052-60.
25. Buu, T. N.; Huyen, M. N.; Lan, N. T.; Quy, H. T.; Hen, N. V.; Zignol, M.; Borgdorff, M. W.; Cobelens, F. G.; van Soolingen, D., The Beijing genotype is associated with young age and multidrug-resistant tuberculosis in rural Vietnam. *Int J Tuberc Lung Dis* **2009**, 13, (7), 900-6.
26. Buu, T. N.; van Soolingen, D.; Huyen, M. N.; Lan, N. T.; Quy, H. T.; Tiemersma, E. W.; Kremer, K.; Borgdorff, M. W.; Cobelens, F. G., Increased transmission of *Mycobacterium tuberculosis* Beijing genotype strains associated with resistance to streptomycin: a population-based study. *PLoS One* **2012**, 7, (8), e42323.
27. Glynn, J. R.; Whiteley, J.; Bifani, P. J.; Kremer, K.; van Soolingen, D., Worldwide occurrence of Beijing/W strains of *Mycobacterium tuberculosis*: a systematic review. *Emerg Infect Dis* **2002**, 8, (8), 843-9.
28. Parwati, I.; Alisjahbana, B.; Apriani, L.; Soetikno, R. D.; Ottenhoff, T. H.; van der Zanden, A. G.; van der Meer, J.; van Soolingen, D.; van Crevel, R., *Mycobacterium tuberculosis* Beijing genotype is an independent risk factor for tuberculosis treatment failure in Indonesia. *J Infect Dis* **2010**, 201, (4), 553-7.
29. Ford, C. B.; Lin, P. L.; Chase, M. R.; Shah, R. R.; Iartchouk, O.; Galagan, J.; Mohaideen, N.; Iøerger, T. R.; Sacchettini, J. C.; Lipsitch, M.; Flynn, J. L.; Fortune, S. M., Use of whole genome sequencing to estimate the mutation rate of *Mycobacterium tuberculosis* during latent infection. *Nat Genet* **2011**, 43, (5), 482-6.

30. Brauner, A.; Fridman, O.; Gefen, O.; Balaban, N. Q., Distinguishing between resistance, tolerance and persistence to antibiotic treatment. *Nat Rev Microbiol* **2016**, 14, (5), 320-30.
31. Wayne, L. G.; Sohaskey, C. D., Nonreplicating persistence of mycobacterium tuberculosis. *Annu Rev Microbiol* **2001**, 55, 139-63.
32. Voskuil, M. I.; Schnappinger, D.; Visconti, K. C.; Harrell, M. I.; Dolganov, G. M.; Sherman, D. R.; Schoolnik, G. K., Inhibition of respiration by nitric oxide induces a Mycobacterium tuberculosis dormancy program. *J Exp Med* **2003**, 198, (5), 705-13.
33. Schnappinger, D.; Ehrt, S.; Voskuil, M. I.; Liu, Y.; Mangan, J. A.; Monahan, I. M.; Dolganov, G.; Efron, B.; Butcher, P. D.; Nathan, C.; Schoolnik, G. K., Transcriptional Adaptation of Mycobacterium tuberculosis within Macrophages: Insights into the Phagosomal Environment. *J Exp Med* **2003**, 198, (5), 693-704.
34. Betts, J. C.; Lukey, P. T.; Robb, L. C.; McAdam, R. A.; Duncan, K., Evaluation of a nutrient starvation model of Mycobacterium tuberculosis persistence by gene and protein expression profiling. *Mol Microbiol* **2002**, 43, (3), 717-31.
35. Danelishvili, L.; Shulzhenko, N.; Chinison, J. J. J.; Babrak, L.; Hu, J.; Morgun, A.; Burrows, G.; Bermudez, L. E., Mycobacterium tuberculosis Proteome Response to Antituberculosis Compounds Reveals Metabolic "Escape" Pathways That Prolong Bacterial Survival. *Antimicrob Agents Chemother* **2017**, 61, (7).
36. Sharma, S.; Tyagi, J. S., Mycobacterium tuberculosis DevR/DosR Dormancy Regulator Activation Mechanism: Dispensability of Phosphorylation, Cooperativity and Essentiality of alpha10 Helix. *PLoS One* **2016**, 11, (8), e0160723.
37. Hu, Y.; Liu, A.; Menendez, M. C.; Garcia, M. J.; Oravcova, K.; Gillespie, S. H.; Davies, G. R.; Mitchison, D. A.; Coates, A. R., HspX knock-out in Mycobacterium tuberculosis leads to shorter antibiotic treatment and lower relapse rate in a mouse model—a potential novel therapeutic target. *Tuberculosis (Edinb)* **2015**, 95, (1), 31-6.
38. Yang, C.; Luo, T.; Sun, G.; Qiao, K.; Sun, G.; DeRiemer, K.; Mei, J.; Gao, Q., Mycobacterium tuberculosis Beijing strains favor transmission but not drug resistance in China. *Clin Infect Dis* **2012**, 55, (9), 1179-87.
39. Mokrousov, I.; Ly, H. M.; Otten, T.; Lan, N. N.; Vyshnevskiy, B.; Hoffner, S.; Narvskaya, O., Origin and primary dispersal of the Mycobacterium tuberculosis Beijing genotype: clues from human phylogeography. *Genome Res* **2005**, 15, (10), 1357-64.
40. Bifani, P. J.; Mathema, B.; Kurepina, N. E.; Kreiswirth, B. N., Global dissemination of the Mycobacterium tuberculosis W-Beijing family strains. *Trends Microbiol* **2002**, 10, (1), 45-52.
41. Schurch, A. C.; Kremer, K.; Warren, R. M.; Hung, N. V.; Zhao, Y.; Wan, K.; Boeree, M. J.; Siezen, R. J.; Smith, N. H.; van Soolingen, D., Mutations in the regulatory network underlie the recent clonal expansion of a dominant subclone of the Mycobacterium tuberculosis Beijing genotype. *Infect Genet Evol* **2011**, 11, (3), 587-97.
42. Rengarajan, J.; Bloom, B. R.; Rubin, E. J., Genome-wide requirements for Mycobacterium tuberculosis adaptation and survival in macrophages. *Proc Natl Acad Sci U S A* **2005**, 102, (23), 8327-32.
43. Wells, R. M.; Jones, C. M.; Xi, Z.; Speer, A.; Danilchanka, O.; Doornbos, K. S.; Sun, P.; Wu, F.; Tian, C.; Niederweis, M., Discovery of a siderophore export system essential for virulence of Mycobacterium

tuberculosis. *PLoS Pathog* **2013**, 9, (1), e1003120.

44. van Crevel, R.; Parwati, I.; Sahiratmadja, E.; Marzuki, S.; Ottenhoff, T. H.; Netea, M. G.; van der Ven, A.; Nelwan, R. H.; van der Meer, J. W.; Alisjahbana, B.; van de Vosse, E., Infection with *Mycobacterium tuberculosis* Beijing genotype strains is associated with polymorphisms in SLC11A1/NRAMP1 in Indonesian patients with tuberculosis. *J Infect Dis* **2009**, 200, (11), 1671-4.
45. Pandey, S. D.; Choudhury, M.; Yousuf, S.; Wheeler, P. R.; Gordon, S. V.; Ranjan, A.; Sritharan, M., Iron-regulated protein HupB of *Mycobacterium tuberculosis* positively regulates siderophore biosynthesis and is essential for growth in macrophages. *J Bacteriol* **2014**, 196, (10), 1853-65.
46. Yeruva, V. C.; Duggirala, S.; Lakshmi, V.; Kolarich, D.; Altmann, F.; Sritharan, M., Identification and characterization of a major cell wall-associated iron-regulated envelope protein (Irep-28) in *Mycobacterium tuberculosis*. *Clin Vaccine Immunol* **2006**, 13, (10), 1137-42.
47. Rao, P. K.; Rodriguez, G. M.; Smith, I.; Li, Q., Protein dynamics in iron-starved *Mycobacterium tuberculosis* revealed by turnover and abundance measurement using hybrid-linear ion trap-Fourier transform mass spectrometry. *Anal Chem* **2008**, 80, (18), 6860-9.
48. Pandey, R.; Rodriguez, G. M., A ferritin mutant of *Mycobacterium tuberculosis* is highly susceptible to killing by antibiotics and is unable to establish a chronic infection in mice. *Infect Immun* **2012**, 80, (10), 3650-9.
49. Peters, J. S.; Calder, B.; Gonnelli, G.; Degroove, S.; Rajaonarifara, E.; Mulder, N.; Soares, N. C.; Martens, L.; Blackburn, J. M., Identification of Quantitative Proteomic Differences between *Mycobacterium tuberculosis* Lineages with Altered Virulence. *Front Microbiol* **2016**, 7, 813.
50. Voskuil, M. I.; Visconti, K. C.; Schoolnik, G. K., *Mycobacterium tuberculosis* gene expression during adaptation to stationary phase and low-oxygen dormancy. *Tuberculosis (Edinb)* **2004**, 84, (3-4), 218-27.
51. Hampshire, T.; Soneji, S.; Bacon, J.; James, B. W.; Hinds, J.; Laing, K.; Stabler, R. A.; Marsh, P. D.; Butcher, P. D., Stationary phase gene expression of *Mycobacterium tuberculosis* following a progressive nutrient depletion: a model for persistent organisms? *Tuberculosis (Edinb)* **2004**, 84, (3-4), 228-38.
52. Fallow, A.; Domenech, P.; Reed, M. B., Strains of the East Asian (W/Beijing) lineage of *Mycobacterium tuberculosis* are DosS/DosT-DosR two-component regulatory system natural mutants. *J Bacteriol* **2010**, 192, (8), 2228-38.
53. WHO, Multidrug-resistant tuberculosis (MDR-TB) 2013 Update. Factsheet. Available at: [http://www.who.int/tb/challenges/mdr/MDR\\_TB\\_FactSheet.pdf](http://www.who.int/tb/challenges/mdr/MDR_TB_FactSheet.pdf) **2013**, (Accessed: 16 January 2015).
54. Xie, Z.; Siddiqi, N.; Rubin, E. J., Differential antibiotic susceptibilities of starved *Mycobacterium tuberculosis* isolates. *Antimicrob Agents Chemother* **2005**, 49, (11), 4778-80.
55. de Steenwinkel, J. E.; de Knecht, G. J.; ten Kate, M. T.; van Belkum, A.; Verbrugh, H. A.; Kremer, K.; van Soolingen, D.; Bakker-Woudenberg, I. A., Time-kill kinetics of anti-tuberculosis drugs, and emergence of resistance, in relation to metabolic activity of *Mycobacterium tuberculosis*. *J Antimicrob Chemother* **2010**, 65, (12), 2582-9.
56. Deb, C.; Lee, C. M.; Dubey, V. S.; Daniel, J.; Abomoelak, B.; Sirakova, T. D.; Pawar, S.; Rogers, L.; Kolattukudy, P. E., A novel in vitro multiple-stress dormancy model for *Mycobacterium tuberculosis*

- generates a lipid-loaded, drug-tolerant, dormant pathogen. *PLoS One* **2009**, 4, (6), e6077.
57. Zahrt, T. C., Molecular mechanisms regulating persistent *Mycobacterium tuberculosis* infection. *Microbes Infect* **2003**, 5, (2), 159-67.
  58. Kapoor, N.; Pawar, S.; Sirakova, T. D.; Deb, C.; Warren, W. L.; Kolattukudy, P. E., Human granuloma in vitro model, for TB dormancy and resuscitation. *PLoS One* **2013**, 8, (1), e53657.
  59. Kristiansen, J. E.; Dastidar, S. G.; Palchoudhuri, S.; Roy, D. S.; Das, S.; Hendricks, O.; Christensen, J. B., Phenothiazines as a solution for multidrug resistant tuberculosis: From the origin to present. *Int Microbiol* **2015**, 18, (1), 1-12.
  60. Amaral, L.; Boeree, M. J.; Gillespie, S. H.; Udwadia, Z. F.; van Soolingen, D., Thioridazine cures extensively drug-resistant tuberculosis (XDR-TB) and the need for global trials is now! *Int J Antimicrob Agents* **2010**, 35, (6), 524-6.
  61. Dutta, N. K.; Pinn, M. L.; Karakousis, P. C., Reduced emergence of isoniazid resistance with concurrent use of thioridazine against acute murine tuberculosis. *Antimicrob Agents Chemother* **2014**, 58, (7), 4048-53.
  62. Machado, D.; Couto, I.; Perdigo, J.; Rodrigues, L.; Portugal, I.; Baptista, P.; Veigas, B.; Amaral, L.; Viveiros, M., Contribution of efflux to the emergence of isoniazid and multidrug resistance in *Mycobacterium tuberculosis*. *PLoS One* **2012**, 7, (4), e34538.
  63. Viveiros, M.; Amaral, L., Enhancement of antibiotic activity against poly-drug resistant *Mycobacterium tuberculosis* by phenothiazines. *Int J Antimicrob Agents* **2001**, 17, (3), 225-8.
  64. Amaral, L.; Viveiros, M., Why thioridazine in combination with antibiotics cures extensively drug-resistant *Mycobacterium tuberculosis* infections. *Int J Antimicrob Agents* **2012**, 39, (5), 376-80.
  65. Sareen, M.; Khuller, G. K., Effect of ethambutol on the phospholipids of ethambutol susceptible and resistant strains of *Mycobacterium smegmatis* ATCC 607. *Indian J Biochem Biophys* **1990**, 27, (1), 39-42.
  66. Kopec, W.; Khandelia, H., Reinforcing the membrane-mediated mechanism of action of the anti-tuberculosis candidate drug thioridazine with molecular simulations. *J Comput Aided Mol Des* **2014**, 28, (2), 123-34.
  67. Amaral, L.; Viveiros, M., Thioridazine: A Non-Antibiotic Drug Highly Effective, in Combination with First Line Anti-Tuberculosis Drugs, against Any Form of Antibiotic Resistance of *Mycobacterium tuberculosis* Due to Its Multi-Mechanisms of Action. *Antibiotics (Basel)* **2017**, 6, (1).
  68. Pieroni, M.; Machado, D.; Azzali, E.; Santos Costa, S.; Couto, I.; Costantino, G.; Viveiros, M., Rational Design and Synthesis of Thioridazine Analogues as Enhancers of the Antituberculosis Therapy. *J Med Chem* **2015**, 58, (15), 5842-53.
  69. van Ingen, J., Diagnosis of nontuberculous mycobacterial infections. *Semin Respir Crit Care Med* **2013**, 34, (1), 103-9.
  70. Johnson, M. M.; Odell, J. A., Nontuberculous mycobacterial pulmonary infections. *J Thorac Dis* **2014**, 6, (3), 210-20.
  71. Li, W.; Raoult, D.; Fournier, P. E., Bacterial strain typing in the genomic era. *FEMS Microbiol Rev* **2009**, 33, (5), 892-916.



72. Zhang, Y., Persisters, persistent infections and the Yin-Yang model. *Emerg Microbes Infect* **2014**, 3, (1), e3.
73. Ohana, D.; Dalebout, H.; Marissen, R. J.; Wulff, T.; Bergquist, J.; Deelder, A. M.; Palmblad, M., Identification of meat products by shotgun spectral matching. *Food Chem* **2016**, 203, 28-34.







Nederlandstalige samenvatting

List of publications

Curriculum Vitae

Dankwoord

# Nederlandstalige samenvatting

## Algemene inleiding

Tuberculose (TB) is een ernstige infectieziekte die veroorzaakt wordt door *Mycobacterium tuberculosis*. Wereldwijd worden er jaarlijks ruim 10 miljoen nieuwe gevallen van actieve TB gediagnosticeerd. Ondanks dat er sinds de jaren 50 meerdere medicijnen op de markt zijn gekomen om TB succesvol te behandelen, eist deze ziekte nog altijd vele mensenlevens, met een geschat aantal sterfgevallen van 890.000 mannen, 490.000 vrouwen en 140.000 kinderen per jaar. Hiermee is TB wereldwijd de meest dodelijke bacteriële infectieziekte. Buiten deze hoge sterftecijfers zijn er naar schatting wereldwijd nog ca. twee miljard individuen die een latente vorm van TB bij zich dragen, waarbij *M. tuberculosis* in een soort slapende toestand aanwezig is. Van deze twee miljard mensen zal uiteindelijk 3-30% actieve TB ontwikkelen en deze gevallen kunnen opnieuw voor verspreiding van de ziekte zorgen. Hoewel TB wereldwijd nog steeds veel slachtoffers eist, is er in de Westerse wereld sinds halverwege de 20ste eeuw, met de introductie van antibiotica, een gestage afname van het aantal TB infecties.

Momenteel is TB in het algemeen goed te behandelen met werkzame antibiotica. De huidige eerstelijns antibiotica worden echter al ruim 50 jaar gebruikt voor de behandeling van TB. Tijdens dit tijdsbestek zijn er antibiotica resistente vormen van TB ontstaan. Wereldwijd wordt momenteel in 3.5% van alle TB gevallen een vorm van TB gevonden die resistent is voor tenminste rifampicine en isoniazide, de twee belangrijkste eerstelijns antibiotica voor de behandeling van TB. Deze vorm van antibiotica resistente TB staat bekend als Multidrug Resistant TB (MDR-TB). Wanneer er sprake is van additionele resistentie tegen fluoroquinolonen en aminoglycosiden wordt deze vorm van TB extensively drug resistant (XDR-TB) genoemd. Tenslotte is er ook totally drug resistant TB (TDR-TB); een verzamelnaam voor TB gevallen die resistentie hebben ontwikkeld tegen alle beschikbare TB antibiotica waar in een bepaalde setting op getest kan worden. Vanwege het beperkte aantal nieuwe anti-TB medicamenten dat op de markt komt, is er een groeiende angst dat MDR-TB, XDR-TB en TDR-TB uitbraken vaker voor zullen komen en moeilijker te bestrijden worden.

MDR-TB gevallen komen relatief vaak voor in Centraal-Azië en Oost-Europese landen. Zo is beschreven dat in Wit-Rusland bij 35% van alle nieuwe TB gevallen er sprake is van MDR-TB. Dit betekent dat resistente vormen van TB actief worden overgedragen. De verspreiding van MDR-TB wordt in Wit-Rusland, Europa, Zuid-Afrika en grote delen van Azië vaak geassocieerd met het Beijing genotype van *M. tuberculosis*, dat in 1995 door het RIVM werd beschreven. Hoewel dit genotype genetisch niet veel verschilt van andere *M. tuberculosis* stammen, vertonen stam-

men van het Beijing genotype een hogere antibiotica tolerantie, een hogere pathogeniciteit en een afwijkende inductie van immuunresponsen in diverse gastheren, waaronder de mens. Vanwege de toenemende antibioticaresistentie bij TB is het belangrijk om verdere verspreiding van resistente bacteriën te voorkomen. Verbetering van de huidige diagnostiek, behandelstrategieën en de ontwikkeling van nieuwe medicijnen kunnen hiertoe bijdragen.

## Dit proefschrift

Eiwitten zijn relatief grote biomoleculen die verantwoordelijk zijn voor allerlei processen in de bacteriële cel, zoals energiehuishouding, celdeling, infectie van de gastheer en ontwikkeling van antibioticaresistentie. Het proteoom, bestaande uit de eiwitten die aanwezig zijn in de cel op een specifiek moment, bepaalt voor een groot deel de eigenschappen van de cel. Het onderzoek dat beschreven is in dit proefschrift werd uitgevoerd om een completer beeld te krijgen van de mycobacteriële eiwitten die van belang zijn voor de ontwikkeling van antibioticaresistentie en verspreiding van TB. Daarnaast is er gekeken naar toepassingen in de diagnostiek.

Een *M. tuberculosis* genotype dat zich de laatste decennia snel verspreid heeft is de ‘moderne’ of ‘typische’ Beijing lineage. Deze typische Beijing genotype familie is in een veelheid aan studies geassocieerd met antibioticaresistentie, de inductie van een alternatieve immuunrespons en een verhoogde prevalentie, terwijl deze genotype familie genetisch zeer sterk geconserveerd is. Tezamen zijn dit sterke aanwijzingen dat de typische Beijing genotype familie een evolutionair voordeel heeft ten opzichte van andere *M. tuberculosis* families.

In **hoofdstuk 2** is onderzocht of er eiwitten aanwezig zijn in het proteoom van de typische Beijing genotype familie die deze stammen een evolutionair voordeel geven. Hiervoor is het proteoom van typische Beijing isolaten vergeleken met het proteoom van atypische Beijing isolaten. De atypische, of ‘ancient’ Beijing familie is evolutionair gezien van alle *M. tuberculosis* families het meest verwant aan de typische Beijing genotype familie. De atypische Beijing genotype familie is echter niet zo sterk geassocieerd met een verhoogde prevalentie en antibioticaresistentie als de typische Beijing strain.

Uit de resultaten bleek dat het proteoom van de onderzochte typische en atypische Beijing isolaten in grote mate overeenkomstig zijn. Slechts vier eiwitten kwamen in verschillende relatieve hoeveelheden voor in stammen van beide families: Rv0450c/MmpL4, Rv1269c, Rv3137, and Rv3283/sseA. Transcriptionele en functionele analyse van deze vier eiwitten in een cohort van 29 klinische Beijing isolaten liet zien dat typische Beijing isolaten meer Rv0450c/MmpL4 tot expressie brengen dan de geteste atypische Beijing isolaten. Rv0450c/MmpL4 is betrokken

bij de ijzerhuishouding van *M. tuberculosis*. De verhoogde aanwezigheid van Rv0450c/MmpL4 eiwit en mRNA in typische Beijing isolaten is een eerste verklaring waarom individuen met een mutatie in SLC11A1/NRAMP1, een eiwit dat betrokken is bij de ijzerhuishouding in de gastheer, een verhoogde kans op een infectie met Beijing stammen hebben.

In tegenstelling tot Rv0450c/MmpL4, was het eiwit Rv3283/sseA verminderd aanwezig in de onderzochte typische Beijing isolaten. Uit de bioinformatische analyse, beschreven in **hoofdstuk 2**, blijkt dat de verminderde aanwezigheid van Rv3283/sseA in typische Beijing isolaten ten opzichte van atypische Beijing isolaten veroorzaakt wordt door een specifieke mutatie in typische Beijing stammen, die een instabiliteit van het eiwit veroorzaakt. Daarmee demonstreert deze studie een direct verband tussen het afwijkende genotype en fenotype van typische Beijing stammen ten opzichte van de nauwverwante atypische Beijing stammen.

De bevinding dat de relatieve kwantiteit van Rv0450c/MmpL4 en Rv3283/sseA verschilt tussen typische en atypische Beijing isolaten is een eerste stap om de hogere prevalentie van typische Beijing stammen te verklaren aan de hand van het mycobacteriële fenotype. Echter biedt het nog geen verklaring voor de correlatie met antibioticaresistentie. Om erachter te komen welke eiwitten een rol spelen bij de initiële respons van typische Beijing stammen op antibiotica is in **hoofdstuk 3** een typische Beijing stam blootgesteld aan een hoge concentratie rifampicine, één van de belangrijkste eerstelijns antibiotica voor de behandeling van TB.

Gedurende de eerste 24 uren na blootstelling aan rifampicine steeg de relatieve hoeveelheid van zogenaamde ‘dormancy regulon encoded genes’ (DosR) in het proteoom van typische Beijing stammen opvallend veel. DosR genen komen sterk verhoogd tot expressie komen wanneer de bacterie in een zuurstofarm milieu terecht komt. Door de aanwezigheid van DosR eiwitten zal *M. tuberculosis* snel in een latente of ‘dormancy’ fase terechtkomen, waarin deze minder vatbaar is voor antibiotica. Door blootstelling aan rifampicine steeg niet alleen de relatieve hoeveelheid DosR eiwitten. Na het bestuderen van fenotypische dormancy markers bleek ook dat de gehele kweekpopulatie van het onderzochte typische Beijing isolaat een pre-dormant fenotype heeft dat nog ‘meer’ dormant wordt na blootstelling aan rifampicine. De bevinding dat DosR eiwitten een belangrijke rol spelen bij de initiële respons van typische Beijing stammen op antibiotica is nieuw en is een nog niet eerder beschreven manier van *M. tuberculosis* om op een actieve manier fenotypische antibiotica tolerantie te ontwikkelen.

In **hoofdstuk 4** is onderzocht of de initiële respons van typische Beijing stammen op rifampicine uniek is, of dat deze reactie ook waar te nemen is bij andere *M. tuberculosis* stammen. Om deze onderzoeksvraag te beantwoorden is eerst het proteoom van een typische Beijing stam vergeleken met het proteoom van *M. tuberculosis* controle stam H37Rv, zowel voor- als na blootstelling

aan rifampicine. In beide *M. tuberculosis* stammen nam de relatieve hoeveelheid DosR eiwitten toe in de eerste 24 uur na blootstelling aan rifampicine. Echter, de relatieve hoeveelheid van meerdere DosR eiwitten was al hoger in typische Beijing stammen voordat rifampicine werd toegevoegd aan de kweek. Ook steeg de relatieve hoeveelheid van meerdere DosR eiwitten sneller in de onderzochte typische Beijing stam dan bij andere stammen. De verhoogde aanwezigheid van DosR eiwitten in typische Beijing stammen, nog voordat de bacterie in aanraking is gekomen met een antibioticum, duidt erop dat de typische Beijing stammen te allen tijde voorbereid zijn om effectief in een dormancy stadium over te gaan.

Om te bepalen of typische Beijing stammen relatief grote hoeveelheden DosR eiwitten bevatten t.o.v. andere stammen, werden meerdere DosR eiwitten gekwantificeerd in 27 klinische *M. tuberculosis* isolaten, afkomstig van vijf van de meest voorkomende *M. tuberculosis* geotype families. De regulatoire DosR eiwitten waren verhoogd aanwezig waren in zowel typische als atypische Beijing stammen. Deze observatie duidt op een evolutionair voordeel voor de gehele *M. tuberculosis* Beijing familie. Dit biedt deze specifieke *M. tuberculosis* genotype familie de mogelijkheid om te persisteren tijdens behandeling met antibiotica en resistentie te selecteren. Daarom staat de in dit proefschrift beschreven observatie mogelijk in direct verband met de associatie tussen Beijing stammen en antibioticaresistentie in diverse regio's in de wereld, waaronder Europa en Azië.

De bevinding dat eiwitten van het DosR regulon verhoogd aanwezig zijn in Beijing stammen biedt niet alleen een mogelijke verklaring voor de associatie tussen dit genotype en antibioticaresistentie, maar geeft ook een nieuwe kijk op huidige antibioticaresistentie testen. Een veelgebruikte test voor het bepalen van antibioticaresistentie is de Minimum Inhibitory Concentration (MIC) test. Hierbij wordt de antibioticaconcentratie bepaald waarbij de *M. tuberculosis* bacterie stopt met groeien. De aanname is dat boven de MIC de bacterie niet meer groeit omdat de concentratie antibiotica toxisch of remmend is voor het pathogeen. De bevindingen beschreven in dit proefschrift laten zien dat *M. tuberculosis* blootstelling aan antibiotica kan overleven doordat deze in een stadium van dormancy over gaat om zich te beschermen tegen de invloed van antibiotica, om later alsnog opnieuw uit te groeien. De mogelijkheid bestaat zelfs dat de bacterie vele malen hogere concentraties van antibiotica kan tolereren. Concluderend kan gesteld worden dat een MIC bepaling uitsluitend iets zegt over de laagste concentratie waarbij bacteriële groei geremd wordt, maar dat deze niet noodzakelijkerwijs direct verband houdt met het overleven van het pathogeen onder invloed van antibiotica. Deze observatie dient als mogelijke verklaring voor de vele TB relapsen na 'geslaagde' behandelingen.

Vanwege de toenemende mate van antibioticaresistentie wereldwijd en het feit dat de meeste beschikbare antibiotica met name werkzaam zijn tegen metabool actieve en delende mycobacteriën is het belangrijk om de zoektocht naar nieuwe antibiotica voort te zetten. Dit wordt



verder onderstreept door de in dit proefschrift beschreven bevindingen dat blootstelling aan antibiotica ook direct antibiotica tolerantie kan veroorzaken door het induceren van dormancy. Een medicijn dat mogelijk geschikt is voor de behandeling van dormant TB, MDR-TB, XDR-TB en mogelijk zelfs TDR-TB, is thioridazine. Thioridazine is een antipsychoticum dat met succes off-label gebruikt is voor de behandeling van XDR-TB patiënten en *in vitro* actief is tegen zowel metabool actieve als metabool inactieve, dormant, *M. tuberculosis*. Buiten de anti-TB activiteit van thioridazine, werkt dit middel synergistisch met reeds bestaande eerstelijns antibiotica. De theorie voor het werkingsmechanisme is dat het de effluxpompen (afvoerpompen) van bacteriën zou remmen, waardoor er een stapeling van stoffen als antibiotica zo ontstaan. Hoewel het potentieel van thioridazine als nieuw middel voor de behandeling van TB is aangetoond, zoals blijkt uit zowel *in vitro* als *in vivo* data, is het exacte mechanisme van thioridazine onbekend.

In **hoofdstuk 5** is onderzocht op welke manier thioridazine *M. tuberculosis* weet te bestrijden en waarom dit middel met name goed werkt in combinatie met andere antibiotica. Door het bestuderen van het *M. tuberculosis* proteoom in de aan- en afwezigheid van thioridazine is ontdekt welke eiwitten betrokken zijn bij het in stand houden van het pathogeen. De theorie als basis voor deze studie was dat eiwitten die differentieel tot expressie komen tijdens de behandeling met thioridazine betrokken zijn bij cellulaire processen die moeten compenseren voor de door het antibioticum toegebrachte schade.

Meerdere van de eiwitten die differentieel gereguleerd werden tijdens behandeling met thioridazine bleken betrokken bij het produceren en in stand houden van de celenvlop. Aan de hand van de gegenereerde proteomics data en beschikbare literatuur kwam de hypothese tot stand dat thioridazine de celenvlop van *M. tuberculosis* beschadigt. Analyse van de vetzuur compositie in de plasmamembraan van *M. tuberculosis* liet zien dat behandeling met thioridazine de relatieve hoeveelheid 'tuberculostearic acid' beïnvloedt, hetgeen kan wijzen op een verandering van de celenvlop permeabiliteit.

Als de celenvlop van *M. tuberculosis* permeabeler wordt, betekent dit dat antibiotica gemakkelijker de cel in komen om hun anti-TB functie uit te oefenen. Om te testen of langdurige blootstelling van *M. tuberculosis* aan thioridazine de permeabiliteit van de celenvlop inderdaad beïnvloedt, werd een cellulair assay ontwikkeld waarmee cel permeabiliteit en efflux pomp activiteit gemeten kan worden, omdat beide mechanismes bijdragen aan de accumulatie van componenten in de cel. Uit deze data bleek dat thioridazine de celenvlop permeabiliteit beïnvloedt, maar er werd geen direct bewijs gevonden dat thioridazine de activiteit van efflux pompen remt.

Aan de hand van de data uit **hoofdstuk 5** kan worden beredeneerd dat thioridazine *M. tuberculosis* kan doden doordat deze zich richt op de mycobacteriële celenvlop. Een verhoogde per-

meabiliteit van de celenvelop zorgt er ook voor dat andere antibiotica makkelijker accumuleren in de cel. Nu er een beter beeld is van het mechanisme van thioridazine kan dit hopelijk leiden tot beter, efficiënter gebruik van dit medicijn, of derivaten van dit veelbelovende medicijn.

Tenslotte is er binnen de studies in dit proefschrift gekeken hoe massaspectrometrie gebruikt kan worden voor de identificatie van mycobacteriën. Binnen het *Mycobacterium* geslacht zijn momenteel meer dan 140 species beschreven. Hoewel alle species binnen hetzelfde geslacht vallen als *M. tuberculosis*, zijn niet alle mycobacteriën van klinisch belang en zijn niet alle species gevoelig voor dezelfde antibiotica. Identificatie van het mycobacteriële species is van belang om tot een juiste behandeling van de patiënt te komen en de epidemiologie te begrijpen.

In **hoofdstuk 6** laten wij zien dat de mate van verwantschap tussen nauw verwante mycobacteriën bepaald kan worden met behulp van massaspectrometrie. De in dit proefschrift beschreven methode vergelijkt het aantal overeenkomstige tandem massaspectra tussen verschillende proteolytische digesten van de onderzochte mycobacteriële species. De voordelen van de beschreven methodologie ten opzichte van bestaande diagnostische technieken is dat er geen *a priori* kennis van het te identificeren pathogeen nodig is, de methode naar alle waarschijnlijkheid kan worden toegepast op andere micro-organismen, alle tandem massaspectra gebruikt kunnen worden voor het clusteren van de verschillende species en dat de methode werkt op zowel hoge als lage resolutie massa spectrometers.

De limitaties en verdere mogelijkheden van de methode beschreven in **hoofdstuk 6** en **hoofdstuk 7** zullen verder onderzocht moeten worden voordat overwogen kan worden of deze benadering in een klinische setting toegepast kan worden. Desalniettemin kan op basis van de in dit proefschrift beschreven informatie geconcludeerd worden dat deze methode de potentie heeft om onze kennis omtrent de fenotypische verwantschap tussen de verschillende mycobacteriële species te vergroten. Hoewel er in **hoofdstuk 6** uitsluitend een 'proof of principle' van de methode is gedemonstreerd, zou het principe van deze techniek gebruikt kunnen worden voor snellere en accurate identificatie van pathogenen. Uiteindelijk zal dit kunnen leiden tot een effectievere behandeling van patiënten met infecties van nontuberculeuze mycobacteriën in de toekomst.

## Conclusie

Het onderzoek beschreven in dit proefschrift biedt inzicht in de moleculaire mechanismes die betrokken zijn bij het ontstaan rifampicine tolerantie; de limitaties van de huidige antibiotica gevoeligheidstesten; inter- en intra-stam variatie binnen de *M. tuberculosis* genus; het anti-my-

cobacteriële mechanisme van thioridazine en potentiële nieuwe diagnostische methoden voor identificatie. Deze bevindingen onderstrepen dat antibioticaresistentie niet enkel een genetisch probleem is, maar dat eiwit regulatie een belangrijke rol speelt bij de totstandkoming van antibioticaresistentie. Hoewel dit proefschrift aantoont dat het fenotype van Beijing stammen er voor zorgt dat dit pathogeen relatief goed bestand is tegen veel van de momenteel beschikbare antibiotica, laten de uitkomsten van dit proefschrift ook zien dat wanneer kennis met betrekking tot het ontstaan van antibioticaresistentie wordt vergroot, nieuwe verbeterde diagnostische- en behandelmethodes aan de horizon zullen verschijnen.

## List of publications

1. **de Keijzer, J.**, Mulder, A., de Ru, A. H., van Soolingen, D. and van Veelen, P.A. (2016) Parallel reaction monitoring of clinical *Mycobacterium tuberculosis* lineages reveals pre-existent markers of rifampicin tolerance in the emerging Beijing lineage. *Journal of Proteomics* 6;150:9-17.
2. **de Keijzer, J.**, Mulder, A., de Haas, P. E., de Ru, A. H., Heerkens, E.M., Amaral, L., van Soolingen, D. and van Veelen, P. A. (2016) Thioridazine alters the cell envelope permeability of *Mycobacterium tuberculosis*. *Journal of Proteome Research* 15(6):1776-86.
3. **de Keijzer, J.**, Mulder, A., de Beer, J., de Ru, A. H., van Veelen, P. A., and van Soolingen, D. (2016) Mechanisms of phenotypic rifampicin tolerance in *Mycobacterium tuberculosis* Beijing B0/W148. *Journal of Proteome Research*: 15(4):1194-1204.
4. **de Keijzer, J.**, de Haas, P. E., de Ru, A. H., van Veelen, P. A., and van Soolingen, D. (2014) Disclosure of selective advantages in the “modern” sublineage of the *Mycobacterium tuberculosis* Beijing genotype family by quantitative proteomics. *Molecular & cellular proteomics: MCP* 13, 2632-2645.
5. **de Keijzer, J.**, van der Plas – Duivesteijn, S.J., Mulder, A., de Zwaan, R., de Ru, A.H., van Veelen, P.A., van Soolingen, D., Palmblad, N.M. Rapid identification of phylogenetic relationships in the *Mycobacterium* genus by direct comparison of shared spectral content (submitted)
6. van der Plas – Duivesteijn, S.J., Wulff, T., Klychnikov, O., Ohana, D., Dalebout, H., van Veelen, P.A., **de Keijzer, J.**, Nessen, A.M., van der Burgt, Y.E.M., Deelder, A.M., Palmblad, N.M. (2016) Differentiating Samples and Experimental Protocols by Direct Comparison of Tandem Mass Spectra. *Rapid Communications in Mass Spectrometry* (30):731-738

## **Curriculum Vitae**

Jeroen de Keijzer werd geboren op 08 juni 1988 te Rotterdam. In 2005 behaalde hij zijn HAVO diploma aan het Christelijk Lyceum Delft. Het jaar daarop ontving hij zijn propedeuse van de opleiding Hoger Laboratorium Onderwijs aan de Hogeschool Leiden. Drie jaar later rondde hij de opleiding succesvol af. Tijdens zijn bachelor liep hij stage bij Centocor B.V. onder begeleiding van Maurice van der Meij. Hier werkte hij aan de overdracht en kwalificatie van chromatografische technieken voor de identificatie en kwantificatie van verontreinigingen in biopharmaceutische producten. Na zijn bachelor begon hij aan de masteropleiding BioMolecular Sciences aan de Vrije Universiteit Amsterdam. Tijdens de masteropleiding liep hij twee onderzoeksstages. De eerste stage liep hij bij de structuurbiologie groep van de Vrije Universiteit Amsterdam onder begeleiding van dr. Dirk Bald. Hier werkte hij aan het recombinant tot expressie brengen en crosslinken van protein motors. Zijn afstudeerstage voerde hij uit bij Erasmus Medisch Centrum te Rotterdam onder begeleiding van dr. Andre Boonstra. Tijdens deze stage deed hij onderzoek naar de interactie partners en signaalcascades van interferon lambda. Na het behalen van zijn masterdiploma in 2011 begon hij als promotiestudent aan een samenwerkingsproject tussen de massaspectrometrie groep van dr. Peter van Veelen (LUMC) en het laboratorium voor Mycobacteriologie van prof. dr. Dick van Soolingen (RIVM). Het promotieonderzoek is beschreven in dit proefschrift. Sinds februari 2016 is Jeroen werkzaam als Scientist Analytical Development bij Bioceros, waar hij zijn werk en interesse in eiwit identificatie, kwantificatie en characterisatie continueert.

## **Dankwoord**

Het zelfstandig uitvoeren van een promotieonderzoek en het schrijven van het bijbehorende proefschrift doe je niet alleen. Op de laatste pagina's van dit proefschrift wil ik dan ook iedereen bedanken die, op welke manier dan ook, heeft bijgedragen aan de totstandkoming van "mijn boekje".

De afgelopen jaren heb ik veel geleerd over het opzetten, uitvoeren, documenteren en presenteren van wetenschappelijk onderzoek. Hier wil ik met name prof. dr. Dick van Soelingen en dr. Peter van Veelen voor bedanken.

Peter, de eerste keer dat ik jouw kamer binnen stapte was in mei 2011 toen ik kwam solliciteren voor een promotieplek bij de massaspectrometrie groep van de IHB, ik voelde gelijk een klik. In de vier(+) jaren die volgden heb jij mij niet alleen veel geleerd, maar hebben wij vooral ook veel gesproken over wetenschap, wielrennen en de minder belangrijke zaken des leven. Tijdens mijn promotieonderzoek ben ik veel obstakels tegen gekomen als wetenschapper, maar ook als mens. Bedankt dat ik altijd op jouw kamer welkom was om hierover met je spreken.

Dick, door jouw passie voor onderzoek, aanstekelijke enthousiasme en wetenschappelijke ideeën creëerde je voor mij een erg stimulerende omgeving om onderzoek te doen. Ik ben je erg dankbaar voor je begeleiding en advies, maar zeker ook voor het vertrouwen dat je in mij had. Dick en Peter, bedankt dat jullie mij deze kans hebben gegeven en mij hebben gevormd tot de wetenschapper die ik nu ben.

To all my co-authors, you are gratefully acknowledged for your interest in the projects, useful comments, suggestions, discussions and help.

George en Arnoud, jullie waren niet alleen mijn prettige kantoorkamergenoten die mij hebben wegwijs gemaakt op het lab, maar ook in de wereld van de biochemie, analytische technieken en natuurlijk proteomics.

Petra, Jessica, Tridia, Rina, Mimount, Miranda en natuurlijk Arnout, bedankt voor de gezelligheid op het RIVM, maar natuurlijk ook voor alle keren dat jullie mij hebben geholpen met kweken, PCRs, VNTRs en nog veel meer.

Chopie en Emmely, bedankt voor jullie gezelligheid als mede-OIO'ers, maar ook bedankt dat ik de kunst van het promoveren bij jullie heb kunnen afkijken.

Jer-Gung, thank you for all the great talks and trips we had during and after our time at the LUMC.

Frits, bedankt voor het faciliteren van dit promotieonderzoek. Mede IHB'ers Jeroen, Yvonne, Jan Wouter, Willemien, Robert, Natasja, Allen, Veronica, Frederike, Vincent en halve IHB'ers Kees & Lianne, bedankt voor de gezelligheid en jullie andere, niet proteomics/ microbiologische, kijk op mijn onderzoek.

Vrienden en (schoon)familie, de laatste jaren heb ik regelmatig een verjaardag of afspraak gemist omdat ik wilde schrijven aan mijn boekje. Bedankt voor jullie begrip en geduld, maar bovenal bedankt dat jullie mij lieten zien dat er meer in het leven is dan pipetteren.

Mamma, dankzij jouw onvermoeibare steun en hulp ben ik in de mogelijkheid gekomen om aan een promotietraject te beginnen. Pappa, je hebt mij meer dan eens gezegd dat je naast je schoenen zou lopen van trots mocht ik op een dag promoveren. Hoe erg ik het ook vind dat je er niet bij kan zijn, denk ik warm terug aan alle momenten die wij samen hebben gedeeld en die uiteindelijk hebben geleid tot dit moment. Als ouders staan jullie aan de basis van dit proefschrift, ik hoop dat jullie zo trots op mij zijn als ik op jullie ben.

Lieve Talitha, het moeilijkste deel van het proefschrift is misschien wel op papier zetten hoe dankbaar ik ben voor alles wat je de afgelopen jaren voor mij hebt gedaan. Hoewel ik altijd enthousiast ben als het over mijn promotieonderzoek gaat, weet jij als geen ander dat er ook moeilijkere momenten zijn geweest. Jouw liefde, onvermoeibare geduld en steun, ook als ik weer eens een weekend aan dit proefschrift spendeerde, zijn de belangrijkste redenen dat het tot een afgerond geheel is gekomen. Ik ben dan ook blij de laatste zin van mijn proefschrift te hebben geschreven, zodat ik vanaf nu mijn vrije tijd met jou en onze kudde kan doorbrengen!





